Copyright is owned by the Author of the thesis. Permission is given for a copy to be downloaded by an individual for the purpose of research and private study only. The thesis may not be reproduced elsewhere without the permission of the Author.

QUANTIFYING HILLSLOPE RESPONSE TO GLACIER RETREAT:

LANDSLIDE MECHANICS, PROCESSES AND IMPACTS

A dissertation presented in partial fulfillment of the requirements for the degree of

Doctor of Philosophy

in

Physical Geography

At Massey University, Palmerston North, New Zealand.

EMMA CODY

2021

ABSTRACT

Landslides are a natural hazard experienced in all countries around the world. Their formation is heavily influenced by internal and external processes including geology, earthworks, rainfall and in some instances glacier ice. This thesis investigates the response of alpine hillslopes to glacier retreat through the utilisation of movement monitoring techniques, subsurface investigations and geotechnical slope stability analysis.

Three objectives are proposed and guide the research outcomes of this thesis. The first objective is to investigate the underlying preconditions, preparatory factors and triggers which control and enhance paraglacial rock slope failures through the study of the Mueller Rockslide in New Zealand's South Island. Preconditioning and progressive weakening of the rockslide began over 8000 years prior to current glacier retreat, with the rockslide forming ~7500 years ago. Movement monitoring shows the rockslide to accelerate gradually over its history, culminating in maximum movement rates of ~6 m per year. Movement is constrained along structurally conditioned discontinuities, identified through a novel ground investigation combining geophysical and geotechnical techniques. Glacier debuttressing is considered a primary trigger of controlled slope failure, with increased displacement in spring attributed to snow melt and rainfall. Step-path failure of the rockslide is ongoing with tensile stress accumulating in the landslide body leading to segmentation of the rockslide into four zones. Ongoing progressive failure will likely lead to block sliding of the rockslide.

The second objective of this thesis was to identify drivers of movement in paraglacial sediment slopes. A novel suite of monitoring techniques was used at Fox Glacier which showed clear correlation between hillslope failure and glacier retreat and downwasting. Unlike previous studies, this thesis found debuttressing to be the primary trigger of slope failure with rainfall acting as an accelerant. Debris flows, once thought to be a dominant process in sediment slope adjustment did not begin until debuttressing was completed.

Finally, this thesis investigated the potential impacts of paraglacial landsliding on the broader environment. Both the rock and sediment slope failures in this study have deformed their supporting glaciers and a combination of monitoring techniques have uncovered to how sediment is delivered to the proglacial zone. Due to both sites being located within a high seismic hazard zone, catastrophic failure of both sites is possible. Continued failure of the Mueller Rockslide will likely result in a landslide dam and will also lead to continued retrogression of the headscarp and weakening of the surrounding hillslope. Continued failure of the sediment slopes at Fox Glacier will contribute large volumes of sediment to the proglacial zone, allowing for remobilisation of sediment in flood conditions. Both landslides have apparently created morphological change in their supporting glaciers.

A unique combination of monitoring methodologies was used to provide insight into landslide movement and evolution, but their usage should not be limited only to studies of landslides. The methodologies used in this thesis provided context across a range of spatial and temporal scales.

ACKNOWLEDGEMENTS

It's been a long road, akin I would say to the drive to Mt Cook; too long, pretty windy and with the occasional wayward driver, but then you arrive and see the view.

Each section within this thesis has its own acknowledgements but there have been a few who were instrumental in helping me write the next few pages.

Sam McColl, you have been ever patient, always honest and most helpful. I said at the beginning I wanted a PhD which was broad, taught me "skills" and had some cool fieldwork. Well after climbing that hill I can say all of the above was true. I have never met someone who can review a 40 page paper in 24 hours, but thank you for that and everything else.

To my co-supervisors Ian Fuller, Brian Anderson, Daniel Draebing and Jon Carey, thank you for tolerating my often very unintelligent questions, willing ears and enthusiasm. Your passion for research, work ethic and kindness have made it a privilege to learn from you, collaborate with you and find answers to long-held and important questions.

To my other willing (or not so willing) conspirators who have imparted knowledge or assisted with technical help. Marc-Andre Brideau; your help has been instrumental, and you are always willing to listen and offer advice. Kevin Norton, Albert Zondervan and Julia Collins from the GNS and Victoria University cosmo crew; thank you for allowing me to use your facilities and running cosmo samples. David Feek and the Massey technicians; thank you for your technical support. Sorry the keas ate everything. Thank you to GNS Science and the Technical University of Munich and Michael Krautblatter for hosting me, allowing me to run models and prepare samples. Thanks to the geology and geophysics teams at VUW and Canterbury University for allowing me to borrow your gear and return it in one piece.

Funding and support for this research has also come from a variety of external sources. A big thank you to DOC for allowing as to complete research in your backyard. The same goes to Fox Glacier Guides and Snowgrass for providing valuable data on the Fox Glacier and surrounding landslides and for providing us with a helicopter ride or two. Funding for this project has been provided by the John Beavan Geodetic Fieldwork Award, the Massey University Doctoral Scholarship and the Brian Mason Scientific and Technical Trust.

And finally, thank you to my friends and family. Your interest in what I do, your willingness to be talked to on natural hazards and your unwavering support has been much appreciated behind the scenes. To my parents Jenny and Steve, you have always encouraged my love of science. Mum - although you didn't really understand what I was doing, you are always enthusiastic and entertaining. Dad, thanks for the constant science discussions (much to Mums dismay) and your never-ending belief that I can achieve anything.

My husband, William. You have successfully evaded my requests to make you carry really heavy things up big hills. Thanks for holding the fort, buying me chocolate and being a constant inspiration in how to work hard.

Contents

Table of Figure

1. Introduction

1.1 General Introduction

The world's climate is changing. Normal fluctuations in temperature, which ordinarily take centuries or millennia are occurring in decades (Marcott et al., 2013). The retreat of glaciers globally has been a well-documented phenomenon following the end of the Little Ice Age ~150 years ago, however this retreat has accelerated in recent decades and has been attributed to anthropogenic climate changes (Gellatly, 1985, Chinn, 1996, Marzeion et al., 2014, Baumann et al., 2020). The impacts of this recent glacier retreat are not only restricted to the loss of glacier ice; deglaciation has a significant impact on the surrounding environment through the increase in erosion, transportation and deposition of sediment (Ballantyne, 2002b). While the rapid retreat of glaciers globally acts as a reminder of the negative impacts of accelerated climate warming, it also presents an opportunity to study and witness substantial glacier retreat and its associated impacts which has not occurred for hundreds or thousands of years.

Glaciers alter landscapes in several ways. During periods of advance, glaciers erode mountains and transport sediment, depositing this sediment along their margins as moraines (Hallet et al., 1996). During periods of retreat they leave behind steepened rock slopes and large deposits of unconsolidated sediment which now lack lateral support and are susceptible to erosion (Augustinus, 1995, Ballantyne, 2000a, Ballantyne, 2002c). With the right preconditions, these unsupported rock and sediment slopes may begin to fail as landslides resulting in the creation and transportation of sediment to the valley floor. Landslides have also been a primary producer of sediment during glacial and interglacial cycles, however during deglaciation this process is accelerated, as glacial support is removed, leading to increased sedimentation rates several times higher than what is measured during glacial or interglacial periods (Church and Ryder, 1972).

Landslides are not only recognised as producers of sediment. Of the many natural hazards, landslides are one of the most commonly occurring (Crozier and Glade, 2005a), and highly variable in how they occur (Hungr et al., 2014). From small individual sized block falls, to fluidised debris flows and deep-seated failures which stretch from hill crest to valley, landslides are responsible for causing billions of dollars in damage and hundreds of deaths each year (Schuster, 1996, Petley, 2012, Froude et al., 2018). Unlike most landslides, landslides which form following glacier retreat, and are known as paraglacial landslides, are poorly understood due to their as yet limited occurrence within human history. In fact, most studies on paraglacial landslides have focused on prehistoric events which failed thousands of years ago following the last major episode of adjustment between a glacial and interglacial period (Ballantyne and Benn, 1994, Shakesby and Matthews, 1996, El Bedoui et al., 2011, Ballantyne and Stone, 2013, Mercier et al., 2013, Cossart et al., 2013, Mercier et al., 2017, Curry, 2020). These studies found paraglacial landslides developed over long time periods, with failure often occurring

several thousand years after glacier retreat. It is this long lag time between glacier retreat and landslide failure that makes paraglacial landslides particularly hazardous, especially given fewer studies have so far focused on quantifying movement rates to determine how paraglacial landslides evolve. As glacier retreat will continue to lead to the destabilization of hillslopes which will continue to deform and act as a hazard thousands of years from now.

There is a lack of empirical data into paraglacial landslide development which has driven recent research on the subject, particularly given the identification of many newly developing paraglacial landslides in heavily touristed areas around the world (Hugenholtz et al., 2008a, McColl and Davies, 2013, Grämiger et al., 2017). Understanding how paraglacial landslides affect people and the surrounding environment first requires an understanding of paraglacial landslide development and failure mechanics. A primary focus of research so far has been to determine how periods of glaciation and deglaciation condition hillslopes over long periods of time (McColl and Davies, 2013) to identify underlying preconditions in landslide prone areas (Glueer et al., 2019) and to begin monitoring movement of paraglacial landslides to determine movement patterns and drivers (Kos et al., 2016, Fey et al., 2017).

A specific emphasis within these studies has been placed on rock slope failures. Sediment or debris slopes such as moraine have also been known to deform and fail following glacier retreat with this process often occurring over decades rather than centuries (Blair Jr, 1994, Curry et al., 2006, Hugenholtz et al., 2008a, Curry et al., 2009b, Draebing and Eichel, 2018, Eichel et al., 2018). Because of this relatively fast adjustment rate, many sediment slopes have already adjusted following Little Ice Age (LIA) retreat 200 years ago and there is only one study (with the exception of this thesis) which has monitored sediment slope failures during the final stages of debuttressing (Emmer et al., 2020). A similar problem occurs in early studies on paraglacial rock slope failures where landslide deposits have often been reworked in the long time frames since failure occurred. Without this information, it is difficult to assess and understand how paraglacial landslides evolve from their formation to eventual failure. It is this lack of quantitative evidence on paraglacial landslide development which governs the focus of this thesis. By utilising traditional and novel investigative techniques, underlying controls on landslide morphology and failure processes are identified and described. By gaining an understanding of paraglacial landslide failure mechanisms and development, scientists can better understand how to study rock and sediment slope failures through various methodologies, identify underlying geological and geotechnical controls which may increase the potential for failure to occur and quantify the environmental and socio-economic impacts of paraglacial hillslope failures.

1.2 Aims and Objectives

The aim of this thesis is to quantify the response of rock and sediment slopes to contemporary glacier retreat with a focus on spatiotemporal patterns in movement, paraglacial landslide causes and potential impacts. To achieve this, three objectives are proposed:

- Objective 1: Determine the movement and evolution of a paraglacial rockslide and the underlying preconditions, preparatory and triggering factors which govern these in a tectonically active alpine setting.
- Objective 2: Evaluate the movement and evolution of paraglacial sediment slope failures and the underlying preparatory and triggering factors which govern these in a tectonically active maritime setting.
- Objective 3: Investigate the contribution of paraglacial slope failures to surrounding landscape morphology and processes.

1.3 Organisation of thesis

This thesis combines a literature review, two published articles, one article in preparation and a synthesis. Each has been written and prepared for this thesis, with each focusing on one or more of the thesis objectives outlined in Chapter 1. The thesis is presented as a literature review (Chapter 2), three original research contribution chapters (Chapters 3-5), and a final discussion chapter (Chapter 6), which are summarised below:

CHAPTER 2: *Literature Review*

A review of the literature related to paraglacial hillslope failures is presented in Chapter 2. This chapter first outlines key terminology which will be used within this thesis, including describing a variety of paraglacial landslides which are included within this thesis. Next, a review of the current understanding on paraglacial landslide preconditions, preparatory factors and triggers are presented. The final section of Chapter 2 a review of past studies on paraglacial landslides and a discussion of the potential impacts of paraglacial landsliding, including the contribution paraglacial landslides play in producing and transporting sediment and previous examples of catastrophic paraglacial landslides which have impacted people.

CHAPTER 3: *Geomorphology and geological controls of an active paraglacial rock slide in the New Zealand Southern Alps. (Published journal article, Landslides, Cody et al. 2019).*

This journal article utilises a variety of field and laboratory techniques to identify and describe preconditioning factors of the Mueller Rockslide, a large paraglacial rock slope failure in the New Zealand Southern Alps. For the first time, a combination of geophysical field techniques (GPR, SRT) were used to identify an extensive fracture network within the headscarp zone of a paraglacial rockslide. Geological and geotechnical mapping was also used to further define this fracture network and kinematic analysis was then used to model the potential for planar, wedge and toppling failure. Finally, a simple numerical model was created based on rock slope geology to identify what impact underlying structural controls have on controlling landslide formation and morphology.

The main findings of this chapter included the identification of an extensive retrogressive development zone that has extended underneath a popular tourist hut (Mueller Hut) with morphology of the rockslide and the development zone controlled by tectonically derived fold structures. Numerical modelling of the rockslide shows anisotropy of the rock mass is required for failure to occur on the hillslope and a review of geomechanical and morphological features of the rockslide indicate a potential for it to fail catastrophically. This chapter presents findings relevant to Objectives 1 and 2 as geophysical monitoring and geotechnical mapping identified structurally controlled conditioning of the rock mass is responsible for controlling the size and extent of the rockslide, the rockslide is currently growing and causing extensive fracturing and scarp development within the surrounding hillslope and rockslide development has now encroached on a tramping hut.

This chapter also highlighted the successful utilization of multiple monitoring techniques for the identification of geological and geotechnical landslide properties controlling landslide failure.

CHAPTER 4: *Paraglacial history and development of the Mueller Rockslide, New Zealand. (Manuscript in prep).*

Following the investigation of the underlying preconditioning factors controlling Mueller Rockslide morphology, this chapter provides a detailed history of the Mueller Rockslide from its formation prior to glacier debuttressing, through to current deformation as the Mueller Glacier has retreated from the landslide. This chapter combined annual surveying, cosmogenic dating, historic aerial imagery and crack meter monitoring to track landslide movement to identify movement drivers and quantify landslide evolution.

Cosmogenic dating of the rockslide revealed it to have formed at least 7600 years ago, reaffirming international studies which found progressive failure within paraglacial rockslides to occur thousands of years prior to headscarp formation. Movement of the rockslide has resulted in deformation of the Mueller Glacier causing it to become elongate and crevassed. Movement of the rockslide has increased over its history and current movement can exceed 5 m per year in the lower slope. Movement monitoring shows potential seasonal variability in movement within the headscarp and retrogressive zone with increased movement over spring. Comparisons between movement and rainfall showed no clear link although increased movement in spring, captured within the headscarp crack meter may coincide with snowmelt.

This chapter presents new knowledge on the development, movement drivers and impacts of paraglacial rockslides fulfilling objectives 1 and 3. The development of the Mueller Rockslide over the last ~8000 years was revealed showing progressive failure and acceleration of the rockslide over time. Monitoring of landslide movement identified several potential triggers including debuttressing, snowmelt, rainfall and earthquakes. These observations also identified opening of the fractures around Mueller Hut and movement of the lower landslide has begun to block the valley and caused deformation of the Mueller Glacier.

Movement patterns, combined with earlier findings within Chapter 3, also indicate a potential relationship between underlying geological controls (discontinuity kinematics) and landslide movement rates, including landslide failure potential. Paraglacial rock slope failures governed by sliding failure mechanisms may move slower than those governed by toppling failure mechanisms and be at lower risk of developing into rapid or catastrophic landslides.

CHAPTER 5: *Paraglacial adjustment of sediment slopes during and immediately after glacial debuttressing. (Published journal article, Geomorphology, Cody et al. 2020).*

Findings in chapter 5 are presented which involve the monitoring of two large sediment slope failures during and after glacier retreat. This research utilised novel pixel tracking of daily timelapse images over a four-year period. Pixels were tracked in 3D and 2D space allowing for the quantification of daily movement which was then compared to rainfall. Visual monitoring of timelapse imagery also allowed for the tracking of spatial and temporal changes in paraglacial sediment slopes which until now have only been conducted after glacier retreat. This paper also explores the impact hillslope failure is having on the broader environment through a focus on sediment connectivity between paraglacial hillslopes and the proglacial zone.

Pixel tracking of the sediment slope failures unveiled seasonal changes in movement rate which coincided with fluctuations in the rate of glacier retreat. Debuttressing was identified as the primary trigger of slope failure and resulted in the sediment slopes failing as slides prior to and during the final stages of glacier retreat. Heavy rainfall during this time acted as an accelerant of sliding failure. Following glacier retreat, the mode of failure transitioned to debris flows which were triggered by rainfall. Movement rates also decreased rapidly following glacier retreat. Unlike other studies on paraglacial sediment failures which found debris flows to be a main process in paraglacial sediment slope adjustment (Ballantyne and Benn, 1994, Blair Jr, 1994, Curry and Ballantyne, 1999), observations from Fox Glacier found debris flows are not an initial failure mechanism and in fact, only occur after debuttressing is completed. Instead, sliding of a sediment mantle was the first form of adjustment to occur, followed by debris flow initiation and gullying. Finally, observations of how sediment is transported from hillslope to valley floor showed connectivity between the hillslope and proglacial zone to be high. An unusual method of sediment delivery was also uncovered, with one paraglacial landslide sliding directly underneath the glacier, rather than on top of the glacier.

This study highlighted the variability in response of hillslopes and changes in landslide mechanics that occur throughout the paraglacial period and provided new research relating to objectives 2 and 3. The evolution of paraglacial sediment slope failures is more complex than originally thought and originates as relatively cohesive sliding before transitioning to debris flows and gullying. Movement is primarily controlled by debuttressing and movement rates change seasonally with changes in the rate of glacier retreat and downwasting. This is much faster than rock slope failures which are thought to respond on a decadal timescale. Sediment slopes also contribute large volumes of sediment

to the proglacial environment, should connectivity be high. Remobilisation of this paraglacial sediment has already begun and proglacial zone and sandur is now prone to flooding and avulsion.

CHAPTER 6: *Synthesis of results and general recommendations.*

The final chapter of this thesis provides a synthesis of Chapters 2-5 with a focus on paraglacial landslide development and impacts. This synthesis first discusses how rock and sediment slopes respond through the various stages of glacier retreat. Fallowing this, potential implications of paraglacial landsliding are discussed with a focus on the localised impacts of landsliding on the surrounding hillslopes and proglacial zone.

2. Literature Review

2.1 Introduction

Landslides or mass movements, here defined as the collapse of material (rock or soil) under gravity (Cruden, 1991) are a fundamental but often dangerous natural process in landscape evolution (Crozier and Glade, 2005a, Petley, 2012). Landslides have the potential to occur in all areas of the globe but are particularly common in mountainous areas with steep relief where slopes are susceptible to and often impacted by extreme temperatures (Krautblatter et al., 2013, Draebing et al., 2014), earthquakes (Keefer, 2002, Malamud et al., 2004, Yin et al., 2009), groundwater fluctuations (Premchitt et al., 1986, Brönnimann, 2011) and glacial erosion and oversteepening (Augustinus, 1995, Ballantyne, 2002b, Holm et al., 2004, Cossart, 2008). Landslides vary greatly in size, from individual block sized (<50 cm) failures to large, deep seated failures exceeding 100 million m^3 and have widespread impacts on the broader geornorphic environment through the formation of landslide darns (Schuster and Costa, 1986, Costa and Schuster, 1988, Korup, 2005c, Fan et al., 2020), delivery of sediment to rivers (Korup et al., 2004, Korup, 2005b, Meigs et al., 2006, Vehling et al., 2017) and delivery of sediment onto glaciers (Gardner and Hewitt, 1990, Deline, 2009, Hewitt, 2009, Reznichenko et al., 2011, Deline et al., 2015b, Dunning et al., 2015) which can alter or enhance sediment pathways and sediment entrainment. While these effects can be significant, the impacts to people have historically been minimised with most alpine landslides occurring in remote, sparsely populated locations. As the world's population increases and technology advances, this is no longer the case and more people have begun to live in or visit these once remote locations. With recent increases in global temperatures attributed to anthropogenic climate warming, the occurrence of large landslides in mountainous regions has begun to increase and have been attributed to melting glacier ice or permafrost (Ballantyne and Benn, 1994, Corominas and Moya, 1999, Evans et al., 2001, Geertsema et al., 2006, Kenner et al., 2011). As these mountainous areas are further developed, the likelihood of landslides impacting on people has risen. Understanding the risks and impacts of these landslides involves gaining an understanding of their development including landslide mechanics and movement processes.

Landslides form due to a number of inherent internal properties and acting external processes. Known as preconditioning, preparatory and triggering factors (Crozier, 1986) they work to influence landslide morphology, weaken hillslopes and eventually lead to failure. Underlying rock or sediment slope characteristics such as bedding, structural discontinuities and material strength precondition hillslopes and make them more susceptible to external stressors. These external stressors which can include earthquake shaking, rainfall and glacial debuttressing then act on hillslopes, weakening them and preparing them for failure. These external stressors can also act as landslide triggers, resulting in rapid or catastrophic failure of the hillslope. In alpine environments, which are regularly exposed to natural extremes in climate and mountain forming processes like earthquakes, it is often a combination

of preparatory and trigger factors which lead to landslide formation and failure (Schulz et al., 2012, Oswald et al., 2021). Identifying how glacial debuttressing and ice loss has contributed to an increase in alpine landslide activity is therefore a complex process, as there are potentially many influencing factors at play. Understanding the specific role debuttressing plays in destabilising hillslopes has been an important topic in geomorphology for the last few decades (Ballantyne and Benn, 1994, Ballantyne, 2002c, Grämiger et al., 2017).

The response of many hillslopes to glacier retreat has been ongoing throughout the Holocene as the worlds climate transitioned from glacial to interglacial conditions. Enhanced climate warming in the past century has accelerated this process with glaciers and hillslopes responding through rapid retreat and increased movement (Kirkbride et al., 1999, Roe et al., 2017, Chinn, 1996). Glaciers weaken hillslopes and potentially trigger landsliding in several ways. During cooler periods when glaciers advance, they erode surrounding hillslopes, making them steeper and deposit this eroded material as moraines along the front and sides of the glacier (Augustinus, 1995). During periods of warming when glaciers begin to retreat and thin, debuttressing of glaciers from hillslopes begins, resulting in a loss of lateral support (Fig 2.1) and in some cases, the development of landslides (Ballantyne, 2002a). These landslides, which form or fail in response to glacier retreat are known as paraglacial landslides. Traditionally, past research into paraglacial landslides and paraglacial slope stability has focused on landslides triggered by pre-historic glacier retreat throughout the early Holocene. Many of these landslides have already failed (Ballantyne and Benn, 1994, El Bedoui et al., 2011, Mercier et al., 2011, Ballantyne et al., 2013, Cossart et al., 2013, Mercier et al., 2013) with a delay identified between glacier retreat and eventual failure. Dating of these landslide deposits shows coincidental timing between periods of rapid and extensive glacier retreat and catastrophic landsliding. For many paraglacial landslides, failure occurred hundreds or thousands of years following glacier retreat, indicating the impacts of glaciation are long lasting and can have significant effects on hillslopes long after glaciers have gone. This also implies that slope failures caused by current climate warming and glacier retreat may continue to deform and remain unstable long into the future, with the final impact not known for hundreds to thousands of years.

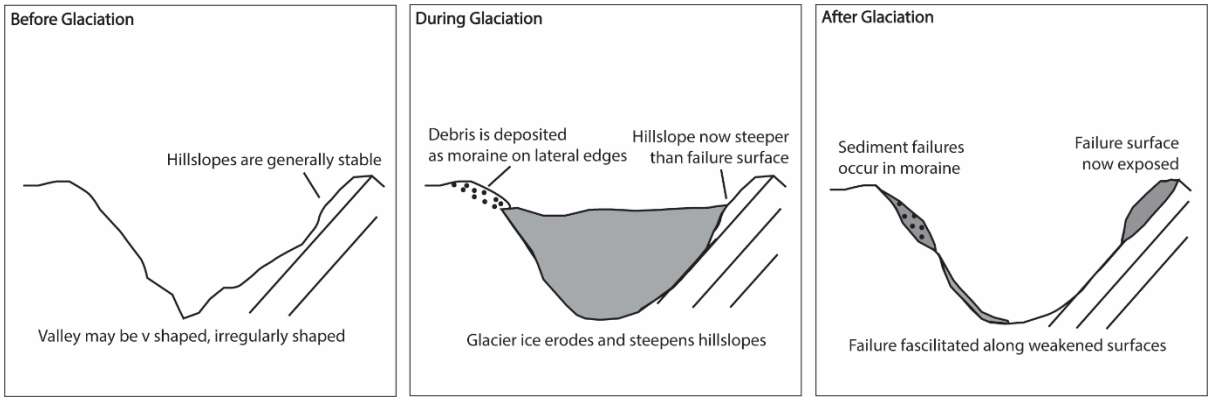

Figure 2-1: Effects of glacial advance and retreat on valley morphology.

As climate warming has accelerated glacier retreat, paraglacial adjustment of hillslopes is also accelerating. Studies into recent paraglacial failures in North America show instances of landslides occurring in areas with a history of deep-seated slope failure and near LIA trimlines, linked in some instances to permafrost degradation (Holm et al., 2004, Higman et al., 2018, Bessette-Kirton and Coe, 2020, Dai et al., 2020). In Europe, several instances of acceleration have been seen in deep seated slope failures within ten years ofrecent retreat (Kos et al., 2016, Fey et al., 2017). Given the extensive retreat of glaciers globally, this increase in occurrence of landsliding in mountainous regions is being attributed to ice loss and glacier retreat (Crozier, 2010, Huggel et al., 2012). Ongoing glacier retreat and debuttressing will only enhance this phenomenon but there is now an opportunity to study how hillslopes respond to glacier retreat as it happens, as opposed to retrospectively investigating the cause of failure thousands of years after failure and glaciers have retreated.

Recently, studies have begun to focus on more contemporary paraglacial slope failures i.e. those which are forming or continue to deform in response to warming following the Little Ice Age (LIA) approximately 250 years ago. These studies have begun to provide an understanding of the spatial and temporal patterns of deformation seen within paraglacial slope failures and identify exactly how debuttressing prepares and triggers landslides. Observations by Kos et al. (2016) showed acceleration of the Moosfluh Rockslide in the Swiss Alps occurring within 10 years of debuttressing. Glueer et al. (2019) and (Manconi et al., 2017) also provided historical data on movement of the Moosfluh Rockslide and showed movement to be episodic with the highest movement rates seen during periods of rapid debuttressing. They further postulate that progressive failure of the Moosfluh Rockslide is controlled by joint set failure following repeated glacial cycles, with repeated loading and unloading of ice responsible for strength degradation of the rockslide. This is confirmed by Grämiger et al. (2017) through analysis of hillslope failures around the Aletsch Glacier including the Moosfluh and Dryas rockslides, all of which are in the Swiss Alps. Grämiger et al. (2017) also states that first deglaciation causes the most mechanical damage to rock slopes with repeated cycles offering less impact, until a state of equilibrium is reached and significant glacier retreat again destabilises rock slopes. These findings appear to contradict the original notion that hillslope response to debuttressing occurs over as a gradual process that leads to a steady reduction in rock strength. In fact, as indicated by Glueer et al. (2019), the response is likely episodic and inconsistent, with periods of rapid acceleration separated by periods of relative quiescence. The research by Grämiger et al. (2017) and Grämiger et al. (2020) shows not all periods of glacier advance and retreat are created equal; it may be that consequential reductions in rock mass strength from debuttressing only occur following major changes in glacier extent (cold periods) like following the LGM (23,000 years ago), the Antarctic Cold Reversal (ACR 13,000 years ago), Younger Dryas (12,000 years ago) and the LIA (250 years ago).

Fey et al. (2017) provide the first comprehensive study of rock slope movement during the final stages of glacier retreat and showed deceleration in the latter stages of monitoring as the rock slope was debuttressed, and the delay between debuttressing and slope response is minimal. This mirrors findings

by Kos et al. (2016) and Glueer et al. (2019) who found rock slopes responded within a decade to rapid glacier retreat. From these studies it appears rock slopes are most responsive during debuttressing and then begin to stabilize and movement rates reduce as debuttressing is completed Kos et al. (2016). No studies have yet investigated how this relates to long term stability in slopes. Given many studies of historic slope failures show failure can occur thousands of years after retreat, it may indicate the potential for failure decreases following debuttressing before alternative preparatory or triggering factors act upon the slope.

While there are still many questions around long term paraglacial rock slope stability, it should also be noted that many of these studies have occurred in high alpine environments in Europe. The studies on contemporary failures mentioned above have occurred, in some cases, at the same glacier or are the same failure i.e. investigation of the Moosfluh failure (Grämiger et al., 2017, Manconi et al., 2017, Glueer et al., 2019, Storni et al., 2020). Given glaciers are retreating globally, more attempts should be made to explore the impacts of debuttressing outside of traditional study sites in the Northern Hemisphere.

Paraglacial hillslope failures are not restricted to rock slopes; sediment slopes also respond to glacier retreat with failures occurring in moraine, talus and other unconsolidated materials. When they have been described, sediment slope failures were predominantly described as debris flows before transitioning to gullying over several decades (Ballantyne and Benn, 1994, Ballantyne, 2002b, Curry et al., 2006, Mercier et al., 2009). In particular these studies found debris flow activity and gullying "peaked" at around 50 years following deglaciation in alpine settings before the slope begins to stabilise. Similar findings have been found by Draebing and Eichel (2018) and Eichel et al. (2018) who have stated gullying is the first in a three step process of paraglacial adjustment of lateral moraines, followed by solifluction (gradual movement of soil or material downslope during freeze thaw cycles) and final stabilisation. Rainfall was considered the primary trigger of debris flows in these studies and in paraglacial environments, debuttressing was considered a mere precursor which allowed for rainfall to initiate slope failure. Debris flows are not the only way slope failures are facilitated in sediment slope failures in paraglacial environments. A study in Canada showed the potential for sliding failure within lateral moraines at the Athabascar Glacier, Canada, which are still buttressed by their supporting glaciers (Hugenholtz et al., 2008a). This study shows sliding to be a primary failure mechanism and debris flows to be a minor process. Long term monitoring of the moraines around the Athabasca Glacier shows moraine deformation to be similar to that seen within rock slope failures, with movement occurring progressively leading to an extensive network of scarps, trenches and fractures.

The impact of hillslope failures is not only isolated to areas immediately impacted by landsliding. Through landsliding and mass movements, sediment is produced, transported and deposited to areas of lower elevation and valley floors. In alpine environments, this sediment can then be entrained by glaciers and rivers and transported and deposited in the proglacial system. Some studies have investigated how sediment systems are responding to increased sediment flux as a result of paraglacial

landscape response. Increased sedimentation as a result of glacial adjustment was first noted by Church and Ryder (1972) through research into rapid alluvial fan formation following glacier retreat. However, a disconnect between sediment sources (hillslopes) and transport pathways (rivers) has been found by those expanding on this area of research, with reduced connectivity in many alpine systems, predominantly due to large clast size present in many glacial deposits (Church and Slaymaker, 1989, Cossart, 2013, Cossart et al., 2008, Lane et al., 2017). In fact, Cossart (2013) notes paraglacial periods merely create sediment storage systems which are then transported in subsequent paraglacial periods.

The study of contemporary paraglacial hillslopes is still relatively new and there is particular focus on rock slope failures. This literature review provides a critical evaluation of the understanding from previous studies on historic failures preceding the LGM, to current studies which have begun to explore hillslope response during active debuttressing. The last significant review on paraglacial rock-slope stability by McColl (2012a) did not include a review on sediment slope failures. Instead, Ballantyne (2002b) was the first and only detailed review of both rock and sediment slope failures. Sediment slope failure are included in this review. In addition, this review investigates the impact paraglacial hillslope failures have on the broader environment, particularly how paraglacial adjustment within the proglacial zone is delayed through reduced connectivity and sediment transport. Finally, this review evaluates the concept of paraglacial landslides as a hazard, especially given the extended timeframes at which paraglacial adjustment occurs within the broader geomorphic system.

2.2 Nomenclature

2.2.1 Review of the paraglacial concept

The adjustment of geomorphic systems to glacier retreat and ice loss was first observed in alluvial fans which formed from reworked glacial sediment (Ryder, 1971). It's noted that alluvial fan construction was reliant on temporary conditions as a result of glaciation and continued until 6000 years B .P. In 1972, Church and Ryder formalised this concept and derived the term paraglacial to refer to "non-glacial processes that are directly conditioned by glaciation". In 2002, Ballantyne revised the paraglacial concept to mean "non-glacial earth surface processes, sediment accumulations, landforms, land systems and landscapes that are directly conditioned by glaciation and deglaciation. There are two notable outcomes from Ballantyne's review: 1) the term paraglacial does not refer to one specific environment but refers instead to the time it takes for these environments to adjust after deglaciation and 2) that paraglacial processes vary across environments and therefore adjustment time also varies.

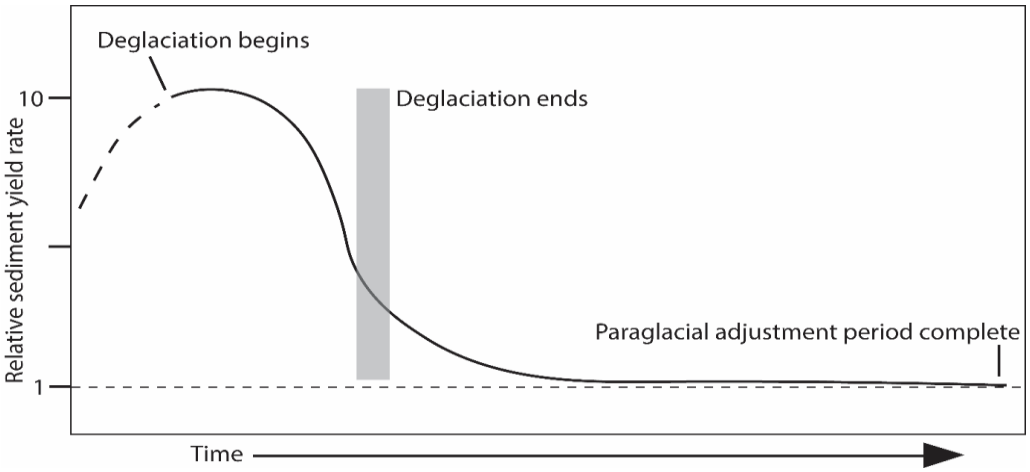

Figure 2-2: Paraglacial adjustment rates according to Church and Ryder (1972).

Following the creation of the paraglacial concept, a majority of studies focused on the reworking of glaciogenic sediment as a primary process (Long, 1974, Jackson Jr et al., 1982, Jijun et al., 1984). Within this initial paraglacial framework, the concept of paraglacial slope stability was considered a secondary process as a result of fluvial erosion or weathering. Wyrwoll (1977) was the first to identify glacial conditioning as a cause of rock fall through stress redistribution. Additional studies followed, noting the timing of rock slope failures in areas that had previously been glaciated (Moore and Mathews, 1978, Johnson, 1984, Bovis, 1990, Ballantyne and Benn, 1994, Shakesby and Matthews, 1996) although the true relationship between hillslope failure and glacier retreat was yet to be explored.

A review on the paraglacial concept by Ballantyne (2002b) was the first to present a detailed analysis of the influence of paraglacial adjustment in geomorphology as well as outline the importance of paraglacial slope adjustment as a research subject. Not only do hillslope failures modify landscapes; they are the primary source of sediment in sediment cascades and can drastically impact downstream sediment transport (Korup, 2005b, Davies et al., 2010, Cossart, 2013). Since Ballantyne's 2002 review, the investigation of paraglacial slope failures has increased considerably. Studies by Mercier et al. (2009), Cossart et al. (2008) and Vehling et al. (2017) have investigated the occurrence of paraglacial rock slope failures following prehistoric glacier retreat, predominantly following the Younger Dryas 12,000 years BP and show it can take thousands of years for some rock slopes to fail following debuttressing. In contrast, sediment slopes like those studied by Ballantyne and Benn (1994), Blair Jr (1994), Hugenholtz et al. (2008a) and Shulmeister et al. (2009) respond rapidly, within decades, with paraglacial adjustment of sediment hillslopes concluding within one to two centuries of glacier retreat.

Although the paraglacial concept is well known and now well utilised in the literature, there is concern from some (Slaymaker, 2009, Slaymaker, 2011) that the term has become overinflated in its use and may be applied to processes that occur well after glaciation has ended. Ballantyne (2002b) outlines his rationale for extending the paraglacial concept to include long term sediment adjustment

seen in river systems or coasts, rather than confining it to rapid adjustment seen immediately following glacier retreat. This definition acknowledges the variable temporal scales upon which paraglacial adjustment occurs, however there is still a lack of understanding of how these temporal scales are defined.

While this thesis does not attempt to resolve issues around nomenclature and defining a hillslope as paraglacial, it does present findings on hillslope failures that fall under the current definition of paraglacial provided by Ballantyne (2002b). The case studies in this thesis are also referred to as contemporary due to their formation or movement occurring following LIA retreat.

2.3 Landslide classifications and area of study

Due to the often harsh environments in which they occur, paraglacial landslides primarily occur in rock and debris slopes (Hungr et al., 2014) rather than in soils. Rock slope failures can occur in intact or fractured bedrock in all rock types like sandstone, schist or volcanic material. Debris slope failures in paraglacial environments commonly include failure of talus, scree and moraine. Within this thesis, paraglacial failures in debris slopes are more commonly classified as sediment slope failures i.e. landslides occurring in superficial material which do not involve failure of bedrock. Hillslope failures in both materials can occur in variety of styles including slides, topples and avalanches. A variety of landslide types that are discussed within this thesis are described below (Fig. 2.2).

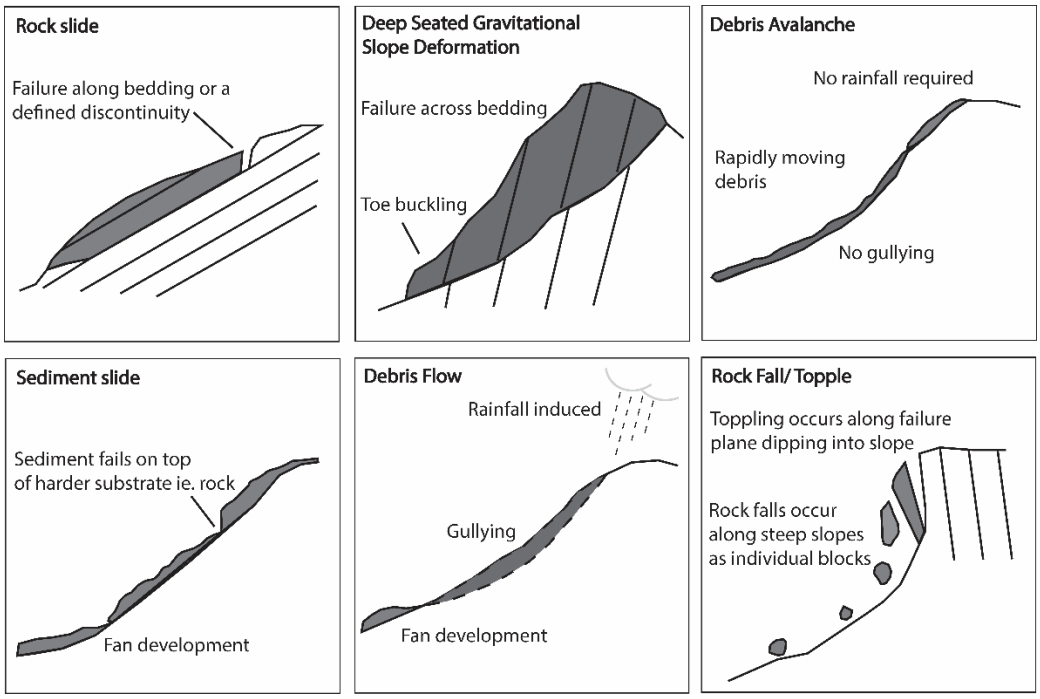

Figure 2-3: Landslide classifications included in this thesis.

Slides

Rock or sediment slides occur along a recognised rupture surface such as bedding. Rupture surfaces can vary from well-defined to poorly defined, with the shape (e.g. roughness) of the rupture

surface controlling how rapidly the landslide deforms. Planar or translational slides occur along defined rupture planes which are predominantly flat i.e. along a single bedding plane. Sliding along multiple bedding planes or along a stepped or intersection failure surface can occur in compound or wedge slides respectively. Rotational slides occur along curved rupture surfaces in weak rock and often result in slumping and rotation of the landslide. As a result of failing along a rupture surface, slides in rock and sediment have similar morphological features although sediment slides often involve internal deformation of unconsolidated material. Defined head scarps are common, as are signs of head scarp retrogression like tension cracks and minor scarp development. Lateral scarps can also be present if sufficient downslope movement has occurred.

Slides in sediment or rock range greatly in size from several m^3 to km^3. Similarly, rock and sediment slides move at variable speeds; some, like rotational slides move mm or cm per year, while some can move cm to m per day prior to failure (Glastonbury and Fell, 2008b, Lacroix et al., 2018). While some rock or sediment slides continue to deform slowly for extended periods of time, some continue to weaken to the point where rapid, catastrophic failure occurs. When this happens, rock and sediment slides transition to rock or debris avalanches (see 2.2.4) and can travel downslope at over 30 m per second (Sosio et al., 2008).

Deep Seated Gravitational Slope Deformations (DSGSDs)

Deep seated gravitational slope deformations (DSGSDs herein) are recognised as large mass movements that involve the deformation of entire mountains or ridgelines (Hungr et al., 2014). As they lack a fully defined rupture surface, movement is often extremely slow (<5 mm/year) as failure occurs through internal deformation of the rock mass. However, DSGSDs do have the potential to fail catastrophically as rock avalanches (Pánek and Klimeš, 2016). Aside from the omission of a defined rupture surface, DSGSDs differ to slides through a range of morphological features. Backwards facing scarps, tension cracks and trenches can commonly be seen within a zone of deformation, particularly at the summit as opposed to a clearly defined head scarp. Due to the lack of a defined rupture surface, deformation features such as backward facing scarps and trenches can be found throughout the slope, as well as bulging of the slope toe due to internal deformation within the lower landslide.

Debris Flows

Debris flows occur when sediment or soil becomes saturated and flows downhill within a confined channel, often resulting in additional entrainment of material with the flow path (Hungr et al., 2014). They can also occur following rock avalanches which become fluidised as they reach the valley floor (Walter et al., 2020). Given the requirement of channelisation, debris flows are not as large as the largest rock slope failures, (typically <0.1 km^3 (Jakob, 2005b)) however they are incredibly common (Jakob et al., 2005), mobilise quickly and can travel significant distances from their point of origin (Jakob, 2005a, Malet et al., 2005). Combined with possible travel speeds exceeding 200 km/h (Naranjo

and Francis, 1987), debris flows are a significant natural hazard, particularly in paraglacial zones due to an abundance of unconsolidated sediment ready for mobilisation, typically high precipitation levels including water sourced through snow melt and steepened topography.

Debris Avalanches and rock avalanches

Debris and rock avalanches involve the extremely rapid failure of material downslope. Specifically, debris avalanches occur in partially or fully saturated sediment, anywhere on a slope outside of confined channels, differentiating them from debris flows. Rock avalanches occur when rockslides or DSGSDs fail catastrophically and become fragmented, accelerating downslope as a disaggregated mass (Hungr et al., 2014). A defining factor of many rock avalanches is their extreme velocities, particularly for larger events (Evans et al., 2001, Stock et al., 2010) with some events exceeding velocities of 80 m/s (Yin et al., 2012).

Rock topples and falls

Rock falls and topples involve the sudden collapse of individual rock blocks or sections of fractured rock downhill. Rock falls often involve individual blocks or small clusters episodically interacting with the slope as they travel downhill (aka bouncing) combined with periods of free fall. Although rock falls usually involve singular or small groupings of rock bodies, the bodies can be large and exceed several meters in diameter (Haas et al., 2012, Corominas et al., 2018).

Rock topples occur as a result of forward toppling and overturning along steeply dipping discontinuities in rock. Like rock falls, topples can occur at a variety of scales with their size controlled by joint spacing and rock strength although some rock topples can exceed 100,000 m^3 (Couture and Evans, 2002).

2.4 Landslide causes: preconditioning, preparatory and triggering factors

There are a number of internal and external factors which control how and why landslides form and fail. Determining the exact factors impacting on the slope can be difficult, particularly when studying prehistoric events, as its difficult to determine what processes or mechanics led to failure. Even when landslides are observed, it is hard to discern a cause with 50% of landslides occurring with no apparent trigger (McColl, 2012a). Instead landslides are caused by a variety of factors, termed preconditioning (Crozier, 1986). While many preconditioning, preparatory and triggering factors are common in all environments, some like debuttressing - are specific to paraglacial environments.

2.4.1 Preconditioning factors

Preconditioning factors are the intrinsic properties of a slope which make it susceptible to movement without initiating movement (Crozier and Glade, 2005a). Preconditioning factors which affect rock slopes include rock type, structure (degree of faulting and folding), bedding and

discontinuities. Preconditioning factors in sediment slopes include bedding and contacts between the sediment mantle and underlying slope, slope angle, sediment type and sediment roundness. While preconditioning factors are predetermined and inherent within the hillslope they do not actively weaken hillslopes. Instead it is preparatory factors which act to weaken hillslopes. Preconditioning factors have ultimate control over a slope's potential for failure as well as failure mechanics and landslide geometry. When investigating how and why paraglacial hillslopes fail, a first step should be to gain a better understanding of a site's key characteristics through the determination of preconditioning factors, as these have a direct influence on slope strength.

Rock Type: lithology, mineralogy

Rock type is arguably one of the most important preconditioning factors in determining a hillslopes potential for failure due to rock type having a direct correlation with rock strength and rock structure (Gerrard, 1994). When investigating the influence of rock type as a preconditioning factor, several patterns can be found based on rock type formation. Sedimentary rocks like sandstones, mudstones and limestones are often laminated or interbedded which can act as planes of weakness within a rock slope (Bromhead and Ibsen, 2004, Margielewski, 2006). Depending on burial history and mineralogy, sedimentary rocks can be soft and able to be scratched by hand or can be highly indurated and require effort to break which significantly impacts on rock strength. Unlike other sedimentary rocks which are primarily siliclastic, limestones can be highly porous and permeable and are susceptible to chemical and mechanical weathering and changes in groundwater (Zêzere et al., 1999, Gattinoni et al., 2012).

Volcanic rocks can be placed within two groups: extrusive volcanic rocks which have been erupted, or intrusive volcanic rocks which never reach the surface and cool underground. Extrusive volcanic rocks like basalt, andesite and rhyolite can be soft and highly porous, and prone to chemical and mechanical weathering (Crandell et al., 1984, Naranjo and Francis, 1987, Barbano et al., 2014). Like sedimentary rocks, the deposition of extrusive rocks means they build in layers which can act as sliding planes or areas of weakness within a slope. Intrusive volcanic rocks like granite and diorite have cooled underground and are usually massive, without discernible bedding. As a result, they often lack discontinuities, are general indurated and can withstand many external environmental processes which can act as landslide triggers in other rock types. Several examples of landslides within intrusive volcanic rocks have occurred following extensive weathering prior to failure (Durgin, 1977, Chigira et al., 2011).

Metamorphic rocks like schist and gneiss have been altered through tectonic and thermal processes. Metamorphic rocks are usually laminated or foliated and these contacts can act as sliding planes for hillslope failures (Macfarlane, 2009, Brideau et al., 2012).

The degree of metamorphism can increase or decrease rock strength. For example, gneiss is highly altered and its crystalline structure interlocks, increasing stability and strength. In contrast to this, argillite or metamorphosed mudstone is fine-grained and the planar structure can often act as a

sliding plane. Several methods exist to estimate fracture potential or propagation in a variety of rock types. Perras et al. (2014) provides a critical review of comparable techniques to link direct tensile strength to Brazilian tensile strength and the crack initiation threshold. Unfortunately, there was no clear correlation with a wide distribution of results likely caused by rock type variability and testing configuration. They did find that metamorphic rocks showed more correlation across testing techniques than sedimentary rocks. Atkinson (1984) also provides a comprehensive review of parameters which can impact sub-critical crack growth of rock. Residual strain, temperature and pressure were all found to influence crack growth.

Rock type has been shown to play an important role in controlling the occurrence of paraglacial landslides. Fernandes et al. (2020) identified 135 potential paraglacial slope failures which occurred in a variety of rock types. However, they most commonly occurred in slate, lutite and limestone. In this study, no paraglacial landslides were identified in igneous rocks (granite) within the study area. Failure of the Yerba Loca landslide in Chile in 2018, did occur in volcanic rocks comprising slightly dipping breccias and brecciated lava flow deposits which were described as "moderately strong" (Sepúlveda et al., 2021). The Moosfluh Landslide in Switzerland occurs across a variety of rock types include granodiorites and gneiss, with a steeply dipping foliation controlling failure through toppling.

Structural Deformation: faulting and folding

Deformation of rock through faulting and folding gradually impacts a rock mass over millions of years. These processes leave an imprint on the environment creating weaknesses within rock slopes which can then be exploited by preparatory and triggering factors. Faulting and folding primarily impact rock in two ways. First, small breakages in the rock can occur which form discontinuities or joints within the rock mass. Commonly, these breakages are oriented in a certain way depending on how stress was applied to the rock during deformation which may be favourably oriented for failure once the rock mass has been exposed (Badger, 2002). Secondly, folding and faulting tilt and rotate bedding which can then act as sliding planes under the influence of gravity (Chigira et al., 2013, Chigira et al., 2003).

Understanding the structural history of a site may make it possible to predict areas of landsliding. For instance, Gupta (2005) found through a study of 207 landslides in the Himalayas that failure predominantly occurred along dip direction which was directly conditioned by regional folding and faulting. Understanding the tectonic history of a site is also essential for understanding how mechanic damage is accumulated in rock masses from folding and faulting. This is better described in section *2.3.2 Preparatory and triggering factors* where the role of seismic activity on inducing landsliding is described.

Brideau et al. (2009) and Stead and Wolter (2015) both highlight the importance of structural geology in determining slope failure kinematics. For Brideau et al. (2009) it was highlighted that structurally oriented fracture sets often act as sliding planes and as rear and lateral release structures. In fact, failure is unlikely to occur without these rear and lateral release structures which are most

commonly formed through faulting and folding. Stead and Wolter (2015) take this further by using numerical modelling to emphasise the importance of considering structural geology in modelling to assist with predicting failure potential of susceptible slopes, or to back analyse past failures to better understand how they formed.

Discontinuities: fractures, joints and foliation

While both rock type and faulting and folding control rock mass strength which in turn influences the susceptibility of hillslopes to landsliding, the primary role they play is in controlling the formation and occurrence of discontinuities. Discontinuities within a rock mass influence rock mass strength as well as how landslides fail. Discontinuities such as fractures and joints commonly form through tectonic conditioning (folding and faulting) and can further be enhanced by other preparatory factors such as frost weathering, earthquake shaking and rainfall. Bedding can act as a point of weakness within a rock mass, which in turn makes many sedimentary rocks prone to failure, especially if the sedimentary rock has been tilted (Guzzetti et al., 1996). Although discontinuities reduce rock mass quality, orientation is essential for inducing and controlling failure. For large landslides like those considered within this review, discontinuity sets need to be dipping, to facilitate sliding vertically to allow for failure like that seen within rockslides (Humair et al., 2013). However, this does not necessarily equate to bedding dipping down slope. Wedge and toppling failures are also controlled through discontinuity orientation with wedge failure occurring along intersecting joints sets, and toppling occurring along joint sets which dip perpendicular to slope direction. The Moosfluh Landslide adjacent to the Aletsch Glacier, is a large (75 M m^3) landslide involving a toppling failure mechanism. Discontinuity sets oriented parallel to the rockslope surface can act as potential sliding planes for planar failure while sets oriented perpendicular to the surface act as lateral and rear release structures (Brideau et al., 2009).

Discontinuities can also be caused or enhanced through stresses associated with glacier advance and retreat, however these discontinuities have often been classed as preparatory or triggering factors. It may be argued that pre-historic glacier retreat following previous glacial cycles occurred long enough ago to be classed as a preconditioning factor through the creating of discontinuities, rather than a preparatory factor which weakens hillslopes. The act of incision of rock slopes caused by glacial advance leads to increased gravitational stresses acting on the slope (Molnar, 2004). This static fatigue i.e. gravitational stress as a result of steepening during glacier advance and unloading during glacier retreat is thought to be a cause of sheeting joints in rock masses (McColl, 2012a). As McColl (2012a) summarised in their review, these sheeting joints form parallel to sub-parallel to a slope. More recently, Grämiger et al. (2017) showed mechanical loading and unloading of stresses caused by glacial ice does little to produce new damage with rock slopes but does act upon existing fractures which may in turn weaken slopes.

Clast size and roughness

Sediment slopes which consist of poorly sorted, unstratified rock debris like the tills found in moraines are not impacted by structural deformation or discontinuity formation. Instead, sediment slope strength can be directly related to sediment size, clast lithology (strength, friction coefficient) and compaction which reduce or enhance friction within the slope. Sediment slopes are also susceptible to groundwater fluctuations. For example, analysis of the geotechnical properties of moraines in Switzerland (Curry et al., 2009b) showed high slope angles which exceed angles of friction due to clast type being angular mica schists. Commonly, regardless of rock type, moraine and talus slopes are very heterogenous in clast shape, and size, allowing for increased cohesion within the sediment slope mass with positive correlations between clast roughness, clast shape and internal angle of friction (Lebourg et al., 2004).

Slope angle

Changes in slope angle can affect the stability of slopes by changing the ratio of shear stress to shear strength within the slope. Increases in slope angle lead to increases in shear stress and a reduction in shear strength through; should the resisting force within the slope be less than the opposing force i.e. gravity, slope failure will occur. In paraglacial environments, hillslopes are often steepened by previous episodes of glaciation, resulting in a reduction in shear strength and an increase in shear stress. This is particularly important in sediment mantled slopes where stability can be highly influenced by slope angle as their inherent strength is derived predominantly from internal friction between particles. As a result of this, many sediment slopes like moraine are stable at lower angles than rock slopes typically between 30-38° (Blair Jr, 1994, Springman et al., 2003, Hugenholtz et al., 2008a). It is common in sediment mantled slopes to see slope failures occurring in slopes which are only several degrees steeper before stabilising at around 30°. This has been well documented in areas of debris flow activity where debris flows occur in slopes from ~30-40° but slopes below this are stable and do not exhibit landsliding (Wang et al., 2013). In paraglacial environments, oversteepening as a result of glacial erosion and retreat can produce sediment slopes exceeding 70° (Curry et al., 2009b) which, following debuttressing and a loss of lateral support begin to deform before stabilising at ~30°. Similarly, glaciated rock slopes can becomes sufficiently steepened for shear stress to overcome shear strength and the slope to become unstable (Augustinus, 1995, Augustinus, 1996).

2.4.2 Preparatory factors and triggering factors

Preparatory and triggering factors are external processes which act upon slopes to gradually weaken them over time and trigger failure (Crozier, 1986). Specifically, preparatory factors weaken slopes over time without initiating movement of the slope while triggering factors do initiate failure of the slope. Both preparatory factors and triggering factors can be the same process (like earthquake

shaking) however movement of the slope is not seen following a preparatory factor acting on the hillslope. For paraglacial hillslopes, common preparatory and triggering factors can include debuttressing and glacial erosion, earthquakes, rainfall or groundwater fluctuations and chemical and mechanical weathering.

Glacial Erosion

The relationship between stress and strength in hillslopes is strongly defined by slope angle. Through the movement of glacier ice, valley sides erode which steepens and lengthens valley walls, changing the ratio between shear stress and strength in hillslopes (Augustinus, 1995, Augustinus, 1996). When glacier ice fills valleys, it provides lateral support for hillslopes and the impacts of oversteepening due to glacier erosion may not become apparent until glacier ice retreats or thins.

Many glacial valleys have experienced multiple periods of glacier advance and retreat, but the effects of glacial cycling on hillslopes are variable. Grämiger et al. (2017) demonstrated that merely adding or removing glacier ice through loading and unloading does little to create new damage in rock slopes as the forces are insufficient to cause new damage. Erosion of hillslopes is required to weaken slopes and this in itself is also variable; Grämiger et al. (2017) found failure of paraglacial hillslopes is most likely to occur following glacier advancement that produced a significant erosive impact, i.e. during global cold periods like the LGM. Minor cycles of glacier advance and retreat did not produce such an effect. It may be that glacier erosion sufficient to act as a preparatory or triggering factor for hillslope failures only occurs during cold periods like the LGM, Younger Dryas or LIA.

It is proposed that glacial erosion prepares or triggers slope failure in three ways (McColl, 2012a). First, glacial erosion can weaken hillslopes through the growth and alteration of fractures (Leith et al., 2014a, Leith et al., 2014b), that they can then be acted on by other factors like earthquake shaking or rainfall. Second, glacial erosion can weaken hillslopes to a critical level but buttressing of glacier ice is still sufficient to support the slope. Finally, glacial erosion can act as a trigger for hillslope failure by reducing strength of a hillslope to a critical level and glacial ice does not provide sufficient support to the hillslope, resulting in slope deformation under low applied stress (McColl and Davies, 2013). While theoretically, glacial erosion can act as a trigger of slope failure, there are no published studies of this occurring without debuttressing also occurring, i.e. there are no examples of slope failures occurring when they are substantially buttressed by glacier ice. Debuttressing in all cases has occurred to some extent, with failure either occurring into the proglacial zone, or onto the underlying glacier (Deline, 2009, Hewitt, 2009, Reznichenko et al., 2011, Deline et al., 2015b, Dunning et al., 2015).

Glacial debuttressing

The retreat of glacier ice from hillslopes, otherwise known as glacial debuttressing, can be a preparatory factor or triggering factor for hillslope failure through the removal of support. To understand the impact debuttressing has on hillslopes first requires an understanding on how glacial ice

impacts hillslopes. As outlined above, glaciers were thought to impact hillslopes in two ways. First, they erode hillslopes, potentially reducing stability through steepening, and secondly, glacier ice loads and unloads upon the slope as well as adds static load, which also creates stresses within hillslopes. Grämiger et al. (2017) has shown that the mere loading and unloading of ice is insufficient to act as a trigger of landslide and has a minor impact as a preparatory factor. However, the process of debuttressing and removal of support does prepare and trigger slopes for failure.

Debuttressing then affects slopes in the following ways. Following glacier advance where valley sides are eroded, undercut and potentially oversteepened, glacier retreat then alters the relationship between shear stress and shear strength in the hillslope (Ballantyne, 2000a, Ballantyne, 2002b). The impacts of debuttressing on hillslopes can be near instantaneous and synchronous with retreat rates, particularly in sediment slopes (Blair Jr, 1994, Curry et al., 2006, Mercier et al., 2009). In rock slopes, movement rates can be slower with one such example of a large rock slope failure beginning to respond within 10 years of debuttressing (Kos et al., 2016). In many recent cases, complete retreat of the buttressing glacier has not been required to trigger slope failure (Hugenholtz et al., 2008, Kos et al., 2016, Grämiger et al., 2017, Glueer et al., 2019).

Seismicity

Earthquakes are one of the primary preparatory and triggering factors for many slope failures (Keefer, 2002). As a preparatory factor, long term seismicity (thousands to millions of years) in many alpine areas gradually reduces rock mass strength through degradation, fracture propagation and progressive failure (Gischig et al., 2016). Secondly, should the hillslope be sufficiently susceptible, earthquakes can trigger unstable hillslopes to fail catastrophically. While seismic shaking is a proven preparatory factor of landslide in all environments, it is unclear what impact debuttressing has on increasing slope sensitivity to seismic shaking. (McColl et al., 2012) found glacier ice acts as a dampener from seismic shaking by 50 -80% however this effect is reduced to 5 - 20% if the height of the glacier is less than half the height of the valley. Not only does debuttressing increase seismic shaking experienced by hillslopes, but the loss of lateral support provided by glacier ice may also increases the slopes susceptibility to failure or weakening following earthquakes.

Rainfall and groundwater fluctuations

Fluctuations in groundwater, whether it is caused by rainfall, snow melt or groundwater along glacial margins has been recognised as a preparatory factor and trigger of slope failures for decades (Premchitt et al., 1986, Iverson, 2000). Changes in groundwater impact upon hillslopes by reducing cohesion and reducing frictional strength within the slope. The impact of groundwater changes varies greatly within different landslide types, with some being more susceptible to groundwater fluctuations. Slope failures which lack cohesion like sediment slides or shallow soil slides can be more susceptible to groundwater changes due to increased porosity and permeability allowing for groundwater to

permeate through the subsurface. In these types of slope failures, movement can be triggered by individual rainfall events or during abrupt changes to ground water. Slope failures which are more cohesive like large rockslope failures can still be triggered by rainfall or groundwater changes but their response is not as rapid due to lower permeability and size. Failure may be delayed, or rainfall may merely act as a preparatory factor rather than a trigger.

In paraglacial environments, groundwater changes can occur suddenly and can be significant due to climatic conditions and spring snow melt. Many alpine environments have high precipitation rates and are also prone to experiencing intense rainfall during storm events (Sturman et al., 2001). Several examples of alpine landslides triggered by snow melt (Cardinali et al., 2000, Naudet et al., 2008) show failure can be rapid and relatively difficult to predict. In sediment slopes common in paraglacial environments, i.e. moraine, rainfall is known to trigger debris flows and is identified as the primary cause of slope failure in paraglacial sediment slopes following debuttressing (Curry and Ballantyne, 1999, Curry et al., 2006, Mercier et al., 2009). When assessing the influence of glacial cycling on inducing rock slope failure, both Riva et al. (2018) and Grämiger et al. (2020) found groundwater fluctuations were required to weaken rock slopes to a sufficient level for failure to occur. Both noted glacier retreat and debuttressing acted as an insufficient trigger of failure without the presence of groundwater.

Periglacial processes

Alpine environments are highly susceptible to significant climatic events and fluctuations in temperature. Mechanical weathering of hillslopes occurs due to changes in temperature and the freezing of groundwater which both lead to expansion and contraction of rock masses. Both are common superficial processes but permanently frozen groundwater within hillslopes, known as permafrost, is found deep within mountains above certain elevations. In the New Zealand Southern Alps, current permafrost levels are thought to be at -2500 meters above sea level (masl), 600 m above the Mueller Rockslide (Allen et al., 2009). More recently, modelling by Sattler et al. (2016) found permafrost in rock glaciers may be lower (-2100) m based on current climatic conditions. Not only does permafrost cause the expansion of the rock mass which leads to fracturing and rock mass degradation, but permafrost acts as an essential glue binding fractures together. The thawing of permafrost -which is occurring in alpine environments due to warming temperatures destabilises hillslopes through a reduction in cohesion (Krautblatter et al., 2013). In some instances, glacier retreat has actually increased permafrost within a rock mass, as the site is now exposed to climatic conditions and lower temperatures (Wegmann et al., 1998).

There are numerous examples of periglacial rock slope failures in the literature. Permafrost degradation has been a trigger of many deep seated slope failures (Allen et al., 2009, Krautblatter et al., 2013, Haeberli et al., 2017, Baldis and Liaudat, 2019, Patton et al., 2019, Hilger et al., 2020) and is often identified as a trigger of rock fall in alpine areas (Noetzli et al., 2003, Gruber et al., 2004,

Krautblatter et al., 2010, Ravanel et al., 2017). The degradation of permafrost is another primary driver of slope failure in paraglacial environments which presents an issue in that it can be hard to distinguish between the effects of permafrost versus debuttressing. This is particularly true for many of the contemporary paraglacial slope failures in Europe (Wegmann et al., 1998, Kääb et al., 2009, Kos et al., 2016, Grämiger et al., 2017, Glueer et al., 2019) which are located within or near the periglacial zone and may be experiencing or have been influenced by permafrost degradation. This may obscure information on how contemporary paraglacial hillslope failures respond to debuttressing. To accurately study the drivers and mechanisms involving hillslope debuttressing, further case studies need to be identified in areas which are not also exposed to permafrost degradation.

Damage accumulation

While the above preconditioning, preparatory factors and triggering factors act upon hillslopes in a variety of ways, the process of damage accumulation in hillslopes is similar, particularly within rock slopes. External processes like earthquakes, permafrost and glacial erosion apply stresses to rock slopes resulting in the formation of microscopic fractures (Amitrano, 2006). The accumulation of fractures eventual weakens the slope and continued accumulation of fractures can lead to step-path failure wherein discrete fractures in specific orientations eventually join, creating discrete, highly fractured surfaces upon which failure can facilitate (Brideau et al., 2009). In paraglacial environments, damage is accumulated from continuous cycles of glacier advance and retreat, earthquake shaking and groundwater freeze thaw cycles to name a few. Progressive failure of the rock slope occurs over potentially thousands of years (Riva et al., 2018) until rock strength is reduced to the point failure can occur.

2.5 Paraglacial landslide impacts

The study of paraglacial hillslope response is not limited to hillslope failures; landslides can greatly impact their surrounding environment both as a hazard, and through the generation and delivery of sediment. A focus within the broader geomorphic community has been on establishing the effect accelerated paraglacial hillslope adjustment has on sediment supply and sediment connectivity, as well as how these increased or cyclic rates of sediment supply impact downstream sediment entrainment and deposition (Cossart et al., 2008) (Cossart, 2008, Lane et al., 2017). Both rock and sediment slopes are capable of delivering large volumes of sediment into proglacial systems, although at different time scales. If paraglacial rock slope failures develop into catastrophic failures, they tend to fail as a single rapid event with sediment delivery occurring almost instantaneously (Coe et al., 2017). In comparison, sediment slopes failures tend to fail progressively as smaller debris flows for decades after glacier retreat (Curry et al., 2006). Both rock and sediment slopes can greatly impact upon sediment connectivity with sediment slopes having a more immediate impact, which will be seen over the next few decades as hillslopes begin to respond from contemporary retreat.

2.5.1 Hillslope failures and sediment connectivity

Effective delivery and transport of sediment throughout catchments is dependent on several factors, namely the connectivity between geomorphic systems which allows for sediment to be effectively transferred between systems (Wohl et al., 2019). Sediment connectivity has been well studied in the field of geomorphology as quantifying the volume of sediment that exists within a system is vital for accurately assessing sediment budgets, catchment management and fluvial hazards (Cavalli et al., 2013, Heckmann and Schwanghart, 2013, Bracken et al., 2015, Heckmann et al., 2018, Schopper et al., 2019). With an emphasis on understanding the impacts of paraglacial processes have on alpine processes, several researchers have begun to investigate how paraglacial hillslope adjustment impacts sediment connectivity in proglacial systems once glacier retreat has occurred (Cossart et al., 2008, Lane et al., 2017, Mancini and Lane, 2020). While paraglacial hillslope adjustment produces greater quantities of sediment, at an accelerated rate, sediment connectivity is not necessarily increased. In fact, findings from Lane et al. (2017) and Mancini and Lane (2020) found that although sediment transport was high from hillslopes, connectivity was reduced as sediment was stored in alluvial fans (Fig. 2.3).

Increased sediment yield to proglacial environments has been well documented in the past. Church and Ryder (1972) were the first to document increased denudation rates in paraglacial sediments compared to areas not affected by glacier retreat. It was this research and documentation of increased sedimentation rates following deglaciation which inspired the development of the paraglacial concept. Sediment exhaustion models since then have favoured increased sedimentation rates during paraglacial periods, due to the high volumes of sediment which are being produced from hillslopes and other sources (Church and Slaymaker, 1989, Müller, 1999, Ballantyne, 2002a). However, patterns of paraglacial landsliding vary in various environments and an increase in sediment yield is not always associated with an increase in connectivity (Cossart, 2008, Kirkbride et al., 2018). The large sediment size of many paraglacial sediments (i.e. moraine) limits the potential for entrainment or transport and reduces connectivity (Cossart, 2008, Lane et al., 2017). Although sediment is transported and deposited in proglacial valley floors, fluvial processes are insufficiently able to entrain this material. This concept was investigated by Cook et al. (2013) through observations of rock avalanche deposit which had been overridden during a period of glacier advancement. They found armouring of the surface of the rock avalanche (which consisted of large, widely space blocks) resisted entrainment by the glacier and initial advancement was not able to rework the sediment. Lane et al. (2017) also noted connectivity can be reduced due to sediment storage occurring, particularly within alluvial fans along the base of many paraglacial hillslopes inhibiting the ability for sediment to be transported further into the proglacial system.

Figure 2-4: Sediment connectivity in alpine environments. Connectivity is high when connection between hillslope and river is immediate or restricted when sediment deposits in alluvial fans or when valley confinement is low (Wohl et al., 2019).

The study of proglacial catchment variability in New Zealand has shown sediment connectivity may be more varied and dependant on catchment morphology (Carrivick et al., 2009). Both Franz Josef and Fox Glacier valleys in New Zealand are located in adjacent glacial valleys with similar climates, geology and glacial extents. However, Carrivick et al. (2009) show Franz Josef Glacier valley, which is defined by narrower and steeper slopes, is supply limited and entrainment of material occurs through irregular outburst flows. In contrast, Fox Glacier valley is wider and is defined by the presence of numerous alluvial fans and an aggrading braided river. While Fox Glacier has alluvial fans which appear to be a defining characteristic of disconnected paraglacial systems, the valley shows no clear evidence of major outburst floods. Instead sediment is finer grained and indicative of regular fluvial transport, indicating a connection between the paraglacial hillslopes and downstream proglacial system. Ultimately, it appears connectivity is variable within proglacial geomorphic systems following glacier retreat. Further work is needed, conducted in a variety of environments, to understand what controls sediment connectivity except for sediment volume and transport rates.

2.5.2 Paraglacial landslides as natural hazards

Landslides have long been recognised as a significant natural hazard which can occur and impact people in every country around the world (Crozier and Glade, 2005a). Paraglacial landslides are no different, however due to how they are prepared or triggered (through glacier retreat) and due to the remote and often high alpine locations in which they occur, the impacts of paraglacial landslides throughout the last few decades has been minimal in comparison to other landslides outside of

paraglacial environments. As it is, several examples of fatal paraglacial landslides are documented (McSaveney, 2003, Huggel et al., 2005, Walter et al., 2020).

A primary hazard associated with paraglacial landslides is the impact they have on infrastructure. Hugenholtz et al. (2008) described the impact moraine deformation in Canada was having on roading with continuous realignment of the road needed as it crossed the landslide surface. In Europe, several instances of recent landslide activity as a result of glacier retreat or periglacial processes have occurred including the Randa Rockslide (Eberhardt et al., 2004) and the Preonzo Rockslide (Loew et al., 2017). In Austria, Kellerer-Pirklbauer et al. (2010) noted smaller debris flows travelling from an unstable rock-mass to populated alluvial fans. There are also numerous examples of increased landslide activity within the last century as a result of glacier retreat and climate warming which have fortunately not impacted on people (Hugenholtz et al., 2008a, Huggel et al., 2012, Kos et al., 2016, Glueer et al., 2019).

Regardless of whether paraglacial landslides are currently considered to be a significant alpine natural hazard, continued climate warming will only increase this risk. The long time periods under which paraglacial landslides respond to retreat, with some rock slope failures responding over thousands of years (Ballantyne, 2002a), means paraglacial landslides will be a continued risk for thousands of years into the future. With the long time frames in which paraglacial landslides take to deform, it may not be possible to predict their overall failure potential due to the number of external processes acting on the hillslope over such a long period of time.

2.6 Research Gaps

There are a number of research gaps in the literature, primarily associated with a lack of analysis on contemporary paraglacial slope failures which are starting to develop following recent glacier retreat. Studies by Kääb et al. (2009), Kos et al. (2016), Fey et al. (2017), Manconi et al. (2017) and Glueer et al. (2019) have presented observations on contemporary paraglacial rock slope failures in Europe. These studies have shown failure rates are variable with some failures moving meters per day (Manconi et al., 2017) whereas others move less than one meter per year (Kääb et al., 2009). These studies have also highlighted how large accelerations are common in paraglacial rock slope failures as the glacier terminus retreats and approaches the landslide toe (Fey et al., 2017), before movement rates retreat following debuttressing. A limitation of these studies is most have occurred at two rock slide sites – the Dryas Rockslide and Moofluh Rockslide adjacent to the terminus of the Aletsch Glacier. Further analysis should be completed on other paraglacial rock slope failures in different, geologic, tectonic and climatic settings to gain a better understanding of potential failure mechanisms, processes and landslide controls.

Several studies have also been presented on underlying structural and geomechanical controls on paraglacial rock slope failure. Grämiger et al. (2017) and Riva et al. (2018) have both used numerical modelling to determine how the impacts of repeat glacial cycles impact upon rock slopes and how long term mechanical damage is accumulated in paraglacial rock slopes. It is currently unclear how and if

structural controls impact formation and failure potential of paraglacial rock slopes. For instance, the Moosfluh Rockslide, which is dominated by a toppling failure mechanism (Glueer et al., 2019) moves rapidly in comparison to the Marzell Rockslide which is dominated by a sliding failure mechanism (Fey et al., 2017). While there are numerous factors controlling the formation of landslides, collating the results from these initial studies indicates there could be a correlation between movement rate and underlying mechanical properties of paraglacial landslides. Identifying this link could assist with assessing the risks posed by paraglacial rockslides as to whether they fail rapidly (catastrophically) or slowly and self stabilise following glacier retreat.

As outlined earlier within this literature review, most studies into paraglacial slope failures have been conducted on rock slope failures. Sediment slope failures, while generally smaller, are a common occurrence in paraglacial environments due to large volumes of glacial till and moraine which is produced and deposited during glacier advance and retreat. Hugenholtz et al. (2008a), Curry et al. (2009b), Draebing and Eichel (2018) and Eichel et al. (2018) have presented studies on recent sediment slope failures and found gullying to be a primary agent in erosion control, mirroring earlier studies by Blair Jr (1994), Curry and Ballantyne (1999) and Ballantyne (2002b). While these studies contribute to the knowledge on sediment slope failures, they fail to analysis sediment slopes in the initial stages of glacier retreat when they are still buttressed by glacier ice. Hugenholtz et al. (2008) identified other slope failure mechanisms including sliding in moraines at the Athabascar Glacier in British Columbia. Further analysis of other paraglacial sediment slopes is required to determine if failure can occur in other ways, as indicated in the study by Hugenholtz et al. (2008).

Finally, landslides are a common natural hazard that directly impact the lives of people around the world. While this thesis will focus specifically on the study of paraglacial landslides, the research techniques used can be applicable to all landslide studies around the world. In particular, what commonly available and relatively inexpensive monitoring techniques can be used to track movement and infer underlying controls on landslide development? How do these monitoring techniques help inform our understanding of rockslide development?

2.7 Conclusions

This review presents an overview of how the paraglacial concept has evolved through time and now encompasses contemporary slope failures in alpine areas. Paraglacial landslides are now recognised as occurring in a number or ways, whether that be as block sized rockfall failures or as slow, creeping deep seated landslides. Current glacier retreat has also allowed for the identification and study of paraglacial sediment slope failures, which due to their transient nature are often obscured within the sedimentary record. Regardless of whether paraglacial landslides occur in rock or sediment slopes, their development is controlled by a similar grouping of factors including slope angle, rainfall and debuttressing.

This review has identified a number of research gaps in the field of paraglacial landsliding. Studies on the evolution of contemporary failures is limited but provides an opportunity to identify

and monitor how paraglacial landslides evolve through the various stages of glacier retreat. This is achieved in Chapter 3, 4 and 5 within this thesis, fulfilling objectives 1 and 2. This is particularly true for paraglacial sediment slopes, which have been the subject of limited investigations, particularly during debuttressing. Monitoring of paraglacial landslides will also provide valuable insight on movement drivers and potential triggers for catastrophic failure. The linkage between debuttressing and landsliding is becoming more defined and both slope failures studied in this thesis show a clear but delayed movement response to debuttressing. But debuttressing is not the only driver of movement; preconditioning, preparatory and triggering factors of paraglacial hillslope failures are highly varied and tracking changes in slope movement may allow for the better identification of these movement drivers. Chapters 4 and 5 present monitoring results for both rock and sediment slopes over 10 year and 4 year periods respectively.

In particular, key research gaps identified within this literature review, and which define the scope and objectives of this thesis include: a) a lack of data on how contemporary paraglacial rock and sediment slope failures develop, particularly in environments outside of Europe; b) the influence underlying preconditioning factors have on paraglacial landslide development; and c) the impacts paraglacial landslides can have on the surrounding environment.

The purpose of monitoring landslide movement and determining how paraglacial landslides develop is not confined to gaining a better understanding of landslide movement drivers. Ultimately, these findings can assist with the quantification of paraglacial landslide impacts on people and the surrounding environment. These impacts are discussed in Chapter 6. It has already been shown that landsliding may deform glacier ice and the contribution of increased sediment leads to large accumulations of stored sediment. But there is mixed evidence to show some systems may have connectivity between sediment sources (paraglacial hillslopes) and sediment transport pathways like rivers, whereas many others are disconnected with sediment accumulating in alluvial fans. Movement of the stored sediment can also be varied with some systems allowing for gradual movement of sediment by rivers leading to aggradation, whereas others are transported through sudden and potentially hazardous outburst floods. Flooding within proglacial zones is not the only hazard associated with paraglacial landsliding; the landslides themselves can be fatal, or at minimum cause significant damage should failure occur. Within an increase in paraglacial landsliding seen globally, combined with the often significant lag times between formation and catastrophic failure, studying these events while allow for the management of a hazard which may be impacting people and communities for hundreds or thousands of years.

3. Geomorphology and geological controls of an active paraglacial rockslide in the New Zealand Southern Alps.

Summary of chapter 3 for thesis.

Chapter 3 presents findings from a combination of geophysical, geotechnical and field mapping which were used to identify underlying preconditioning factors affecting the development and morphology of a developing paraglacial rockslide and contributes to objectives 2, 3 and 4. While preconditioning factors are unique to every individual landslide, this chapter presents a review of techniques and highlights the uses of combining subsurface imaging techniques to identify structural controls and discontinuities. Using these techniques, a large retrogressive zone was identified above the rockslide. By identifying controls on landslide evolution, an assessment can also be made on the failure potential of the rockslide. Identification of key structural parameters like discontinuity orientations has led to an assessment that the rockslide could develop in a rapid failure which would adversely affect the valley, the tramping hut and the surrounding area.

This chapter has been published as a research article within Landslides as:

CODY, E., DRAEBING, D., MCCOLL, S., COOK, S. & BRIDEAU, M.-A. J. 2019. Geomorphology and geological controls of an active paraglacial rockslide in the New Zealand Southern Alps. Landslides, 1-22.

3.1 Abstract

Geological structures precondition hillslope stability as well as the processes and landslide mechanisms which develop in response to deglaciation. In areas experiencing glacier retreat and debuttressing, identifying landslide preconditions is fundamental for anticipating landslide development and hazard mitigation. Herein, the ~150 M m³ Mueller Rockslide in Aoraki/Mount Cook National Park, New Zealand is described, and we document how preconditions have controlled its morphology and development in response to thinning of the adjacent Mueller Glacier. A combination of geomorphological and geotechnical mapping – based on field, geophysical and remote sensing data – was used to characterise the rock mass and morphology of the rockslide and surrounding hillslope. Mueller Rockslide is identified as a rock compound slide, undergoing dominantly translational failure on a dip slope. The crown of the rockslide is bounded by several discontinuous, stepped scarps whose orientation is controlled by joint sets; these scarps form a zone of toppling that is delivering rock debris to the main rockslide body. Surface and subsurface discontinuity mapping above the crown identified numerous joints, fractures and several scarps that may facilitate continued retrogressive enlargement of the rockslide. The presence of lateral release structures, debuttressing of the rockslide toe and steeply dipping bedding, suggest the rockslide may be capable of evolving to rapid failure.

3.2 Introduction

Topographic, environmental and geological conditions predispose alpine landscapes to hillslope instability (McColl and Draebing, 2019). Consequently, mass movements are a significant process shaping alpine and mountainous areas as well as a significant natural hazard. While slope failure can occur in a variety of ways in mountainous terrain, large deep-seated slope failures such as deep seated gravitational slope deformations (DSGSD) and rockslides are primary hillslope modification processes and their evolution remains a subject of scientific enquiry.

DSGSD predominantly occur in steep relief and are commonly expressed as large interconnected networks of fractures and tensions cracks as well as with toe bulging, uphill and downhill facing scarps and significantly displaced geomorphic features (Beck, 1968, Dramis and Sorriso-Valvo, 1994, Agliardi et al., 2001, Agliardi et al., 2009b). DSGSD deform slowly over centuries to millennia (Agliardi et al., 2009a, El Bedoui et al., 2011, Pánek et al., 2011, Pánek and Klimeš, 2016), however, they have the potential to accelerate and fail catastrophically as large rockslides or rock avalanches (Kilburn and Petley, 2003, Pánek et al., 2009). Rockslides, whether preceded or not by DSGSD activity, can reach similar sizes to DSGSD (>100M m^3) but differ in that they more commonly move via sliding along one or more discrete failure surfaces, rather than through internal deformation and toe bulging (Hungr et al., 2014). Upward facing scarps are less characteristic of rockslides, and they tend to involve more intact rock mass blocks in comparison to DSGSD (Crosta et al., 2014). As with DSGSD, they can fail progressively, evolving towards rapid failure, but may involve different failure processes.

Given the potentially large size (>100 M m^3) of DSGSDs and rockslides and their ability to generate long-runout, rock avalanches, these slope failures are a major natural hazard in alpine

landscapes. Although they have long been recognised within the scientific community (Chigira and Kiho, 1994, Mahr, 1977, Bovis, 1982, Radbruch-Hall, 1978), there is still much to understand of the processes driving their evolution towards failure. Gaining an understanding of their underlying preconditioning factors, which are the primary control of landslide morphology is essential for anticipating their future development.

Worldwide, many large DSGSD and rockslides have been recognised in oversteepened glacial valleys (Agliardi et al., 2009a, McColl and Davies, 2013, Coquin et al., 2015, Barbarano et al., 2015). In alpine landscapes, glacier debuttressing – where ice support is removed from the toe of a hillslope – is considered a primary influence on preparing DSGSD or rockslide formation (Ballantyne, 2000a). However, rainfall and changes in groundwater (Pánek et al., 2011, Nishii et al., 2013), earthquakes (Crozier, 1986, Aringoli et al., 2016), gravitational or topographic stresses (Martinotti et al., 2011) and river incision (Hou et al., 2014) have all been attributed with triggering hillslope failures in both glaciated and non-glaciated terrain. Given that large rock slope failures occur in a variety of rock types and rock masses, climate conditions, and tectonic settings, identifying a common control or main trigger is difficult. As it stands, DSGSD and rockslides appear to commonly form along pre-existing or reactivated tectonic structures (faults, fractures, joints) (Agliardi et al., 2001, Ghirotti et al., 2011, Ambrosi and Crosta, 2011, Jaboyedoff et al., 2013) which constrain their size and morphology. Geological structures and steep relief precondition instabilities and are key for understanding how preparatory factors like debuttressing, fluvial incision and strength degradation allow slopes to evolve to failure.

Investigations into DSGSD and rockslides in glaciated valleys have primarily focused on those which formed or failed following prehistoric (pre Little Ice Age, 1750 AD) glacier retreat as a result of debuttressing and loss of support to the slope (Ballantyne, 2002b, Ballantyne and Stone, 2004, Cossart et al., 2008, Hewitt, 2009, Ballantyne and Stone, 2013). More recently, effort has been directed towards monitoring the response of hillslopes currently undergoing deformation following glacier retreat (Kos et al., 2016, Manconi et al., 2017, Fey et al., 2017, Glueer et al., 2019). For example, an acceleration of landslide movement and a change in movement mechanisms have been observed to coincide with glacier retreat and debuttressing at the Moosfluh Landslide aside the Aletsch Glacier in Switzerland (Kos et al., 2016, Glueer et al., 2019, Manconi et al., 2017) and at the Marzell Rockslide in Austria (Fey et al., 2017).

While monitoring studies have highlighted how some slopes are currently accelerating in response to recent glacier retreat, deformation may have been occurring within the rock slope for centuries to millennia (Eberhardt et al., 2017, Riva et al., 2018, Ballantyne et al., 2013, Brideau et al., 2009). Progressive failure (i.e. the progressive loss of strength of a rock mass) within paraglacial rock slopes occurs through stress changes induced by glacial erosion, ice load fluctuations, in-situ stress modification and thermal and hydro-mechanical processes (McColl, 2012b, Jaboyedoff et al., 2013, Grämiger et al., 2017, Grämiger et al., 2020). While a rock slope may currently be undergoing rapid

deformation, it is likely strength degradation has been ongoing through several repeated cycles of glacier advance and retreat. Further, as glaciated slopes begin to develop instability, their movement might involve deformation of its buttressing glacier (McColl and Davies, 2013), creating a complex interaction between the glacier and the mass movement. Such interactions are likely to affect whether a slope catastrophically collapses, the timing of collapse, and how the mass movement affects glacier and sediment transport dynamics.

In this study, we investigate the geomorphology and structural features of an active deep-seated slope failure, The Mueller Rockslide, whose development coincides with thinning of an adjacent glacier. The Mueller Rockslide was described by McColl and Davies (2013) as an example of a large (~150 M m^3) deep-seated gravitational slope deformation, undergoing gradual deformation adjacent to a retreating glacier. The study combines geomorphological mapping with geotechnical, geophysical and remote sensing techniques to identify discontinuity sets and other structures in and around the rockslide. The structures are interpreted within the context of the geomorphological and geological setting of the rockslide. We explore how these structures have preconditioned failure of this slope and identify the potential for retrogressive enlargement and catastrophic development of the rockslide. Our research contributes to the understanding of how geological structures precondition paraglacial rock slope failures and influence their response to contemporary glacier retreat.

3.2.1 Study Area

Mueller Rockslide is in Aoraki/ Mount Cook National Park, New Zealand (Fig. 3.1), situated on the western flank of the Sealy Range. The rockslide was first identified by (Hancox, 1998) as part of a study on the stability of an alpine mountain hut. At that time, the hut (referenced as Old Hut herein) was located on the eastern edge of the Sealy Range, which was experiencing localised subsidence in a large slump block. Due to safety concerns, the hut was removed and rebuilt 500 m south-west along the range in 2003. During the investigation, Hancox (1998) identified and described a much large slope failure (herein the Mueller Rockslide), affecting the western side of the Sealy Range, which Hancox described as a large block slide with an extensive headscarp area and a large rift-zone / graben. The hut is now about 200 m east of a series of large (10-20 m high, 30-50 m long) scarps that appear to define the headscarp of the rockslide. Above the rockslide, in the vicinity of the newly located Mueller Hut, several large fractures have been monitored since 1994 with opening detected of between 6 and 66 mm (Archibald, 2016). Annual GPS measurements of survey pins about 700 m west of Mueller Hut within the rockslide indicate movement rates of 1 m per year between 2010 and 2012 (McColl et al., 2012).

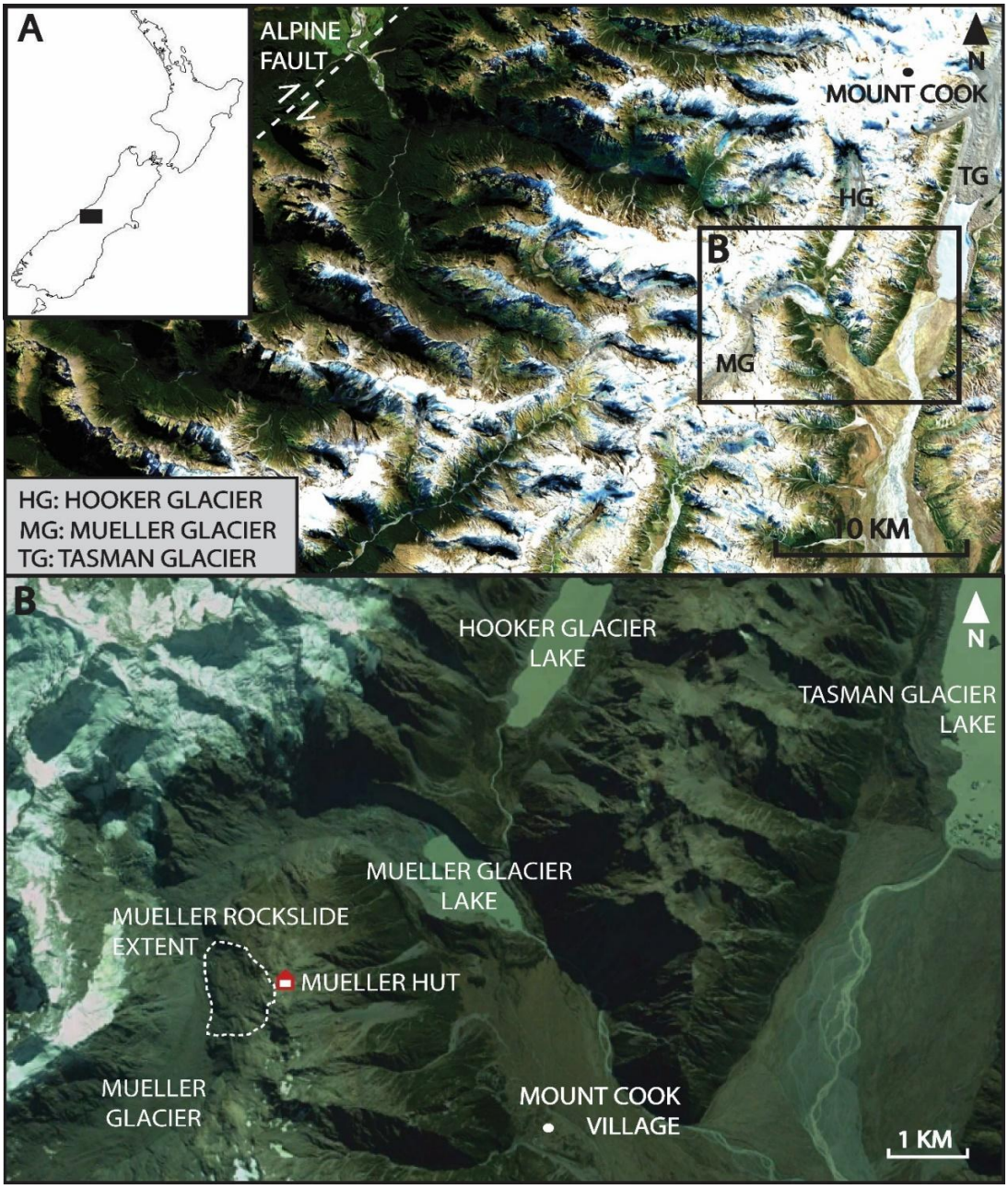

Figure 3-1. Location map of Mount Cook and surrounding area. B) Mount Cook Village and surrounding area. Mueller Rockslide estimated boundary is represented by the dashed white line with Mueller Hut sitting to the east.

The shape and stability of the Sealy Range reflects its history of tectonic and glacial processes. The range is about 25 km east of the boundary between the Pacific and Australian tectonic plates, which for the past 5 million years has been expressed by the Alpine Fault. Regional shortening and compression has resulted in faulting, folding and fracturing of the Torlesse Group greywacke sandstones and argillite, and semischist (low-grade schist of textural zone IA, IIB) which make up the Sealy Range (Cox, 2007). The Mueller Rockslide is located on the western side of the Sealy Range, on the western limb of the tightly folded north-plunging Kitchener anticline (Lillie et al., 1964) which formed initially from east-west compression (Fig. 3.2). Within and near the rockslide body, bedding

dips westward at roughly 30-60 degrees, with the Mueller Rockslide forming within the dip slope of the interbedded greywacke (Lillie et al., 1964, McColl and Davies, 2013) although most of this is heavily mantled with debris material. Currently, the Mueller Rockslide abuts onto the margin of the

Mueller Glacier, which is undergoing rapid thinning and terminus retreat. The Mueller Glacier has retreated by over 1 km (Gellatly, 1985, Kirkbride et al., 1999) since the Little Ice Age (LIA) ~200-250 years ago (Fig. 3.1), but it is still approximately 3.5 km down-valley from the Mueller Rockslide (Winkler, 2000). Glacier debuttressing has occurred through thinning of the glacier and has been in the order of some 100 metres since the LIA, as inferred here from abandoned lateral moraine ridges on the slopes near the rockslide as well as documented at the terminus (Gellatly, 1985, Kirkbride et al., 1999). The remaining thickness of the glacier at the toe of the Mueller Rockslide is unknown, but based on valley cross-section extrapolation, is estimated to be < 100 metres thick at the southern (upper valley) end of the rockslide. The glacier at the northern end may have melted completely, becoming disconnected from the down valley end of the glacier (Fig. 3.2).

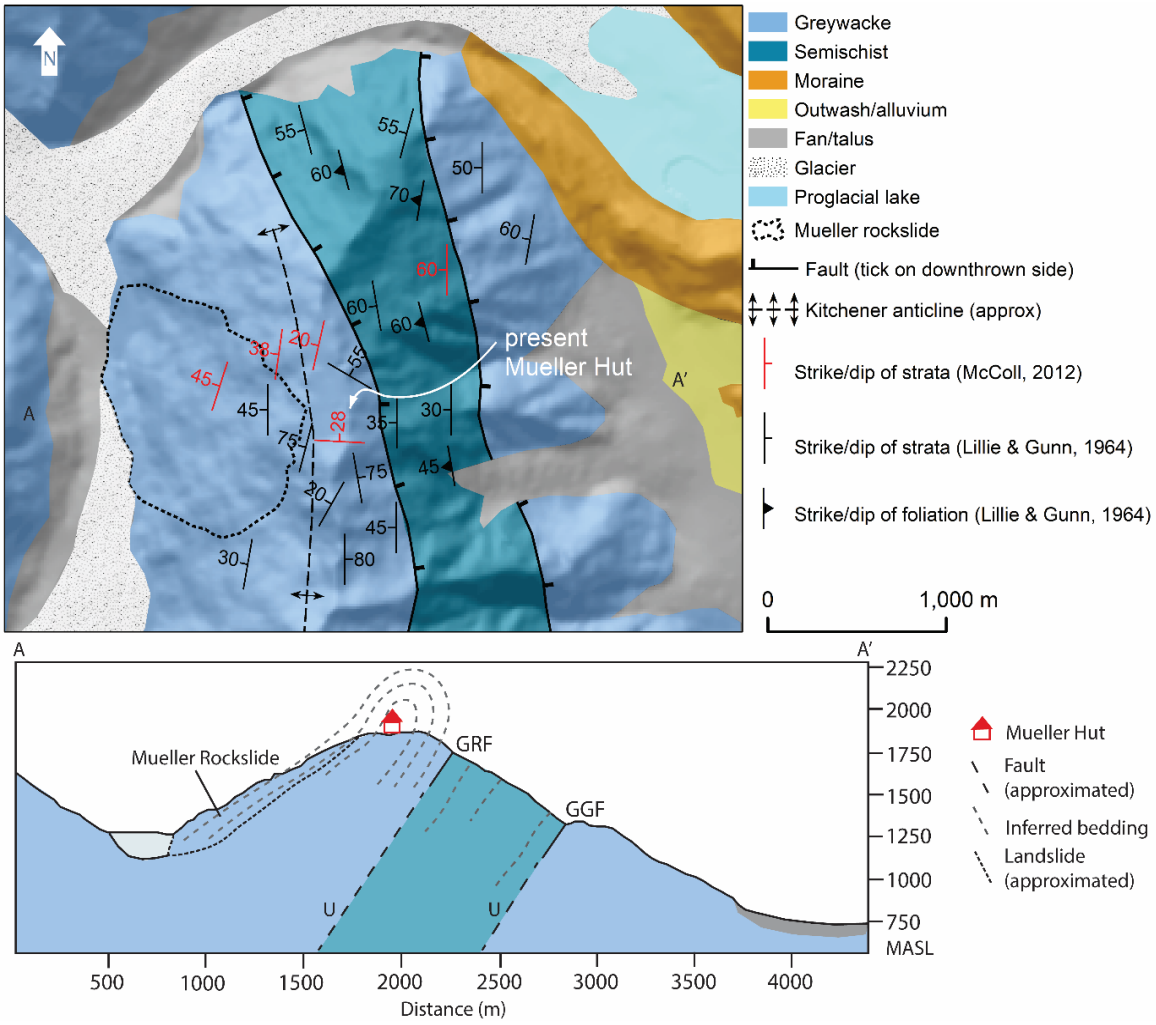

Figure 3-2. Geological map of Sealy Range and cross-sectional profile of the Kitchener Anticline (informed by mapping by Lillie et al. (1964) and (McColl, 2012b)). Glacier extent and Mueller Rockslide outline are as mapped in this study, based on aerial imagery from 2010 – 2017. GRF and GGF represent the Green Rock Fault and the Great Groove Fault respectively.

3.3 Methods

3.3.1 Topographic data and aerial photography

High-resolution topographic data and an orthophoto mosaic were obtained using Structure-from-Motion (SfM) photogrammetry for mapping the rockslide and surrounding slopes (Westoby et al., 2012). Photos were collected in February 2017 from a DJI Phantom 3 Professional unmanned aerial vehicle (UAV). Photos were captured from an above ground altitude of 60-120 m, in both oblique (30° from nadir) and nadir camera orientations to achieve a minimum of 75% forward and 60% side photo overlap. The SfM software Agisoft Photoscan was used to produce a dense point cloud that was decimated to a 0.25 m resolution DEM, and a 5 cm pixel-resolution orthomosaic image (Fig. 3.3).

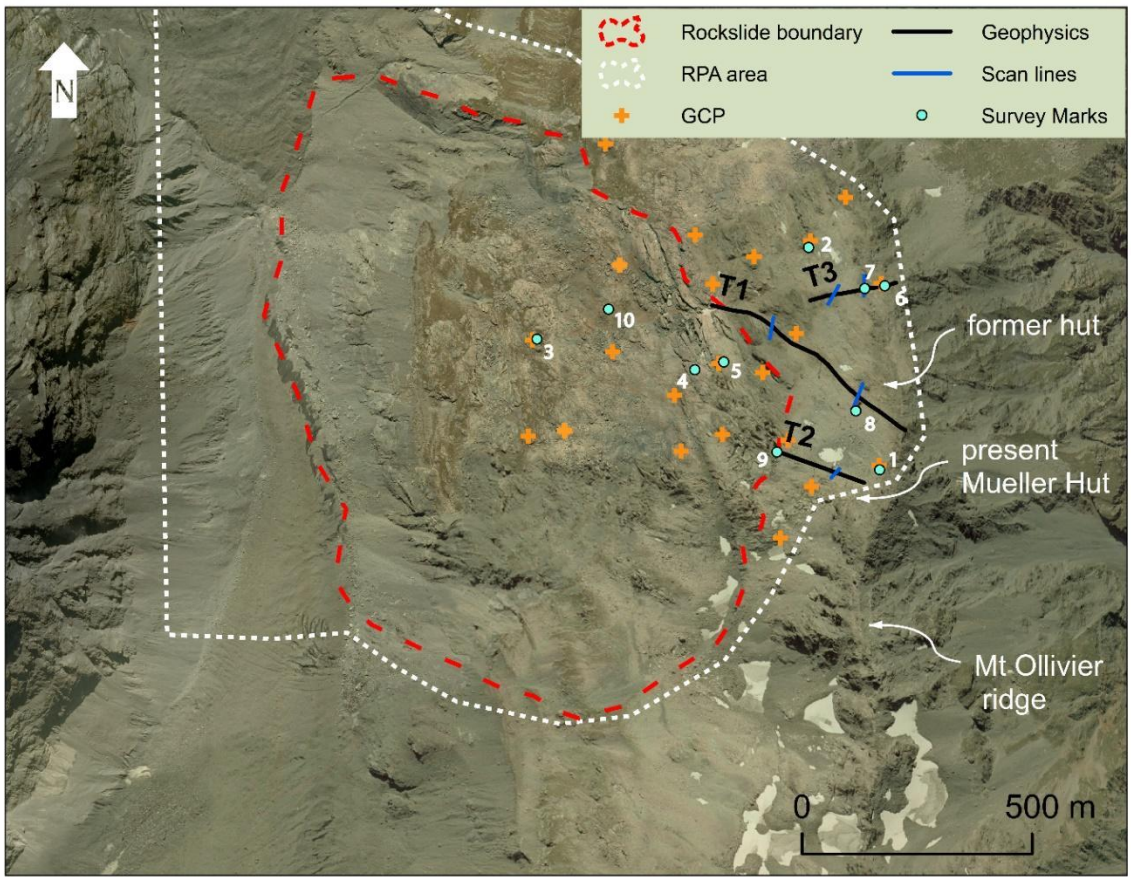

Figure 3-3. Approximate rockslide outline, extent of the UAV flights for photogrammetry and ground control points (GCPs), spot height survey marks used in Table 1, and the geophysics transects. Imagery is 0.75 m LINZ aerial photo (~ 2004-2010).

The georeferencing of the SfM model was provided by 22 ground control point (GCP) targets surveyed with a Trimble R10 GPS, with a 5-km RTK baseline correction, and referenced against the national survey network (using B8Y2 UNWIN geodetic benchmark, and the New Zealand Geodetic Datum 2000 and New Zealand Vertical Datum 2016). The GCPs were distributed asymmetrically, due to difficulty deploying them in steep, fractured terrain along the glacier and lower and southern slopes of the rockslide. The Photoscan estimate of GCP vertical uncertainty was an RMSE 0.156 m. We provided an independent assessment of this modelled error by comparing the modelled DEM elevations with our own 10 independent spot height elevations measured with RTK GPS. The mean difference and

RMSE we calculated were 0.35 m and 0.59 m respectively, with a maximum of 1.75 m (Table 3.1.) These vertical error values are mostly representative of the area inside our GCP distribution and therefore we have lower confidence in the model accuracy in the western and southern parts of the model outside of the GCP distribution. However, the combination of oblique and nadir convergent photographs will have reduced the amount of radial distortion in the model periphery, as shown by James and Robson (2014) and where GCPs were not available, the aircraft's built-in GPS (better than 10 m accuracy) provided camera positions for lens optimisation. We consider the resulting accuracy of the DEM to be adequate for the purposes intended here: to support geomorphological and geotechnical mapping of the rockslide and surrounding slopes.

Table 3-1. Comparison between selected spot heights and equivalent DEM elevations. Distance to nearest GCP indicates model performance away from model control points.

Spot Height ID	Spot Height Elevation (m) (NZVD2016)	DEM Elevation (m) (NZVD2016)	Elevation Difference (m)	Distance to nearest GCP (m)
1	1844.62	1844.69	0.07	16.3
2	1779.28	1779.09	0.19	14.9
3	1472.66	1472.21	0.45	11.1
4	1686.85	1686.55	0.29	54.6
5	1714.83	1714.78	0.05	17.9
6	1787.33	1787.39	0.06	11.5
7	1786.96	1786.70	0.26	37.7
8	1812.91	1812.77	0.15	112.7
9	1815.55	1815.37	0.18	35.9
10	1554.84	1556.59	1.75	99.1
Mean			**0.35**	**41.17**

3.3.2 Geomorphological and fracture mapping

A combination of field observations and remote sensing was used to map the geomorphology and structures present at the site. Using the SfM hillshade model and orthomosaic, landforms and features on and around the rockslide were mapped, including scarps, major fractures, lateral moraines, and areas of debris cover and bedrock outcrop. Detailed field mapping over three consecutive summers was completed in 2017, 2018 and 2019. Features mapped in the field included scarps, fractures, tension cracks and bedding. A total of 41 bedding measurements and 206 joint measurements (including fractures and tension cracks) were taken in the field.

Mapping of discontinuity locations and orientations was done in the field at accessible bedrock outcrops on the rockslide and ridge, and along the geophysical transects (described below). Discontinuities were also measured along one to two scan-line surveys perpendicular to each geophysics transect (Fig. 3.3). For less accessible locations of the site, major fractures were mapped remotely using Point Cloud Viz (Mirage Technologies SL) to select fractures in 3D space using each fracture face. Discontinuities were plotted on stereonets, with pole-to-plane density contours, using the software DIPS (Rocscience, 2018),

to identify orientation patterns and major fracture sets within the fracture network. Discontinuities were grouped into two structural domains; Domain 1 within the rockslide including the rockslide body and headscarp; and Domain 2 outside the rockslide and along the ridgeline. Kinematic analysis was conducted for both structural domains for plane, wedge and flexural toppling failure, with the aim of evaluating the feasibility of simple structurally-controlled failure mechanisms (Kliche, 1999). Average slope dip and dip direction obtained from the SfM derived digital surface model were used in the kinematic analysis. A friction angle of 33 degrees was taken from previous tilt test results (McColl et al., 2012) assuming failure along an argillite bedding surface. Argillite and siltstone beds are a common feature of the greywacke within the study area with the argillites described by Lillie et al. (1964) as sometimes being highly contorted and crushed. The lower strength of these argillites compared to sandstone makes them the most likely structural weakness along which bedding failure may be facilitated. This friction angle may be greater than that of a fully formed sliding surface (i.e. at residual strength) in argillite, so is treated as an upper estimate for the frictional strength of the argillite beds.

3.3.3 Geophysical surveying

Seismic Refraction Tomography (SRT) and Ground Penetrating Radar (GPR) were used to image the subsurface rock mass around the rockslide headscarp, Sealy Range Ridgeline and Mueller Hut. The steep and highly unstable topography of the landslide body made it impossible to conduct geophysical surveys along the rockslide. The geophysical surveys were used to identify rock mass discontinuities and better characterize the subsurface extent and nature of fractures, either identified or obscured by scree at the surface. In particular, the subsurface mapping was to help evaluate the potential for rockslide retrogression through identification of incipient shear surfaces east of the Mueller Rockslide crown. SRT has been previously used to investigate the internal structure of rock slope instabilities, such as the Åknes Rockslide in western Norway (Ganerød et al., 2008, Heincke et al., 2010), the slope instability at Randa in the Swiss Alps (Heincke et al., 2006), the La Séchilienne Rockslide in the French Pre-Alps (Meric et al., 2005) and several rockslides in Tien Shan, Kyrgyzstan (Havenith et al., 2000, Havenith et al., 2002). GPR has been used in previous rockslide and rock fall studies to investigate individual fractures and discontinuities (Toshioka et al., 1995, Theune et al., 2006) as well as stratigraphic analysis (Davis and Annan, 1989). Here we combine both methods to maximize potential information regarding shallow (<20 m) subsurface rock mass conditions.

Three combined geophysics transects using SRT and GPR were deployed along Sealy Ridgeline in a roughly east-west direction (T1-T3 in Fig. 3.3), targeting major fractures visible at the surface, and where possible, following accessible bedrock outcrop. In addition, 3 GPR transects were completed in the immediate area of Mueller Hut. Transect 1 (Mueller Hut transect) extends from the eastern Sealy Range ridgeline, past the present-day Mueller Hut to the main rockslide headscarp. Transect 2 (Mount Ollivier transect) is located farthest to the south, stretched east-west along the northern slope of Mount Ollivier. Transect 3 (Old Hut transect) is nearer to the northern end of the

rockslide and stretches from eastern Sealy Range ridgeline near the former Mueller Hut, west to the rockslide headscarp. SRT was completed using repeated overlapping transects of 24 geophones. Transect 1 had geophone spacing of 6 m and consisted of 4 overlapping transects (each 138 m long) resulting in a total length of 531 m. Transects 2 and 3 had a geophone spacing of 8 m with 3 additional offset shots after geophone 24 resulting in a total transect length of 204 m. Different geophone spacing resulted in different resolutions for the seismic tomographies which range from 1.5 m at T1 to 2 m at T2 and T3.

Seismic waves for the SRT survey were generated by sledgehammer shots between each geophone and three offset shots before or after the first and last geophone. Five shots were stacked to increase signal-to-noise-ratio. Geophone and offset shot positions were recorded using a Trimble R10 RTK DGPS and implemented in the data processing using Reflex W 7.0 (Sandmeier, 2012). First arrivals were picked manually. Raw data analysis was performed using the approach by Krautblatter and Draebing (2014). The raw data were inverted using the SIRT algorithm of Reflex W and ray path tracing was performed to check ray coverage. The quality of the final tomographies was calculated and total absolute time difference (3.96 – 4.72 m^{-s}) and root mean square error (5.58 - 6.27 m^{-s}) are in an acceptable range of 1/4 of the seismic wave amplitudes at Mueller Rockslide (10 to 20 m^{-s}).

The volumetric fracture density (P_f) for the rock mass was calculated using the equation by Clarke and Burbank (2011) and is expressed as a percentage:

$$P_f = \frac{V_f}{(V_r - V_f)}\left(\frac{V_r}{V_p} - 1\right)$$

where V_p is the subsurface p-wave velocity measured by the seismic survey, V_r is the intact rock velocity, and (V_f) is the velocity of the fracture material. Rock samples collected from the field were cut into 6.27 cm wide and 4.5 to 5.8 cm long cores and used to quantify V_r in the lab in parallel and perpendicular directions. A Geotron ultrasonic generator USG40 in combination with Geotron preamplifier VV51 and 350 kHz sensors generated the seismic signal. Seismic signals were recorded using a PICO oscilloscope and data analyzed using the software Geotron Lighthouse UMPC. Intact rock p-wave velocity (V_r) is 0.54 ±0.4 km s^{-1} and anisotropy on rock core scale according to Draebing and Krautblatter (2012) is 6 to 8%. We assumed that the fracture infill is air and, therefore, V_f is the velocity of air (0.33 km s^{-1}).

Ray path tracing was performed to estimate fracture location and persistence using the technique developed by Phillips et al. (2016). Ray density indicates the number of rays crossing a 1.5 x 1.5 m rock column within seismic transects. P-waves travel along layer boundaries (Hauck et al., 2003) which can be different layers of rock mass with different elastic properties or anisotropies caused by macroscopic air-filled faults and joints (Heincke et al., 2006). Therefore, ray density is increased in areas of fracturing in comparison to areas of low fracturing.

To assist with SRT interpretation, and to identify major sub-vertical fractures, faults, and bedding structures, ground penetrating radar reflection surveys were conducted at each seismic transect using a Sensors and Software Pulse Ekko Pro GPR. Three additional GPR transects were deployed around Mueller Hut (GPR 1, 2, 3 in Fig. 3) to evaluate the subsurface persistence of several scarps. They are 30, 55 and 100 m long respectively. For all GPR transects, stepped measurements were taken at 25 cm intervals along each transect using 100 MHz unshielded antennas. Topographic profiles from RTK GPS surveying were applied to correct for topography, and velocity was evaluated from hyperbola-fitting and common mid-point surveys and applied in Sensors and Software Ekko Project 3 software. Gains were adjusted to enhance weaker reflectors, using a combination of SEC2 and AGC methods. Discontinuities were mapped onto the radargrams, guided by matching discontinuities seen in the radargram with those observed in the field.

Subsurface features were identified to a depth of 15 m within the GPR radargrams and up to 20 m in the seismograms. These penetration depths are deemed adequate for identifying surficial rock mass quality around the ridgeline and Mueller Hut as well as identifying a potential sliding surface within the headscarp / toppling zone.

3.3.4 Rock mass characterisation

Descriptions of the rock mass and rock mass characterization were made for the rockslide and surrounding area. The Geological Strength Index (GSI) was utilized to describe rock mass "blockiness" and the presence of discontinuities within the rock mass following the methodology of Marinos and Hoek (2000).

3.3.5 Slope stability modelling

To help evaluate the importance of rock mass anisotropy (i.e. bedding) in influencing the stability conditions and development of the Mueller Rockslide, we used the two-dimensional finite element software RS2 (Rocscience 2019). A cross-section equivalent to that shown in Figure 3.2 was used to set the topographic boundaries of the model. The assumed geomechanical properties (Table 3.2) were selected to be representative of greywacke in New Zealand (Richards and Read, 2007) and conditions observed at the Mueller Rockslide. Equivalent elastic perfectly plastic Mohr-Coulomb strength parameters were estimated using RocLab (Rocscience, 2017). To evaluate the influence of the bedding orientation on the displacement and stability condition at Mueller Ridge, a model with isotropic strength material (no bedding) was compared with a model assuming an anisotropic direction 40° dipping to the west (bedding). The frictional strength along the anisotropy plane was assumed to be 33° using the tilt test results from McColl et al. (2012). The critical shear reduction factor (SRF; (Matsui et al., 1992)) was calculated to assess the relative stability of both the isotropic and anisotropic models.

Table 3-2. Summary of geomechanical parameters used in the exploratory finite element models of the Mueller Rockslide.

Property	Value
Density	2600 kg/m^3
Intact rock Young's modulus	35 GPa
Poisson's ratio	0.25
Unconfined compressive strength	80 MPa
Geological strength index	60
mi	11

3.4 Results

3.4.1 Rockslide geomorphology

From geomorphic mapping, we divide the rockslide and surrounding slope into three major zones, characterised by distinct morphology: 1) a main landside body, 2) a complex headscarp zone of block toppling, block dilation and sliding, and 3) a retrogressive zone with large tension cracks, fractures and small scarps.

Rockslide body

The main rockslide body is expressed as a partly disaggregated rock mass that has been moving downwards and outwards into Mueller Glacier Valley (Fig. 3.4). Extending from 1700 to 1150 masl., the surface of the main rockslide body slopes towards the valley floor at an inclination of approximately 31˚; the upper slope averages 29 to 30°, steepening to 37-39° near the rockslide toe. This transition is marked by a lateral moraine extending across most of the landslide. Much of the rockslide body is mantled with debris from weathering processes, rockfall, glacial deposits, and blocky debris from disaggregation of the rockslide body. Where not covered by debris, the bedrock shows indications of sculpting by glacial or nival erosion (smoothed rock surface and striations), and evidence of brittle deformation (fractures, and scarps). Most of the scarps within the rockslide body are downslope-facing, but in the upper part of the rockslide body there is a low-profile upslope-facing scarp, which is hypothesised to form the downslope edge of a large graben structure (Fig. 3.4) which was identified in field mapping. The graben structure may represent the separation of the rockslide body from the headscarp zone but has little to no vertical geomorphic expression because it is mostly filled with blocky debris from the collapsing headscarp zone.

A prominent lateral moraine can be traced across the rockslide body immediately above a prominent break in slope 160-230 m above the Mueller Glacier surface (Fig. 3.4). Up- and down-valley of the rockslide boundary other lateral moraines were identified, some resting at higher and more eastward locations on the slope. It is inferred that the moraine ridges identified in Figure 3.4 outside the rockslide boundary are of equivalent (LIA) age to the moraine ridge on the rockslide body. If correct, rockslide movement has displaced the lateral moraine on the rockslide by about 100-130 m horizontally west and 110-120 m vertically down. The toe of the rockslide body below the LIA trimline is affected

by shallower mass movement processes, with an apron of debris having built up at the base of the slope. At the southern end of the rockslide toe, and beyond the rockslide extent, shallow mass movement processes have removed parts of the LIA trimline and moraine altogether.

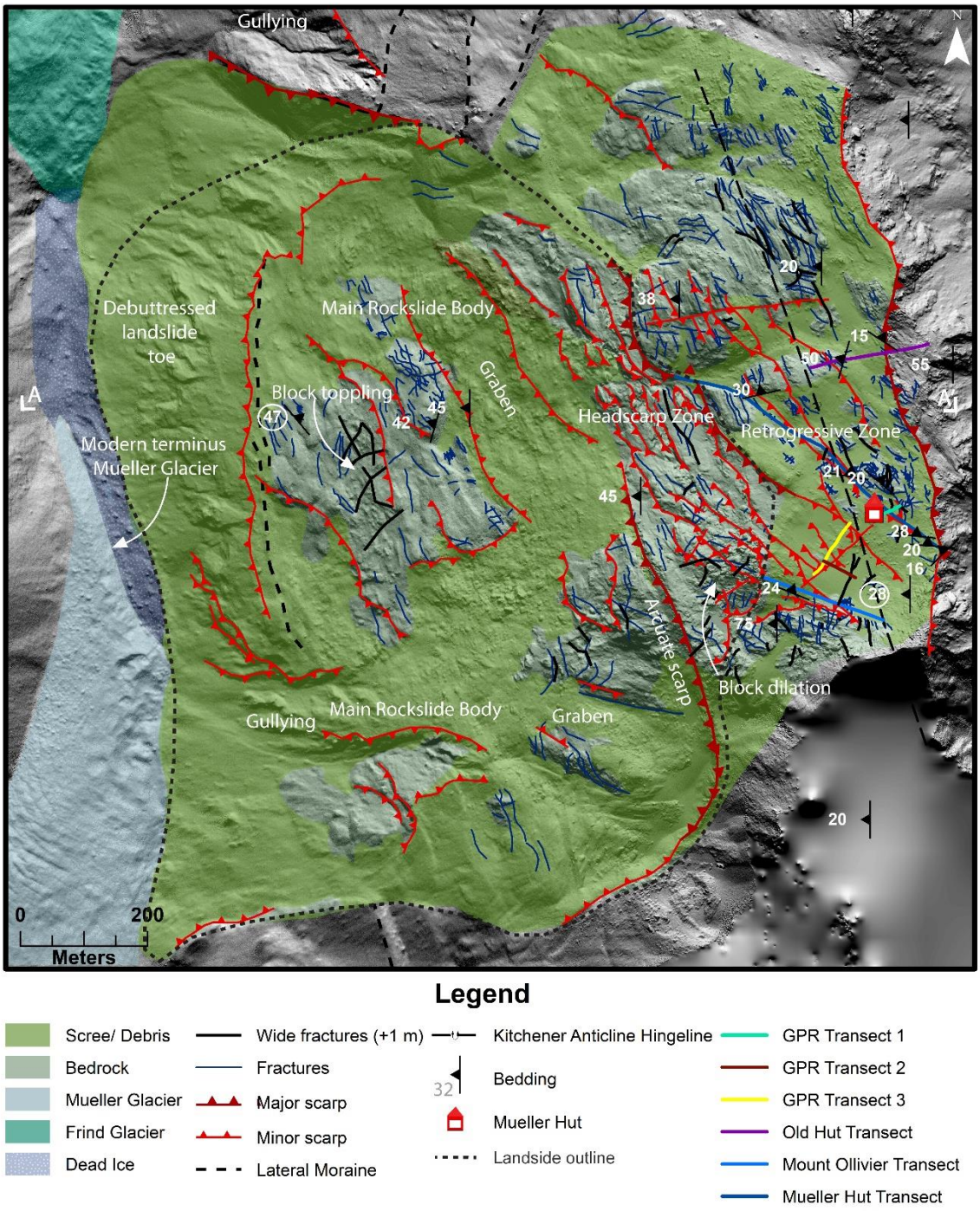

Figure 3-4. Geomorphic map of the Mueller Rockslide. Mapped bedrock (light green) can be seen throughout most of the ridgetop and headscarp but is limited to a central zone with the rockslide. The majority of the rockslide is debris-mantled (darker green). GPR and SRT transects are located near Mueller Hut extend E-W/NE-SW. A to A' marks the location of the cross section in Figure 3.12.

Headscarp and toppling zone

The crown of the rockslide is defined by a network of stepped, discontinuous and en-echelon scarps that form a wide (200-300 m) headscarp zone extending from 1830 to 1700 masl. Slope angle varies from <30° in areas of intact bedrock to 90° along fractures. Individual scarps have vertical offsets of up to 20-30 m (Fig. 3.4). The visible cumulative vertical displacement across these scarps is 55-70 m in the northern/upper section of the headscarp and decreases to 30-40 m in the southern part where the scarp transitions into a single arcuate scarp and becomes the southern lateral boundary of the rockslide. Towards the north, the headscarp is less defined but appears to transition into a lateral scarp that defines the northern extent of the rockslide. The lateral scarp is 50-100 m high, and of varying strike, appearing to follow planar pre-existing structures. The stepped scarps forming the headscarp are facilitating forward-toppling of large (up to 140 m long, ~0.2 M m^3 in volume) blocks of rock (Fig. 3.4). Several incipient block topples/failures are evident from the presence of open cracks. It appears that rock blocks have been breaking up and delivering blocky debris to the main rockslide body.

Retrogressive zone

Above the crown (>1830 masl.) the slope gradient decreases to <10° and is represented by an almost flat-topped ridge heavily mantled with blocky scree, with patches of exposed fractured bedrock. Fractures vary in aperture from tight to the largest open fracture being over 3 m wide to a depth of at least 7 m. Fracture length varies from several metres long to some fractures that extend for over 100 m along the ridgeline. Several large tension cracks (without evidence of vertical displacement) are present. These vary in width from 0.2 m wide to 3m and extend for over 20 m. Smaller tension cracks measured 0.02 to 0.2 m wide and up to 10 m long. While most fractures have no evidence of shearing, some have evidence of vertical displacement represented by low scarps (Fig. 3.4). This vertical displacement varies from 0.5 m to 2 m, extending for tens to hundreds of meters with down-throw towards the SW and SSW. They are often subtly visible in the field where mantled by debris but are more readily recognised and traceable in the DEM hillshade and aerial photography. Where the scarp travels through bedrock, extensive dilated fracturing occurs with some fractures exceeding 2 m in aperture. The scarps are at a similar orientation to the major scarps making up the headscarp zone below the rockslide crown; for example, the southern-most scarp trends northwest and dips southwest through the northern face of Mount Ollivier before intersecting the headscarp zone (Fig. 3.4). To the north, two scarps at similar orientation to the southern-most scarp are located on each side of Mueller Hut and converge 100 m north-west of the hut. Both have subtle surface expression but at their point of intersection there is an area of intense fracturing approximately 30 m long, 1-3 m wide and 1-3 m deep before becoming scree filled.

3.4.2 Rock mass characterisation

The greywacke sandstone is typically weathered orange (lightly weathered, NZGS 2005) with fresh surfaces light grey. Jointing is obvious and quartz veins often fill many open joints with some being over 10 cm wide. Geological Strength Index (GSI) was used to describe the sandstone rock mass quality at the surface as very blocky which represents a GSI range between 50 and 60. The rock is indurated and takes several hard hammer or sledge hammer blows to break. Minor seepage could be seen within the main headscarp zone. Siltstone and argillite bedding within the study area is often dark grey, laminated and highly fractured with small very angular blocks. The argillite rock mass is intensely jointed with fair surface condition and can be broken by hand with effort. The argillite rock mass is considered as blocky, disturbed and seamy which corresponds to a GSI of between 30 and 40.

3.4.3 Discontinuity analysis

Stereographic projections of discontinuity orientations are presented as well as kinematic analysis for planar sliding, wedge and flexural toppling (Fig. 3.5). Discontinuities are grouped into two structural domains 1) ridgetop / retrogressive zone (Fig. 3.5) and 2) headscarp and rockslide body zones (Fig. 3.6) with several discontinuity sets identified within each domain. Identified discontinuities are divided into bedding, joints and faults.

Seven discontinuity sets are identified within the retrogressive zone (Fig. 3.5a). R1 is a strongly defined bedding set dipping north with an average dip of 30°. R2 is a near vertical joint set trending north-south and dipping predominantly to the west from 80°–90° although several joints dip steeply to the east. R3 is a minor joint set dipping steeply north at 85°. R4 is a minor joint set striking east-west and dipping at approximately 50° to the south. R5 strikes northwest and dips steeply to the southwest at 75°–90°. R6 strikes north-south, similar to R2 but with a shallower dip of 60°-70° to the west. R7 strike northwest like R5 but dips east at 70°-80°.

Discontinuities mapped within the rockslide body and headscarp differ from those identified along the ridgeline (Fig. 3.6a). In total 5 discontinuity sets are identified. L1 is a predominantly defined by bedding, dipping to the west from 30°-70° with an average dip of 50°. L2 is a minor joint set again strongly defined by bedding although this set dips to the north-west at approximately 45°. L3 strikes northwest and dips to the south-west at 80°. L4 is an east-west trending joint set, like R2 in orientation with joints dipping to the west with an average dip of 80° to 85°. L5 is a minor joint set dipping to the south-east at approximately 80°.

Kinematic analysis was conducted for both domains, to explore potential differences in kinematics between the upper and lower part of the slope. We assessed the potential for planar, wedge, and toppling failure under the following scenario: an empirically-derived friction angle of 33° for the mudstone, and a slope dip and dip direction of 40/270. The direction (of 270°) is along the steepest path of the slope and is slightly oblique to the dip direction (~285°) of most bedding measurements. Using an average slope angle of 31° (which is below the friction angle of 33°) does not result in kinematic

feasibility by planar failure. However, slope angles of up to 39° were measured at the toe, and we evaluate the kinematic feasibility at a slope angle of 40° to provide a conservative estimate that allows some freedom for a potentially lower friction angle.

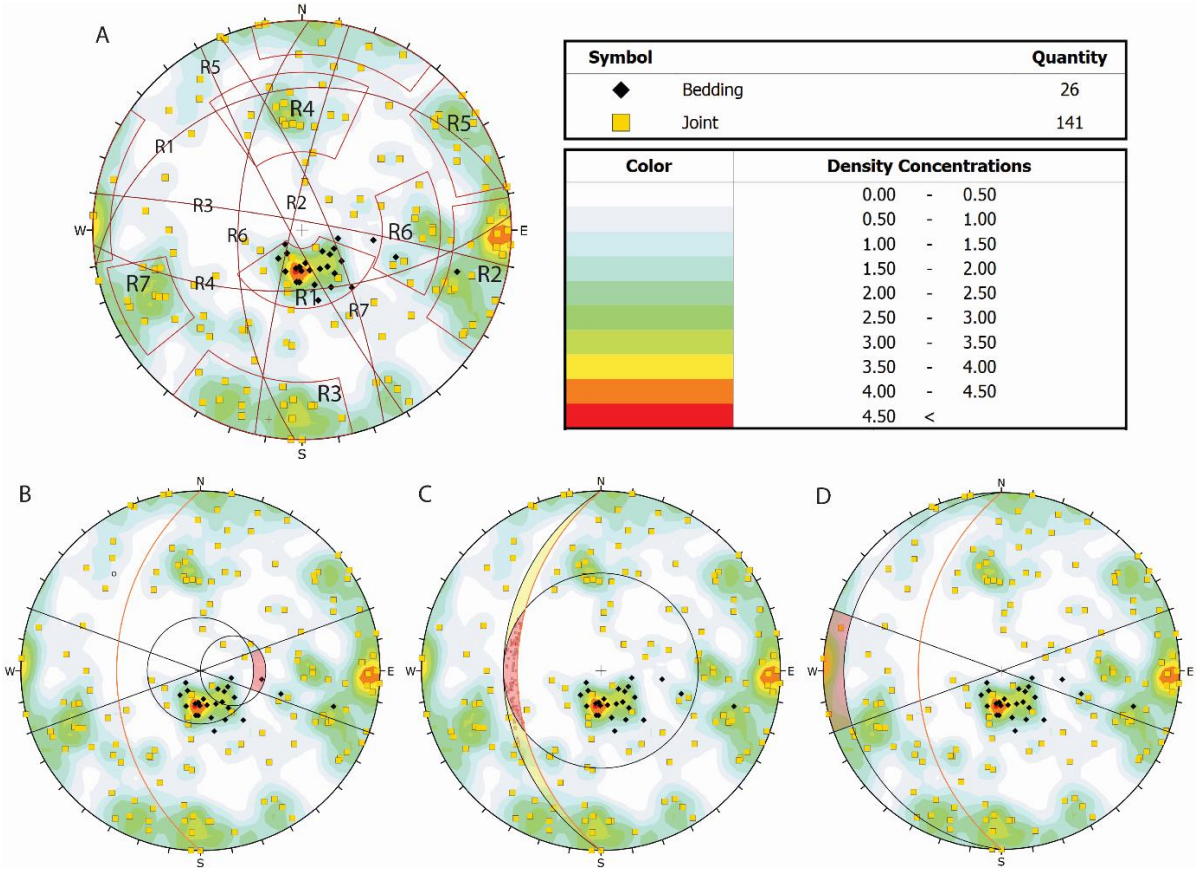

Figure 3-5. A) Joint sets (R1-R7) and corresponding planes for discontinuities within the retrogressive development zone of the rockslide. Kinematic analysis was completed for planar sliding, wedge and flexural toppling respectively (B, C, D).

For the retrogressive zone (Domain 1), the kinematic analysis shows that potential for planar failure is minor (Fig. 3.5b) with only one bedding point (3.8% of total bedding measurements) falling within the failure envelope. Wedge failure analysis shows the potential for failure along the intersection of R3-R6 and R4-R6 joint sets (Fig. 3.5c), however, the failure envelope falls just outside the definitive intersection of these joint sets. Flexural toppling analysis shows potential toppling along the R4 eastward dipping discontinuities (Fig. 3.5d).

For Domain 2, the kinematic analysis showed marginal potential for planar sliding although no discontinuities fall in the failure window; several L1 discontinuities are at the margin or just outside of the failure window. Wedge failure analysis shows potential for L1-L3 and L1-L5 intersections within or just outside the failure envelope (Fig. 3.6c) (2.2% within failure window). Flexural toppling analysis shows L4 discontinuities falling within the failure envelope when the slope angle is 40° (Fig. 3.6d) (1.3% total discontinuities and 16.7% of L4 discontinuities).

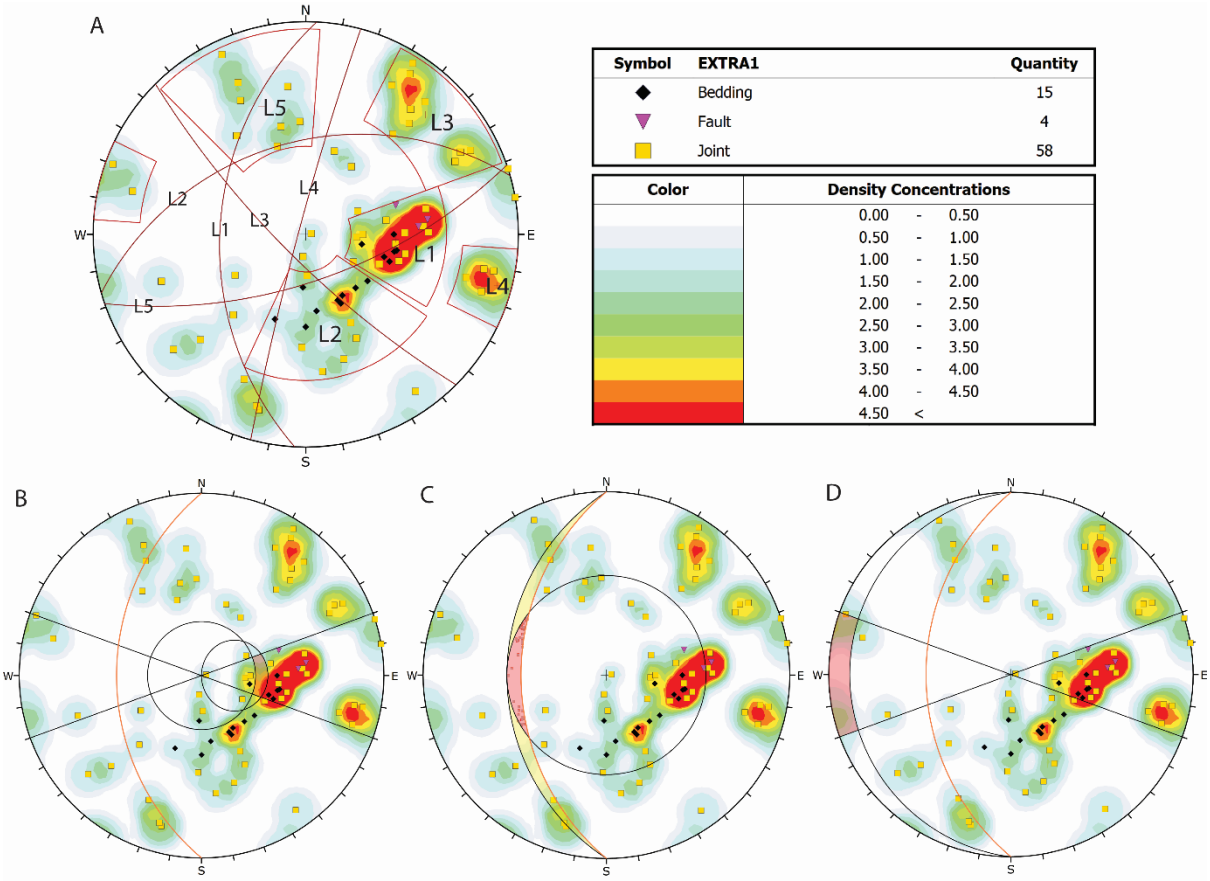

Figure 3-6. A) Joint sets (L1-L5) and corresponding planes for discontinuities within the landslide and headscarp zone of the Mueller Rockslide. B-D) Planar, wedge and flexural toppling kinematic analysis respectively.

3.4.4 Subsurface data: SRT and GPR

Mueller Hut Transect (T1)

The Mueller Hut transect (T1) extends from 100 m east of Mueller Hut in the upper ridge to the rockslide crown for a total length of 500 m (Fig. 3.4). There are three distinct velocity layers recognizable along the seismic transect (Fig 3.7.). The near-surface p-wave velocity layer (0.5-0.95 km s^{-1}) is predominantly located within the first 100 m of the transect to a depth of 5 to 7 m below ground level and from 140 m to 380 m to a depth of 3-5 m. A second, faster, velocity band (0.95 to 1.7 km s^{-1}) is observed predominantly from 140 to 380 m, through localized areas of bedrock outcrop and in the final 150 m of the transect towards the rockslide crown. The third and fastest velocity band (>1.7 km s^{-1}) is found between 400 and 480 m along the transect.

Fracture density results show high values in the first 100 m of the transect as well as between 140 and 280 m, coinciding with the low p-wave velocities outlined above and areas of blocky debris seen on the surface. Fracture density decreases rapidly with depth under areas of scree and in areas of bedrock from 30-50% in scree zones to 10-30% in bedrock and the underlying rock mass. The last 150 m of the transect shows lower fracture densities particularly in relation to the debris-mantled ridgeline.

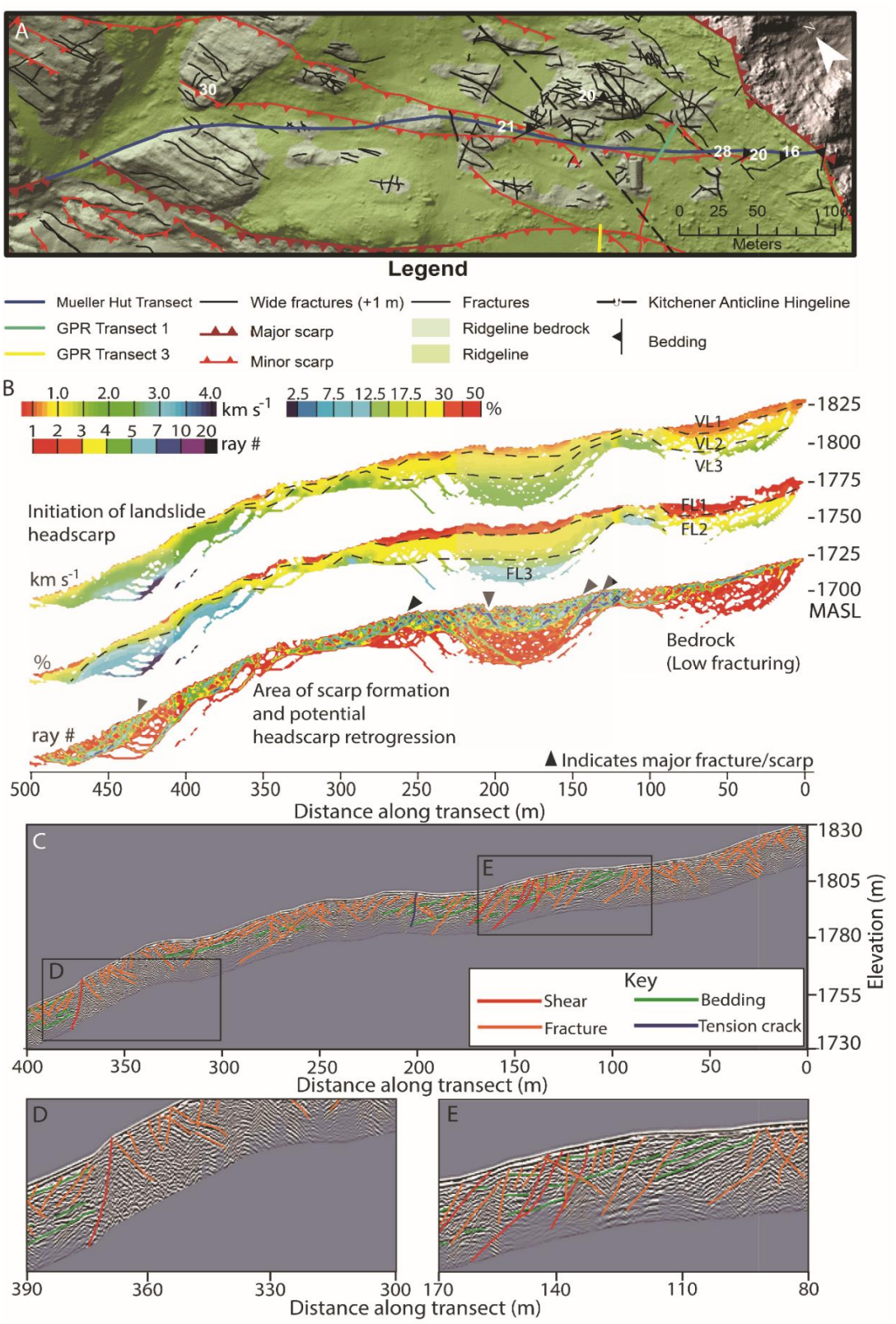

Figure 3-7. Mueller Hut seismic transect (T1). A) Geomorphic map of the transect. B) SRT transect consisting of P-wave velocity, fracture percentage and ray density. High ray density indicates clustering of linear features (black arrows) indicating potential scarp or fracture development. C) GPR transect for 0-400 m. D) Beginning of the block toppling and headscarp zone. E) GPR directly adjacent to Mueller Hut (105 m).

Ray density analysis shows the percentage of rays per 1.5 x 1.5 m grid spacing with high ray density indicating the presence of linear features or discontinuities. In the first 100 m, of the transect, ray density appears to be related to scree, and suggests an absence of large, persistent fractures within the bedrock. Farther down the transect, high ray densities are detected from 140 to 280 m with increased ray density at the surface and moderate density at depth to ~30 m indicating the presence of large, persistent structures (black arrows in Fig. 3.7b). High ray density also indicates a large persistent fracture at 430 m is also indicated by high ray density.

The corresponding GPR profile for Transect 1 is 400 m long, near the rockslide crown. Evidence of bright reflectors which coincide with areas of bedrock at 100-200 m are interpreted as bedding planes. Reflectors with a similar signature can be seen at depth at 175 m along transect and at 380 m (Fig. 3.7c, d). The first 210 m of the transect which bypasses Mueller Hut also shows extensive orthogonal fracturing with apparent dips to the east and west. A highly fractured zone from 140 m to 210 m along the transect is marked by significant fractures which extend for ~8 m through the GPR profile. A scarp identified in the geomorphic mapping and in the field at 140 m is hard to identify within the GPR transect due to both being oriented in a north-west direction however there is evidence of shear planes and displaced bedding around 140 m. From 210 m to 310 m, fractures appear to dip predominantly westward as the transect moves towards the crown of the Mueller Rockslide. A highly fractured zone can be seen between 220 m and 245 m (Fig. 3.7c) which coincides with where the two minor scarps either side of Mueller Hut intersect and with several large fractures identified on the geomorphic map. Bright linear reflectors identified between 290 m and 320 m are interpreted as bedding. From 310 m, fractures have an apparent dip to the east, coinciding with the transition to block toppling as the transect nears the headscarp.

Mount Ollivier Transect (T2)

The Mount Ollivier transect (T2), located south of Mueller Hut, is 200 m long extending from below Mount Ollivier to the rockslide headscarp (Fig.3.4). Two p-wave velocity layers have been identified within the Mount Ollivier Transect (Fig. 3.8). The first (0.5 to 0.95 km s^{-1}) is located mainly in the top 10 m through the entire transect extending to 15 m depth from 120-160 m (Fig. 3.8b). The second, and faster, velocity band (0.95 to 1.7 km s^{-1}) is found from 40 to 160 m. A third velocity layer (>1.7 kms-¹) can be seen in isolation from 25 to 40 m. Fracture density analysis shows the majority of the top 7 m of the transect shows fracture densities greater than 40% with this decreasing to 15-30% underneath the upper scree areas. At 30 m low fracture densities of less than 10% are seen, corresponding with mapped bedrock along the surface of the transect. Ray density analysis shows an area with extensive and persistent fractures at 110 to 190 m (black triangle, Fig.3.8b).

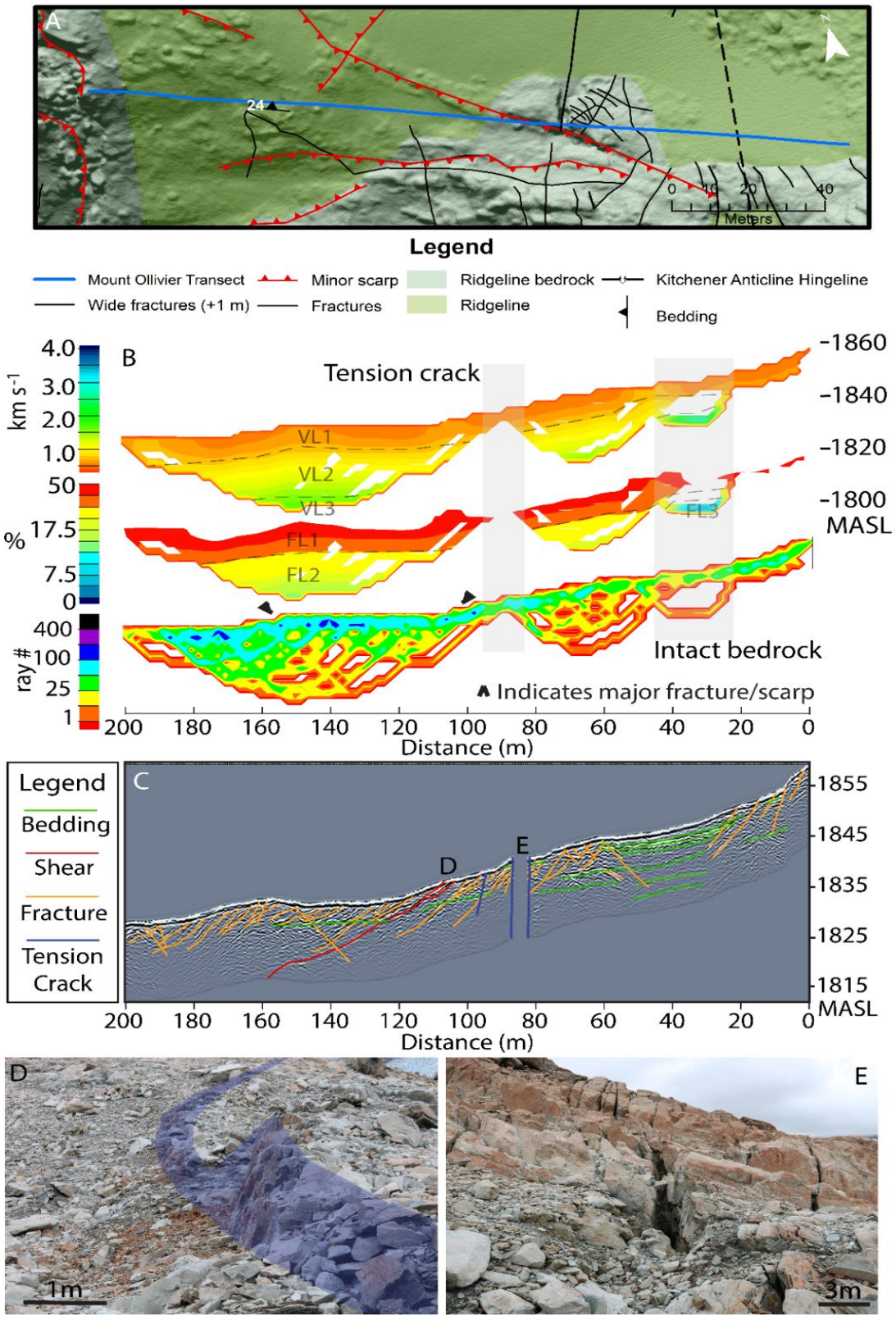

Figure 3-8. SRT and GPR for the Mount Ollivier Transect. A) Geomorphic map of the Mount Ollivier transect. B) SRT showing in order P-Wave velocity, fracture percentage and ray density. C) GPR with identified bedding, fractures, shear planes and tension cracks. D)Scarp associated with the mapped shear surface within the transect dipping to the southwest (left in the image). E) Large dilated tension crack within the transect.

The Mount Ollivier GPR transect shows an apparent dip to the west of several strong reflectors (Fig. 3.8c). At 55 m and 150 m are east-dipping reflectors which extend for over 10 m depth in the GPR profile. A similar albeit small feature is identified at the end of the transect between 160 and 180 m within 20 m of the previously identified rockslide headscarp. Four strong sub-horizontal reflectors are identified in the eastern most extensive feature from 22 m to 55 m, interpreted as (argillite) bedding, consistent with outcrop observations; similar but more steeply dipping reflectors are identified between 120 and 160 m. A large tension crack (Fig. 3.8c, e) extends throughout the transect as well as extending for a total of 40 m to the north (Fig. 3.8a). An extensive shear plane can be seen from 110 m which extends throughout the GPR transect and is represented at the surface by a continuous 1-2 m southwest dipping scarp (Fig. 8c, 8d).

Old Hut Transect (T3)

The Old Hut transect (T3) is located to the north of Mueller Hut extending for 200 m from the eastern headscarp through the ridgeline (Fig. 3.9). P-wave velocity analysis has identified 3 dominant velocity bands. The first, and slowest, velocity band (0.5 to 0.95 kms^{-1}) is found through the upper 1-4 m depth of the majority of the transect particularly in areas mapped as debris or scree. The second band (0.95 to 1.7 kms^{-1}) is at 30 m from 0 to 12 m deep, at 70 m from 2 to 15 m deep and 160 m distance from 5 to 17 m deep (Fig. 9b). The third and fastest p-wave velocity band (>1.7 kms^{-1}) can be found from 0 to 10 m, 40 to 60 m and 80 to 150 m.

Fracture density patterns show fracture zones at 30, 70 and 160 m distance display very high fracture densities of greater than 30% with the fracture zone at 70 m exceeding 50% fracture density (Fig. 3.9b). This fracture zone is characterized by fracture widths at the surface of greater than 0.5 m. At 150 m, both methodologies identified a large fracture zone which also corresponds to high ray densities that the existence of persistent fractures.

GPR results again have highlighted an extensive network of fracturing. Due to the blocky surface in this area and lack of outcrop, identified fractures are mainly isolated to the first 100 m of the transect near the main eastern scarp, and to an isolated but highly fractured bedrock zone from 130 to 170 m (Fig. 3.9e). The most extensive zone of fracturing is located from 25 m to 70 m marked by several crossed eastward and westward dipping fractures and one major failure zone (Fig. 3.9e; red lines) which extends through the GPR profile, marking the headscarp of the eastern rift/graben. Although graben is block filled, vertical displacement of ~5 m is estimated from the GPR profile, consistent with the height of the graben scarp. Minor fracturing from 90 to 130 m in the GPR profile is hidden in the field, the area covered with blocky debris. Strong gently-west-dipping, reflectors through this zone are interpreted as bedding which extends from 85 m to 135 m along the transect.

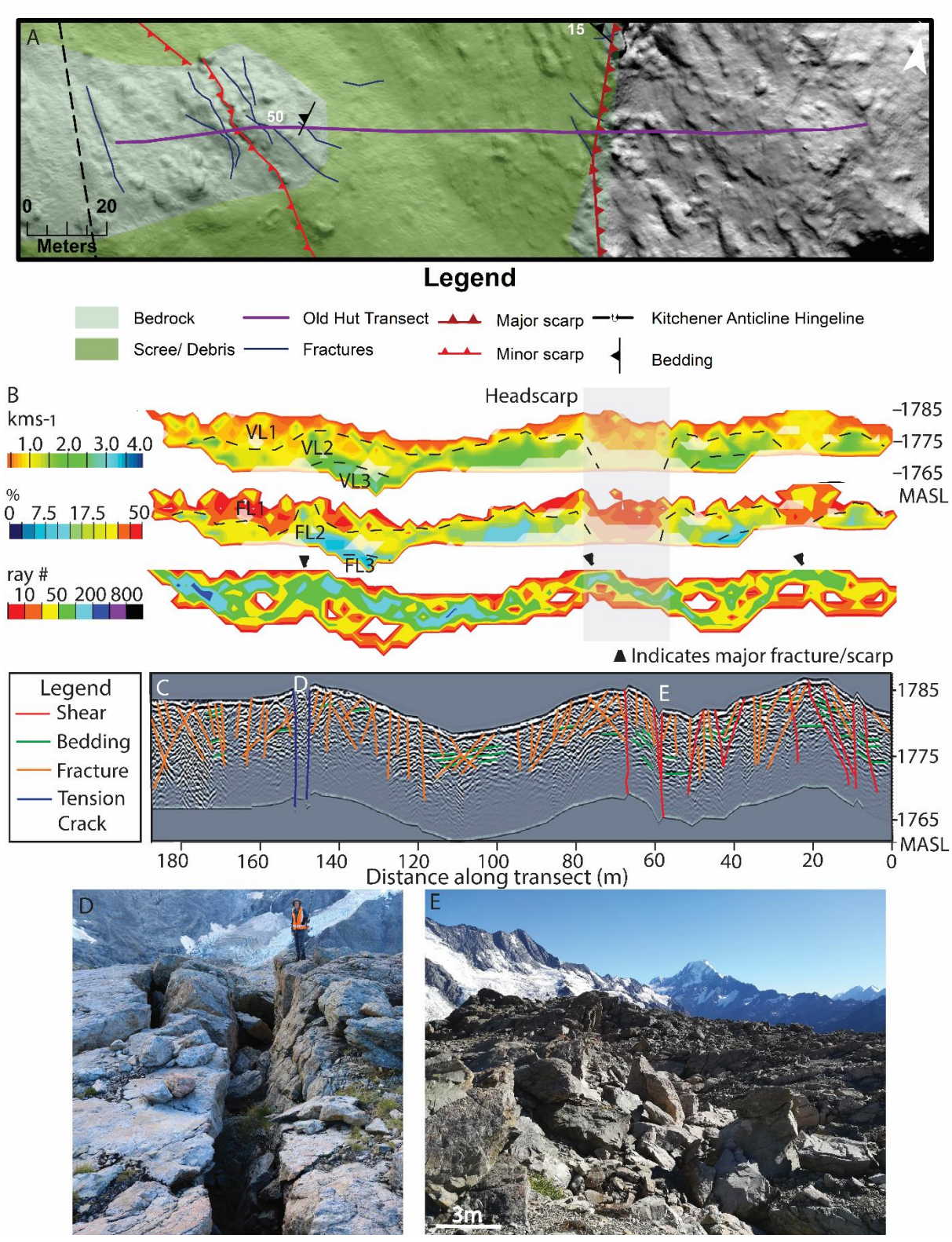

Figure 3-9. Old Hut seismic transect. A) Geomorphic map of the transect and surrounding area. B) SRT showing P-wave velocity, fracture percentage and ray density. C) GPR. D) Large tension crack 150 m along the transect. E) Headscarp for the eastern slope failure which is partly obscured by block fill.

Bedrock outcrop from 130 m to 170 m largely consists of minor superficial fracturing with fractures appearing to only extend for several meters. However, from 155 m to 165 m there two very large parallel vertical dislocations extending through the radargram and marked at the surface by two

large (~30 m long and 0.5 m to 3 m wide) open fractures with a bedrock wedge in between. The wedge sits 2 m lower than the surrounding bedrock and the surfaces corresponding to the dislocations extend for at least 10 m deep in the radargram. There is no obvious vertical displacement between each side of the wedge (i.e. no scarp).

Additional GPR Transects

Radargrams from the three additional GPR transects, in proximity to Mueller Hut, are presented in Fig. 3.10. Transect 1 reveals the scarp identified at the surface is associated with two near vertical shear surfaces that extend through depth of the transect (Fig. 3.10a). Several near vertical fractures can be identified within the graben between the two shears while fractures outside the graben appear to have a shallower dip.

Transect 2 crosses a large north-south trending scarp as well as the large tension crack identified in the Mount Ollivier seismic transect. The tension crack appears to split into at least two large fractures at depth (Fig. 3.10b). Distinct bedding can be seen dipping to the right (west) before being displaced by an obvious shear surface which corresponds with the scarp at 45 m.

Transect 3 shows mapped scarps in the area south of Mueller Hut correspond with shear surfaces at depth. In total, 4 scarps were identified with all scarps corresponding with shear surfaces at. An additional 3 shear surfaces were identified which do not correspond to scarps at the surface (Fig. 3.10c). Determining the depth of these shear surfaces was difficult due to the poor quality of the GPR in the final 50 m of the transect however all extend to at least 10 m depth.

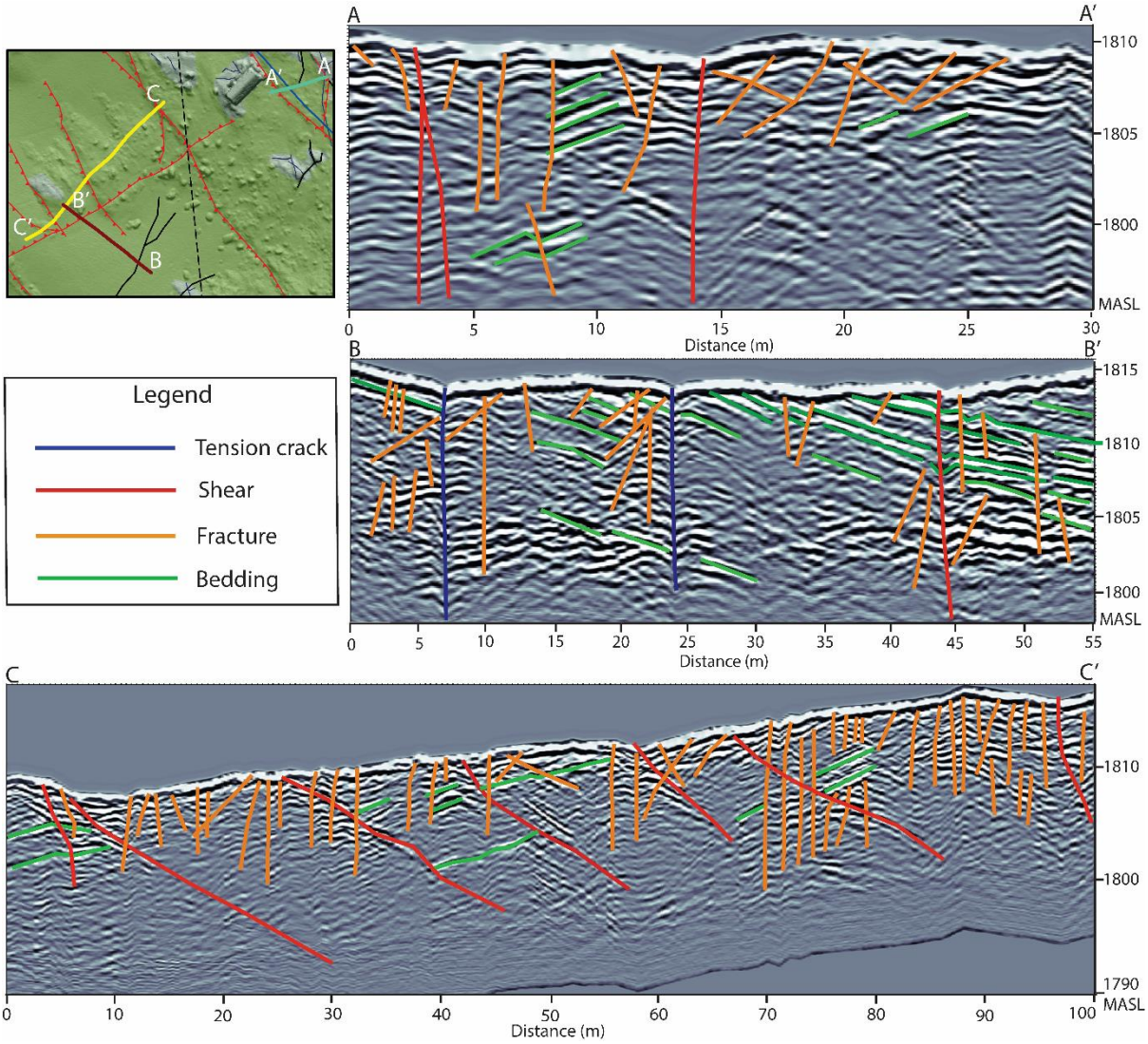

Figure 3-10. GPR transects from the Mueller Hut area. A-A') Transect 1 going NE-SW approximately 20 m from Mueller Hut. The two shear features identified in the left of the image mark the eastern most scarps for the rockslide retrogressive zone. B-B') Transect 2 going NW-SE through the northern limit of a large tension crack. C-C') Transect 3 going NE-SW through several large shear fractures directly south of Mueller Hut.

3.4.5 Slope stability modelling

The calculated critical SRF for the isotropic model was greater than the one obtained for the anisotropic model. More importantly, the displacement pattern at the critical SRF model is on the east side of Mueller Ridge for the isotropic model whereas it shifts to the western (i.e. Mueller Rockslide) side when the bedding anisotropy is considered (Fig. 3.11). This numerical modelling assessment provides simple but useful support for the idea that the Mueller Rockslide is structurally influenced by the bedding. However, neither model produced a SRF approaching a critical value of 1, suggesting that the rock strength parameters used or the bedding orientation were inappropriate (i.e. too strong), or groundwater or other processes not included are important for bringing the slope to a critically-stable

state. Additional models considering a wider range of strength parameters, the influence of more subtle structural weaknesses (e.g. discontinuity sets) and potential triggers should be considered.

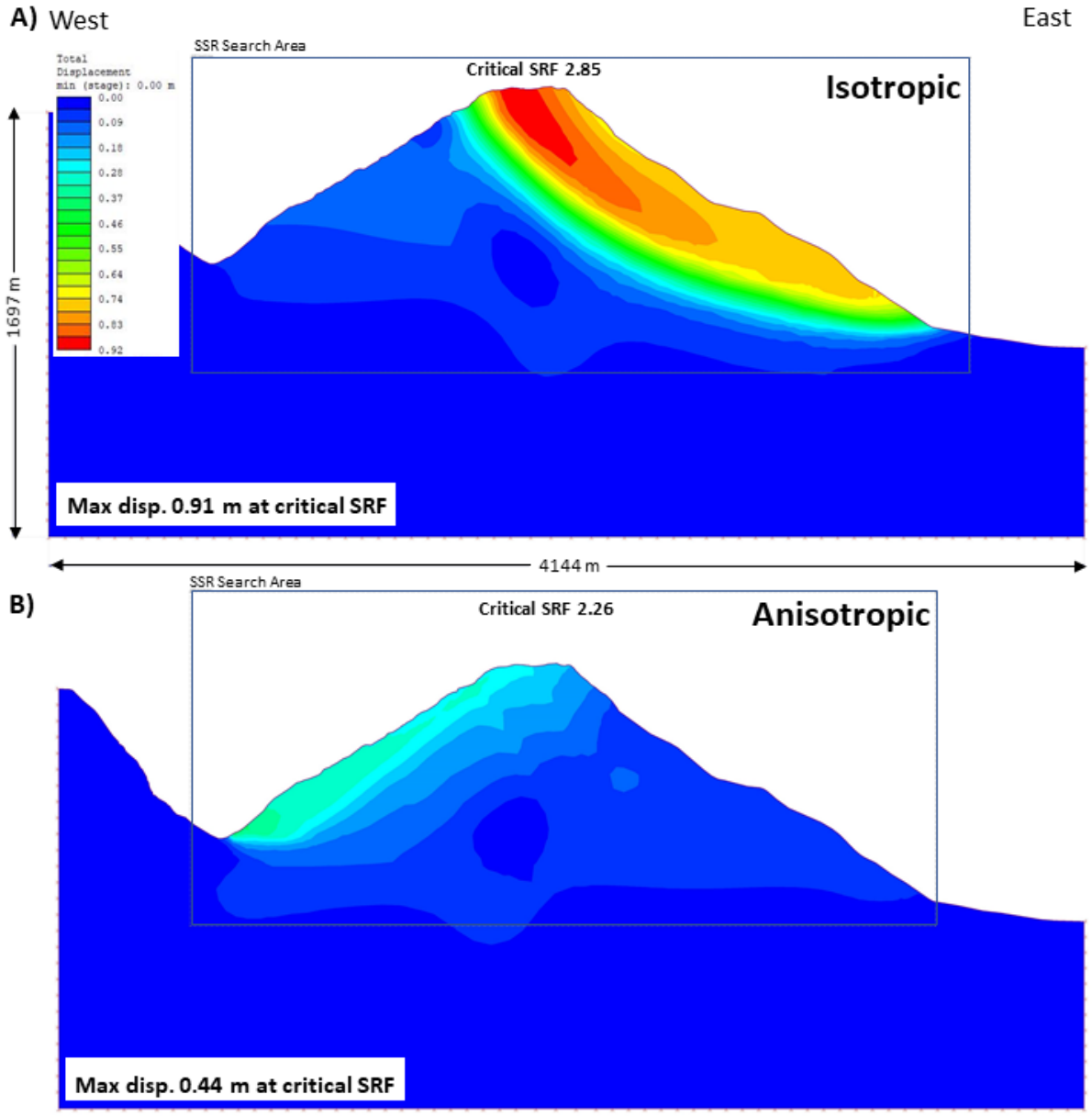

Figure 3-11. Total displacement magnitude across Mueller Ridge at the critical strength reduction factor for an A) isotropic and B) anisotropic models. Location of the cross-section is equivalent to the one shown in Figure 3.2.

3.5 Discussion

3.5.1 Comparisons between SRT, GPR and geomorphic mapping

Geophysical surveys including SRT and GPR, have become common place in recent decades for quantifying rock mass qualities and discontinuities of rock slope failures (Heincke et al., 2010, Meric et al., 2005). SRT and GPR have been previously combined in rock cavity identification or in the study of smaller fracture zones (De Giorgi and Leucci, 2014, Heincke et al., 2006). Herein, we further demonstrate the utility of these two techniques for confirming the presence and subsurface continuity

of deformation indicated at the surface by scarps, and for supporting geotechnical mapping of fractures into the subsurface, especially where bedrock is obscured by debris. In addition, we show how SRT can be used to reveal changes in fracture density at depth, as well as revealing the thickness of surficial materials overlying bedrock.

This study has shown a strong relationship between areas of increased fracturing (high fracture percentage) in the SRT with fractures identified within the GPR. Areas of low P-wave velocity (<2.0 kms-1) and high fracture percentage (>30%) often found in areas with numerous fractures. Several shear surfaces were distinguishable within the SRT in the Old Hut and Mueller Hut transects, consistent with field mapping (scarp identification) and GPR. For the Mueller Hut transect, ray density analysis showed this particularly well as the transect passed through a more intact bedrock zone, allowing for the differentiation between intact and highly fractured bedrock.

Inclusion of the GPR also allowed for the identification of bedding planes which were not readily apparent from the SRT data; this information was useful for identifying shear surfaces at depth and linking them to mapped scarps at the surface. While the GPR was also useful for detecting discontinuities, GPR is not effective at imaging features parallel to the radar transect (i.e. vertical features along the transect). We believe tension cracks and other vertical discontinuities within the GPR data are underrepresented. Combining the two methods (SRT and GPR) helps to minimise some of the shortcomings of the individual techniques and provided richer results. This enabled a more comprehensive assessment of all structural features throughout the surveyed area and the methods complimented each other to provide a view of broader rock mass quality and the relationship to bedding, fractures and shear planes. Overall, the three techniques (GPR, SRT and field mapping) were consistent and complimented each other and here they have confirmed the presence of major open fractures, and vertical deformation along features consistent at the top of the rock slope. The kinematic analysis suggests that planar failure along bedding is unlikely here, and instead the geophysics indicates that this deformation is being accommodated by sub-vertical joints, likely the same ones controlling morphology of the headscarp fractures. This suggests that the rock mass of the upper part of the rock slope is facilitating retrogressive enlargement of the rockslide.

Access and safety made it unfeasible to extend the geophysical surveys across the entire rockslide, and the depth of penetration by SRT was limited by use of mechanical means of seismic signal generation (i.e. sledge hammer). Nonetheless, this study demonstrates the utility of these techniques not only on rock slopes, but in any area in which shallow subsurface mapping of fractures and superficial features is required. The technique is relatively economical and accessible should the gear be available and even short transects (<100 m) have produced favourable results for identifying fractures within the top 10 to 15 m of the surface.

3.5.2 Structural controls on rockslide morphology

Geomorphic mapping, SRT and GPR have identified an extensive fracture network at the Sealy Range. The discontinuity sets in Figures 3.5 and 3.6 are equivalent with fractures commonly associated with folding (Price and Cosgrove, 1990). Specifically, discontinuity sets closely align with fractures oriented parallel, perpendicular and orthogonal to an anticline (Fig. 3.12).

Excluding bedding, discontinuity sets identified along the ridgeline align parallel (R2, R6) and perpendicular (R3, R4) to the main anticline hingeline (Fig. 3.5; Fig. 3.12) and are classed as extensional joint sets. R5 and R7 are orthogonal fractures in the retrogressive zone and are classified as shear fractures. Discontinuity sets within the landslide zone are predominantly orthogonal to the main hingeline and dip to the northwest (L2), southeast (L5) and southwest (L3) and are interpreted as shear fractures.

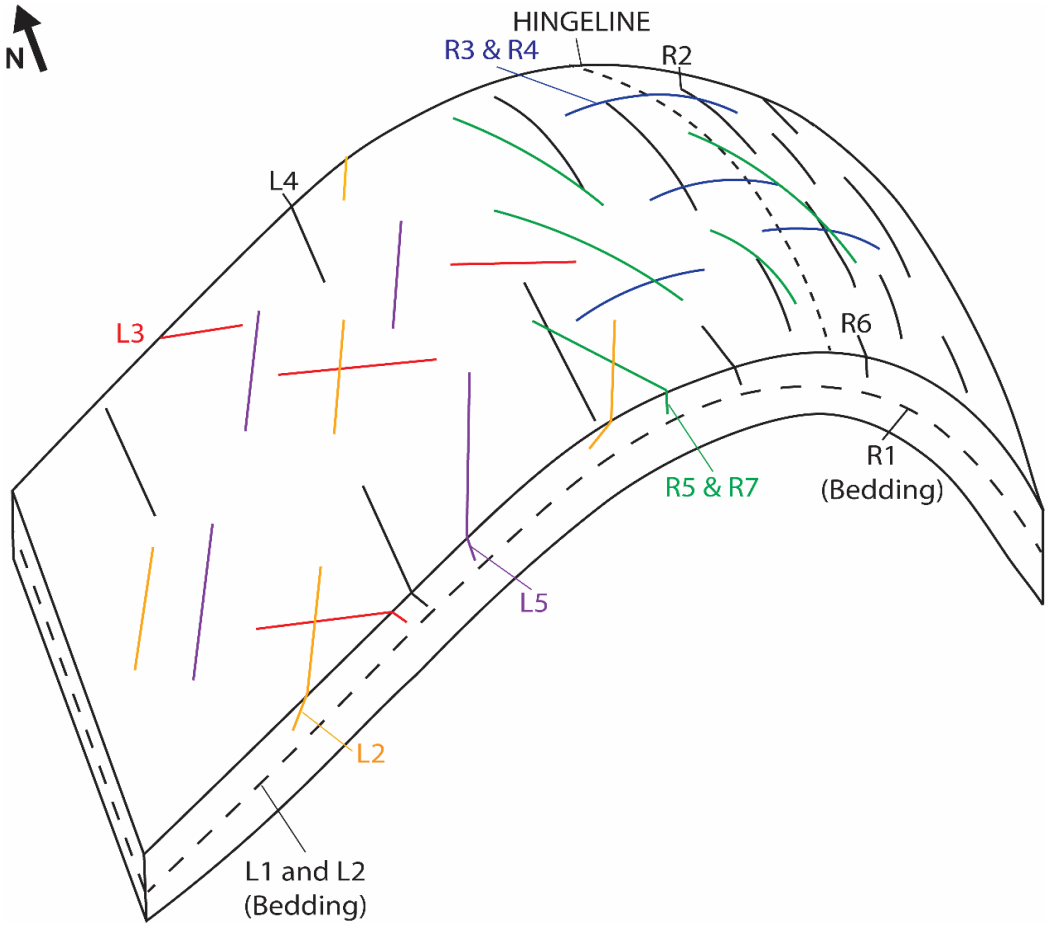

Figure 3-12. Primary discontinuity sets seen within the Sealy Range and northward plunging Kitchener Anticline. Adapted from Price and Cosgrove (1990).

Preconditioning and morphology of the Mueller Rockslide has been strongly controlled by its location on the dip slope of the Kitchener Anticline. In fact, without structural controls and anisotropy, failure of the hillslope would only occur to the east as indicated by modelling (Fig. 3.11). Headscarp morphology has strongly aligned with the L3 and L4 fractures (Fig. 3.12) in a northwest – southeast

direction with steeply dipping fractures causing block toppling in this area. These joint sets also align with the newly mapped scarps developing along the ridgeline (R5 and R7; Fig. 3.12) which appear to be facilitating downslope movement of the upper ridge. They appear to act as rear-release structures, similar to what has been previously observed by Brideau et al. (2009) at the Hope slide in British Columbia and the Randa Rockslide in Switzerland. Continued block toppling and rockslide movement has steepened this headscarp zone, allowing for the potential for daylighting of several joint sets and the increased potential for wedge failure and block toppling as indicated in the kinematic analysis (Fig. 3.6). The north – south oriented R2 and R6 joint sets may also be acting as a minor rear-release mechanism, resulting in the formation of large tension cracks above the headscarp. Lateral release structures are also essential for allowing the rockslide to develop (Brideau et al., 2009). Several east-west oriented releasing scarps were identified (R3 and R4; Fig. 3.12) particularly to the north-west of Mueller Hut and to the south-west of Mueller Hut above the arcuate headscarp (Fig. 3.4). The importance of these rear and lateral release structures is highlighted by Brideau et al. (2012) who demonstrate that persistence of these release surfaces along with their orientation relative to the slope dip direction are essential for controlling rockslide failure initiation as well as rockslide morphology.

The inability to investigate the deep subsurface of the rockslide body has meant that little is directly known about the rockslide failure surface. Instead we make assumptions on the failure surface based on scarp and shear surface morphology resolved from the ridgeline seismic transects, observations of rock type and rock mass quality, and discontinuity mapping. The failure surface is assumed to be along bedding (weak argillite layers), consistent with GPS survey data shows that movement in a down-dip direction (285°) rather than a downslope direction (270°) in the central rockslide (McColl et al., 2012) and supported by the stability modelling (Fig. 3.11). However, kinematic analysis indicates simple planar failure marginal or oblique to the slope direction as only one bedding measurement fell inside the failure window (Fig. 3.6, 3.7), consistent with the observation that measured dip of bedding is steeper than the slope of the rockslide. While this makes daylighting of a failure surface along bedding unlikely, there is very little known of the orientation and condition of bedding at the toe of the slope. It is feasible for bedding to fold back into a different structure (e.g. syncline) at the toe and we observe bedrock on the opposite side of the valley appears lithologically and structurally different. Consequently, bedding may curve into the slope face at the toe of Mueller Rockslide, facilitating kinematic release and sliding along bedding into the valley (Fig. 3.13a). Alternatively, movement may be accommodated at the toe by ductile deformation (buckling; Fig. 3.13b) or release along one or more fractures (Fig. 3.13c).

While toe buckling by ductile processes occurs in the Southern Alps within the highly anisotropic schist, this process is less likely to occur in the high strength brittle greywacke. Finite element modelling with the assumed bedding orientation suggests a low failure potential with a high SRF of 2.26 for the western rock slope with displacement of only 0.44 m at that SRF. We therefore suggest that if bedding orientation does not permit kinematic admissibility, breakout along fractures

that step across bedding is a more likely scenario as a step path failure mechanism (Camones et al., 2013). We observe fractures stepping and shearing across bedding at the top of the slope. GPR and SRT (Mueller Hut transect) show shearing across bedding, facilitated by the joint sets in the retrogressive zone, and at the top of the headscarp where the identified scarp dips near vertically through bedding. Stepping across bedding may in fact be a characteristic feature of the whole failure surface, creating a stepped failure surface connecting planes of weakness (i.e. bedding). Stepped sliding planes have been identified in other large rock slope failures (Oppikofer et al., 2011, Sturzenegger and Stead, 2012, Tannant et al., 2017). Ultimately, failure of the rock slope may be accommodated by acombination of geological structure (bedding) and rock mass conditions (joints), both of which are influenced by the Kitchener Anticline.

While the Mueller Rockslide has previously been described as a DSGSD (McColl and Davies, 2013), observations from field work and geophysical surveys indicate the slope failure does not display many of the normal attributes seen in DSGSDs. Only a single uphill facing scarp (on the landslide body) was identified, which are normally typical of DSGSDs. Instead, we see a discontinuous but clear set of normal scarps defining the crown. While a bedding failure surface has not been confirmed, movement direction down-dip indicates failure along bedding is feasible. Therefore, it is proposed that the Mueller Rockslide can be better described as a rock compound slide. As defined by Hungr et al. (2014) rock compound slides are those which form along several planes or a disconnected sliding surface and must undergo some internal deformation to allow movement. Continued internal deformation and progressive weakening of the rock mass may eventually lead to rapid failure.

3.5.3 Rockslide development towards rapid failure

Slow moving rock slope instabilities can transition to rapid and catastrophic failures (Kilburn and Petley, 2003, Geertsema et al., 2006, Pánek et al., 2011). While assessing the temporal evolution of the Mueller Rockslide has not been the focus of this chapter, the data collected here can allow a qualitative assessment of whether the Mueller Rockslide could accelerate and fail rapidly, either overtime as a progressive failure or through an external trigger like strong earthquake shaking.

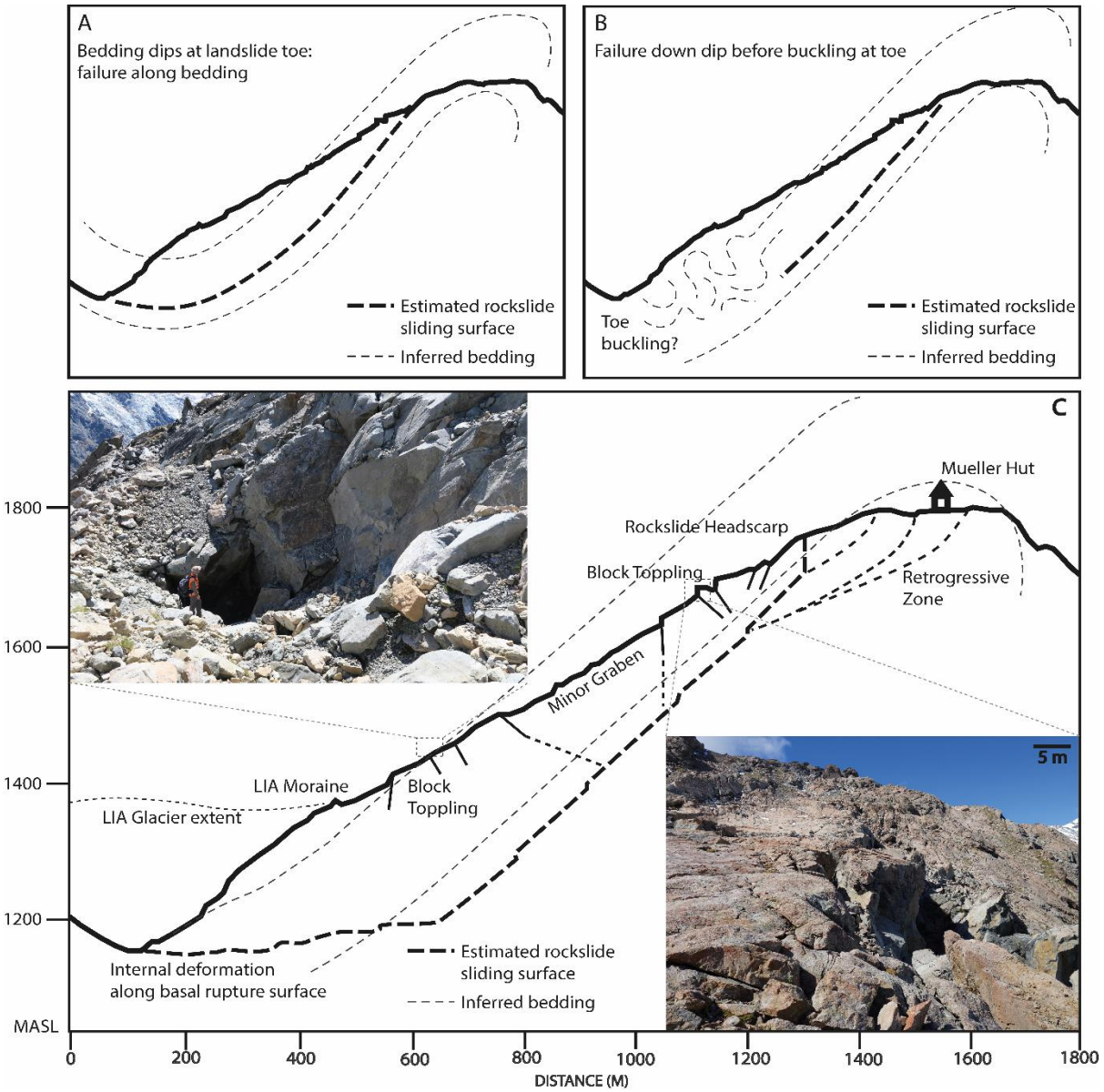

Figure 3-13. Cross section and theoretical of Mueller Rockslide development. A) Sliding failure along downdip bedding. B) Failure occurring due to internal deformation. C) Stepped failure along downdip bedding with internal deformation at toe.

The evolution of large rockslides towards rapid failure is an important avenue of landslide hazard research (Hungr, 2007). Several studies (Crosta and Agliardi, 2003, Eberhardt et al., 2004, Glastonbury and Fell, 2008a, Glastonbury and Fell, 2010) have attempted to identify key structural and geomechanical properties commonly found in rockslides which transition to catastrophic failure and found several common factors, which can indicate potential for catastrophic failure. Common characteristics include a high strength rock mass that facilitates failure en-masse rather than through smaller slope failures from highly disaggregated rock masses, loss of toe buttressing support, and strongly defined lateral margins (particularly important for deep rockslides) which lie normal to anisotropy (Glastonbury and Fell, 2008b, Glastonbury and Fell, 2010). As well, first time failure as opposed to those experiencing reactivation are more likely to progress to rapid failure. In contrast, slow

moving landslides, which do not progress to rapid failure more often occur in weak, disaggregated rock masses and in slopes where the basal rupture surface angle is less than the residual friction angle (Glastonbury and Fell, 2008a).

Our observations show that the Mueller Rockslide has some characteristics in favour of catastrophic failure and others against. GSI values from rock mass characterisation of 50-60 for sandstone and 30-40 for argillite are low to fair, possibly suggesting disintegration rather than failure en-masse, however rock mass strength at depth is likely higher which may facilitate failure en-masse. However, while the rockslide is clearly fractured, it occupies the entire slope from toe to ridge crest and extends for about 1 km along the ridge, further suggesting it is failing as a large mass. The slope has clearly been debuttressed, as a result of thinning of the Mueller Glacier, but has likely undergone erosion by the glacier too, explaining the steepened section of hillslope below the break in slope of the LIA moraine limit (Fig. 3.13). Lateral restraints are identified within the kinematic analysis (R3 and R4 discontinuity sets) and lie normal to anisotropy (perpendicular to bedding) which is characteristic of potential rapid failure. While the Mueller Rockslide is currently unstable (indicated by movement data; (McColl et al., 2012) it is probably not a first time failure i.e. the sliding surface is at residual strength as the rockslide may have been moving for decades to centuries. Displaced lateral moraines shows movement has been ongoing for a significant period of time without yet accelerating to catastrophic failure. This magnitude of displacement, however, suggests that the friction angle of the rupture surface is likely to be at residual values (<33°), and this is considerably less than the dip of the bedding assumed to be the sliding surface (which is a characteristic of rapid failure). Putting some of these conditions together and following the decision tree of Glastonbury and Fell (2008a) for an internally sheared, compound slide, the probability of very rapid to extremely rapid failure for the Mueller Rockslide is between 55-65%. The upper value represents the case of rapid external loading inducing failure (e.g. a strong earthquake). Under this decision tree scenario, we assume that the failure surface is at residual strength (i.e. a through-going, well-developed failure surface extending to the toe); if not at residual strength yet, the probabilities increase to 80-90%. The gradual development of a through-going failure surface at the toe, by connection of fractures and breakage of rock bridges (step-path failure mechanism), may represent progressive failure of this slope and could allow the transition to catastrophic acceleration.

These results appear to contradict the simplified modelling results presented in Figure 3.11 which indicates failure to be unlikely. However, this model does not account for the influence of glacier debuttressing, seismicity and ground water fluctuations. While failure along bedding is feasible, our results indicate it will not occur without external forcing, or without progressive loss of strength. Similar results have been seen within the Moosfluh Landslide and other rock slope instabilities surrounding the Aletsch Glacier. Grämiger et al. (2017) and Glueer et al. (2019)show incremental damage associated with repeat glacier cycles play a significant role in gradually weakening rock masses. Riva et al. (2018) has shown incremental damage can take thousands of years to accumulate to the point of physically

manifesting at the surface through headscarp formation. In addition, while glacier debuttressing has been identified as a preparatory factor for many alpine rock slope failures, in the latter stages of retreat glacier ice can induce viscous flow in unstable rock slopes through deformation (McColl and Davies, 2013), allowing for controlled failure of rockslides. Paraglacial stress release (Ballantyne, 2000b) may also be a cause of failure within the Mueller Rockslide, as the hillslope gradually adjusts to the unloading of the Mueller Glacier.

Future investigations on kinematics and movement history may provide insights on the relationship between movement and environmental drivers (e.g. pore-water pressure) and external forcings (e.g. seismic shaking). Additional modelling is required to assist in the determination of rockslide failure potential.

3.6 Conclusions

This paper summarises a combination of field mapping, fracture mapping, kinematic analysis and geophysical methods to present the structural controls and preconditioning factors of Mueller Rockslide. An extensive fracture network throughout the Sealy Range in proximity to the rockslide as well as several scarps above the main rockslide headscarp were newly identified. SRT and GPR have been successfully combined and show extensive fracturing to at least 10 m depth as well as the presence of several shear planes that coincide with mapped scarps at the surface. Several large tension cracks have also been identified above the main rockslide headscarp. The identification of several scarps and tension cracks indicates retrogressive development of the rockslide into the ridgetop. The novel combination of techniques in this chapter have proven useful in identifying shallow rock mass properties and could be utilised in many other areas of study on rock slope failures.

Kinematic analysis was performed for discontinuities within the rockslide and ridgeline areas. There is a low feasibility for planar sliding and an increased feasibility for wedge and toppling failure was identified through the headscarp and ridgetop. Although there is a limited feasibility for planar sliding, the movement direction of the rockslide is down-dip (285°) as opposed to down-slope (270°), suggesting an influence of bedding, further supported by our stability modelling. We therefore estimate the rockslide is moving along a stepped, discontinuous sliding surface along and through the interbedded argillite and sandstone. This geomechanical properties make the Mueller Rockslide susceptible to rapid failure, particularly after external loading via debuttressing, earthquakes or rainfall/snowmelt.

This research shows the formation of the Mueller Rockslide has been strongly influenced by the folding of Kitchener Anticline with failure controlled by bedding angle and orientation and the presence of joint sets commonly associated with anticline formation. While slow moving, the Mueller Rockslide exhibits some features commonly identified within rock slopes that transition to rapid, catastrophic landslides. A strong and predominantly intact rock mass as well as the presence of strongly defined lateral release structures increases the potential for rapid failure.

Future work should focus on identifying key triggers for rockslide movement and investigate the development of the rockslide through monitoring, modelling and cosmogenic dating. The investigation of potential seismic and hydrological triggers should also be completed given the high seismicity, rainfall and snow melt levels that affect the site.

3.7 Acknowledgements and funding

The research was funded by Massey University Research Grant (MR19350), Brian Mason Trust (2017/24) and Deutsche Forschungsgemeinschaft (DR 1070/1-1). The authors acknowledge support by the Department of Conservation. S. Cook and D. Draebing thank Massey University for funding in the form of the Massey University Visiting International Research Fund (2017 and 2018 respectively). Field work was kindly supported by Jana Eichel, Pat Kailey, Tim Stahl, Michal Brezny, James Fay and Florian Strohmaier with laboratory analysis by Georg Stockinger, Fritz Ettl and Till Mayer.

3.8 Contribution and summary for thesis

This chapter has utilised a variety of field investigative techniques to identify and define underlying structural controls on a developing paraglacial landslide which can be used to estimate future deformation of the rockslide and highlights high hazard areas should landslide development continue to occur. This chapter also showed the effectiveness of combining geophysical, geotechnical and geological mapping techniques which successfully combined to identify fracturing to a depth of 10 – 15 m. This chapter has contributed to objectives 1 and 3 by identifying controls which govern landslide development, provides new insight into how paraglacial landslide develop through the identification of the large retrogressive zone and explores how continued development may impact the surrounding area including the popular tourist site above the landslide.

The findings within this chapter have been utilised in Chapter 4. Knowledge of underlying structural controls was particularly valuable when providing an account of historic movement of the rockslide in the Chapter 4 discussion and allowed for additional monitoring equipment to be placed in specific areas throughout the rockslide.

4. Paraglacial development of the Mueller Rockslide

Introduction of Chapter 4 to Thesis

This chapter builds on original findings in Chapter 3 to present a nearly 8000 year history of paraglacial rockslide development, fulfilling objectives 1 and 3. By combining movement monitoring, historic aerial imagery, cosmogenic dating and rainfall data, a detailed movement history of the rockslide is presented which shows movement to be episodic, accelerating and controlled primarily through glacier retreat and potential groundwater changes. Cosmogenic nuclide exposure age dating of the main rockslide headscarp has shown landslide movement began at least ~8000 years ago, likely as a result of glacier retreat following the Antarctic Cold Reversal ~13,000 years ago (Putnam et al., 2010). Findings within this chapter highlight the variability in paraglacial landslide movement rates and show paraglacial landslides can be long-lived, forming thousands of years before complete debuttressing. This makes the prediction of failure based on accelerations in movement difficult but may help refine future models of landslide development.

This chapter is in preparation for publication within Earth Surface Processes and Landforms (ESPL).

4.1 Introduction

Glacier retreat and debuttressing as a result of climate warming have been recognised as drivers of hillslope failure in many alpine environments. Numerous large landslides occurring in the last 12,000 years are thought to have been triggered or influenced by debuttressing (Shakesby and Matthews, 1996, Kellerer-Pirklbauer et al., 2010, Mercier et al., 2011, Ballantyne and Stone, 2013, Mercier et al., 2017) associated with gradual climate warming throughout the Holocene (Schaefer et al., 2009). Following the end of the Little Ice Age (LIA) approximately 200 years ago, glacier retreat in alpine areas has increased rapidly, leading to the activation or acceleration of many large hillslope failures (Fey et al., 2017, Riva et al., 2018, Glueer et al., 2019). While the current rapid loss of glaciers is devastating, it also provides an opportunity to study the development and progressive failure of these large and potentially hazardous landslides as they undergo debuttressing. These findings can then provide useful context for understanding the causes of prehistoric landslides that developed during the major deglaciations in the past.

Although understanding around paraglacial slope failures is increasing within the scientific community, there are still relatively few studies focusing on more recent, contemporary failures. Primarily, these studies have focused on identifying how glacier retreat and debuttressing condition and weaken hillslopes (Grämiger et al., 2017, Riva et al., 2018), investigating underlying landslide structure and morphology (Glueer et al., 2019), (Chapter 3) and using remote sensing and historic imagery to identify movement patterns and deformation history since the LIA (Fey et al., 2017, Manconi et al., 2017, Glueer et al., 2019). From numerical models, we now understand that repeat cycles of glacier advance and retreat work to gradually weaken hillslopes (Grämiger et al., 2017), with this effect occurring over thousands of years prior to obvious deformation or movement of the hillslope expressed through the surface morphology (Riva et al., 2018). Through recent monitoring of contemporary paraglacial failures in Europe, it is now understood movement rates are highly variable and can sometimes exceed 1 m/day (Oppikofer et al., 2011, Manconi et al., 2017, Glueer et al., 2019), whereas others have maximum movement rates approaching 1 m/ year (Fey et al., 2017). Triggers for these periods of accelerated movement have in some situations been tied to glacier retreat, for example with Fey et al. (2017) finding the Marzell Rockslide in Austria showed the greatest movement rates occurred during partial debuttressing with a deceleration of movement occurring after debuttressing. The Barry Arm landslide in Alaska has also shown enhanced movement following rapid glacier thinning with 120 m of horizontal displacement seen between 2010 and 2017 (Dai et al., 2020). Given paraglacial landslides are the result of thousands of years of preconditioning, current and future glacier retreat may act as a catalyst to further prepare or trigger the final failure of already weakened slopes. Alternatively, the gradual thinning of glaciers may permit the continued slow, and non catastrophic, movement and stabilisation of rock slope failures. Investigation of active paraglacial landslides, through analysis of their movement patterns and historical development, may help to shed light on their future development, which in tum could help to mitigate them as a hazard.

The investigation of active failures can also provide insight into the behaviour of historic paraglacial failures, therefore helping us to interpret the causes of past events.

While the studies above show paraglacial landslides to be variable in their movement patterns, sensitive to environmental changes regardless of size and indicate that long timescales are required to induce progressive failure, there is still little known about spatio-temporal patterns of paraglacial landslide evolution. Accelerations in movement have been tied to debuttressing but greater accelerations as noted by Oppikofer et al. (2011) and Manconi et al. (2017) are also known to occur without a clearly discernible trigger. Few studies have integrated monitoring methods which cover a range of timescale, although the extended timefrarnes over which paraglacial landslides develop makes this difficult. As noted by (Coe, 2020), there are few long-term monitoring projects currently in place providing insight into how paraglacial slope failures develop during final debuttressing.

In situ monitoring of large paraglacial rockslope failures can be difficult due to their inaccessibility, hazardous terrain and extreme environmental conditions. Many are located in remote alpine areas which experience extremes in weather and temperature. The Mueller Rockslide in New Zealand is no exception, located in steep alpine terrain which is prone to these climatic extremes (Figure 4.1). However, the rockslide lies adjacent to a popular tramping hut, 1000 vertical meters above a small alpine village, making it relatively easy to access. The proximity to infrastructure also makes its study relevant due to its potential threat to the nearby village and the people living in or visiting the area. The landslide lies adjacent to the Mueller Glacier which has thinned by many tens of metres and retreated by several hundred meters over the last half century, the latter resulting in the formation of a pro glacial lake north of the rockslide. Current thinning of the glacier has likely contributed to further instability of the Mueller Rockslide, adding urgency to the need to understand the future fate of the rockslide. In situ monitoring of landslide movement was begun in 2010 using annual GPS surveys and monitoring deformation of individual fractures using crack-meters, with a sub-daily measurement frequency, since 2017. In addition, historical aerial photo interpretation and a rockslide scarp exposure history have allowed longer-term development of the landslide to be evaluated. Using these different methods this chapter aims to combine daily, annual, decadal and millennial movement data to analyse current movement patterns and provide an account of paraglacial rockslide evolution over the last -10,000 years. This data combined with other environmental information (e.g. rainfall and glacier changes) then allows some inference of the underlying causes of landslide movement and longer-term development.

4.1.1 Study Site

The Mueller Rockslide is a large (200 Mm3) paraglacial rockslide in the New Zealand Southern Alps, which is currently undergoing debuttressing by the Mueller Glacier (Fig. 4.1). Since the Little Ice Age (LIA) which ended in New Zealand in the mid 1700's (Winkler, 2000), the Mueller Glacier extent remained relatively static, extending to several historic terminal moraines approximately 5 km down valley, until the 1960s (Schaefer et al., 2009). Since the 1960's the glacier has retreated and thinned considerably; lateral moraines along the lower Mueller Rockslide inferred to be from the LIA now sit over 150 m above the current glacier height (Figure 4.1.), and a proglacial lake has developed.

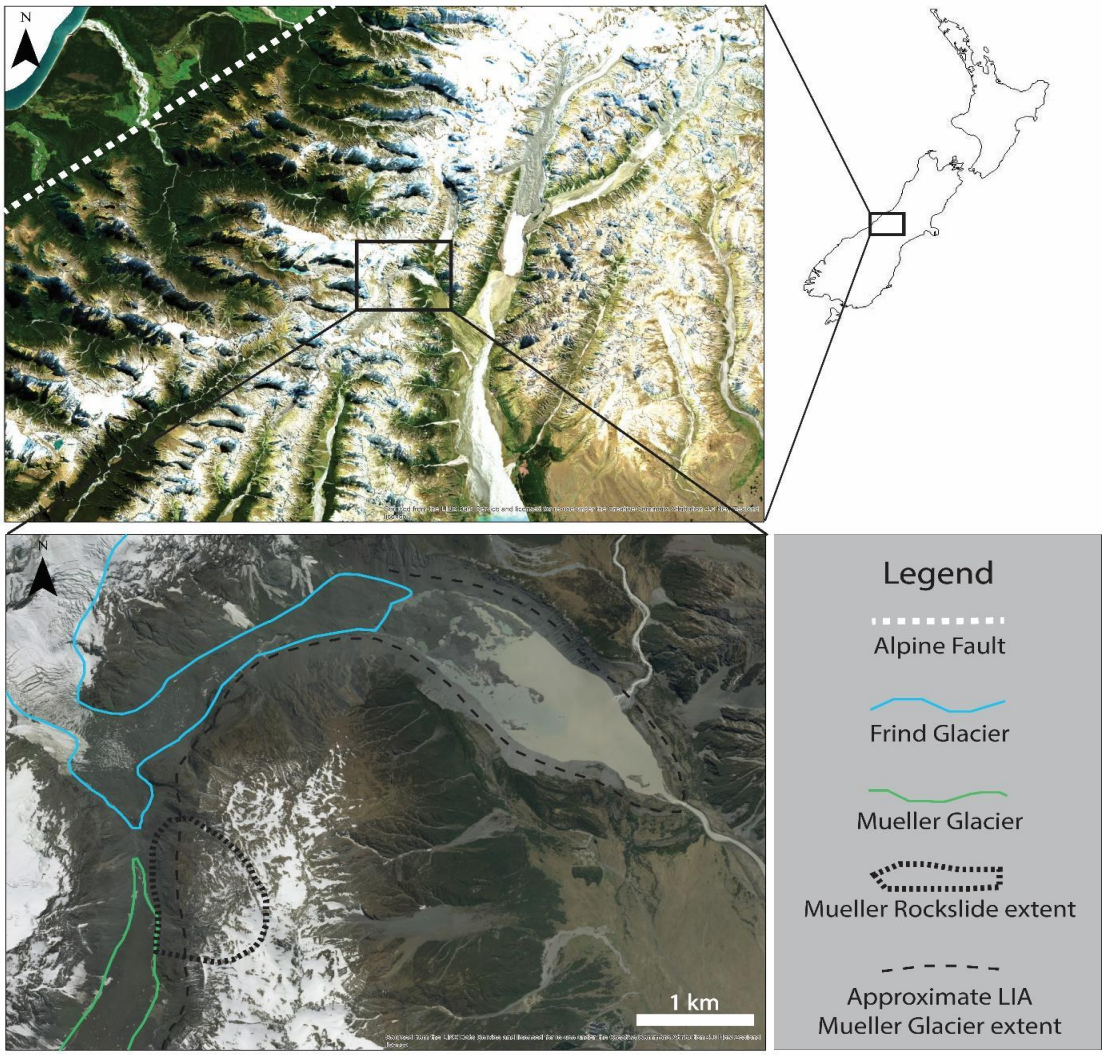

Figure 4-1: Location map of the Mueller Rockslide (black dotted line, bottom image) and the Mueller Glacier (green line, bottom image) based its current extent as seen in aerial imagery.

The rockslide is a high seismic zone within the Southern Alps. A large plate boundary fault system, known as the Alpine Fault, lies within 30 km to the west which has a well recorded history of magnitude 7.5+ earthquakes every ~300 years (Berryman et al., 2012). Geology at the site has been subsequently conditioned by tectonic processes and seismic shaking has likely played a role in

conditioning the slope for failure over the preceding years. The rockslide lies on the western side of the Sealy Range on the western limb of the overturned Kitchener Anticline (Lillie et al., 1964) which is composed of argillite and sandstone. Failure of the rockslide is mainly facilitated along down-dip planar bedding consisting of alternating sandstone/ argillite beds. Discontinuity sets associated with folding of the Kitchener anticline act as lateral and rear release structures controlling landslide failure, as well as controlling fracture orientation and propagation (Chapter 3). Geophysical analysis and geotechnical mapping show an extensive retrogressive zone underneath the tramping hut to the east (Chapter 3).

The study site is at maximum elevation of 1800 meters above sea level (masl), extending to approximately 1200 masl at the toe of the landslide. Due to the site's relatively low elevation, it is unlikely to be affected by permafrost which is thought to begin above 2400 masl in the central Southern Alps (Allen et al., 2009). The Mueller Rockslide and Sealy Range lie on the western edge of the Southern Alps and are influenced by orographic rainfall with very high rainfall experienced along the Main Divide. As a result, Mueller Rockslide is exposed to high magnitude rainfall events which can exceed 400 mm per day. Total annual precipitation near the Mueller Rockslide can exceed 10 m per year (Fitzharris and Garr, 1995) with high snowfall through May- October and high spring melt in November and December. During the Holocene, New Zealand has experienced steadily warming average temperatures since the end of the Antarctic Cold Reversal (ACR) 12,700 years ago (Putnam et al., 2010). During the ACR, glaciers throughout the Southern Alps experienced a resurgence after a period of more widespread retreat that had followed the end of the LGM, with average temperatures 2°C to 3°C lower than current temperatures (Vandergoes et al., 2008). It wasn't until ~6900 years BP where Holocene temperatures approached current temperatures, before remaining steady for several thousand years (Putnam et al., 2012). The Mueller Glacier reached its last maximum extent approximately 500 years BP before a general pattern of retreat began (Schaefer et al., 2009), punctuated by another period of glacial advance during the Little Ice Age (LIA) ~250 years ago (Winkler, 2000). In total, the Mueller Glacier is estimated to have a total volume loss in the last 250 years of 2.27 km^3, equating to total surface lowering of up to 300 m (Carrivick et al., 2020).

4.2 Methods

4.2.1 Cosmogenic 10Be exposure dating of the Mueller Rockslide headscarp

To determine the age of the rockslide, cosmogenic 10Be exposure age dating was completed using three samples obtained from the main (largest) headscarp which lies ~200 m west of Mueller Hut. The scarp selected is near vertical greywacke bedrock with samples taken at differing heights down the headscarp. M1 was taken at 7 m down from the top of the scarp, M2 taken at 10 m and M3 taken from 15 m (Fig. 4.2). The first sample was taken from down the scarp to reduce the occurrence of inherited

10Be from the top of the scarp. Thickness and density for all samples was ~4 cm and 2.76 cm3 respectively. Calculation inputs are presented in Table 4.1.

Quartz was isolated from the samples using standard procedures at Victoria University of Wellington (Gosse and Phillips, 2001). Beryllium concentrations in the samples and blanks were measured with the GNS Science Accelerator Mass Spectrometer. Exposure ages were then calculated using the online exposure age calculator Chronus, using the Macaulay valley production rate (Putnam et al., 2010), and the time-dependant LSDn scaling method (Lifton et al., 2014). A topographic shielding correction factor was applied (Table 4.1), as measured from each sample location, but no erosion or snow shielding corrections were made. To avoid sampling areas of higher than average erosion, samples were selected from areas with apparent uniform weathering discoloration (i.e. no fresh surfaces) and a lack of veining. Snow shielding is likely to have had some bearing on 10Be accumulation due to snow accumulation at the base of the scarp, leading to slightly lower concentrations and therefore younger than real ages.

Table 4-1:Summary of calculation parameter inputs and estimated ages.

Temperature Correction Factor (K)							
	Thickness scaling factor	**Shielding factor**	**Production rate (atoms/g/yr)**	**Internal uncertainty (yr)**	**Exposure age (yr)**	**External uncertainty (yr)**	**Production rate (atoms/g/yr)**
M1	0.9663	0.8233	0.321	200	7882	264	12.52
M2	0.9663	0.8050	0.321	153	2450	162	12.23
M3	0.9663	0.7813	0.321	159	1658	163	11.82

An assessment was made of the site to determine where the scarp was formed as a result of landslide development of glacial erosion. There was no evidence of glacial erosion (striations) along the scarp where sampling was undertaken.

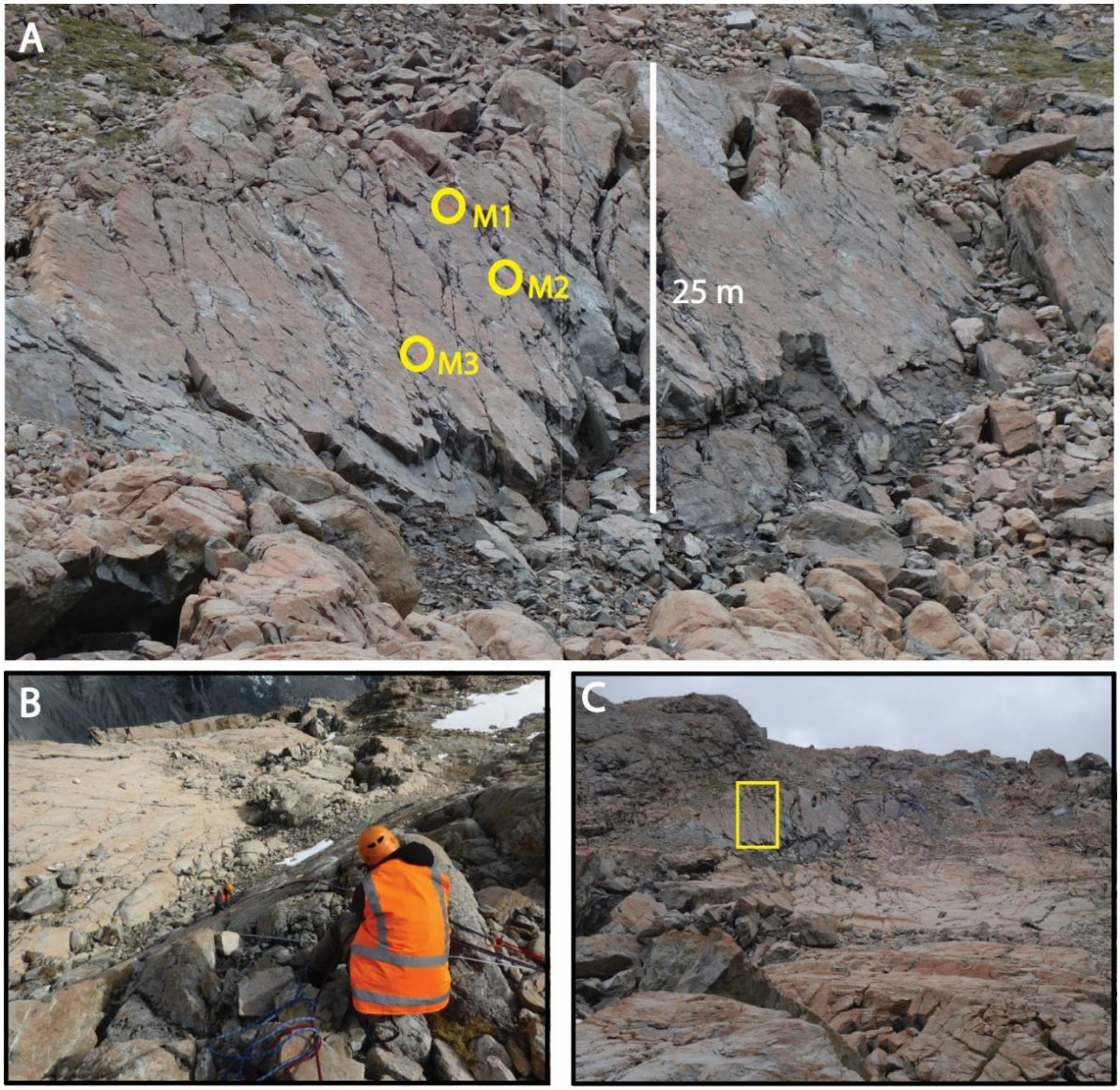

Figure 4-2: A) Sampling locations for 10Be dating. B) Sampling in process. C) Position of scarp relative to the main headscarp zone.

4.2.2 Morphological mapping from historic aerial imagery

To track changes in landslide morphology three orthomosaic models were produced from aerial photography. Historic aerial imagery from 1960 and 1986 from RetroLENs (www.retrolens.nz) were utilised to create a Digital Elevation Model (DEM) and orthoimagery for mapping changes within the landslide. The 2017 structure from motion (SfM) derived orthoimagery was the same used in Chapter 3 and the methodology for its production is described there.

The 1960 imagery was recorded on the 25/02/1960 using a light aircraft at an elevation of 16500 feet, with images were captured using a Wild RC5 camera. In total, 12 images were captured which encompassed the study area within the 1960 survey. The 1986 imagery was obtained on the 02/01/1986 using a Zeiss RMK camera at an elevation of 30000 feet. Ten images were captured within the 1986 survey period which covered the study site and surrounding area. Photo alignment and orthoimage

generation was completed using Agisoft Metashape, using a similar methodology as per Chapter 3 although GCP's were not used for photo alignment. Instead, 22 manually selected tie points identified across both image sets were then used to improve model alignment (Fig. 4.3). Tie points were located on stable bedrock that had not experienced landsliding between the 1960 and 2017 imagery to ensure the points could be accurately identified in all imagery. Following alignment, average horizontal error for the 1960 imagery was 13.4 m and 9.8 m for the 1986 imagery. Error for the 2017 SfM was significantly lower, with a mean elevation difference of 0.35 m recognised between the DEM and other known, measured survey marks. Because georeferencing was not possible, the aerial imagery was used to map morphological changes and estimate horizontal movement rather than estimate elevation changes or volumetric changes in the landslide.

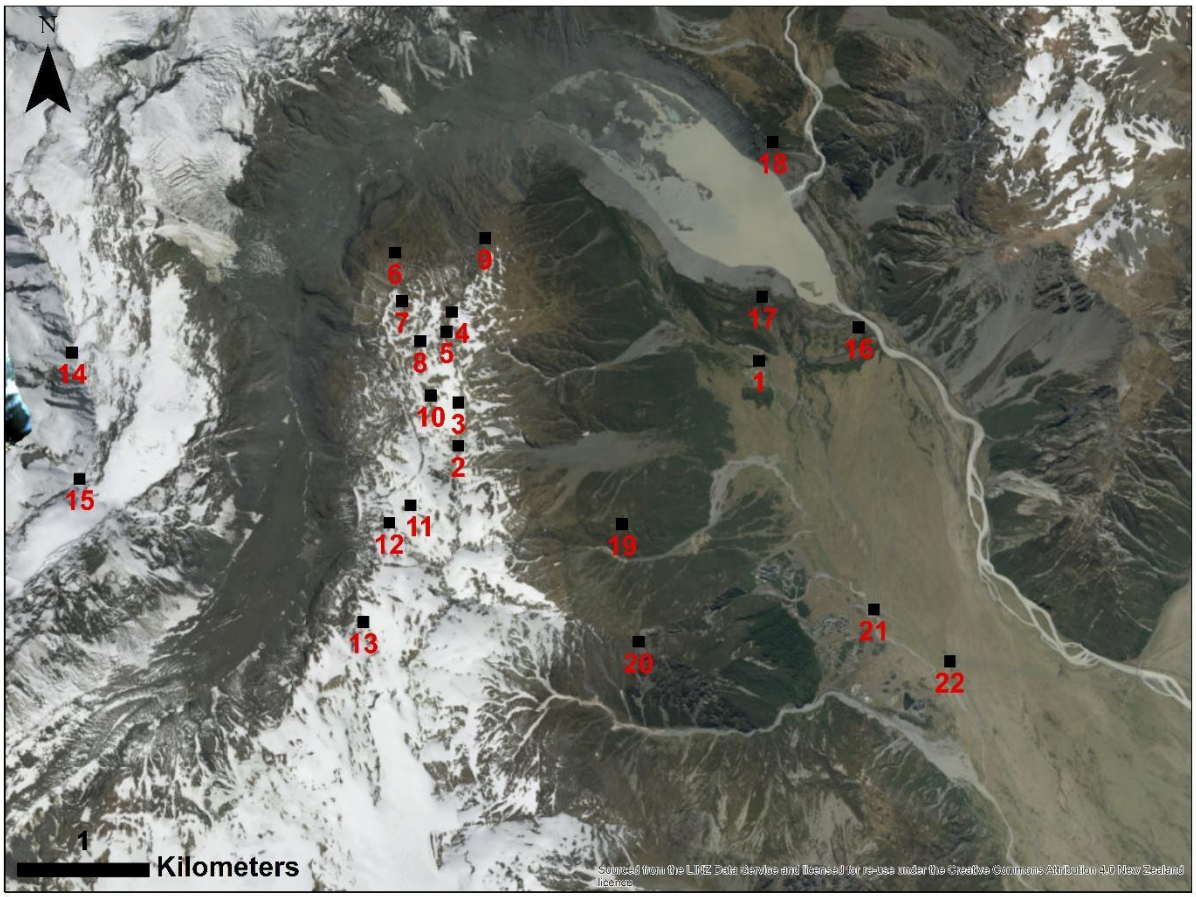

Figure 4-3: Tie points for alignment of the 1960 and 1986 aerial imagery.

4.2.3 Annual GPS survey peg monitoring

To track annual rockslide displacement, GPS surveying of survey pegs on and around the rockslide began in 2010. The survey was initially done using a Trimble GeoHX differential GPS, with baselines corrected against the Mount John Observatory (MJO) continuously operating GPS station which lies approximately 45 km southeast (McColl, 2012b). Following correction against the MJO base station, horizontal and vertical precisions were 0.1 m and 0.2 m respectively. In 2016 the surveying method changed to using a Trimble R10 GPS and an RTK baseline correction against the national

survey network using B8Y2 UNWIN, 5 km from the site. The resulting precision were 0.02 m horizontally and 0.03 m vertically. In total 14 survey marks were placed over the 10 year study with two survey marks lost, six survey marks which cover the entire study period and six survey marks which were added in 2011 (Fig. 4.4). To account for a systematic difference in recorded elevation heights between the two dGPS techniques, a correction of 1.86 m was applied between the 2016 and 2017 measurements.

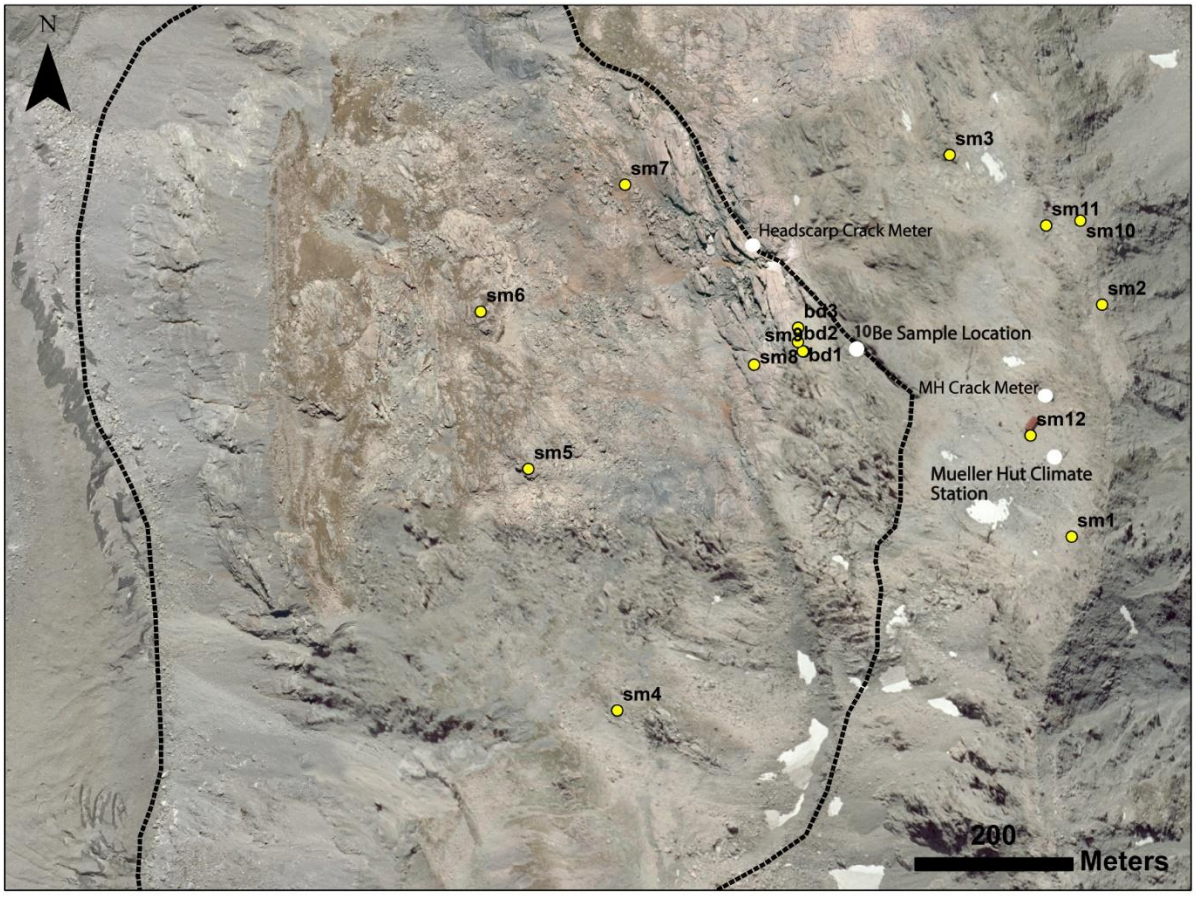

Figure 4-4: Locations for survey marks, crackmeters, cosmogenic sampling and the Mueller Hut Climate Station. Black line indicates the Mueller Rockslide extent.

4.2.4 Continuous monitoring of headscarp fractures

To complement the movement data obtained through annual surveying of the rockslide, two 'RST Instruments' vibrating wire crackmeters were installed to continuously monitor movement around the headscarp and Mueller Hut within the rockslide retrogressive zone. The top crackmeter was located 10 m north of Mueller Hut and was located in a fracture where wastewater drained from the hut (Fig. 4.5). This crackmeter had a maximum reach of 100 mm. The bottom crackmeter was located within the headscarp zone where headscarp retrogression to the north. This crackmeter had a maximum reach of 200 mm.

Figure 4-5: Crackmeter adjacent to Mueller Hut. The crackmeter lies under the protective pipe with the logging equipment connected to the wall of the fracture above the crackmeter.

Monitoring of the 100 mm Mueller Hut crackmeter was done between February 2017 and April 2019 before a battery fault terminated monitoring. Monitoring of the headscarp crackmeter was continued between February 2017 and February 2020. Measurements were taken at a variety of intervals to accommodate data storage and power capacity; between February 2017 and February 2018, measurements were taken at 3 hourly intervals, between February 2018 and February 2019, measurements were taken every 5 minutes, and later were then increased to every 15 minutes from February 2019 for both crackmeters. Data was logged using an RST single channel vibrating wire datalogger with reported accuracies of 0.1% F.S. A temperature correction was applied to the raw data to remove thermal expansion-contraction effects on the components of the crackmeter. A temperature correct factor (K) was first applied using the following equation:

$$K = \big((Rc * M) + B\big) * CF$$

where Rc is the current reading in ohms, M is slope as given in the RST guide, B is constant as given in the RST guide and CF is the Linear Calibration Factor. Used values are presented in Table 4.2.

Table 4-2: Values used for calculating temperature correction factor (K).

Temperature Correction Factor (K)				
	Rc: Current Reading	**M: Slope**	**B: Constant**	**CF: Calibration Factor**
Mueller Hut Crackmeter	Variable	0.0004	-0.7577	0.024055
Headscarp Crackmeter	Variable	0.000306	-0.4498	0.046524

Linear displacement was then calculated using the following equation:

$$Linear\ displacement = (Rc - Ri) * CF + (Tc - Ti) * K$$

with Rc being the current reading in ohms, Ri being the initial reading (in ohms), CF being the Linear Calibration Factor from the RST guide, Tc being current temperature (°C), Ti being initial temperature (°C) and K being the temperature correction factor. Values used are displaced in Table 4.3.

Table 4-3. Values used for calculating linear displacement.

Linear Displacement						
	Rc: Current Reading	**Ri: Initial Reading**	**CF: Calibration Factor**	**Tc: Temperature Current**	**Ti: Temperature Initial**	**K: Temperature Correction Factor**
Mueller Hut Crackmeter	Variable	3952.53	0.024055	Variable	10.02	Variable
Headscarp Crackmeter	Variable	3305.96	0.046524	Variable	9.94	Variable

4.2.5 Comparisons between movement and rainfall

Rainfall data were collected from the Mueller Hut (station number 38102) and Mount Cook (station number 18125) climate stations to evaluate the relationship with crackmeter and annual surveying monitoring data (Cliflo, NIWA). Mueller Hut climate station, which lies at an elevation of 1800 meters above sea level (masl) has rainfall data available over the last decade. The site experiences an average of 3800 mm of rainfall annually, with most of this falling through the warmer summer months from December to April.

To coincide with crackmeter monitoring, daily rainfall records were obtained from 2017 through to February 2020. To estimate winter precipitation levels, rainfall was also compared again the Mount Cook Village climate station which lies at approximately 740 masl. (Fig. 4.6). The Mueller Hut climate station measured, on average, 98 mm of rainfall more than the Mount Cook village climate station over the summer months from December to April with a variation of between 23 to 206 mm. In comparison, the Mount Cook Village station measured an average of 106 mm more rainfall in winter than the Mueller Hut station, with a maximum range of between 5 to 267 mm. To account for this

discrepancy due to a lack of snowfall data, the difference in summer rainfall between Mueller Hut and Mount Cook (98 mm) was added to Mount Cook climate station winter totals, to represent an estimated minimum precipitation total for Mueller Hut. Following this change, total rainfall for Mueller Hut increased from 3874 mm without a precipitation correction, to 5297 mm with a correction.

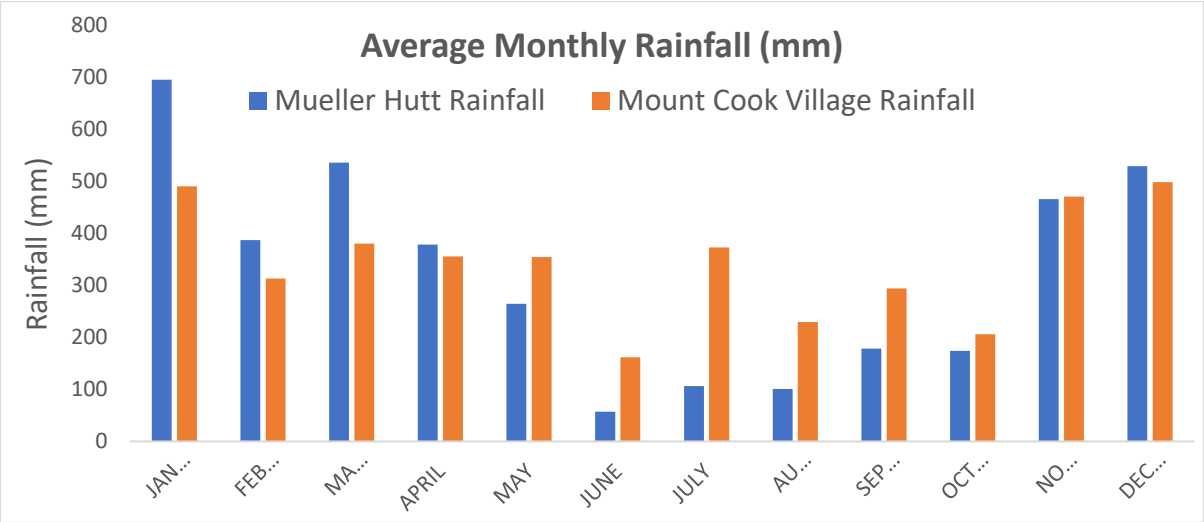

Figure 4-6: Average monthly rainfall comparison between Mueller Hut and Mount Cook Village.

In addition, rainfall records from Mueller Hut and the Mount Cook Village climate stations were obtained from 2010 for comparison against annual survey results. Annual rainfall totals for each site were compared up until 31/12/2019 (Fig. 4.7). In total, Mueller Hut recorded higher rainfall in five of the ten years where rainfall data was obtained. Of note, rainfall at Mueller Hut in 2012 was lower than all other study years by almost half, whereas there was no notable change in rainfall recorded at Mount Cook Village. This is likely due to higher than normal snowfall at Mueller Hut in 2012. Additionally, another snowfall correction was applied to the Mueller Hut data to estimate total minimum precipitation at the site each year. When comparing pre- and post- snowfall correction values (3874 mm and 5279 mm respectively) outlined above for Mueller Hut in the 2017 – 2019 data, total precipitation was 1.4 times higher following snowfall correction. This value was then applied to the Mueller Hut values in Fig. 4.7 to provide an estimate of minimum annual precipitation for Mueller Hut. Given the much lower rainfall recorded in 2012, overall minimum annual precipitation for this year is under-estimated as it is presumed more precipitation fell as snow that year. Following this correction against all annual data, average minimum precipitation for the site increases to 5478 mm per year.

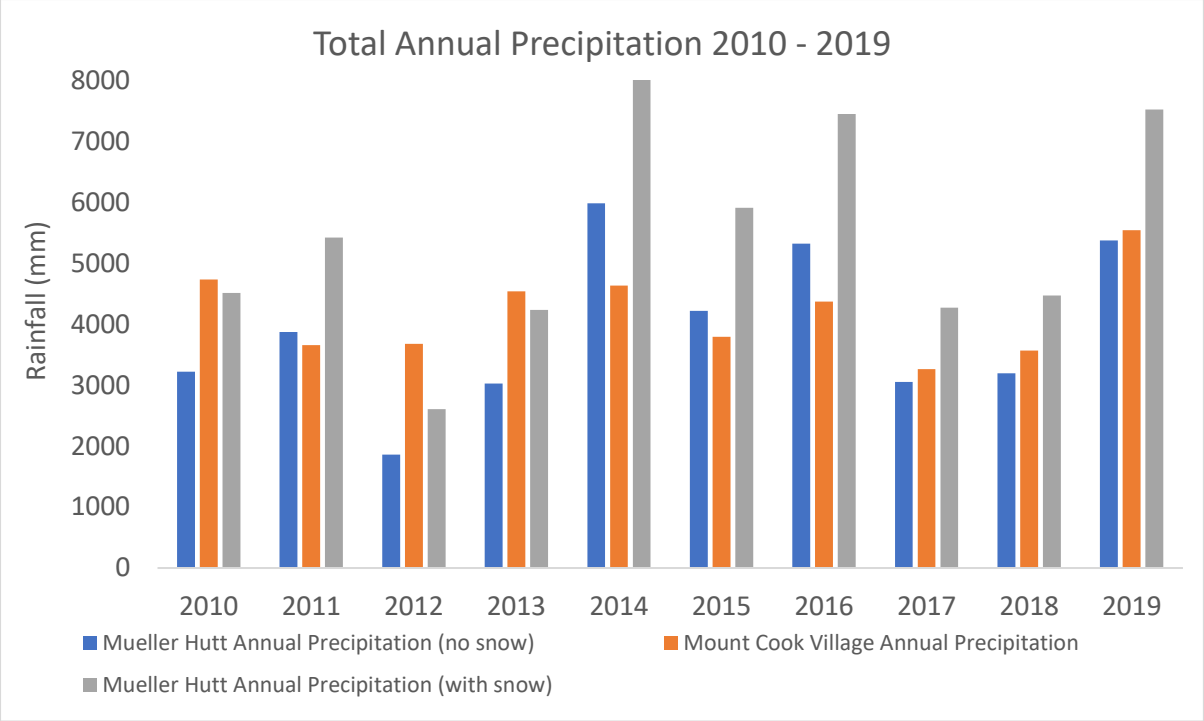

Figure 4-7:Corrected Mueller Hut annual precipitation with estimated snowfall allowance.

4.3 Results

4.3.1 Cosmogenic age dating of the Mueller Rockslide headscarp

^{10}Be dating of the main rockslide headscarp provides an approximate age of the Mueller Rockslide. Sample M1, the oldest result taken from 7 m from the top of the headscarp had an exposure age of 7481 ± 222 years. Sample M2, which was taken from 10 m down the headscarp had an exposure age of 2289 ± 147 years. Sample M3, which was taken from 15 m down the headscarp had an exposure age of 1507 ± 146 years.

Averaged annual movement rates of the headscarp were then calculated between each dated sample for the headscarp zone, providing an estimate of annual movement which can be compared against current movement rates obtained from annual surveying. The difference in exposure age between M1 and M2 was 5192 ± 369 years while the height difference between M1 and M2 was 3 m, equating to an average annual movement rate during this time of 0.57 ± 0.3 mm. The difference in exposure age between M2 and M3 of 782 ± 293 years combined with a height difference of 5 m gives an approximate average annual movement rate of 6.39 ± 1.74 mm. Using the scale available in Figure 4.2, we can also estimate the average annual movement rate of the headscarp zone from when M3 was taken at 15 m, to the base of the headscarp at approximately 25 m. This provides a height difference of approximately 10 m, over a period of 1507 ± 146 years, equating to an average annual movement rate of 6.63 ± 0.58 mm per year.

4.3.2 Historic morphological mapping

Orthoimagery obtained from historic aerial imagery and the 2017 SfM show large changes in both the Mueller rockslide extent and the extent of the Mueller Glacier (Fig. 4.8). Between 1960 and 1986 the Mueller Glacier narrowed by approximately 200 m although the glacier still extended throughout the valley and buttressed the rockslide. Between 1986 and 2017, the glacier retreated to the centre of the Mueller Rockslide, disconnecting from the Frind Glacier to the north and debuttressing completely from the northern section of the rockslide. Within the 2017 imagery, the glacier has thinned and become elongate, deforming around the landslide boundary. The eastern margin of the glacier which lies against the base of the rockslide appears thinner and pockmarked compared to the western boundary.

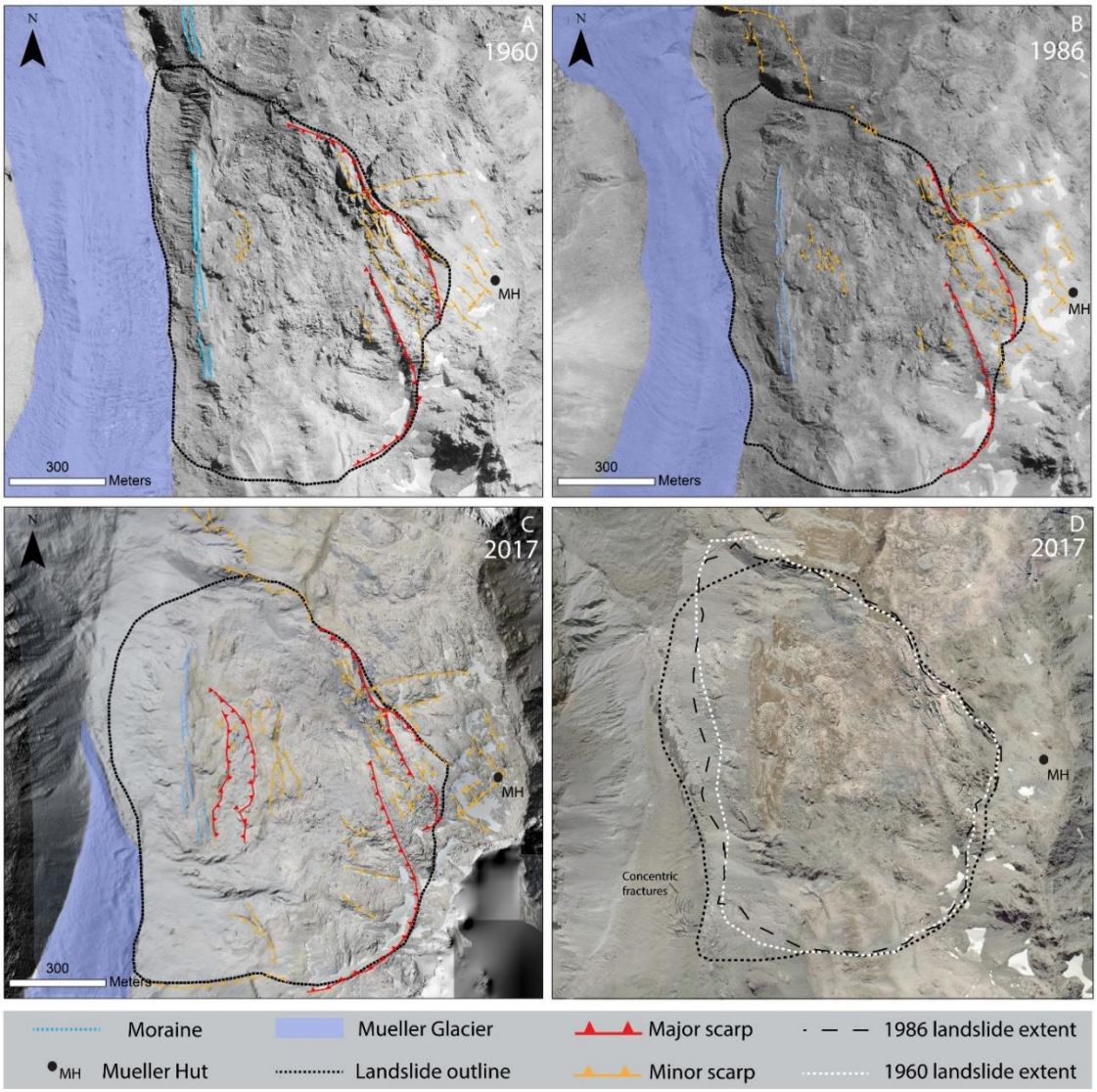

Figure 4-8:Comparisons between historic and current aerial imagery. A) 1960 aerial imagery. B) 1986 aerial imagery. C) 2017 orthomosaic and hillshade imagery. D) Comparison between 1960, 1986 and 2017 landslide extent.

Deformation of the rockslide has followed on from retreat of the glacier. Between 1960 and 1986, minor changes in landslide toe morphology show a slight extension of the toe to the west by approximately 50 – 100 m by comparing the location of the lateral moraines in the lower landslide toe. Several small scarps can also be seen within the central landslide zone above the lateral moraines although the rock mass of the lower landslide appears relatively intact. From 1986 to 2017 growth of the landslide toe infills the valley floor, pushing the glacier to the left. As a result, the western boundary of the landslide reaches almost to the opposite valley wall, displacing and thinning the glacier. Failure of the landslide toe increases by 100 – 150 m meters horizontally between 1960 and 2017 by comparing the position of the moraines relative rockslide headscarp and Mueller Hut location. Scarp development within the central landslide increases with several smaller grabens forming and disintegration of the rock mass can be seen (Fig. 4.8). Changes within the lateral moraines can be seen within the 2017 imagery, with a 50 m offset in horizontal distance seen between the moraines and the top of the headscarp compared to the 1960 and 1986 imagery. Several small and presumably superficial slope failures can also be seen at the bounding margins of the rockslide (south and north) where the glacier and rockslide meet.

Movement rates are approximated for the landslide over the last 60 years by tracking changes in moraine displacement. As the moraines are located at the landslide toe, these movement rates are considered to be a maximum average movement rate of the time period. Between 1960 and 1986, moraine displacement is minor and estimated to be no more than 5 m over the 26 year period. This equates to 0.19 m per year. Estimating movement from 1986 to 2017 is easier due to obvious deformation of the lower slope. During this time, moraine displacement is estimated to be 50 ± 10 m over the 29 year period equating to 1.7 ± 0.5 m with error inferred based on measuring error across the width of the moraine ridge. This acceleration in movement aligns with increased retreat of the Mueller Glacier over the same time period.

While large changes in landslide extent and morphology can be seen in the lower slopes, no significant changes can be identified within the landslide headscarp. Several minor scarps can be seen in all imagery around the Mueller Hut and headscarp zones. Major scarp morphology within the headscarp zone is also relatively unchanged with poor imagery quality in 1986 obscuring some of the minor scarps near Mueller Hut. Some changes in tension crack width can be seen within the retrogressive zone, particularly to the south between the 1960 and 2017 imagery.

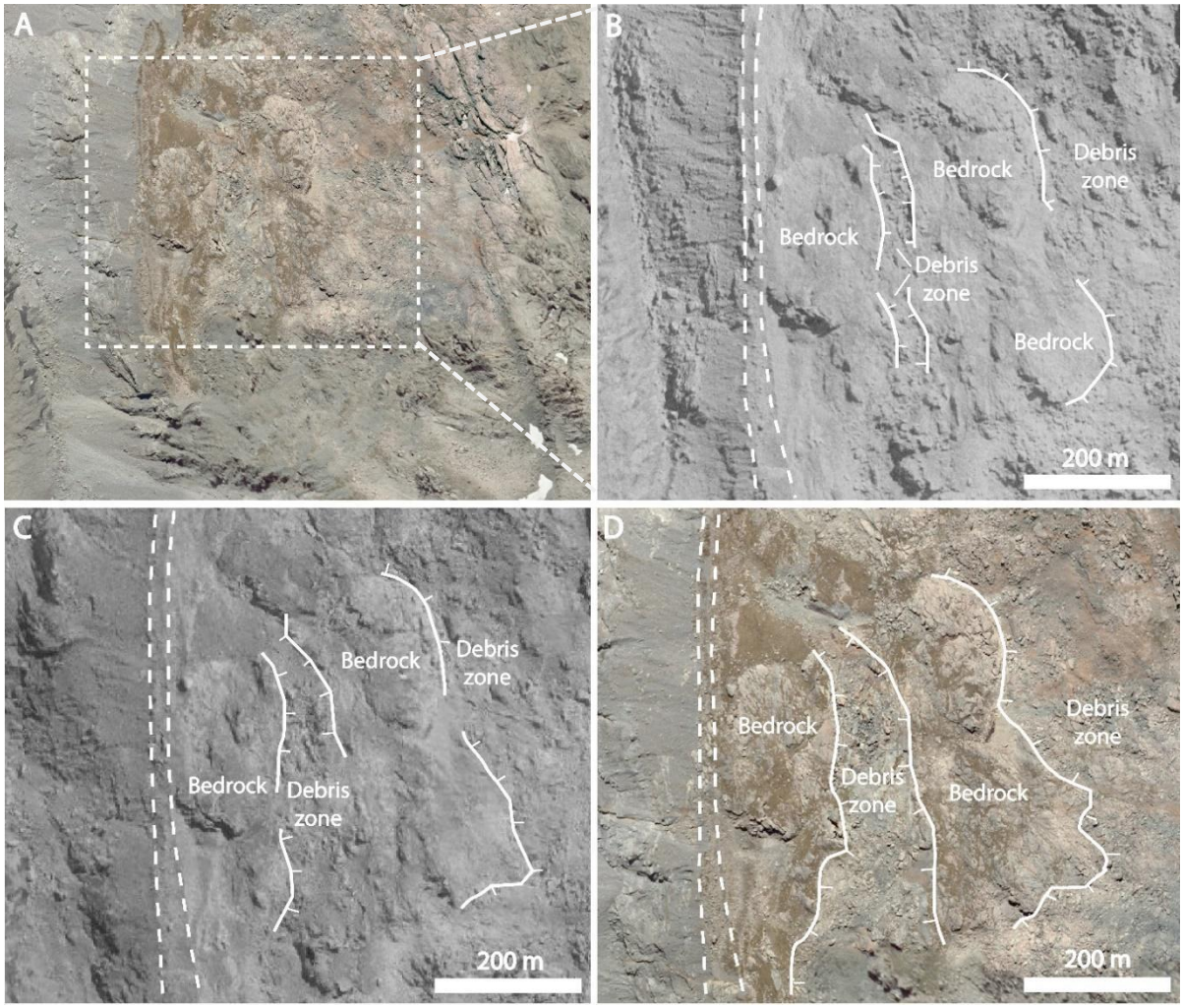

Figure 4-8. Close up of the lower landslide showing development of the lower graben. A) location map, B) 1960 imagery, C) 1986 imagery and D) 2017 imagery. Dashed lines represent lateral moraines.

4.3.3 Annual survey

Annual survey results from April 2010 to February 2020 are presented in Figure 4.9. Survey marks from within the landslide and the retrogressive zone show variations in movement annually. Average total displacement within the headscarp and retrogressive zone is 1.2 m with maximum and minimum displacement of 1.7 m and 0.27 m seen at survey marks 7 and 12 which are in the headscarp and underneath Mueller Hut. The sudden change at SM9 is attributed to measurement error as are decreases in movement between 2012 and 2013.

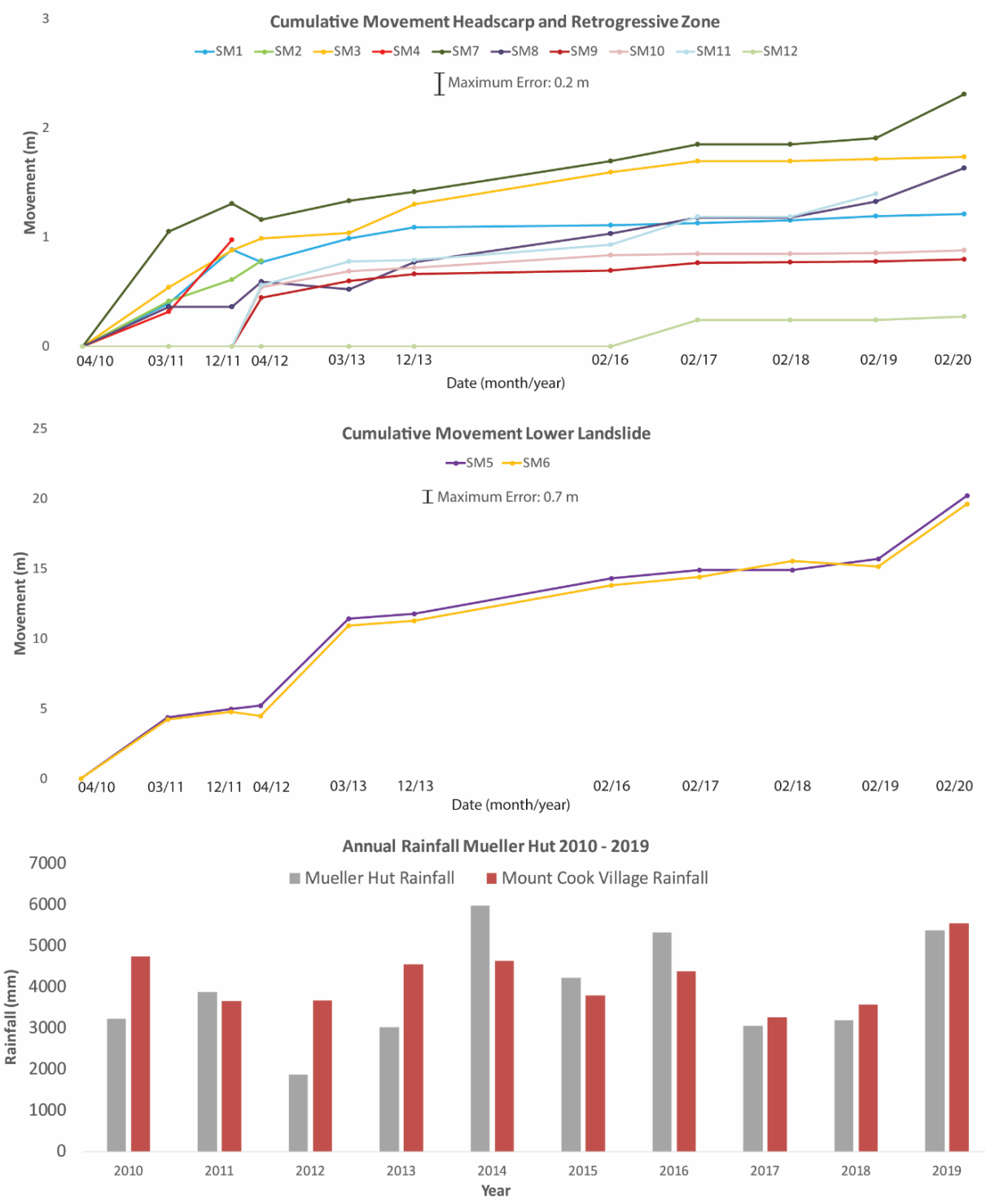

Figure 4-9: Cumulative net movement data from 2010 – 2020. Movement downslope is indicated through negative movement values.

Within the lower landslide, both survey marks 5 and 6 show 20.2 and 19.6 m of movement respectively over the study period, which equates to an average of 19.9 m. Two epochs with larger displacement are observed. The first in 2012 had ~6 m of total displacement and the second occurring in 2019 and had ~4.5 m of displacement. An above-average displacement in 2019 was also seen in

survey marks 7 and 8 which lie within the upper landslide just below the headscarp. Survey mark 9 which is located in the headscarp did not show increased displacement in 2019.

Annual rainfall totals for Mueller Hut were compared to movement rates for all survey marks. Overall, rainfall varied from approximately 1800 mm in 2012 to ~5900 mm in 2014. Average annual rainfall over the decade was 3913 m, however total precipitation is higher as this doesn't include snowfall. Comparisons with the Mount Cook Village rain gauge show higher annual rainfall totals compared to Mueller Hut which were displayed in Figure 4.7. Comparisons between rainfall totals and displacement show variable linkage. Accelerated movement in 2019 coincided with above average rainfall for the year. Similar high annual rainfall in 2014 and 2016 showed no correspondence with greatest displacement. Accelerated movement in 2012, particularly of survey marks 5 and 6 corresponded with the lowest annual rainfall total of ~1800 mm. Movement direction was also derived for survey marks within the landslide and represented as vectors (Fig.4.10). Movement vectors varied from west to north. Survey mark 4 – which was destroyed in 2011 – shows a nearly northward trend, as did survey mark 9 within the headscarp zone. Survey marks 5, 6 and 7 show a roughly westward trend while survey mark 8 within the headscarp zone, showed a northwest trend.

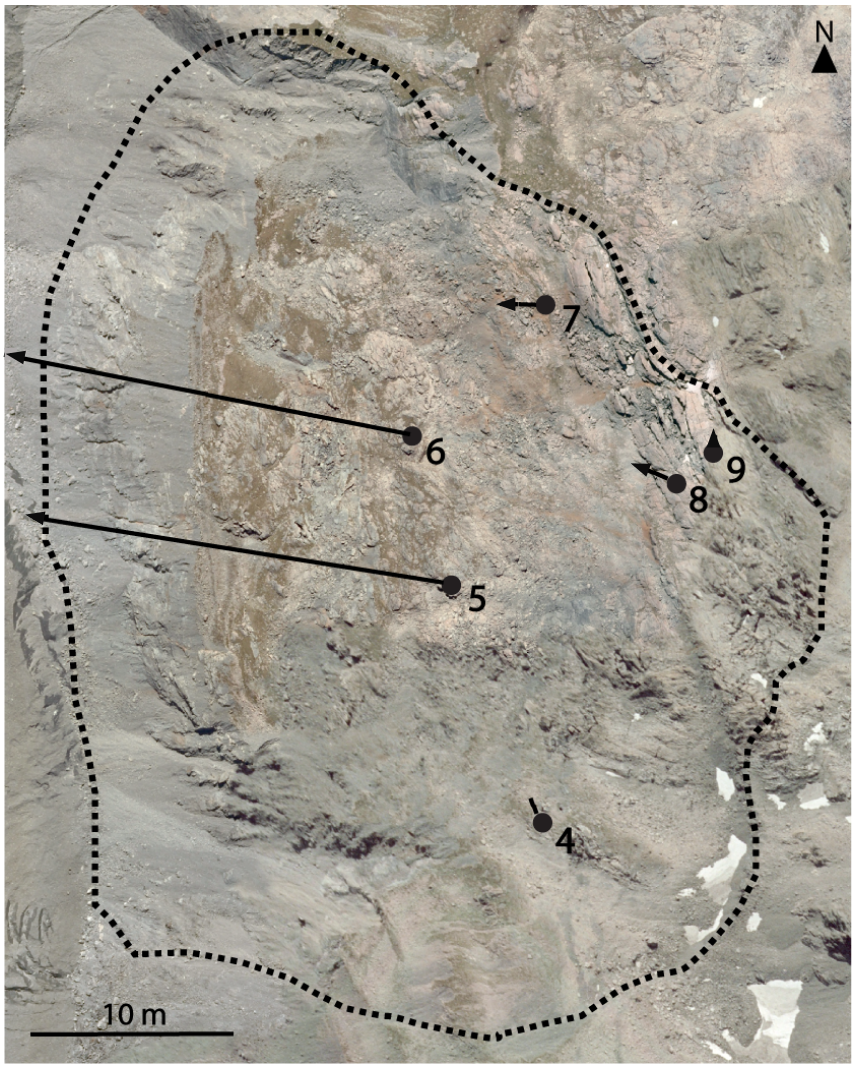

Figure 4-10: Movement vectors for survey marks within the landslide from 2010 – 2019.

4.3.4 Crackmeter measurements of headscarp and retrogressive zone

Crackmeter results from the Mueller Hut and headscarp crackmeters are presented to track changes in fracture dilation and contraction. Results show variability in measurements with expansion and contraction occurring as well as variability in temperature at the site throughout the year (Fig. 4.11). Crackmeter measurements over summer show daily variability of 0.4 mm with peak reduction of the crackmeter measurements occurring at midday due to thermal expansion of the rock mass, and peak extension of the crackmeter occurring at midnight. A reduction in crackmeter measurement corresponds with fracture contraction as the rock mass expanded (narrowed) while an increased in crackmeter measurement at night indicated the rockmass was contracting due to lower temperatures or no sunlight. Winter movement measurements varied from winter 2017 to winter 2018. Measurements throughout winter 2017 was minimal and temperature readings show the fracture to remain at roughly 0°C until spring. In contrast, winter 2018 showed several fluctuations in movement across a 2 mm range through contraction and expansion. Temperatures during this time remained at 0°C. Monitoring of the fracture does show a gradual widening of 0.3 ± 0.04 mm over the two year monitoring period with the first crackmeter measurements at 1200 hours starting at 97.209 mm and finishing at 97.554 mm.

The headscarp crackmeter covered a three year period from February 2017 to February 2020 (Fig. 4.12). Unlike the Mueller Hut crackmeter the headscarp crackmeter shows expansion throughout winter of approximately 0.5 mm before movement reduces or moves negatively in spring, indicating fracture closure. Temperature results show minor fluctuations in winter, although these stay within 1°C. Overall, there is a trend of gradual expansion recorded by the crackmeter which continues throughout the year, rather than stopping or slowing in winter like the Mueller Hut crackmeter. During this time, total movement of the fracture was 2.5 ± 0.05 mm over the three year study period with the first and last measurements taken at 1200 hours being 153.86 mm and 156.37 mm.

Two rapid periods of rapid and sustained crackmeter extension can be seen in Spring 2018 and Spring/Summer 2019 – 2020 with a close up of the 2019/2020 movement seen in the bottom of the image. Movement in spring 2018 occurs from the 29/10/2018 while rainfall occurs on the 9/11/2018 indicating no correlation to rainfall. However, as the movement corrects after this event it could be an error in measurement or could be an example of an avalanche impacting the crackmeter. Four periods of extension can be seen within the end of 2019 and beginning of 2020. The first occurs on the 4th of November and shows no correlation with rainfall. Movement on the 7th November occurs following several days of moderate rainfall (maximum 119.4 mm per day). A third period of extension occurs on the 28th November and continues until the 5th December. Rainfall occurs throughout this period and peaks at 289 mm per day. The final period of gradual extension seen within the crackmeter monitor occurs on the 5th February 2020 and occurs following a period of sustained rainfall which culminates with peak rainfall of 327 mm per day.

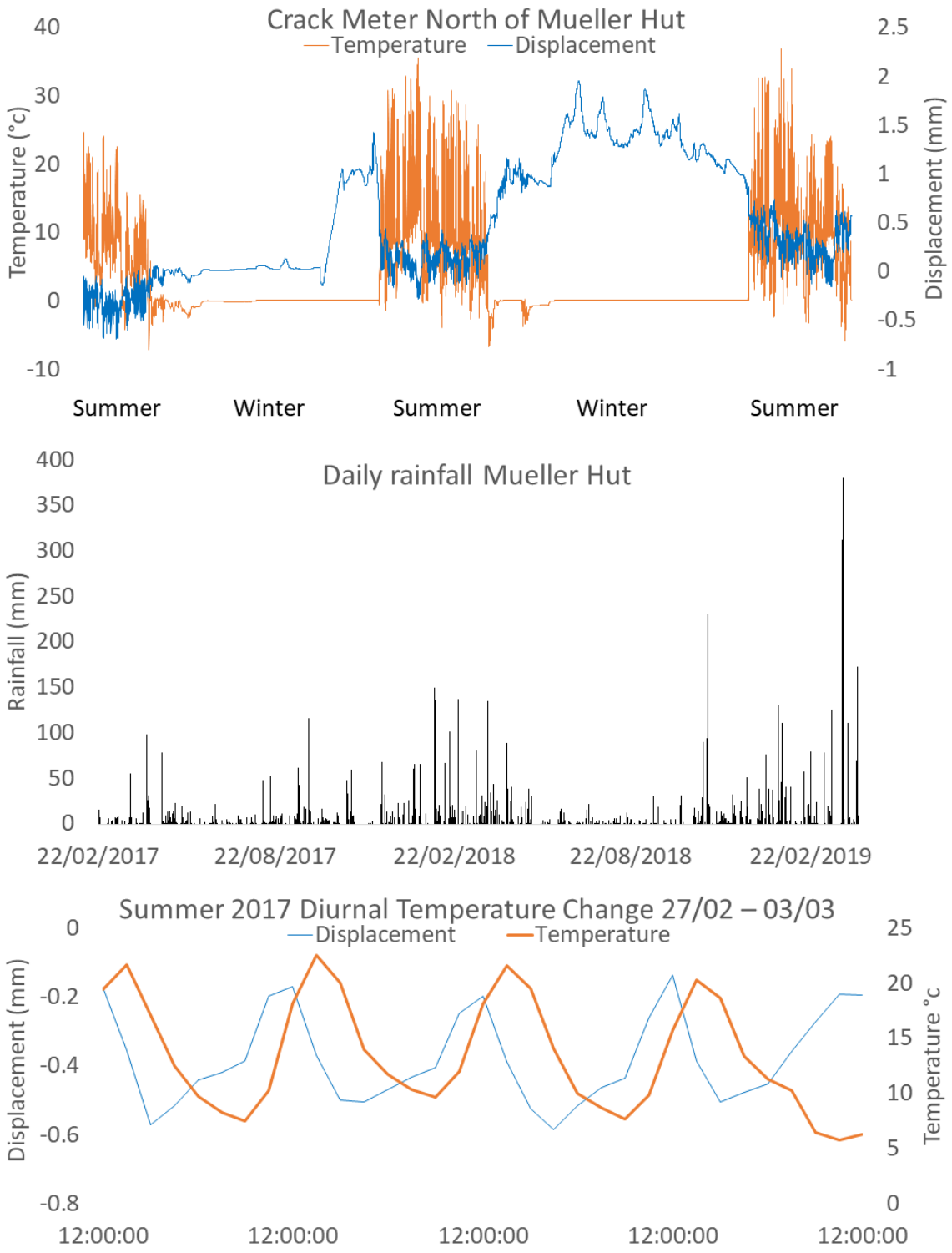

Figure 4-11: Results from the crackmeter above Mueller Hut showing movement (top of image), rainfall over the same time period (middle of image) and diurnal changes in movement and temperature through a typical 5 day block in summer.

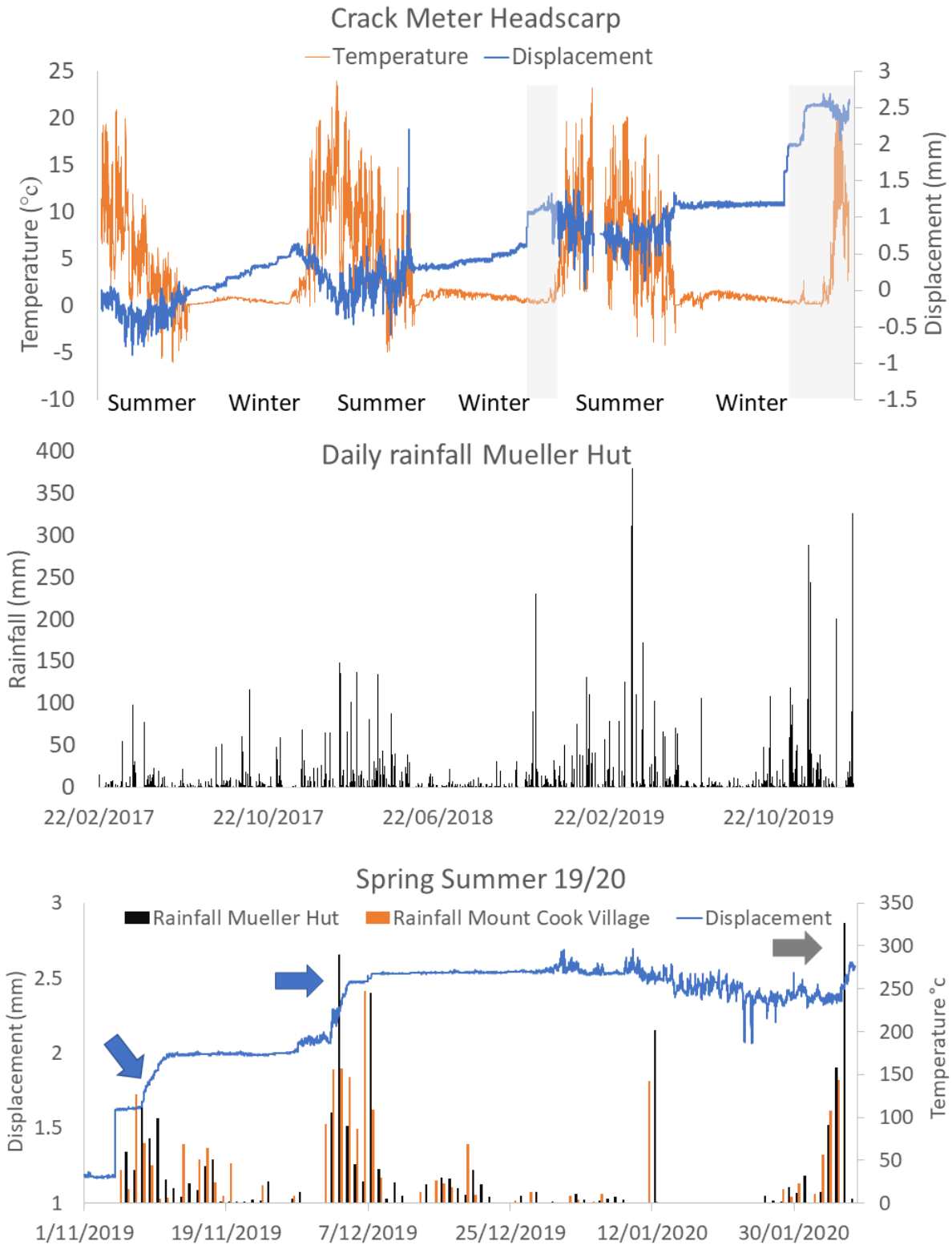

Figure 4-12: Crackmeter results from the Mueller Rockslide headscarp zone, showing annual movement compared to temperature (top of image) and daily rainfall over the same time period (middle of image). The bottom of the image shows a close up of movement and rainfall during Summer 2019 – 2020.

4.4 Discussion

4.4.1 Changes in landslide and glacier morphology

Historic aerial imagery reveals several changes to the morphology of the rockslide over the last 60 years coincident with changes to Mueller Glacier. The most obvious morphological change within the landslide has occurred near the toe where extension or displacement of the slope into the valley can be seen by approximately 50 m. This appears to be directly related to the almost complete retreat and detachment of the Mueller Glacier from the northern portion of the landslide toe and has allowed the Frind Glacier to flow up valley towards the rockslide. The Mueller Glacier in this location has also become elongate and sits on the western side of the valley. This is likely due to growth of the landslide toe to deform and move the glacier to the left. While deformation of glacier ice in this way has not been documented before, McColl et al. (2010) and McColl and Davies (2013) have used numerical models to show glacier ice can deform under low-applied stress, which in this case is occurring due to slow and continuous failure of the Mueller Rockslide. The Mueller Glacier is no longer providing support within this section of the rockslide.

In the southern portion of the landslide it is unclear to what degree the slope is still supported. Due to a lack of movement data there is also a limited understanding of whether the landslide moves as a cohesive block. Aerial imagery shows minimal change in this area. No changes can be seen within the headscarp, except for the development of several small scarps roughly 150 m below the headscarp. The only major change within the southern landslide zone is the formation of what appears to be small, superficial slope failures at the landslide toe in this location. By 2017, gullying is seen as a result of these superficial slope failures and extends up to 450 – 500 m above the glacier. The glacier in this location has thinned considerably from the earlier imagery and shows an area of depression along the eastern margin at the base of the area of gullying and sediment failure. This has not been documented in other studies on contemporary paraglacial slope failures (Fey et al., 2017, Glueer et al., 2019, Manconi et al., 2017). There is also faint evidence of concentric cracks or crevasses in the ice at the location, which resemble landslide scarps. Increased thinning of the glacier in this area, as well as the presence of the concentric scarp-like bands indicates the landslide is having a detrimental impact on the glacier by causing deformation of the ice surface potentially enhancing melting.

By combining observations and changes in landslide morphology and movement data from the landslide, five different landslide zones were created (Fig. 4.13). Zone 1 which covers the lower northern slope of the rockslide has been fully debuttressed by the glacier and exhibits the fastest movement rates and is colloquially termed as an active zone due to this. Morphologically, Zone 1 has also exhibited the greatest changes as seen within the historic aerial imagery. Several scarps were seen to form between 1986 and 2017 as well as tension cracks within this lower part of the landslide. This was also noted following geotechnical mapping in Chapter 3. The zone is now defined by a rift zone through the centre and another bounding the eastern edge of the zone, where grabens have formed, likely caused by differential rates of movement. The presence of a graben and open fractures below

survey marks 5 and 6 suggests the lower slope near the relic lateral moraines is moving faster again in comparison to survey marks 5 and 6.

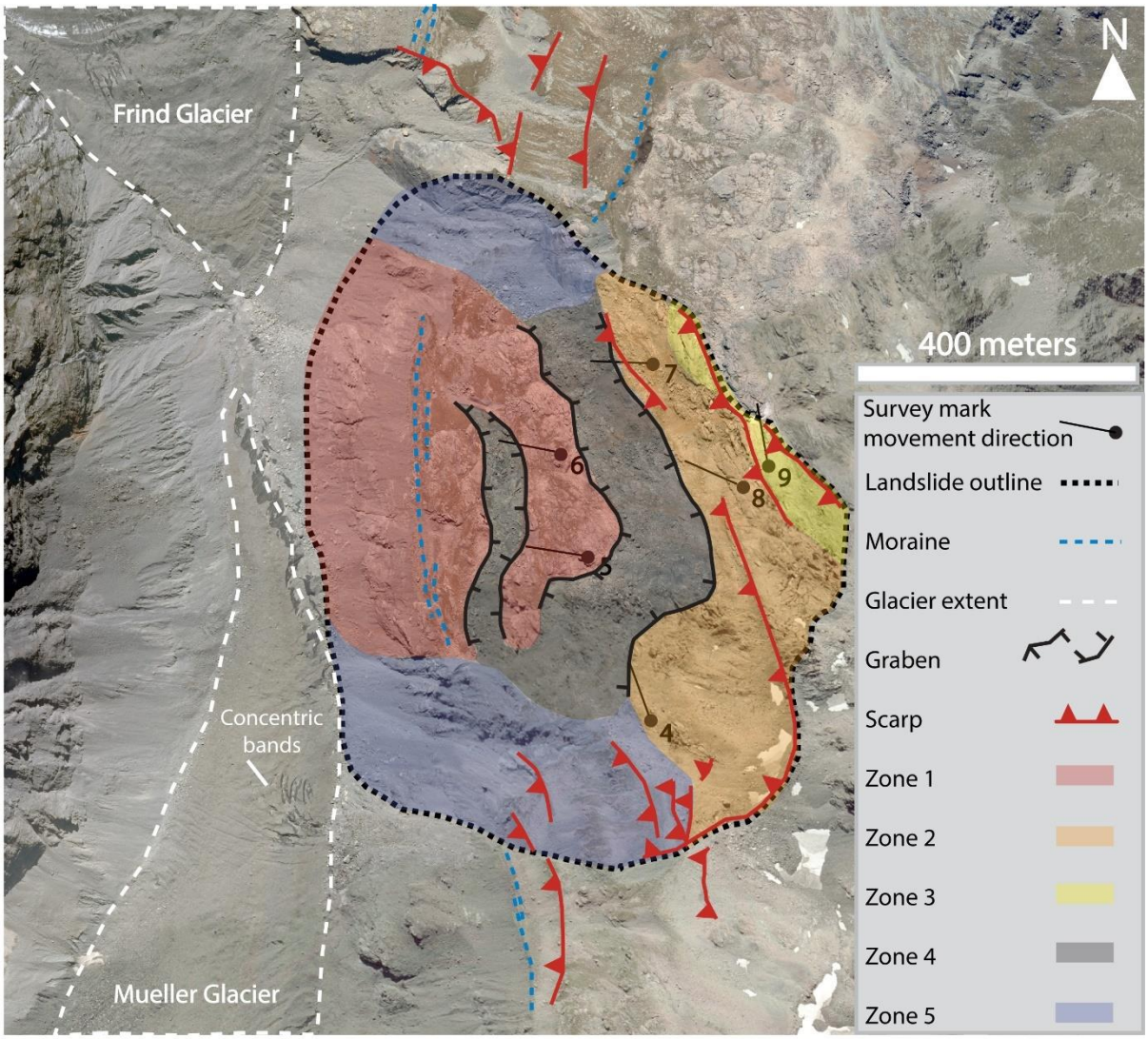

Figure 4-13: Landslide movement zones. Zone 1 is an active landslide zone, Zone 2 and 3 are reactive zones, Zone 4 are graben structures represented by scree and Zone 5 represent sediment slope failures.

Movement within Zones 2 and 3 is reduced in comparison to zone 1 with maximum movement not exceeding 3 m. Zone 2, which includes survey marks 7 and 8 shows similar accelerations in movement to zone 1 at a smaller scale with increased movement rates seen in 2012 and 2019. Consequently, Zone 2 is referred to as a reactive zone, moving in sync with Zone 1. Zone 2 also includes survey mark 4 which was destroyed in 2011 but still records a movement direction towards the northwest, as opposed to down slope to the west. Movement directions of the three survey marks indicates failure of this zone occurs as a result of movement of Zone 1. The geometry and shape of bedrock in comparison to scree also aligns strongly between Zones 1 and 2, indicating the eastern edge of Zone 1 was juxtaposed against the western edge of zone two, approximately 150 m further up slope. Movement direction of survey mark 4 also indicates failure of Zone 2 occurs into the space made

available by the removal of Zone 1, rather than along bedding. Zone 3 which lies above Zone 2 and is represented by the headscarp and cosmogenic sampling area, records the lowest movement rates within the landslide with maximum displacement not exceeding 2 m. Zone 3 is also a reactive zone, with movement occurring throughout the year. There were no obvious correlations in movement between survey mark 9 and survey marks 5, 6, 7 and 8. Movement within Zone 3, which also includes the headscarp crackmeter is also episodic but without experiencing the periods of acceleration the lower zones experience, the zone may have different controls affecting movement than the lower slopes.

The change in movement rates across the landslide may be due to a step-path failure mechanism, with mechanical weakening of the lower slope allowing for failure at a higher rate compared to the upper slope. As noted by Huang et al. (2015), the nature of the step-path failure mechanism allows for fractures to coalesce and joint together from top to bottom under the influence of gravity. This appears to be happening on a large scale across the rockslide. Vertical fracturing seen in the headscarp and graben are also indicative of tensile fractures with form perpendicular to the step-path failure surface.

Zones 4 and 5 represent areas of scree and apparently superficial rotational slope failures. Zone 4 which lies within the grabens between zones 1 and 2 is block filled with no apparent bedding or intact rock structure. Zone 5 which lie along the northern and southern boundaries show evidence of gullying and minor listric scarp development. This is particularly evident to the southern, where several stepped scarps begin below the main arcuate scarp belonging to the Mueller Rockslide. These scarps continue to the south of the rockslide, indicating the potential for future development of the hillslope with continued glacier retreat.

Overall, average movement rates within the various zones of the Mueller Rockslide can be compared to other examples of monitored paraglacial rockslope failures. The Moosfluh Landslide buttressed by the Aletsch Glacier (Glueer et al., 2019, Manconi et al., 2017) has exhibited movement rates of up to 10 m/day without transitioning to a catastrophic failure, much greater than the movement rates exhibited at Mueller Rockslide. In comparison the Marzell Rockslide had maximum movement rates of 1.5 m/year (Fey et al., 2017) which appears to be more in line with movement rates generally observed at the Mueller Rockslide. In comparison, rockfall at the Eiger in Switzerland occurred after almost 60 m of displacement in the year preceding the collapse. When analysing structural controls of each respective failure both the Eiger rockfall and the Moosfluh Landslide occur in anti-dip slopes with bedding dipping into the slope or near vertically. Both of these slope failures had very high movement rates. The Marzell Rockslide and the Mueller Rockslide both occur in dip slopes along downward dipping bedding failure surfaces and have movement rates of only several meters per year at a maximum. It appears that structural controls and bedding impact upon landslide movement rates and could be an indicator for identifying more at risk paraglacial rockslopes susceptible to rapid accelerations in movement or catastrophic failure.

Changes in glacier morphology include reductions in glacier thickness and length. This is particularly evident when comparing imagery from 1960 to 2017 which track the glacier retreating past the rockslide and thinning by ~100 m. Historically, the glacier terminus extended about 5 km down valley to terminate near a set of historic terminal moraines (Fig. 4.1). In fact, numerous dated terminal moraines show the glacier stayed at a relatively consistent length for several thousand years and rarely advanced past this point (Reznichenko et al., 2016). While the length of the glacier has remained consistent, temperature fluctuations and changes in glacier mass balance may have primarily been accommodated through changes in glacier thickness. A second moraine to the north of the rockslide is located further up the slope the interpreted LIA moraines (Fig. 4.13). Although this is not dated it shows the Mueller Glacier would have been substantially thicker in the past, during the formation of the rockslide.

4.4.2 Landslide age and long term movement history

Cosmogenic dating of Mueller Rockslide headscarp has resulted in three exposure ages of 7481 ± 222, 2289 ± 147 years and 1507 ± 146 years taken from 7 m, 10 m and 15 m down the headscarp respectively. This minimum oldest age of 7481 years aligns with many examples of dated paraglacial rockslides in Europe that have since failed catastrophically as rock avalanches. A majority of these studies including Cossart et al. (2008), El Bedoui et al. (2011), Mercier et al. (2013) and Mercier et al. (2017) show failures occurring catastrophically between 6000 and 10,000 years ago following the Younger Dryas. Other studies (Ballantyne and Stone, 2004, Ballantyne and Stone, 2013) identified paraglacial landslide deposits ranging in age from 11,000 to 17,000 years ago which may have formed as a result of the transition from the Last Glacial Maximum (LGM) 20,000 years ago (Kageyama et al., 2001), or more closely following the Younger Dryas. These dates show a lag time between deglaciation and catastrophic failure of several thousand years. Ballantyne and Stone (2013) noted an average lag time of 2000 years between deglaciation and failure with the greatest lag times approaching 5000 years between deglaciation and failure. While the Mueller Rockslide has been progressively failing over more than 7000 years, the rockslide is only now experiencing complete debuttressing and will continue to deform. Catastrophic failure of the rockslide is still possible for thousands of years following current debuttressing.

Long term development of the Mueller Rockslide is not limited to the ~7000 year history of deformation identified with the cosmogenic dating. The top cosmogenic sample, which returned an exposure age of 7481 ± 222 years ago was taken 7 m from the top of the headscarp and does not represent the beginning of landslide movement. Based on this approximate age, it is estimated the Mueller Rockslide began to form following the LGM (~22,000 years ago) or following the ACR which began in New Zealand 13,000 years ago (Putnam et al., 2010).

Average movement rates between cosmogenic samples shows movement rates have been variable with these results mirrored within crack meter monitoring and surveying, particularly within

the lower landslide. Annual surveying shows fluctuations in movement from 0.2 m per year to >5 m per year. In the headscarp zone below where the cosmogenic samples were taken, survey marker 8 and 9 have shown total movement of 1.487 m and 0.374 m respectively, equating to annual movement rates of 148.7 mm and 37.4 mm. In comparison, crackmeter data from Mueller Hut, and the headscarp shows annual movement to be 0.15 mm and 1.7 mm respectively. It is unclear whether this measured expansion of the fracture network near Mueller Hut is associated with landslide headscarp retrogression (i.e. movement of the Mueller Rockslide) or whether it is as a result of mechanical weathering (i.e. localised fracture expansion driven by thermal cycles). Likely, it is a combination of both. However, the headscarp crackmeter shows several instances of sudden extension in the warmer months which could be associated with movement and the crackmeter was installed in a fracture which marks the edge of a toppling block.

Movement monitoring of the rockslide also shows a large difference between movement of the landslide toe and the upper slopes and headscarp zone. Survey marks 5 and 6 moved ~15 m vertically and ~ 14 m horizontally over the 10 year monitoring period. Compared to survey mark 9 which moved a total of 0.374 m, differential movement rates between the top and bottom of the landslide may indicate a delay between movement triggered at the landslide toe before it is expressed further up the slope. However, survey marks 7 and 8 show a similar trend in movement, albeit at a smaller scale, to survey marks 5 and 6 indicating the landslide is potentially moving as a cohesive block at different orders of magnitude. This is particularly evident during the last year where survey marks 5 and 6 increased to 3.4 m total movement, and survey marks 7 and 8 accelerated to 0.42 and 0.32 m. While movement rates at the headscarp are smaller than those at the toe, similar movement trends indicate the potential for an underlying trigger or triggers affecting the entire slope, as opposed to the landslide failing as a series of discrete blocks.

By combining a variety of monitoring techniques, the results indicate that while the Mueller Rockslide has likely undergone a gradual acceleration in movement following its initiation. Detailed monitoring shows movement rates to be both spatially and temporally variable and long term development of the rockslide has likely mirrored this. Not only do changes in movement rate occur annually, crackmeter data shows rapid movement occurs in spring within the headscarp zone, during the period when spring snowmelt is expected as groundwater levels within the hillslope and landslide increase. It can be assumed that similar movement patterns affect the rest of the rockslide at a larger scale, particularly within the lower landslide. While these fluctuations in movement make determining the landslides age difficult, from cosmogenic dating, we can estimate the rockslide is at least ~7500 years old and intiated following the Last Glacial Maximum or Antarctic Cold Reversal. Regardless when the main headscarp formed, development of the rockslide has likely been a long process; Riva et al. (2018), has shown it can take up to 10,000 years for sufficient damage to condition paraglacial rockslopes for progressive failure, prior to movement. Riva et al. (2018) also states that progressive failure is improbable without both the cyclic stresses applied during periods of glaciation and

groundwater changes. In the case of the Mueller Rockslide, it could be the rockslope was preconditioned for failure through slope adjustment associated with the LGM. This preconditioning was then enhanced following the ACR when temperatures increased, and movement of the rockslide began thereafter. Since then, movement of the landslide has been irregular but has resulted in an extensive rockslide complex where differential rates of movement can now be seen throughout the rockslide, represented by Zones 1, 2 and 3. Like the Dryas Rockslide (Grämiger et al., 2017), movement of the Mueller Rockslide began after minor to moderate retreat of the Mueller Glacier and has continued slowly while the glacier was a dominant feature within the valley.

4.4.3 Movement triggers and future development

There are likely several factors controlling the failure of the Mueller Rockslide including the structural controls that were outlined and discussed in Chapter 3. The first and primary control for triggering movement is likely the Mueller Glacier and conditioning of the slope through repeated cycles of glacial advance and retreat. Downwasting of the glacier is predicted to be around 300 m from the LIA to 2019 (Carrivick et al., 2020). Effectively, the rock slope has gone from being buttressed for 30% of its height, to being buttressed by <5% in a short amount of time. Earthquakes are also considered as a potential trigger or preparatory factor for the Mueller Rockslide, particularly due to its close proximity to an active plate boundary fault system. The Alpine Fault, which has a recurrence interval of ~330 years (Berryman et al., 2012) lies within 30 km west of the rockslide. The fault has experienced 24 magnitude 7.5+ earthquakes in the last 6000 years at very regular intervals, almost certainly acting as a preparatory factor to weaken the hillslope. As well as dozens of large Alpine Fault earthquakes, the site is located within a high seismic hazard zone (Stirling et al., 2012) and has likely experienced many strong or very strong earthquakes through its history. The last very strong earthquake in 1717, coincided with the Little Ice Age where the glacier was ~100 m thicker than it currently is. Modelling by McColl et al. (2012) has also shown seismic shaking is amplified on hillslopes without glacial ice. The impacts of earthquakes from the Alpine Fault or other nearby faults in the future will be more substantial now the slope is partly debuttressed compared to earthquakes near the site throughout the rest of the Holocene. The last major earthquakes in the South Island ranging in magnitude from 7.1 to 7.8 (Christchurch earthquake sequence 2010-2011 and Kaikoura Earthquake sequence 2016) did not coincide with increased movement.

Regardless of when movement initiated, landslide movement has accelerated in recent decades from 0.5 mm per year to >4 m per year, following accelerated retreat of the Mueller Glacier and remains high especially within the lower landslide. The impact of a warming climate is not only limited to enhanced glacier retreat; permafrost degradation is another potential cause of hillslope movement, particularly during early stages of movement. Permafrost degradation has been linked to several large rockslope failures as the removal of permafrost reduces internal cohesion within the rock mass and increasing pore pressure (Gruber et al., 2004, Gude and Barsch, 2005, Blikra and Christiansen, 2014,

Keuschnig et al., 2015, Baldis and Liaudat, 2019). Modelling of permafrost in New Zealand shows the potential for permafrost to occur at lower elevations of ~2500 masl (Allen et al., 2009). Given mean annual temperatures 13,000 years ago were on inferred to be 2°C to 2.5°C cooler than they currently are (Vandergoes et al., 2008), permafrost may have been present within the landslide and permafrost degradation may have been an additional factor which has enhanced instability with the rockslope over the life time of the rockslide. Of particular note is the findings by Baldis and Liaudat (2019) in the Andes that show long term permafrost degradation favours deep seated hillslope deformation, such as what is seen at Mueller Rockslide. Studies by Hilger et al. (2020) on the impacts of permafrost on enhancing or reducing hillslope failure deformation shows sites with no permafrost activated shortly after glacier retreat, whereas sites with permafrost (even if it was degrading) showed a delayed response in landslide activation following debuttressing. When applied to the Mueller Rockslide, it could explain the delay between glacier retreat following the ACR or the LGM, and the formation of the Mueller Rockslide.

Further potential triggers or processes controlling rockslide dynamics include rainfall and earthquakes. The site is exposed to very high precipitation totals due to its topographic position in the Southern Alps. Rainfall data showed the site received on average 3800 mm of rainfall per year, although total precipitation is higher due to additional high snowfall in the winter. Rainfall is a common trigger of landslides with several examples of large deep seated slope failures (Crosta et al., 2014, Helmstetter and Garambois, 2010) occurring in high alpine environments as a result of rainfall. However, monitoring of the Mueller Rockslide does not provide a clear link to rainfall as a potential trigger or accelerator of current movement even with high annual rainfall compared to many European sites. Accelerated movement of the rockslide in 2012 corresponded with the lowest recorded annual rainfall of the study, with ~1800 mm recorded that year. This may be due to rainfall not significantly impacting the rockslide or it could be due to a delay in response to triggers by the landslide. Kos et al. (2016) showed a delay of a decade in a large paraglacial rockslope failure. Given the size of the Mueller Rockslide, a delay between preparatory process or trigger is likely and long-term monitoring is required to patterns in movement which can identify this delay period.

Crackmeter monitoring of the headscarp shows some instances of sudden movement occurring during high rainfall periods and several periods of accelerated movement with no rainfall correlation. When modelling progressive deformation within the Spriana Rockslide in Italy, Riva et al. (2018) found both hydromechanical damage caused by ground water and mechanical damage caused by glacial stressors was required to conform with damage seen at the rockslide. Individually, each trigger or preparatory factor (groundwater changes or glacial retreat) were insufficient to cause the rockslide to reach its current state of degradation. Given the size of the rockslide, it is also unclear how quickly the Mueller Rockslide would respond to rainfall and how delayed movement could be. Higher movement rates were noted within the crackmeters in spring from September to December which may coincide with spring snow melt. Crosta et al. (2014) noted an acceleration in movement with spring snow melt

at the La Saxe rockslide. It may be that a combination of spring snow melt and high rainfall events are required to sufficiently act as an aid in triggering movement episodes at the landslide.

Modelling the susceptibility of the rockslope to seismic shaking would provide valuable insight into not only the Mueller Rockslides development, but also investigate the susceptibility recently debuttressed rockslopes will have to seismic shaking. It could also present valuable knowledge on the future development of other paraglacial rockslides. Given the variability in annual and potentially seasonal movement rates, predicting failure based on accelerated movement is not likely to be accurate. Predictions on failure potential may require long term monitoring (decades) to determine whether changes in movement rate are a sufficient precursor of potential rapid failure. Alternatively, glacier retreat and debuttressing may be a sufficient trigger to control these fluctuations in movement and they do not represent increased periods of instability.

Ultimately, failure of the rockslide will continue to be controlled by the step-path failure mechanism. Modelling by Huang et al. (2015) showed failure of rockslopes through step-path failure occurs in four stages. Stage one is elastic deformation, stage two is failure of rock bridges in the lower slope, stage three is progressive failure of rock bridges up the slope and stage four is final compete failure of the slope and block sliding. The Mueller Rockslide is now in stage three, with movement seen in the upper slopes of the rockslide and clear scarp development through the upper slope. Huang et al. (2015) also noted that during step-path propagation, tensile stress accumulates in the main landslide body and the formation of tensile fractures (vertical fractures) eventually happens and the landslide body is split in four zones, separated by tensile fracture zones. This is seen at Mueller Rockslide with tensile zones at the toe, mid slope and headscarp and four discrete zones created along the rockslide body.

4.4.4 Hazards associated with paraglacial landsliding

There are several potential hazards which could develop if further movement of the rockslide was to occur. These are not only limited to the immediate hazard posed by the landslide itself which was discussed in Chapter 3; regardless of whether the landslide continues to develop slowly or fail rapidly, ongoing movement will continue to lead to fracturing and growth of the landslide retrogressive zone and may also lead to damming of the valley.

The most immediate hazard associated with continued or current landslide development is the continued retrogression of the headscarp and formation of tension cracks and open fractures. Although changes in headscarp morphology seen within the aerial imagery are minor, movement monitoring of the headscarp and retrogressive zone shows between 0.3 and 2.4 rn of movement in the last decade. Crack meter monitoring shows gradual opening of fractures at 0.3 mm to 1.5 mm per year near Mueller Hut and within the headscarp respectively. Continued development of the headscarp and retrogressive zone will increase the chance of damage or danger to Mueller Hut and those who visit the area. Mitigation measures may need to be considered in the corning decades at the site.

The second major hazard excluding the landslide itself is the formation of a landslide darn. Landslide darns traditionally form following rapid landslide failure. It is their unpredictable ability to remain stable or fail that makes them a particular hazard, with 50% of landslide darns forming and failing within 10 days (Schuster and Costa, 1986, Costa and Schuster, 1988) and 80% failing within a year (Fan et al., 2020). Estimating the chance of landslide darn forming is difficult, particularly given the unusual way in which it may form. Traditionally, landslide darns form through rapid failure such that erosive action (i.e. river erosion at the base of the valley) is unable to act upon the landslide. Stefanelli et al. (2016) provides a summary of way of estimating whether landslide darn formation will occur by presenting a summary of several indices which can be used to estimate dam formation probability. The annual constriction ratio (ACR) (Swanson et al., 1986) is presented as

$$ACR = \log\left(\frac{Wv}{V}\right)$$

Where velocity (V) is presented as m/s and valley width is presented in m. An ACR value of <4.26 is required to form a landslide dam. Based on the ACR, the Mueller Rockslide would not form a landslide dam at current movement rates (~6 m/a). However if the Mueller Rockslide was to fail rapidly as a rock avalanche and an estimated velocity of 50 m/s was used, the rockslide would form a landslide dam. Stefanelli et al. (2016) also presents a link between landslide volume and percentage of landslide dams which formed and were stable, formed and were unstable or didn't form. For landslides over 100 Mm^3, 69% formed stable landslide dams whereas 8% did not form landslide dams.

4.4.5 Review of landslide monitoring methodologies

The object of this thesis was initially not to assess the viability of monitoring methodologies as the methodologies used were commonly available and utilised in landslide research. However, this study has highlighted the unique application of multiple, relatively inexpensive methodologies which combined have provided valuable insight in paraglacial rock slide development. Methodologies were chosen to provide movement information at differing spatial and temporal scales i.e. crackmeters were used to analyse movement of a specific fracture or scarp at minute to hourly interviews, compared to annual GPS surveying which provided an overview across the landslide on a yearly basis. This allowed for a holistic, encompassing assessment of landslide movement for an extended period of time with minimal fieldwork required to obtain monitoring information.

However this methodology is not without flaw. Limited samples were obtained from cosmogenic dating from an inferred headscarp. This small dataset from a localised area makes it difficult to draw a conclusion on the onset of rock slide failure and consequently, cosmogenic dates on scarp formation are a guide only. For the annual surveying, access to the landslide is difficult and consequently, there is limited data available for the southern half of the landslide, limiting our understanding of how movement occurs in the area still partially buttressed by the glacier. For the crack meter data, the equipment is susceptible to damage and placement should be carefully considered to minimise the risk of equipment breaking.

For all of these methodologies there was limitations on their use or application, but combined the complimented other methodologies are assisted in supplementing the shortcomings of other methods. These specific methodologies could be combined or alternatively more consideration should be placed on developing a suite of the methods which are conveyed across a variety of spatial and temporal scales.

4.5 Conclusions

By combining a new and novel range of monitoring methodologies, we present a detailed record of the movement and development of the Mueller Rockslide. Following a period of conditioning by prehistoric glacier retreat, the rockslide began to develop at minimum ~8000 years ago following conditioning from the Antarctic Cold Reversal and Last Glacial Maximum. Cosmogenic dating and crack meter monitoring show movement of the rockslide to be episodic and ranging from mm per year to m per year at its current rate of movement. From 1960, the landslide has continued to deform and begin to infill the Mueller Valley as the Mueller Glacier has retreated. Between 1986 and 2017 the slope underwent near complete debuttressing of the Mueller Glacier and has moved approximately 50 m into the valley, based on displacement of lateral moraine ridges. Detailed surveying of the rockslide over the last decade has shown movement to be variable and inconsistent with no discernible trigger for accelerations in movement rate, including no links with high annual rainfall or earthquakes. The lower landslide shows the greatest movement with a maximum of ~14 m horizontal movement and ~15 m vertical movement seen since 2010. From 2017, crackmeter monitoring within the retrogressive zone of the rockslide shows gradual expansion occurring from daily changes in temperature. Accelerations in movement are seen within the rockslide headscarp every spring, likely caused by spring snowmelt. Glacier retreat is considered a primary trigger for landslide movement, as indicated by increased movement coinciding with increasing glacier retreat although high rainfall and snowmelt in spring likely enhance movement.

Finally, this study presented an overview of the potential impacts paraglacial landsliding can have on the surrounding environment. Deformation of the rockslide toe has led to deformation and potentially accelerated melting of the Mueller Glacier. Continued movement of the rockslide may also lead to the complete blocking of the Mueller Glacier valley, causing a landslide dam should it occur. Monitoring of the landslide and retrogressive zone identified movement throughout the hillside, including under Mueller Hut of at least 0.3 m over the last decade. Continued deformation is likely in response to continued glacier retreat and may continue for several thousand years as indicated by other examples.

4.6 Acknowledgements and funding

We wish to thank Albert Zondervan and Julia Collins from GNS Science and Kevin Norton from Victoria University of Wellington for assisting with the running the cosmogenic samples. We also thank Florian Strohmaier, Daniel Draebing and Marc-Andre Brideau for assisting with crackmeter

installation and maintenance. Pat Kailey, Natasha Reznichenko, James Fay, Michal Brezny, Simon Cook, Jana Eichel, Tim Stahl, Jan Blahut, Lorraine Cook, Louise Vick, Michael Cronin, Anna Sintenie, and Simon Stewart provided field assistance for the surveying.

4.7 Contribution and summary for thesis

This chapter contributes to the knowledge of paraglacial landslide development and movement drivers in several ways. A novel suite of monitoring methodologies were combined successfully and provided information on the long-term development and evolution of a paraglacial rockslide from its formation through to the final stages of debuttressing. Not only can paraglacial landslides develop thousands of years prior to complete glacier retreat and debuttressing but their movement rates can be highly episodic and may make estimating future failure potential difficult. Regardless of whether the landslide develops into a catastrophic failure, growth of the landslide toe in recent decades is likely to continue and potentially block the Mueller Glacier valley. This highlights that the hazards associated with paraglacial landslide developments are not isolated to failure of the landslide itself; landslide dams, outburst floods and increased fracturing within the retrogressive zone are all likely to act as a hazard in the future.

5. Paraglacial adjustment of sediment slopes before and immediately after glacial debuttressing

Summary of chapter 3 for thesis.

While Chapters 3 and 4 focused on quantifying the response of rock slope failures to glacier retreat, Chapter 5 focuses on assessing the response of sediment slopes. This chapter presents the first findings of the response of sediment slopes to glacier retreat during the final stages of debuttressing. The objective addressed in this chapter include assessing spatial and temporal patterns in paraglacial sediment slope development during and immediately after glacier retreat. To achieve this objective, and to determine underling triggers of landsliding, a detailed four year period of daily monitoring is outlined and compared with rainfall data. This system of monitoring using daily timelapse images not only allowed for the quantification of movement; timelapse imagery provided a continuous and detailed visual aid for assessing changes in hillslopes, glacier and landscape response.

This chapter has been published as a research article within Landslides as:

CODY, E., ANDERSON, B., MCCOLL, S., FULLER, I. & PURDIE, H. 2020. Paraglacial adjustment of sediment slopes during and immediately after glacial debuttressing. *Geomorphology*.

5.1 Abstract

Daily time lapse imagery and pixel tracking was used to monitor and track spatial and temporal changes in sediment-mantled hillslopes, during and immediately after glacier retreat in the Fox Glacier/ Te Moeka o Tuawe valley, New Zealand. Observations from 2014 to 2018 of the Fox Glacier and surrounding hillslopes show hillslope failure is primarily coincident with, and triggered by, glacier retreat with rainfall accelerating movement of the hillslope. During glacier retreat, failure of the hillslope primarily occurred through sediment sliding, internal deformation of the sediment and occasional surficial debris falls, flows and avalanches delivering approximately 9.2 M m^3 of sediment directly to the underside of the glacier over the study period with a maximum daily averaged movement of 0.4 m per day of the main sediment mass. Following debuttressing, hillslope failure became dominated by localised rainfall-induced debris flows which initiated gullying of the sediment-mantled slope. Ongoing instability of the slope and associated movement is maintained by toe erosion from the Fox River and melting dead ice, while continued rapid failure is facilitated through localised debris flows. The tracking of temporal and spatial changes of sediment-mantled hillslopes during glacier retreat has shown broad-scale hillslope response to occur quickly within days of rainfall or accelerated glacier retreat, particularly during summer. Debris flows, commonly thought to be a dominant erosion process within paraglacial environments, only occur following complete debuttressing and are supply-limited, only occurring after sediment sliding has occurred. Unlike many other case studies, sediment connectivity immediately following glacier retreat is high due to a lack of storage space and high rainfall inducing mass movements, efficiently delivering hillslope sediments to the proglacial stream channel. Attempts to quantify displaced volumes of sediment from paraglacial systems are likely underestimated due to a) a lack of focus on the early and latter stages of debuttressing b) a reliance on debris flows being a primary transport mechanism, and c) sediment being delivered sub-glacially rather than supra-glacially, further enhancing connectivity.

5.2 Introduction

Glacier retreat and ice loss in alpine regions has commonly been seen following periods of climate warming (Oerlemans et al., 1998, Purdie et al., 2014). Anthropogenically enhanced warming has led to accelerated retreat and down-wasting of many glaciers (Marzeion et al., 2014, Roe et al., 2017). One consequence of this ice loss is destabilisation of adjacent hillslopes. Paraglacial hillslope failures (i.e. those which develop following periods of glaciation) are recognised as a significant geomorphic process in many alpine areas (Ballantyne and Benn, 1994, Curry, 1999, Ballantyne, 2002b) as they deform and modify mountains (Crozier and Glade, 2005b), increase sediment input to glaciers (Hewitt, 2009, Reznichenko et al., 2011), act as a primary source for sediment cascades (Church and Ryder, 1972, Crozier, 1986, Korup, 2005b, Korup, 2005a), and present a significant natural hazard (Purdie et al., 2015). In recent decades, there has been an increase in paraglacial landslide activity in alpine areas through increased ice loss and glacier retreat (Geertsema et al., 2006, Deline et al., 2015a, Coe et al., 2017), with many of these fortunately occurring in unpopulated areas. However, as the rate

of paraglacial landslides increases globally, coupled with increasing human population in alpine areas, the hazard posed by paraglacial landslides is increasing. To allow for better planning and risk mitigation, research is required to better understand how these landslides form and effect processes in their surrounding environment.

Paraglacial slope failures affect both rock and sediment slopes. In many cases, these landslides evolve through time, progressively failing as hillslope strength degrades through external forcing such as weathering, earthquake shaking, rainfall and glacier retreat (Crozier, 1986). Following glacier retreat and progressive failure, many paraglacial landslides have since accelerated and failed catastrophically as rock avalanches (for rock slope failures) (Holm et al., 2004, Geertsema et al., 2006, Owen et al., 2010, Coe et al., 2017) or in the case of sediment slopes, through debris flows (Blair Jr, 1994, Curry and Ballantyne, 1999, Ballantyne, 2002b, Curry et al., 2006, Curry et al., 2009a). These studies of past events rock and sediment slope failure events have reinforced the notion that glacier retreat commonly prepares hillslopes for failure even if eventual failure can occur hundreds or thousands of years following slope-debuttressing. However, studying prehistoric or historic events makes it difficult to analyse pre-failure conditions and the evolution of stability conditions and hillslope failure processes.

More recently, studies have investigated contemporary paraglacial hillslope failures, which have begun to form or have accelerated as a response to Little Ice Age (LIA) glacier retreat. Several observations of sediment slopes which have undergone complete debuttressing show adjustment is rapid with debris flows and gullying leading to almost complete removal of superficial sediment within decades of retreat (Blair Jr, 1994, Curry et al., 2006, Hugenholtz et al., 2008b, Curry et al., 2009a). Moraine deformation at the Athabasca Glacier, British Columbia, is one of the few studied examples of contemporary paraglacial sediment slope failure currently undergoing debuttressing by its supporting glacier (Hugenholtz et al., 2008b) and shows failure occurring primarily through rotational sliding in contrast to debris flow dominated systems identified by Curry et al. (2006), Blair Jr, (1994) and Curry et al. (2009). So far, there are an insufficient number of sediment slope failure case studies to draw conclusions on whether sediment sliding is a normal or exceptional response to glacier retreat. It is also unclear what impact sediment delivery from deep seated moraine deformation may have on sediment connectivity and sediment cascades compared with debris flows, which are generally smaller and mobilise more rapidly. While paraglacial sediment slope failures are known to have significant localised effects in the immediate failure vicinity, they can also impact on sediment delivery and transport processes downstream between hillslopes and glaciers as well as hillslopes and rivers (Cossart, 2008). An assumption may be that increased slope failure following glacier retreat leads to increased connectivity between hillslopes and glaciers or rivers allowing for enhanced transport of sediment between systems. However, several studies (Cossart, 2008, Lane et al., 2017) indicate sediment connectivity is comparably low during paraglacial periods due to the glacial sediment commonly resisting entrainment, contradicting the fundamental concept underlying the paraglacial concept where sedimentation adjustment rates are accelerated during and after glacier retreat (Church and Ryder,

1972). Instead, Lane et al. (2017) proposed connectivity may be episodic and may be influenced by temporal and spatial changes in mass movements within the sediment slope.

To gain a more thorough understanding of how paraglacial sediment slope failures occur and their impact on connectivity, quantification via monitoring of process is needed. With the exception of the study on the Athabasca Glacier moraine, very little long term monitoring of sediment slopes has been done and there is a lack of quantitative information that can shed light on landslide movement rates, drivers and mechanisms. Is glacier retreat a primary trigger and what impact do other common triggers like earthquakes and rainfall have on inducing sediment slope failure (as debris flows or as rotational sliding)? Finally, the adjustment of paraglacial sediment slopes has been shown to be rapid (Ballantyne and Benn, 1994, Curry and Ballantyne, 1999, Ballantyne, 2002a), occurring within decades of retreat. In the latter stages of paraglacial adjustment slope angle, vegetation availability and type, and slope material type all play an important role in slope adjustment towards stability (Eichel et al., 2018). While this process can occur through solifluction in alpine areas (Draebing and Eichel, 2018), no studies have investigated how this adjustment occurs in temperate paraglacial environments which are less susceptible to freeze-thaw processes.

This study addresses these gaps in understanding by presenting new observations and analysis of sediment slope failures occurring at the temperate (43°S) Fox Glacier/ Te Moeka o Tuawe, New Zealand (hereafter Fox Glacier). Daily time-lapse camera imagery and pixel tracking were used to monitor temporal and spatial changes in hillslope deformation from 2014-2018. The objectives of this study are:

- To identify internal and external factors affecting the formation and development of temperate, maritime paraglacial sediment slope failures. As a result of this, we aim to identify various slope deformation processes affecting the hillslopes adjacent to Fox Glacier terminus to determine how paraglacial sediment slopes deform and interact with other geomorphic systems (glaciers and rivers) during and immediately after glacier retreat.
- To track deformation rates during and after glacier retreat to compare rates of change with known adjustment rates for paraglacial sediment slopes and investigate how off-slope sediment delivery impacts sediment connectivity and other geomorphic systems (glaciers and rivers).

5.2.1 Study site

Fox Glacier is a temperate, maritime glacier located within Westland Tai Poutini National Park, New Zealand (Fig. 1). Covering an area of 32.5 km^2, the glacier descends from a starting elevation of 2900 m asl in the Southern Alps/Kā Tiritiri o Te Moana westward for 12 km before terminating at an elevation of ~ 350 m asl (Purdie et al., 2008). The study site focuses on the area around the terminus of the glacier, extending from Straight Creek to the icefall and the hillslopes on the southern side of the valley (Fig. 1).

Two large landslides are included within the study. The largest of these is lower Sam Slip, which has been recognised and described as a large rotational composite slide with an arcuate headscarp, bounded by two streams. The lower slope of Sam Slip is heavily mantled with sediment which has shown considerably failure in the last few years. Although the there is a history of displacement at Sam Slip, it is the lower sediment slope which is the focus of this study and is herein referred to as lower Sam Slip. The second sediment slope failure Passchendale Slip, has also exhibited evidence of failure within the sediment slope. Unlike Sam Slip, Passchendale Slip has no defined headscarp and it is unclear whether bedrock failure is involved at this location.

Unlike previously studied paraglacial environments, the site is not susceptible to permafrost or other periglacial processes. Fox Glacier township at an elevation of 180 m asl has an average temperature of 11.5°c. The West Coast region is an area with high rainfall; the closest long-term rain gauge, in Fox Glacier township (3 km away, 200 m asl), measured a mean annual precipitation total of 4548 mm (station 4069: 1951-1980; Cliflo, NIWA). However, the precipitation at Fox Glacier terminus is higher than that due to the strong orographic precipitation gradient. Mean annual rainfall within the Fox Glacier terminus area (study site) totalled 7382 +/- 369 mm with precipitation measured from 2/09/1981 to 4/01/1983 (Kerr et al., 2018).

High glacier mass balance turnover as well as a steep and tightly confined valley geometry mean Fox Glacier has a high velocity of as much as 6 m/day (Herman et al., 2011). These conditions mean the glacier is sensitive to climatic variations and the terminus reacts quickly to changes in mass balance, with a reaction time of 3-4 years (Purdie et al., 2014). While the glacier has retreated 2.8 km since it was first mapped in 1893, retreat has been interrupted by several periods of advance (Sara, 1968, Purdie et al., 2014). Following the most recent stage of advance in 2009, the glacier has retreated by several hundred metres (Fig 1.C) and is now at its shortest in recorded history.

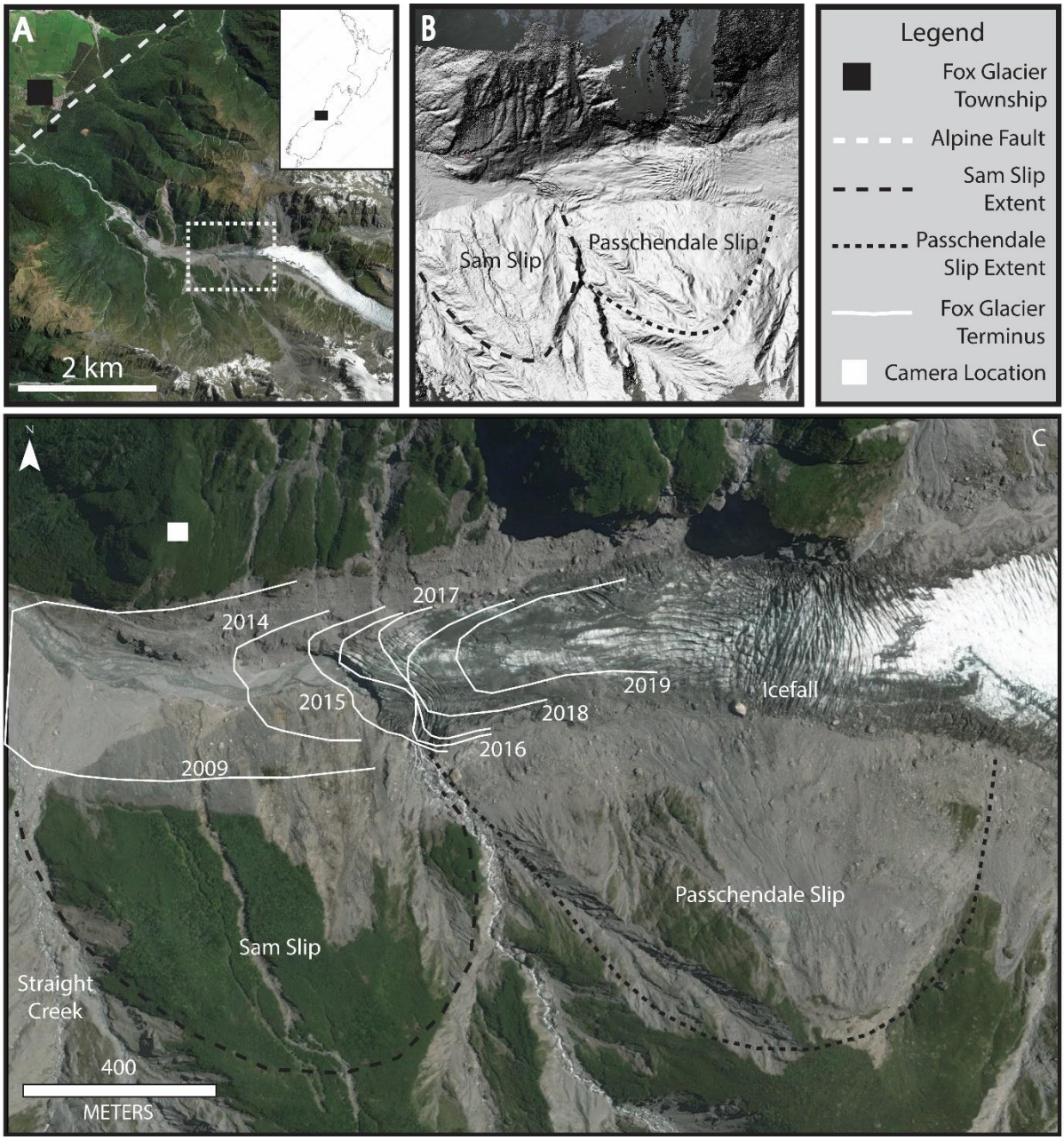

Figure 5-1: Fox Glacier and surrounding area. A) Fox Glacier inset, Alpine Fault and Fox Glacier township. B) Hillshade of Fox Glacier valley showing relief and scarps of Sam Slip and Passchendale Slip. C) Fox Glacier with marked history of glacier terminus, camera location and landslide boundaries.

The study site at the terminus of Fox Glacier extends from Straight Creek (lower left corner) to the Fox Glacier icefall over an approximately 5 km^2 area. The site has an elevation change of ~300 m from the icefall to the terminus with an average slope angle of 21° (30° through the icefall area). Close proximity (<5 km) to the Alpine Fault, which marks the boundary of the Australian and Pacific Plates, means bedrock within the valley is mostly composed of schist. Although glacially derived sediments - which cover many hillslopes - consist of schists, greywackes and other metasedimentary rocks sourced from the east. Hillslopes on the true-right (north) of the terminus are predominantly rock or partly till covered with slope angles from 20° to vertical. Slopes to the true-left (south) are mostly till covered and

have slope angles of 15° to 50°. The glaciogenic sediments are poorly sorted and sub-angular to sub-rounded, with some clasts exceeding several metres in length.

Following the LIA, glacier retreat of over 3 km (Chinn, 1996) has exposed steep, sediment-mantled slopes and lateral moraines. lower Sam Slip. A detailed site investigation of natural hazards in the valley was conducted in 1994, which identified several small slope failures within the valley, as well as noted the existence of a large slope failure between “Straight creek and Boyd Creek” (Hovius, 1995), in what is now identified as Sam Slip. Exposure of the lower slope below the glacier trimline began in 2008 as the glacier retreated (Purdie et al., 2014). A large headscarp ~700 m above the glacier (Fig. 2) marks the upper most boundary of the landslide with vertical displacement of ~100 m measured at the headscarp. Within the valley floor, several alluvial fans have formed from the base of each stream and talus cones have built up below several rockfall zones on both sides of the valley.

The site has a history of hazardous rockfall; in 2014 and 2019 show rockfalls narrowly missed climbing parties on the glacier. Studies on rockfall hazard indicate a greater risk as the glacier continues to downwaste increasing runout potential (Purdie et al., 2015, Roy et al., 2015). Debris flows, flooding and icefall are also known hazards within the area, a result of a highly dynamic environment with paraglacial adjustment amplifying these effects. In 2019, the road to the glacier was washed out as a result of debris flow activity from a nearby stream and will not be rebuilt due to continued debris flow activity.

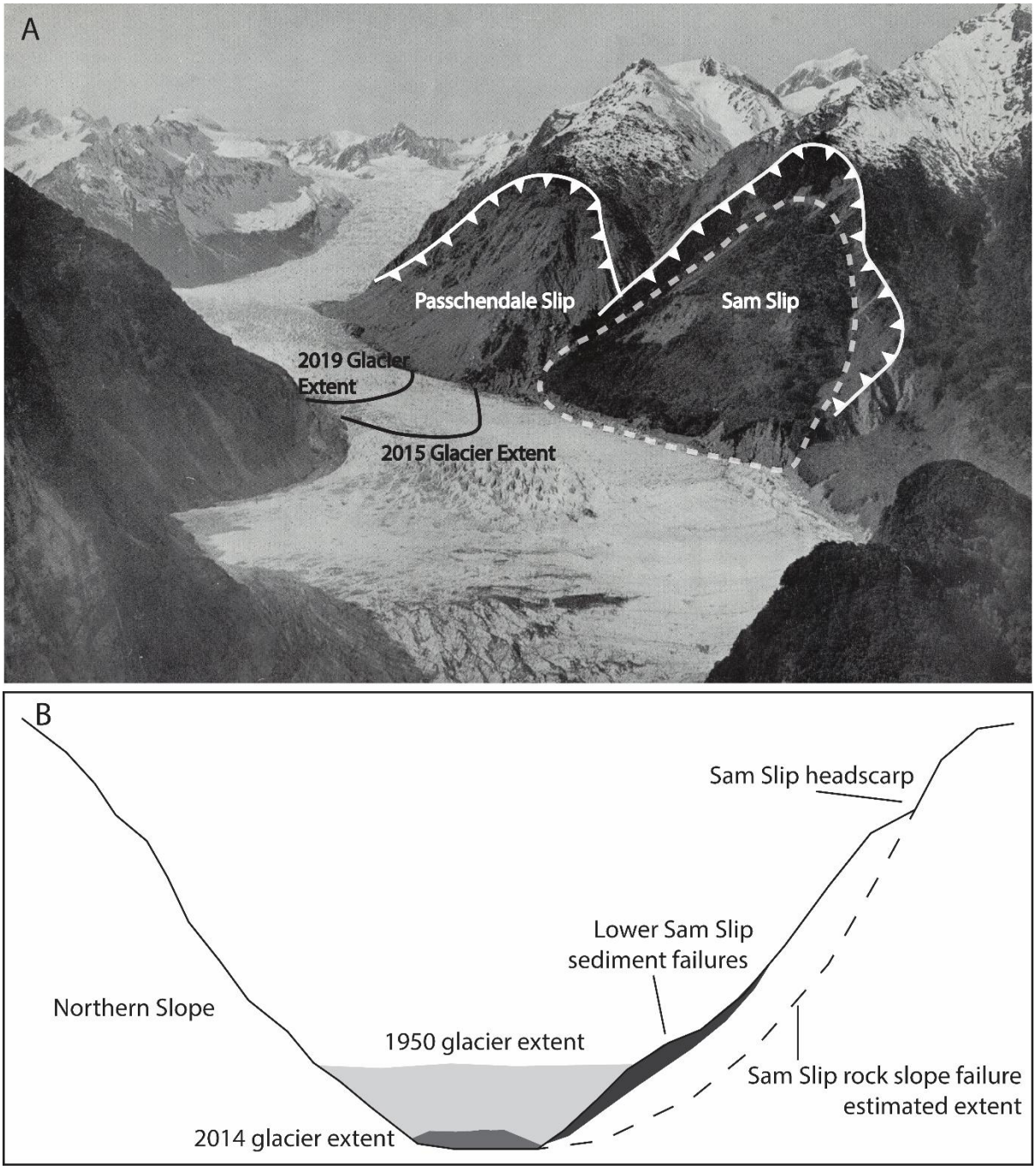

Figure 5-2:A) Sam Slip (white dotted line), Passchendale Slip and Fox Glacier in 1950. Image by Trevor Chinn. B) Schematic valley profile cross section showing historic and present glacier extent, Sam Slip and the shallow sediment failures which are the focus of this study.

5.3 Methods

5.3.1 Timelapse imagery

In January 2014, a time-lapse camera was installed to monitor the behaviour and retreat of the Fox Glacier terminus and the activity of lower Sam Slip. The images revealed major adjustments of the surrounding hillslopes in response to the glacier retreat. This research presents observations and measurements of the hillslope responses captured by this camera.

The camera was installed at 450 m asl looking across the glacier terminus to the toe of lower Sam Slip (Fig 1). As the glacier continued to retreat, the camera was rotated in March 2015 and captured the icefall and Passchendale Slip. Images were taken at hourly intervals using a Nikon D5100 camera with a 28 mm lens with the focus fixed at infinity. The camera was controlled using a custom-built timer and a Raspberry Pi computer board, which uploaded the images to a remote server via a wireless network. The camera was powered by a solar panel and, as it was sited on a south-facing slope, it did not receive any direct sunlight for approximately 3 months during winter. At times during this period there was not enough power to run the camera system and there are some gaps in the record during July - August 2014 and June to October 2016. The images were captured with a fixed aperture of f11 and recorded in raw format (Nikon NEF).

Figure 5-3: A) Camera views, B) Passchendale Slip points and C and D) lower Sam Slip points.

5.3.2 Digital Elevation Model

Two digital elevation models (DEMs) were produced or used in this study to support the time-lapse image interpretations and measurements. The first was obtained using Structure from Motion photogrammetry in 2015 and was used in primary analysis for georeferencing of the pixel tracking. The second was obtained in 2018 using LiDAR and was used to evaluate the net topographic changes of the monitored hillslopes.

Geotagged airborne and ground based photographs were used to produce the 2015 Structure from Motion (SfM) derived DEM with the images processed in Agisoft Metashape using a standard workflow. On 14 March 2015, 4 days after camera installation, an airborne photography survey, which included the Fox Glacier terminus area, was undertaken. A total of 55 images of the study site were

captured using three different cameras: Nikon D800E with 35 mm lens, Nikon D5100 with 50 mm lens, and Nikon D200 with a zoom lens. Camera positions were measured with a Septentrio PolarX GNSS receiver and the image acquisition time with a custom-built timer at 1 m precision, using the same method as Vargo et al. (2017). The high altitude of the flight (~3000 m asl) meant that the positioning of this DEM without GCP's was not sufficiently accurate. The hazardous and mobile nature of the study area meant that only four GCP's could be obtained (their position measured with a Trimble GeoXH reciever). An additional nine points were derived from an orthophoto and DEM captured in April 2015 (Gomez and Purdie, 2016). This 2015 DEM does not cover the Passchendale Slip area, so the nine control points are used to georeferenced the larger DEM. The uncertainty of the alignment using these nine points is 1.15 m and an independent test against the three GCP's shows an overall accuracy of 1.35 m.

The 2018 DEM was created using aerial LiDAR with a Leica RCD30 80MP RGBN image sensor and a Leica ALS60 LiDAR sensor. Control was provided by GNS Science using a Leica GS18 GNSS base and rover, Riegl Z-420i Terrestrial Laser Scanner and a MapTek XR3 Terrestrial Laser Scanner. In total 20 measured positions were used for terrestrial laser scanning and positions corrected against LINZ COR QUAR. DEM uncertainty equated to 0.1 m.

Both the 2015 and 2018 DEMs are in the same vertical reference system (NZVD2016) but due to differences in how each DEM was acquired, there are minor differences in elevation. To account for this, the average difference between DEM's was determined from 10 stable points with a mean difference of 1.2 m and maximum difference of 1.6 m noted between each DEM.

Differencing of DEMs to calculate geomorphic change was completed using Geomorphic Change Detection (GCD) (Wheaton, 2015). DEM differencing (DoD) was completed using both DEMs with a minimum level of detection calculated using error values from both DEM's. Root Mean Square Error (RMSE) for differencing equated to 1.2 m. A conservative value of 1.5 m was used for the GCD.

5.3.3 Pixel tracking

To analyse movement of the slope, individual pixels were tracked in 2D and 3D space by overlaying the georeferenced 2015 DEM. Pixels were selected that were located on easily trackable features including large boulders or areas of discolouration. Movement tracking was completed using Pointcatcher – freely-available pixel-tracking software which allows movement data to be analysed semi-autonomously and derives three dimensional coordinates for selected geomorphic features (James et al., 2016) by projecting selected pixels onto a DEM.

Using time-lapse imagery, one image per day was selected from the same time of day (1200 hours.) to maintain consistency in lighting for feature identification. Images of low quality e.g. due to low cloud cover were not used. In these situations, either the image (and day) was excluded or an image at 1100 or 1300 hours was selected if the cloud cover was absent.

In total 12 points were selected within the lower Sam Slip imagery and 14 points from the Passchendale imagery with a further 10 points selected which were considered to be static. Static points were used for image registration although 3 were found to actually move through the course of the study (and were consequently excluded for image registration purposes) and were instead included within the Passchendale points. To capture movement across the majority of lower Sam Slip within the field of view, points were grouped in an approximate 3x3 pixel grid initially, on easily trackable features. Additional points were added at the top of the imagery as failure occurred and new trackable features moved into frame. Once points moved to the toe of the slope and disappeared into the river or glacier tracking ceased. Similar methods were applied within the Passchendale area however, due to slope orientation and rock outcrop locations, points were grouped into two rows through the centre of the imagery and then additional points were added up the slope. Ultimately, feature visibility was a major deciding factor in its suitability as a trackable feature and was the deciding factor in final point location. Larger features were preferred and their movement was considered to be representative for the broader slope failure.

A combination of manual tracking and automatic tracking was used. When picking manually, a three-pixel error was used to account for error when selecting trackable features due to changes in lighting. To account for camera movement, image registration was completed using stable points with Pointcatcher. All images passed a Chi-squared test for normality following analysis with a mean RMS for static point residuals of 0.59 pixels.

To track pixels in 3D space for lower Sam Slip and convert displacement units from pixels to metres, DEM alignment with the tracked pixels was completed manually using specific features identified within the 2015 DEM and within the images. Reliable alignment of the DEM was not possible within the Passchendale imagery due to an extremely oblique camera angle. Instead movement of points was tracked using changes in x-y coordinates for each pixel with the method proving adequate for the analysis of relative movement rates.

5.3.4 Rainfall data

To investigate the relationship between slope movement and external forcing (rainfall), daily rainfall data were collected. The closest automatic rain gauge to the Fox Glacier terminus operating over the study interval was at Franz Josef airport, 16 km to the north at an elevation of 170 m. This site records rainfall hourly, and rainfall annual totals average 4125 mm (2004-2014, data from cliflo.niwa.co.nz). Given the close proximity of the sites, the timing of rain events, according to previous measurements of Kerr et al. (2018) is very similar and can be considered simultaneous (Kerr et al., 2018). However, given the very strong rainfall gradients in the area, it is presumed there is more rainfall at Fox Glacier terminus than Franz Josef airport. A rain gauge was installed in Fox Glacier valley near the top of Mills Creek in 2019, and here it was used to compare differences between rainfall at between Fox Valley and Franz Josef Airport over a 48 day period (7/02/2019 – 26/03/2019). This was done to

further evaluate whether the Franz Josef rain gauge can be used as a reliable representation of rainfall at Fox Glacier for the study period.

Comparisons between Fox Glacier and Franz Josef airport rain gauges show rainfall is higher at Fox Glacier over the same time period. Total rainfall over the 48 days at Fox Glacier was 1120.8 mm (Table 1) with almost half of this total coming from a rainfall event at the end of the survey period (Fig 4.) There were three days in which Franz Josef airport received more rainfall than Fox Glacier; on the 26th February, 5th March and 7th March. From the 12th February to the 15th February, malfunction of the Fox Glacier rain gauge meant no rainfall was recorded and this data was not used in the analysis.

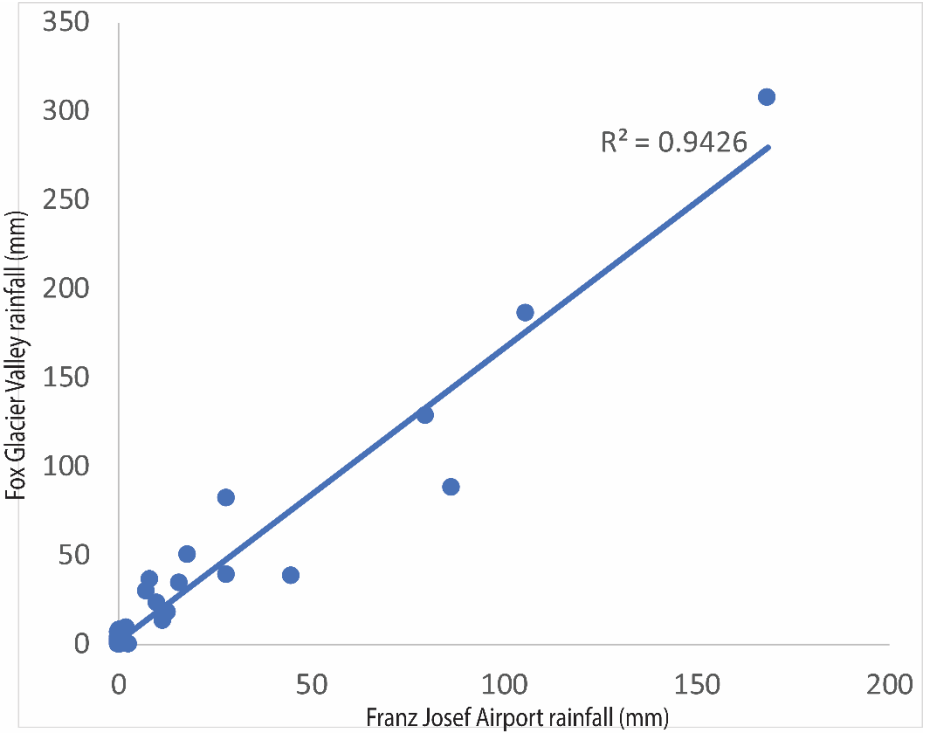

Figure 5-4: Rainfall comparisons between Fox Glacier (Alpine Garden) and Franz Josef airport. In total, Fox Glacier valley received 431 mm (63 %) more rainfall than Franz Josef airport.

Table 5-1: Rainfall comparison between Fox Glacier and Franz Josef Glacier.

	Fox Glacier	Franz Josef Glacier
Total Rainfall	1120.8 mm	689 mm
Average Daily Rainfall	25.5 mm	14.6 mm
Ratio Rainfall/ No Rainfall	11/43	26/49
Maximum Daily Rainfall	307.6 mm	168.4 mm
Maximum Daily Rainfall (when other site had no rain)	6.8 mm	0.6 mm

5.4 Results

5.4.1 Lower Sam Slip

Time-lapse imagery

Time-lapse imagery of lower Sam Slip showed substantial slope movement over the monitoring period, as the glacier terminus retreated past the slope. Sediment sliding was identified as the primary failure process within lower Sam Slip with localised debris flow activity increasing towards the end of the monitoring period. Once the glacier had retreated beyond lower Sam Slip and completely debuttressed, river erosion and melting of buried ice led to toe undercutting of the slope and continued movement of the slope.

Time-lapse images (Figure 5) and time-lapse videos (supplementary materials) of lower Sam Slip showed the dominant landslide failure mechanisms changed through time from debris or sediment sliding, to debris fall and debris flows. By the end of the study, sliding of sediment was localised and controlled by melting of detached ice under the slope and through toe undercutting by the Fox River. Periodic toe undercutting of the lower sediment slope occurred from December 2014 through to the end of the time-lapse imagery. Field work at the site in 2018 showed undercutting was ongoing combined with river incision and evidence of minor scarp development (<10 cm) within the lower slope.

Debris flows were uncommon on the slope prior to August 2014. After this date, several large debris flows were seen in the upper slope. Evidence of gullying was seen following debris flow activity. Several smaller debris flows were identified which do not induce gullying. Rarely, singular debris falls occurred from undercutting of the slope.

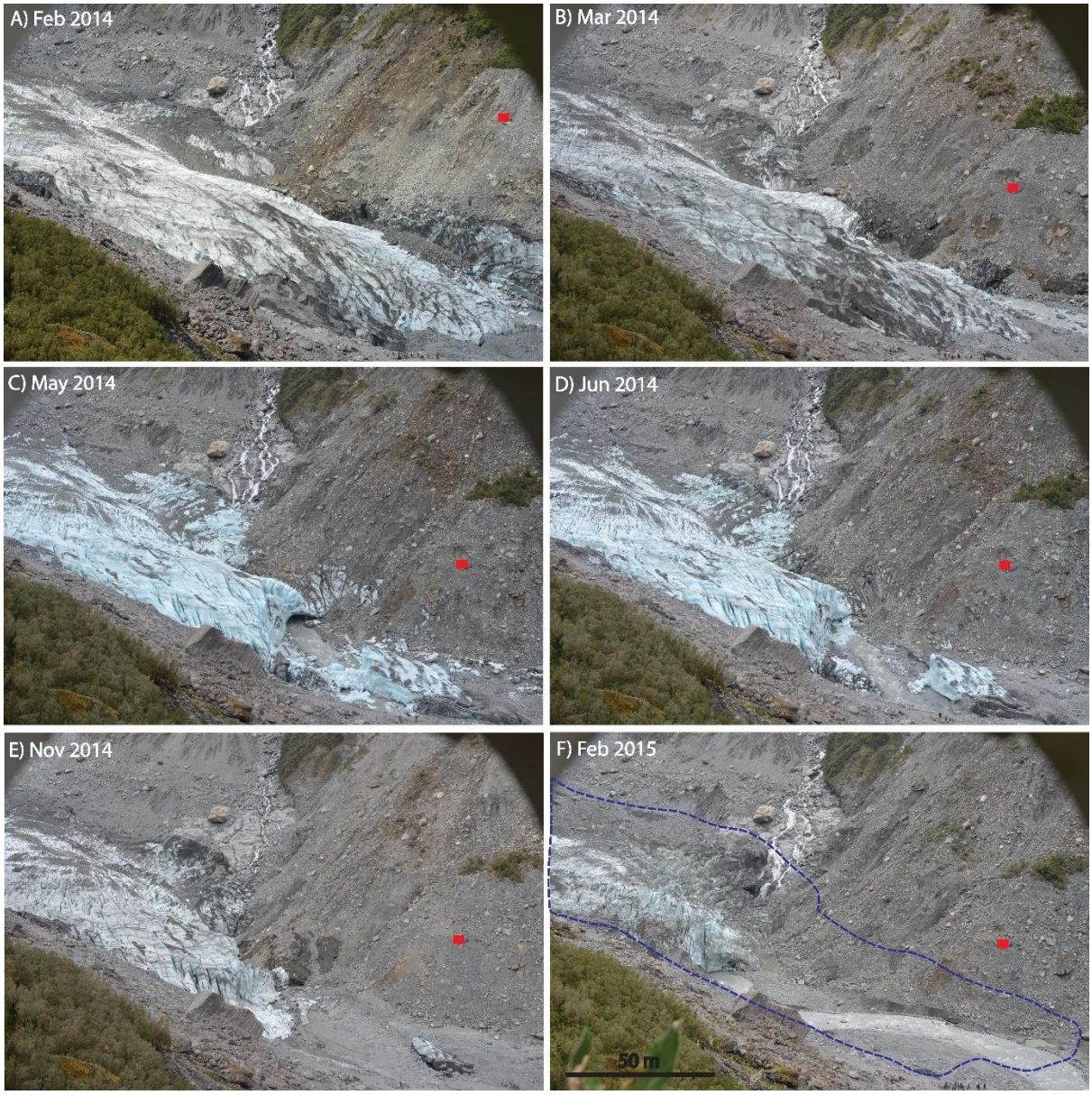

Figure 5-5: Time-lapse imagery of lower Sam Slip from Feb 2014 to Feb 2015. Red mark indicates Point 8. Blue dotted line indicates location of glacier from 2014. The Fox Glacier viewing area is in the bottom right of each image.

Movement tracking of lower Sam Slip

Thirteen points were tracked on lower Sam Slip (Fig. 6). All points with the exception of points 19 and 20, moved rapidly through their first few months of tracking, sometimes exceeding 1 m per day. The first five months of monitoring occurred when Lower Sam Slip was almost entirely buttressed by the Fox Glacier. Average daily movement through this period was 0.5 m with a maximum average movement rate of 0.81 m observed for Point 8. Following a time gap due to lack of data in July 2014, movement rates slowed to an average of 0.29 m per day. This coincided with lower Sam Slip being partially buttressed by the Fox Glacier.Overal, Point 13 had the highest movement rate of 0.8 m per day. The slope was completely debuttressed by December 2014 after which average slope movement

for all points reduced to 0.09 m per day, with the exception of Point 15 which showed more rapid movement of 0.32 m per day.

A decrease in daily movement was recorded with ongoing debuttressing. From August 2014, most movement occurred sporadically and coincided with rainfall. Imagery at the time of this movement shows localised failure of the slope, which are interpreted as debris flows triggered by rainfall. Points 13 and 15 show several periods of rapid failure through debris flow activity and by the end of the study these points were located in several small gullies. These debris flows were not spatially connected and often occurred on different parts of the slope during different rainfall events. The exception was in January 2015 when a rainfall event triggered debris flows at two different pixel tracked points. Periods of high rainfall intensity (>100 mm/ day) or duration (>3 days of rainfall) appear to have resulted in debris flow activity, with 9 events identified within the tracked points. However, similar sized heavy rainfall events in October and November 2014 failed to initiate debris flows at the monitored locations. Conversely, a debris flow or debris avalanche on the 11th December (point 18) occurred following a much smaller rainfall event, although the month prior had seen high antecedent rainfall exceeding 800 mm.

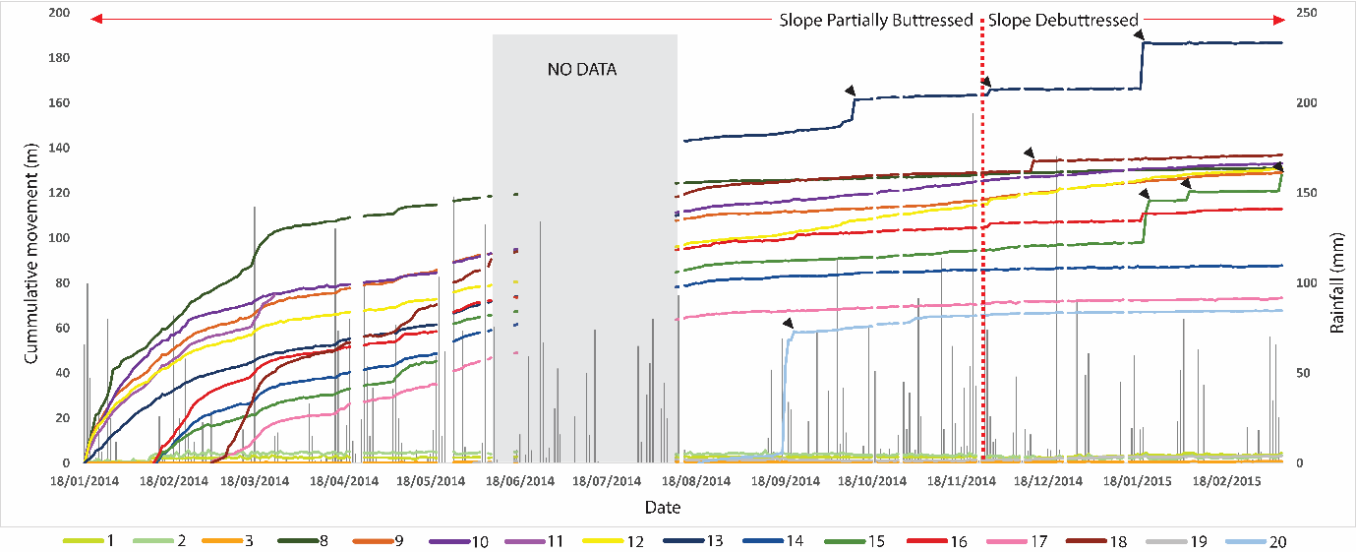

Figure 5-6: Cumulative movement of tracked points at lower Sam Slip. Points 1-3 were considered stationary prior to the study and showed ~3 to 5 m of movement throughout the study period. Black arrows represent instances of debris flow or debris avalanches.

There is no evidence of sudden accelerations within the pixel tracking during the early months of the study. The sudden periods of fast movement that occurred later on coincided with debris flows and debris avalanches recorded in the time-lapse imagery. Instead, movement in the early months was gradual and when rainfall did occur, accelerations in movement occurred across several days, like that seen on 18/03/2014. These gradual accelerations occurred across all points within lower Sam Slip following large volume or longer-duration rainfall events. The largest movement event occurred from the 18th March 2014 and continued for five days before diminishing. Ongoing rainfall continued to

trigger synchronous slope-wide accelerated deformation through lower Sam Slip, although rates were lower than during the start of the study. Ongoing movement - which facilitated through sliding - decreased as debuttressing continued. Overall, the mean total displacement of all points was 110 m, but total displacement varied from 3 m at Point 19 to 187 m for Point 13 (Figure 7).

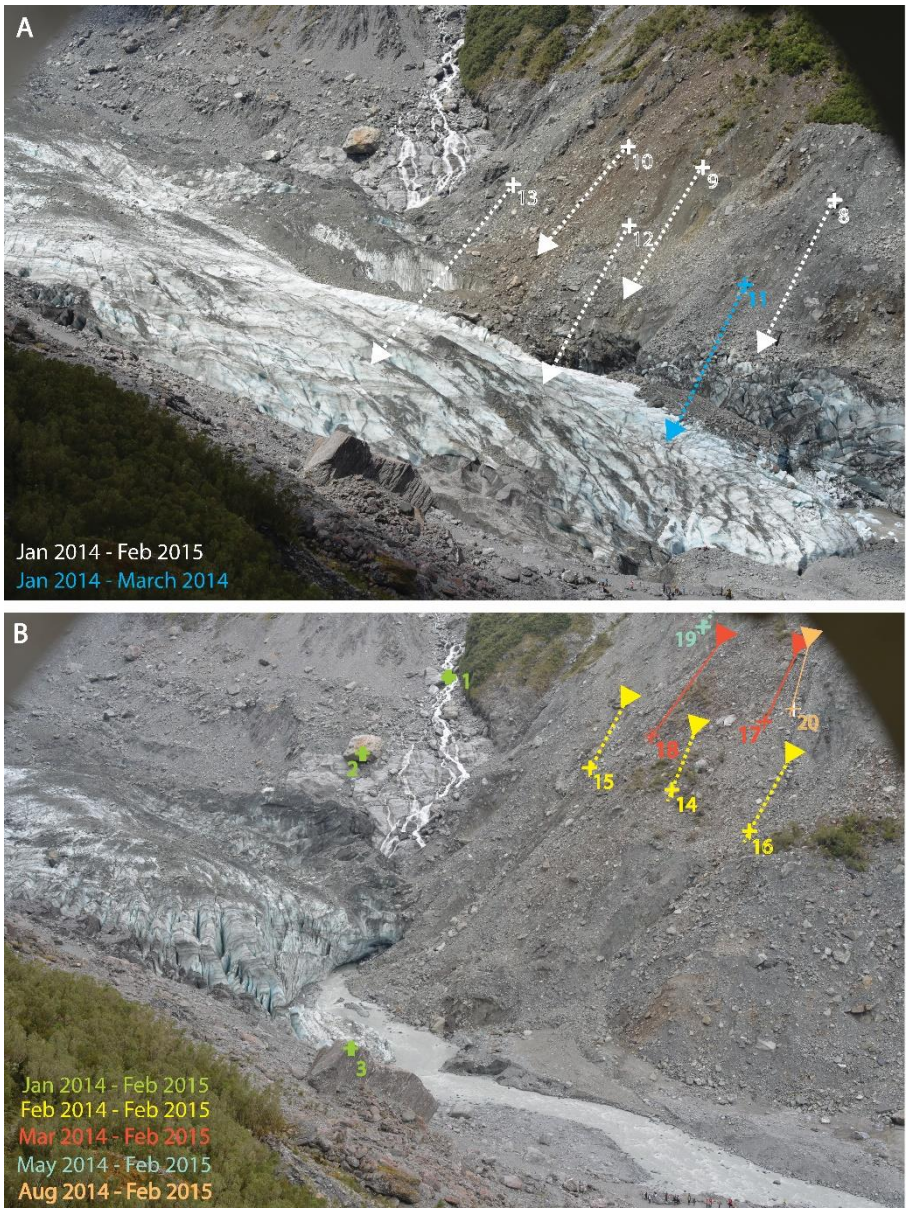

Figure 5-7:Movement vectors for tracked points, lower Sam Slip.

5.4.2 Passchendale slope failures

Time-lapse Imagery

Time-lapse imagery from 2015-2018 (Fig. 8) showed significant change in both Fox Glacier and the surrounding hillslopes (Supplementary material). During the first months of the study, slope failure in the area adjacent to the Fox Glacier icefall was the most active, with continuous movement. In this same area, several boulders were seen disappearing directly underneath the glacier (as opposed

to being delivered onto the glacier surface). In fact, all displaced sediment near the icefall and on the southern side of the valley was transported directly underneath the glacier as the slope failed.

Down valley from the icefall, the Fox Glacier experienced rapid downwasting particularly over the summer months. The terminus of the glacier stayed relatively static through 2015, 2016 and early 2017 before retreating by several hundred metres over the summer of 2017 and 2018. The hillslope above the glacier terminus responded rapidly to this downwasting and retreat, which coincided with the acceleration in displacement rate from December 2017. An earlier episode of rapid slope movement through sliding at the beginning of the study period also coincided with downwasting over the summer of 2016 and 2017.

From December 2017, the down-valley flow of the glacier reduced with tracked boulders on the glacier surface travelling less than 50 m from April 2017 to May 2018, in comparison with 250 m from March 2015 to April 2017. These observed movement rates coincided with ice flow velocities of 0.15 m per day and 0.34 m per day respectively. This reduction in ice flow velocity at the terminus coincides with changes in increased sediment delivery to the glacier. As outlined earlier, there are few examples of sediment being transported onto the glacier surface; instead, sediment including large boulders, was transported directly underneath the glacier. From April 2017, the occurrence of lateral-subglacial sediment delivery was reduced and sediment began to be delivered supra-glacially onto the lateral margins of the glacier.

Time-lapse imagery unveils other geomorphic changes within the valley. Hillslope failure and sliding was evident on the north side of the valley (Fig. 8) during the initial months of the study in an area above the Fox Glacier viewing platform (bottom right of the imagery). The primary slope movement process was an encompassing sliding of the slope with separation of the overlying sediment slope along an underlying sliding plane of consolidated sediment, seen from 2017 to 2018 at Passchendale Slip (Figure 9). A large rockfall was also visible during the middle of 2017 in the top left of the imagery. At the base of lower Sam Slip in the lower right, toe erosion continued as did aggradation of the valley floor from the Fox Glacier river. The river bed in the bottom right of the time-lapse imagery also appears rise, presumably driven upwards as lower Sam Slip fails directly underneath the valley floor (supplementary material).

Figure 5-8: Passchendale time-lapse imagery taken from March 2015 to March 2018. Red square marks point 10 and the blue dotted line indicates glacier extent from 2015.

Figure 5-9:Passchendale slip movement of lower unconsolidated sediment along intact sediment boundary. Once exposed, gullying can be seen in the intact underlying sediment.

Movement tracking of Passchendale Slip

Monitoring of slope displacement of the Passchendale Slip spanned 24/03/2015 to 21/05/2018 (Fig. 10). In total, 14 points were tracked within this period including 3 points which were initially thought to be on stable ground. Movement rates were highly variable throughout the study period. Point 18, located along the lower slope showed the most movement of ~380 pixels before falling onto the glacier towards the end of the study period. In contrast, Point 16, located on a large boulder experienced very minor displacement, prior to retrogressive undercutting of the slope below the boulder led the boulder to fall towards the glacier.

Three major changes in movement rate were noted. Firstly, between January and May 2016, all points moved together with an average displacement of 0.18 pixels per day/ Another period of acceleration was seen through summer from December 2016 to March 2017; however, movement rates were not as high as the previous year. A third notable change in movement rate was evident in points 10,11, 12 and 14 from January 2018 resulting in an average displacement of 0.34 pixels per day.

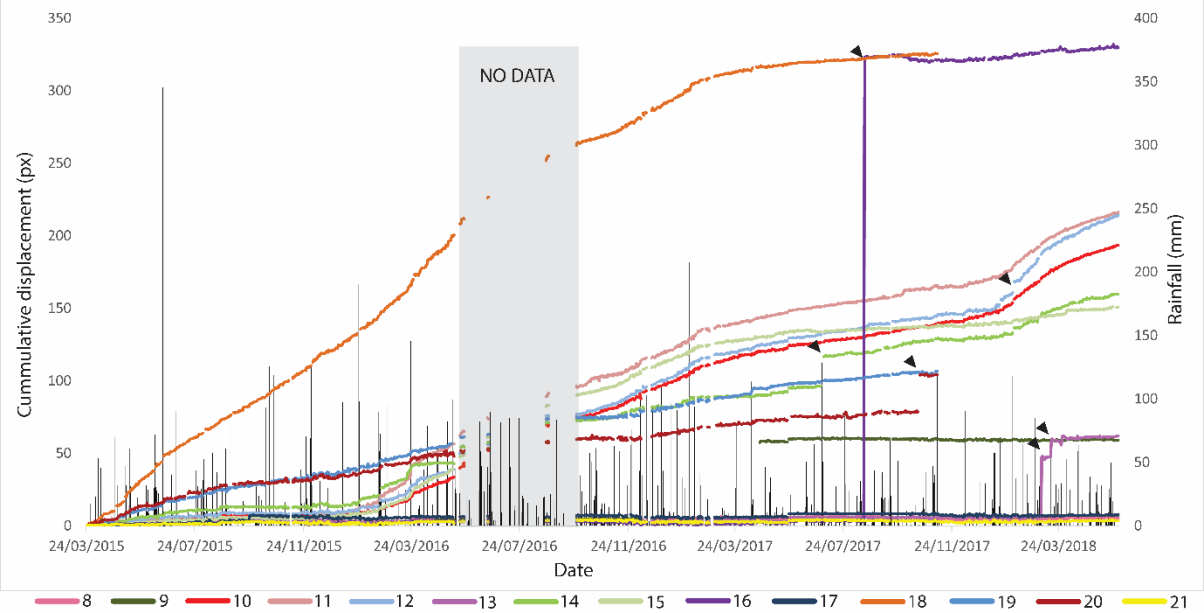

Figure 5-10: Cumulative movement in pixels for the Passchendale points. Black arrows indicate debris flow, debris avalanche or rock fall activity. Points 8, 17 and 21 were considered stationary prior to pixel tracking (were placed on bedrock or stationary boulder).

Like lower Sam Slip, rainfall had a variable effect on accelerating slope failure. Rainfall events on 08/05/2015, 18/06/2015, 24/01/2016, 18/02/2016 and 23/03/2016 initiated a short (several days) increase in displacement rate of all points following the rainfall event. Following the data gap in June to August 2016, the impact of rainfall on the slope appears to be reduced with several large rainfall events (>100 mm per day) occurring, but no significant acceleration in slope failure rate detected. Rainfall on 31/01/2017 coincided with a minor increase in slope displacement rate. An increase in sudden displacement of monitored points was evident as debuttressing continued in the latter months of the study. Sudden movement of points 13 and 16 coincided with rockfall observed within the time-lapse imagery (purple vertical lines in Fig. 10). Sudden movement of all other points (12,14 and 20)

occurred with or without rainfall and are identified as debris flows or debris avalanches. Debris avalanches that occurred without the presence of rainfall can be seen at points 12 and 14 above the orange rock and Point 20 above the icefall.

Points 8,17 and 21 were considered to be stationary prior to monitoring and were located on bedrock or stable ground (Fig. 11). Point 8 shows a total displacement 5.2 pixels, outside the 3 pixel selection error. Point 21 shows total displacement of 3.7 pixels which could be accounted for within the 3 pixel error. Point 17 shows total displacement of 7.8 pixels. Given movement of the camera is minimised and is represented by an average pixel movement of 1.14 pixels, movement of stationary points appears to be real and indicates broadscale movement within the rock slopes surrounding Fox Glacier.

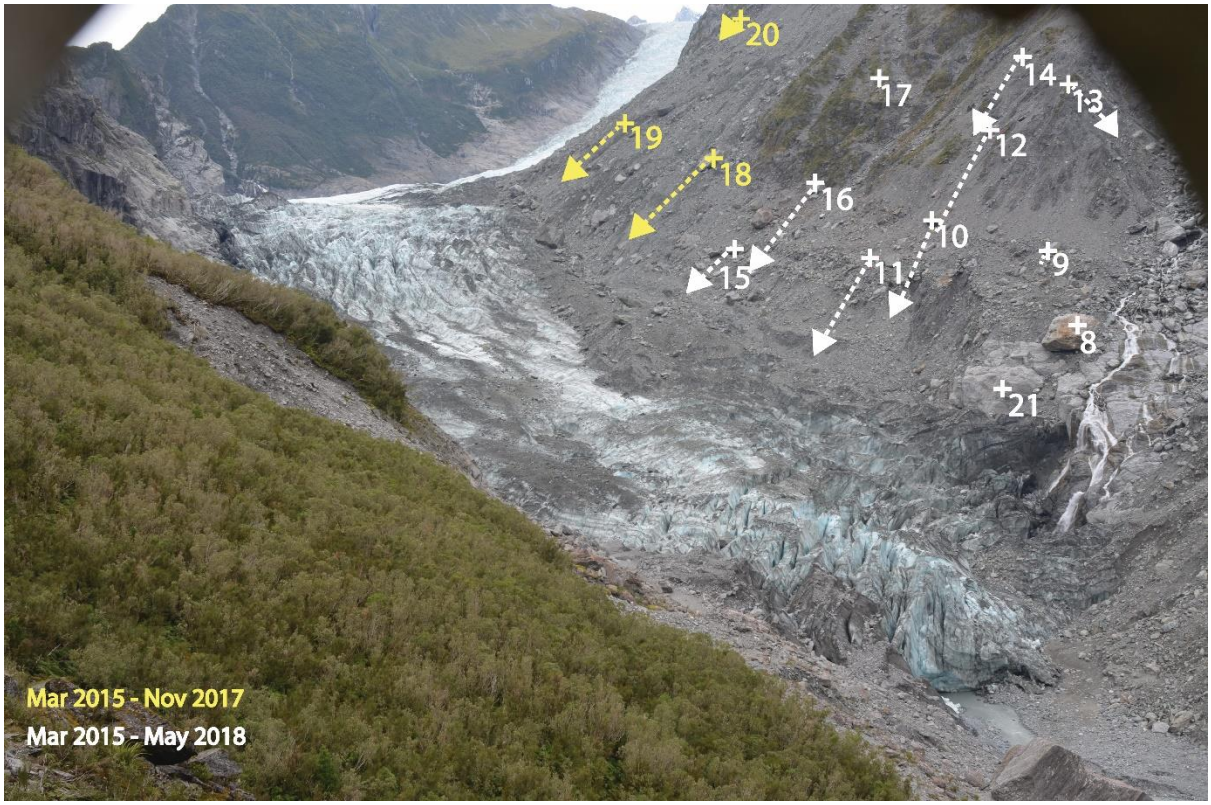

Figure 5-11: Point locations and movement vectors for the Passchendale points. Imagery is from 2015 at the start of the monitoring period.

5.4.3 Geomorphic change detection

Differences between the 2015 and 2018 DEMs showed over 100 m surface lowering from the glacier terminus to the icefall (Figure 12). lower Sam Slip on the left side of the image showed up to 14 m of surface lowering. At the base of lower Sam Slip, a small debris cone has begun to form, fed from the small stream to the east of lower Sam Slip, which showed a maximum elevation gain of 6 m. Small gullies are visible within lower Sam Slip, particularly on the right closer to the glacier terminus. Sediment failure oflower Sam Slip has led to the collapse of vegetated sections of slope, particularly in

the bottom left of Fig. 12, however, due to variable tree height and error near the outer DEM extent, it is difficult to quantify exact elevation change of the hillslope.

Hillslopes within the centre of the image closer to the glacier terminus show variable elevation changes. Areas of surface raising are mostly found along the lateral extent of several small ridges, which have accumulated sediment from the ridgeline. The area immediately debuttressed in the bottom of the image shows an average lowering of 9 m. Closer to the glacier, areas of increased surface lowering (darker red) in the centre experienced an increase in sliding towards the end of the study. On the other side of the valley near the viewing platform, surface lowering ranged from 0.5 m to 7 m, increasing towards the glacier.

Areas currently buttressed by the glacier showed the most movement on both sides of the valley. The most movement in the bottom right of the image exceeded 40 m change in elevation from 2015 to 2018. Average change in the areas of movement was approximately 25 m. Some faint indication of gullying is evident within the slopes nearer to the glacier.

Volumetric analysis for lower Sam Slip and Passchendale Slip was completed and associated errors displayed in Table 2. In total, lower lower Sam Slip showed a total volume reduction of 1.3 M m^3 across an area of approximately 0.16 km^2. Passchendale slip shows two main areas of slope failure, which are both included within the volumetric analysis (Fig. 12). In total, volume change for Passchendale Slip was 7.9 Mm^3 across an area of approximately 0.38 km^2. Across lower Sam Slip and Passchendale Slip, total volumetric change equated to 9.2 ± 0.7 Mm^3.

Table 5-2: Volumetric and depth of surface lowering at Passchendale Slip and lower Sam Slip from DEM of Difference analysis.

	Threshold volume	**Error volume**	**Error %**
Passchendale Slip Total Volume Surface Lowering	7,900,000. m3	500,000 m3	6.58%
Sam Slip Total Volume Surface Lowering	1,300,000 m3	200,000 m3	15.94%
Total Volume Surface Lowering	**9,200,000 m3**	**700,000 m3**	
Passchendale Slip Average Depth Surface Lowering	22.74	1.5 m	7.22%
Sam Slip Average Depth Surface Lowering	9.21 m	1.5 m	15.94%

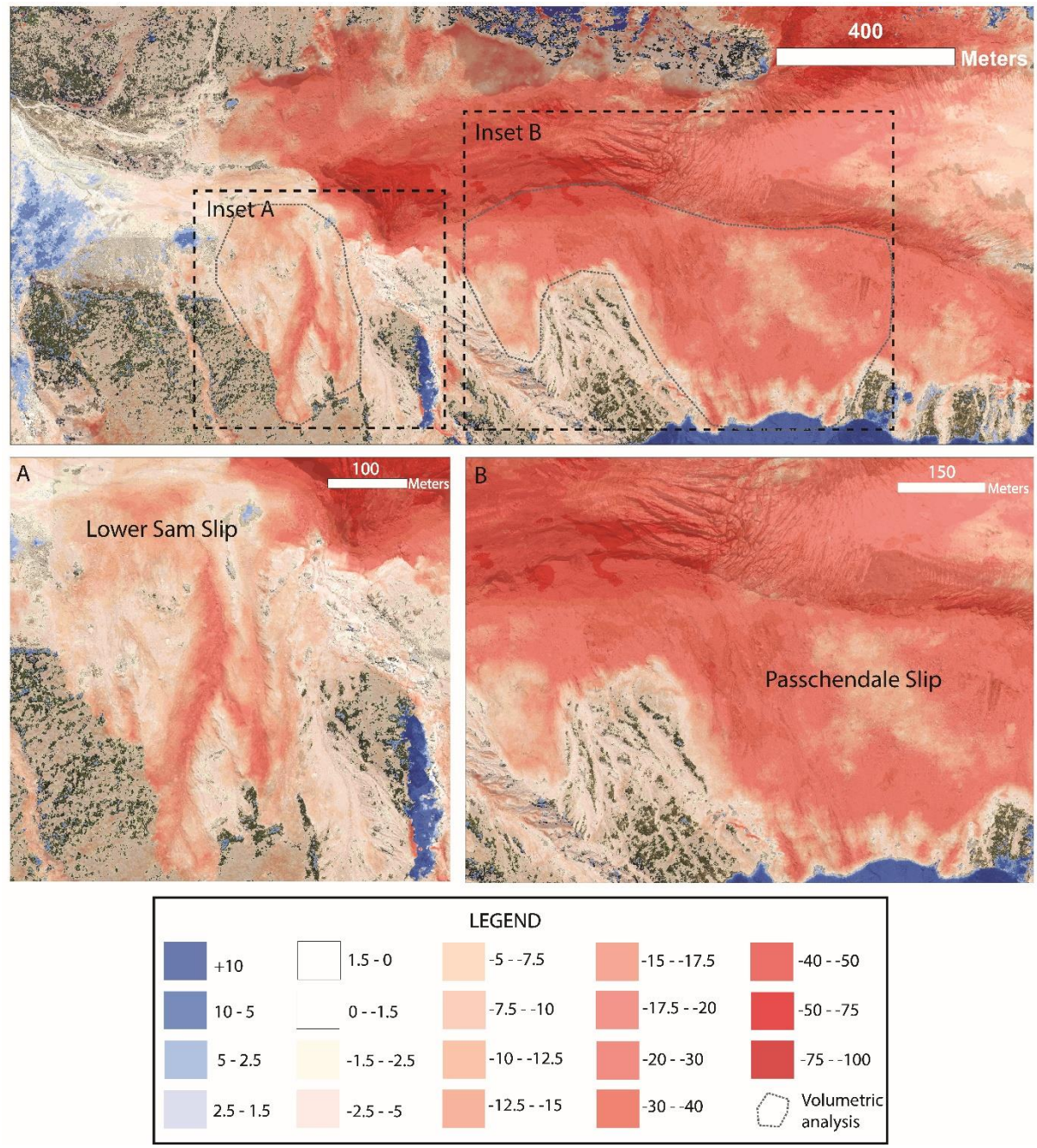

Figure 5-12: DOD for lower Sam Slip and Passchendale Slip. A) Valley view with glacier and associated mass movements. B) lower Sam Slip. C) Passchendale Slip. Bounding boxes mark inset A and inset B.

5.5 Discussion

The hillslope activity captured at Fox Glacier provides new insights into the changes in stability factors and mass movement processes that develop in sediment slopes in response to retreating glacier ice.

5.5.1 Processes and erosion controls affecting paraglacial sediment slopes

Glacier debuttressing has generally been considered as a preparatory factor in destabilising hillslope failures with little empirical evidence to show it also directly triggers failure (McColl, 2012). At Fox Glacier we show that the debuttressing has acted as both a trigger for slope movement (via internal deformation and sliding) as well as a preparatory factor for other mass movements (debris flows and avalanches) triggered by rainfall, as well as minor movement at the toe due to melting of buried dead ice.

In most studies on paraglacial sediment slope failures, rainfall was a primary observed trigger and as a result, rainfall-triggered debris flows were the most commonly identified slope failure process of debuttressed slopes (Curry et al. 1999; Ballantyne, 2002). Debris flows were recognised as a primary erosional process in paraglacial environments through the study of debris cone formation following LIA retreat (Ballantyne and Benn, 1994). For example, several instances of debris cone formation through debris flow activity within moraines were noted in Norway (Ballantyne and Benn, 1994, Curry, 1999) in the decades after retreat. While these studies have greatly enhanced understanding of long term paraglacial sediment slope adjustment, they focused on hillslopes in the latter stages of paraglacial adjustment. Very few studies have documented how sediment slopes respond during the process of debuttressing and capture the critical stages of response that immediately follow. While debris flows are a dominant erosional process following complete retreat, our observations from Fox Glacier show slow sediment sliding and deformation to be the dominant mass movement process driving sediment slope adjustment while the slope is still partially buttressed by the Fox Glacier.

Debuttressing is considered to be the primary trigger for slope failure at Fox Glacier as opposed to rainfall for several reasons. Firstly, time-lapse camera imagery and pixel tracking shows hillslope movement increases in response to rapid downwasting from December to March in summer, regardless of rainfall. Secondly, monitoring shows movement rates plateau during winter months (when downwasting and glacier retreat was minimised) and reduce significantly once the slope has been fully debuttressed. At lower Sam Slip, average movement rates decreased from 0.5 m per day at the beginning of the study to 0.09 m per day once the slope is debuttressed. Finally, while rainfall caused periodic acceleration of rotational sliding at the beginning of the study for each hillslope failure, this impact reduced until rainfall had a limited impact on enhancing debris sliding. It was at this point debris flows began to appear and become the dominant failure process.

The debris flows observed at lower Sam Slip and Passchendale Slip primarily occurred in material that had already been reworked through sliding at the foot of the slope. This mobilisation and disturbance of the sediment (and vegetation in the case of lower Sam Slip) may make sediment more readily available or reduce the thresholds for debris flow initiation Jakob (2005b) and Bovis and Jakob (1999) suggest the importance of sediment supply in controlling debris flows and state that in supply-limited basins, debris flows are often small to medium size ($<10^5$ m^3) and require larger recharge times between events. There are large sediment slopes throughout Fox Glacier valley that can be mobilised,

however, debris flows were not a common feature throughout the study period and the basin may in-fact be supply-limited. The first indication is that there is little evidence of debris flow activity within the time-lapse imagery or within the pixel tracking of points within the valley until after rotational sliding has occurred and transported significant volumes of sediment to the lower slopes. Secondly, although the site is exposed to very high rainfall events, debris flows are not documented as occurring until the end of this study period. In some cases, large rainfall events do not trigger debris flows, indicating a greater recharge time between events. Slow sliding and internal deformation appear necessary to mobilise sediment and transport it to the lower slopes where it can be reworked and further transported through debris flows. This appears to reduce strength within the slope sufficiently for future rainfall events to trigger debris flows within the lower slope material.

5.5.2 Temporal and spatial changes

Debuttressing not only triggers sediment sliding but controls how and when sediment slopes deform within the Fox Glacier Valley. Rather than triggering rapid, one-off failure, gradual debuttressing allows for sediment slopes to deform slowly through sustained failure (sliding and deformation) partly-supported by the adjacent glacier ice. Similar instances of gravitational deformation have been seen on hillslopes adjacent to the Athabasca Glacier, British Columbia (Hugenholtz et al., 2008b) and near the Tasman Glacier (Blair Jr, 1994). Deformation of a moraine ridge has been ongoing since the 1950s, as monitored with aerial imagery used to track broad scale and long-term deformation of the hillslope. Imagery of the site shows most of the moraine to be debuttressed by 2006, indicating the majority of movement occurred within the 50 years prior to complete retreat. When comparing these results with those seen within Fox Glacier Valley, results suggests these previous studies on paraglacial slopes were not observing sediment slopes during their peak deformation period. Ballantyne and Benn (1994) note average minimum erosion rates of 100 mm per year of sediment slopes in Norway. The results of Ballantyne and Benn (1994) align with those found by Curry (1999) who also identified that gullying and incision begins to occur with lowering of the sediment surface by 2-3 m following debris flow activity.

Our results at Fox Glacier show sediment adjustment occurs much more rapidly that previously described by Church and Ryder (1972), in which they suggest the highest movement rates seen in the final stages of debuttressing, instead of the initial stages of debuttressing (Fig. 13). In fact, movement rates from Fox Valley show a steep decline as the glacier fully retreats from the toe of the slope, indicating observed response rates for other paraglacial sediment slopes may be underestimating total response rates and consequently displaced sediment volume. Our results at Fox Glacier also show average minimum erosions rates were exceeding 1000 mm per year in this study period, ten times higher than those average minimum erosion rates recorded by Ballantyne and Benn (1994), Curry and Ballantyne (1999), Curry et al. (2006) and Mercier et al. (2009). A closer approximation to the environment at Fox Glacier may be the San Rafael Glacier (Harrison and Winchester, 1997) where

rainfall of 4000 to 10,000 mm per year is expected. Although surface lowering rates are not presented, Harrison and Winchester (1997) note the rapid rate in which cone development occurred with almost 6 m of debris accumulation in 15 years. The maximum erosion rate for lower Sam Slip was 2500 mm per year whereas at Passchendale, erosion rates were exceeding 4000 mm per year during debuttressing. This is due to the high rainfall observed at Fox Glacier compared to the above studies which are located in high alpine, tectonically passive environments. While pixel tracking of lower Sam Slip following complete debuttressing was not possible, visual observations from time-lapse imagery show a reduced rate of movement towards the end of the study which may be more comparable to those rates noted by Ballantyne and Benn (1994), Curry and Ballantyne (1999), Curry et al. (2006), Mercier et al. (2009). Our results are evidence of early adjustment at the peak of the adjustment curve and indicate erosion rates of sediment slopes may be an order of magnitude higher than previously thought as previous studies have been conducted following slope debuttressing when erosion rates had already reduced considerably.

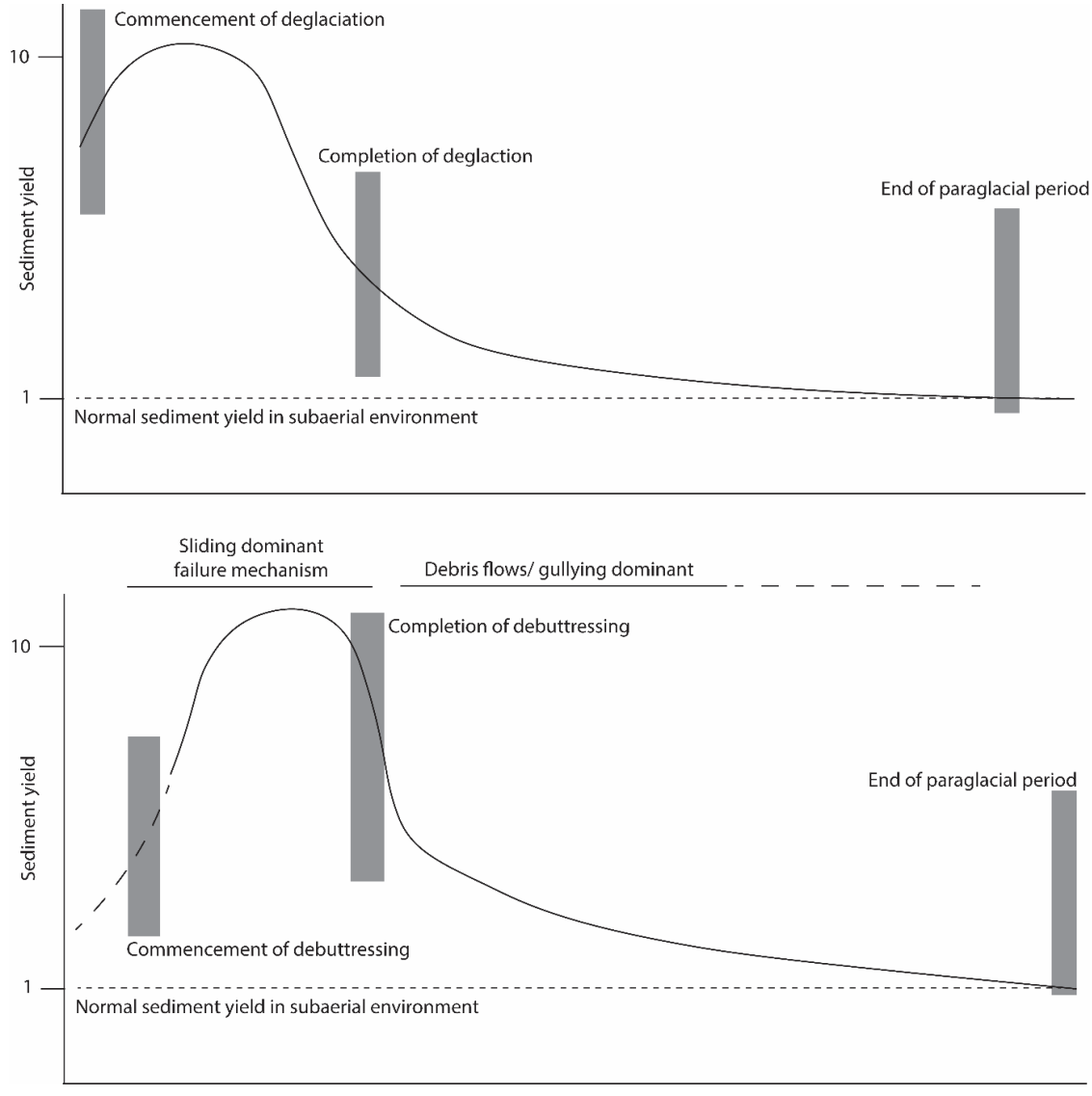

Figure 5-13: Paraglacial adjustment curve as assumed by Church and Ryder (1972) (top image). Paraglacial sediment slope adjustment as inferred from study (bottom image).

5.5.3 Broader impacts of hillslope adjustment

Quantifying sediment volumes and erosion rates is important as hillslopes and glaciers are primary sources of sediment delivered into proglacial stream networks and catchments (Ballantyne, 2002a). However, clear pathways must exist to deliver sediment from the upper catchment to the valley floor and beyond. While ordinarily sediment generation and connectivity may be perceived to increase in paraglacial settings in response to an increase in hillslope failure, this is not necessarily the case. Lane et al. (2017) reiterate this and suggest coarse sediment common in moraine and talus slopes plus rapid reworking during times of retreat, make entrainment into proglacial streams difficult and consequently reduce connectivity. Within our study site, there is no evidence of reduced connectivity due to clast size, with large boulders regularly being delivered to the glacier surface and valley floor. There is however, a lack of sediment storage in the Fox Glacier systems and the GCD shows net erosion across lower Sam Slip and Passchendale Slip and few areas showing minor increases in elevation, which would indicate areas of sediment storage. It is likely that steep valley morphology and the site being located in a temperate climate with high rainfall increases connectivity to the proglacial zone. This doesn't necessarily equate to an increase in connectivity within the proglacial zone and further work should be done to identify how successfully fluvial entrainment of sediment occurs within the area. These factors should be considered when determining the connectivity of other paraglacial catchments with similar morphology.

Further evidence of increased connectivity within the Fox Glacier paraglacial zone is the unusual way in which sediment is being transported along the Fox Glacier margin. The delivery of hillslope sediment to glaciers is usually onto glacier surfaces, creating supraglacial debris cover. The supply of supraglacial sediment from landslides and the effects on the glacier are well-recognised (Gardner and Hewitt, 1990, Hewitt, 2009, Scherler et al., 2011, Deline et al., 2015b). Large landslides that fall onto the ablation zones of glaciers represent a sudden influx of protective sediment, which can increase glacial mass balance through reduced ablation, driving glacier advance, and influence glacial processes such as moraine formation (Hewitt, 2009, Reznichenko et al., 2011, Reznichenko et al., 2016). The supraglacial landslide sediment is transported passively on the glacier surface, unlikely to experience clast modification, and be delivered slowly to the proglacial system at the rate of the flow of the glacier. Landslides that fall onto glacier accumulation zones (unless of significant size) do little to ablation rates, being quickly buried by snowfall, and likely undergo predominantly englacial sediment transport (Dunning et al., 2015). In contrast to both of these transport pathways, the landslide process observed at Fox Glacier delivers sediment directly to the bed of the glacier. McColl and Davies (2013) recognised that partly-buttressed failing rock slopes could deliver sediment to glaciers in this way, but this is the first study to document such a sediment transport pathway via failure of moraine or sediment-mantled slopes. This sediment is therefore likely to undergo active glacial transport at the glacier bed and within subglacial streams, modifying these sediments and potentially contributing to additional erosion at the glacier bed if there is otherwise insufficient basal debris. Furthermore,

entrainment into the subglacial drainage network will likely result in much faster transport of that material through the glacier and into the proglacial stream system compared to delivery of landslide material via supraglacial or englacial transport pathways. This transport pathway therefore may add to the sediment yields at the glacier terminus, and it would be difficult to distinguish this legacy paraglacial sediment source from other sources of glacigenic sediment exiting the glacier. This has implications for the interpretation of contemporary measurements of glacial erosion. For example, in a study comparing the relative contributions of sediment produced from glacial erosion and (proglacial) paraglacial sediment yields during glacier retreat, Williams and Koppes (2019) assume that the majority of measured sediment yield from Tyndall Glacier in Alaska is derived from glacial erosion alone. However, this neglects the potentially significant sources of sediment entering a thinning glacier via sub-, en- and supra-glacial paraglacial mass movements and any resultant increases in the erosivity of the glacier bed (from any actively transported mass movement sediments). Consequently, the sediment yields of a retreating glacier likely represent a combination of both classic glacial erosion mechanisms and the supply and reworking of paraglacial sediments destabilised by thinning of the glacier and are therefore enhanced during deglaciation.

5.6 Conclusions

Monitoring of the hillslopes within the Fox Glacier valley have advanced the understanding of how sediment slopes respond to the latter stages of glacier retreat. Key findings include:

1. During glacier retreat, movement develops primarily via rotational sliding at an average rate of 0.4 m per day, decreasing to 0.2 m per day as the response to debuttressing reduces. Once the slope has been completely debuttressed it self-stabilises and stops deforming en-masse. Rainfall-triggered debris flows and debris avalanches then become the dominant failure process with associated gullying.
2. Glacier retreat is the dominant trigger and sustaining factor of hillslope failure as seen by a reduction in movement following complete retreat. Rainfall is an accelerant and amplifier of mass movement via sliding and internal deformation, as opposed to a trigger.
3. The freshly debuttressed sediment slopes may begin in a supply-limited state more resistant to debris flows, given there is often sufficient rainfall at the site to initiate debris flow activity. Once sliding and internal deformation of the slope has disturbed the sediment, and the angle of repose becomes more conducive to debris flow activity, there is an increase in loose sediment and consequent debris flow activity.
4. Previous studies on paraglacial sediment slopes have suggested most moraine deformation occurs in the latter stages of the sediment exhaustion curve model. Unlike those studies, this study shows substantial mass movement taking place during the debuttressing process and a slowing of rate of movement in the latter stages of debuttressing. Minimum erosion rates at Fox Glacier are at least ten times higher than those reported in previous examples due to high rainfall rates at Fox Glacier.

5. Fox Glacier valley shows evidence of high connectivity between hillslopes, glaciers and rivers. This is due to a lack of sediment storage capacity induced by steep valley side morphology, high rainfall leading to debris flow activity due to the site's temperate climate with high orographic rainfall and propensity for landslide-derived sediment to be delivered sub-glacially rather than supra-glacially.

5.7 Acknowledgements

The authors would like to thank the following people and companies for their assistance in data collection, analysis and manuscript production. First, many thanks to Marius Bron from Fox Glacier Guiding for assisting with field work and camera installation, and for general assistance in the collection of data for this study. We would like to thank the Department of Conservation (DOC) for allowing us to install equipment and monitor the site which is located within a National Park. For data collection, we would like to thank Snowgrass Solutions for their time-lapse data which they freely and happily provided (data co-owned with DOC and Fox Glacier Guiding). Finally, we would like to thank Saskia de Vilder and Chris Massey from GNS Science for their use of the LiDAR data set.

5.8 Contribution and summary for thesis

Chapter 5 contributes to the primary objectives of thesis by presenting the first detailed study of paraglacial sediment slope development in the final stages of debuttressing. The evolution of sediment slopes is far more rapid than observed from rock slope failures, and their contribution of sediment into proglacial systems can be substantial, leading to adverse impacts in the proglacial zone and further down-valley. This chapter has also highlighted the role rainfall plays in inducing failure in paraglacial sediment slopes, although debris flow activity was low initially until mobilisation of sediment had occurred through sliding. While these results have unveiled new information on movement rates of triggers of paraglacial sediment slopes, these findings also highlight the lack of understanding we have on this subject. It is likely the sedimentation rates and impacts of paraglacial adjustment are under representative of true sedimentation rates, connectivity and movement rates. A greater focus should be applied to sediment slope failures within the research community.

6. Synthesis

6.1 Development of paraglacial rock slope failures

The development and conditioning of paraglacial rock slope failures has been a topic of conversation within the geomorphic community following the early classification of the paraglacial concept and its recognition as a major influence on alpine processes and hillslope evolution. A primary observation within many early studies established the linkage between glacier retreat and rockslope failures, finding many large alpine rock slope failures occurred after glacier retreat. These studies (Ballantyne and Stone, 2004, Agliardi et al., 2009a, Cossart et al., 2013, Sturzenegger et al., 2015, Mercier et al., 2017) found glacier retreat and debuttressing to have occurred prior to failure although there was often a significant lag between this glacier retreat and eventual rapid failure, sometimes exceeding thousands of years. Rather than acting as a trigger of failure, debuttressing was most likely a preparatory factor, weakening hillslopes over time. While the linkage between glacier retreat and landsliding has been shown, there are limitations on what can be deduced through the analysis of prehistoric landslide deposits. In recent years, as active paraglacial hillslopes have been identified in alpine areas, research including that found within this thesis has begun to focus on these research gaps including deducing rates, patterns and causes of landslide movement and deformation.

By utilising a novel suite of monitoring techniques, this thesis has successfully presented a history of paraglacial landslide development through various stages of glacier debuttressing. The first finding relates to the long timescales under which paraglacial rockslides can deform prior to glacier retreat. Riva et al. (2018) and Grämiger et al. (2017) have used numerical modelling and cosmogenic dating to better estimate the role repeat glacial cycles play on reducing hillslope stability and found progressive failure of the rock mass occurs as a gradual process. Riva et al. (2018) particularly noted that in relation to the Spriana Rockslide, damage nucleation was noted within their time-dependant model 16,000 thousand years ago, some 6,000 to 10,000 years prior to the formation of the rockslide headscarp. Dating of the headscarp of the Driest Rockslide shows scarp formation beginning around 8000 years ago (Grämiger et al., 2017). Both studies indicate that the development of paraglacial rock slope failures occurs over large timescales and the movement or formation of previously studied paraglacial rock slope failures has been preceded by thousands of years of development.

This has a number of implications for the Mueller Rockslide regarding its development. Current movement of the rockslide and the formation of the headscarp has likely occurred following thousands of years of mechanical damage accumulation. Cosmogenic dating within this thesis found headscarp initiation occurred at minimum ~7500 years ago. While this methodology was limited due to limited sampling, it provides an estimate of rockslide age. Based on the cosmogenic dating results and the study by Riva et al. (2018), it is estimated that development of the Mueller Rockslide began at a similar time as the Spriana Rockslide, which is estimated to be ~16,000 years ago.

At the Mueller Rockslide, glacial cycles as well as regular seismic shaking have likely contributed to the progressive failure of the slope. The findings of both this thesis and the Driest Rockslide study indicate that paraglacial rock slope deformation can begin without significant or complete debuttressing. Instead, slow deformation of paraglacial rock slopes can begin soon after climate warming and glacier retreat begins, following an extensive history of progressive weakening following earlier cycles of glacier advance and retreat, or seismicity. From the findings within this thesis and those obtained by Riva et al. 2018 and Grämiger et al. (2017) formation of the Mueller Rockslide has likely been influenced by glacier retreat at the end of the Last Glacial Maximum (~20,000 years ago) and the Antarctic Cold Reversal (~12,000 years ago) which eventuated with the formation of the headscarp and incremental movement of the rockslide. Further glacier retreat and consistent, large seismic events nearby have continued to condition the slope, increasing fracture patterns and increasing permeability within the rock slope. With an extensive fracture network, the slope is now particularly susceptible to external triggers including groundwater fluctuations and earthquake shaking.

Although the period when the rockslide initiated movement (-7500 years bp) is marked by warmer temperatures following the end of the ACR, the Mueller Glacier extent at this time was far greater than its current extent, with the Mueller, Hooker and Tasman Glaciers combining and extending 20 km further down valley (Putnam et al., 2010). The second key finding of this thesis relates to the influence glacier ice has on controlling and initiating landslide movement and movement rates. Theoretical modelling by McColl and Davies (2013) proposed that glacier ice provides insufficient support to hillslopes and can deform under low applied stresses and that hillslope deformation and landslide development could occur prior to debuttressing. Both the Mueller Rockslide and Driest Rockslide have formed and movement intiated prior to glacier retreat and debuttressing. Evidence of glacier ice deformation is seen at Mueller Glacier in 2017, with concentric banding and crevassing of the glacier ice adjacent to an area of active movement along the southern half of the landslide toe (Fig. 4.13). These concentric crevasses which step towards the slope represent a depression forming within the glacier where the glacier ice interacts with the slope. Referred to as ice cauldrons, these areas of concentric banding and depression are associated with sub-glacial melting. Their cause has been attributed to geothermal activity or volcanic activity with no other causes proposed (Gudmundsson, 2021). With no evidence of geothermal activity in the study area, another process must be attributed to causing ice cauldroning at the Mueller Glacier. It is likely that the ice is thin in this area to facilitate melting without intensive heat due to an accumulation of meltwater or a sub-glacial lake in this area.

It may be that this very slow retreat over 13,000 years of the Mueller Glacier resulted in controlled failure of the slope and more rapid glacier retreat may have resulted in more rapid or catastrophic failure of the Mueller Rockslide. Alternatively, other factors such as preconditioning factors or alternative triggers such as rainfall may be responsible for varying rates of paraglacial hillslope failure. Overseas, there are examples of hillslopes failing rapidly or gradually (like Mueller) during debuttressing and glacier retreat. A recent example of a catastrophic failure of a

rockslope during glacier retreat is the Taan Fiord landslide and tsunami which occurred at the terminus of the Tyndall Glacier (Higman et al., 2018). Meanwhile, examples of gradual retreat include the Moosfluh Landslide and Marzell Rockslide which have yet to fail rapidly even following average movement rates exceeding 1 m per day at Moosfluh. This variation in movement rates across different paraglacial rock slope failures makes assessing the likelihood of paraglacial landslides failing rapidly more difficult to determine, with further work required to identify common patterns which distinguish those which have failed rapidly from those which have failed gradually.

The third key finding of this research relates to the spatiotemporal changes in movement that occur in paraglacial rock slope failures during their development. Fey et al. (2017), Manconi et al. (2017) and Glueer et al. (2019) provided the first detailed monitoring studies of contemporary paraglacial rock slope failures and found movement rates were generally high (in some instances exceeding 1 m per day) and reached their maximum extent when the glacier terminus was located midway along the landslide toe (i.e. when the rock slope was partially debuttressed). Movement rates were then seen to slow with continued retreat. The Mueller Rockslide is also partially buttressed and it is expected, based on these analogous studies, that movement rates of the rockslide are near or have reached their maximum rate and will decrease in the near future. Like these studies, movement rates of the Mueller Rockslide also accelerated during late stage glacier retreat, especially between 1986 and 2017 when average movement rates eclipsed those currently occurring and indicate that although movement rates still fluctuate, rockslide movement rates are decreasing.

By utilising a variety of monitoring techniques, movement patterns of the European paraglacial rock slope failures can be deduced. This has primarily been done to investigate the role debuttressing plays in enhancing and controlling movement. Fey et al. (2017), Manconi et al. (2017)and Glueer et al. (2019) have established that landslide movement rates (although delayed) accelerated with increased glacier retreat. Similar patterns have been found in this thesis with gradual increases in movement rate identified over the last -8000 years. However annual movement data from this study has shown movement to be episodic and variable, and similar variability in movement rates may have occurred throughout long-term development of the Mueller Rockslide and other similar paraglacial slope failures.

Through the synthesis of these results, a general model of paraglacial rock slope deformation can be developed with several caveats. These caveats are: i) This thesis has only included analysis of one paraglacial rock slope failure which has its own unique set of preconditioning factors and preparatory factors i.e. the site is exposed to different climatic conditions than those studies in Europe including differences in precipitation, temperature and lack of permafrost and ii), the movement mechanics and processes within this thesis are based on those commonly identified within large rockslides and does not account for other types of rock slope failures. Smaller rock slope failures or those governed by wedge or toppling failure kinematics are likely to form and evolve differently both spatially and temporally.

To that end, the development of paraglacial rock slopes begins slowly with conditioning and progressive failure slowly weakening the rock slope over thousands of years. In the case of the Mueller Rockslide, preconditioning of the rock slope occurred following the Last Glacial Maximum and Antarctic Cold Reversal and likely repeat seismic events over the last ~20,000 years. Gradual deformation of the rockslope began following an extending period of conditioning through several glacial cycles, including the formation of scarps which are structurally controlled and conditioned by underlying structural controls (folding and faulting). These discontinuities make the slope favourable for failure with fracture sets daylighting within the slope. Following preconditioning, failure began along favourably orientated fracture sets in the early Holocene. As glacier retreat and downwasting has continued, the movement rate of the rockslide has appeared to accelerate. With the rockslide now in the final stages of debuttressing, movement rates have increased and fluctuate both spatially and temporally. Headscarp retrogression is now seen along controlling discontinuity sets and obvious deformation of the landslide toe is seen as it begins to grow into the glacial valley where the glacier has fully retreated from the landslide toe. Tension cracks and increased fracturing are now seen in the middle of the rockslide as the landslide toe continued to accelerate relative to the landslide headscarp.

Based on the work by Fey et al. (2017) and Glueer et al. (2019) it would be expected for landslide movement rates to slow as debuttressing continues. Based on the narrow morphology of the Mueller Glacier Valley and the size of the Mueller Rockslide, continued movement of the rockslide may end as the rockslide toe interacts with the valley floor and adjacent valley wall. Following retreat, gradual growth of the Mueller Rockslide into the valley may also increase its stability through enhanced friction at the landslide toe. Continued monitoring of the site would be beneficial as a way to determine whether the changes seen at Mueller Glacier improve stability or simply delay the occurrence of rapid failure. Alternatively, if the rockslide were to fail rapidly as a rock avalanche, narrow valley morphology would likely confine the rockslide, making it difficult for the rock avalanche to travel a large distance down valley. Without continued monitoring of active failures post debuttressing it is hard to make assumption on continued development. However, it could be that if paraglacial landslides reach the valley floor through controlled debuttressing, they are at a reduced likelihood of failing rapidly and the landslide as a hazard is reduced.

6.2 Development of paraglacial sediment slope failures

The adjustment of sediment slopes to glacier retreat has been observed for several decades, with many studies noting rapid changes in sediment slopes occurring following LIA or more recent glacier retreat (Blair Jr, 1994, Curry et al., 2006, Curry and Ballantyne, 1999, Hugenholtz et al., 2008a, Mercier et al., 2009, Kuschel et al., 2020). In particular, it has been noted that a primary erosive activity impacting paraglacial sediment slopes are debris flows which lead to gullying and rapid incision of the often unconsolidated material (Ballantyne, 2002b). More recently, efforts have been made to identify how final adjustment of paraglacial sediment slopes occurs i.e. observing the transition from active gullying to stable vegetated slopes (Eichel et al., 2018, Draebing and Eichel, 2018) and it is proposed

that this process takes place over centuries, culminating in the growth of established shrubs and bushes, or in the return of glacial conditions. There is still a lack of evidence detailing the early response of adjustment paraglacial sediment slopes undergo during retreat, with greater emphasis placed on rock slope failures, likely due to a heighten perception of rock slope failures as a hazard, the arguably more complex nature of rockslope failure development and the highly transient nature of sediment slopes undergoing paraglacial adjustment, limiting their ability to be observed and studied. The findings on sediment slopes within this thesis combat these assumptions in a number of ways, namely through the monitoring of paraglacial sediment slope failures which have been shown to move rapidly, displace large volumes of sediment and involve a complex interplay of triggering processes including glacier retreat and rainfall. This thesis has also provided a detailed study of paraglacial sediment slope adjustment during the final stages of debuttressing, before debris flows become a dominant erosion process. From these findings, and those studies included above, a comprehensive overview of paraglacial sediment slope response can now be developed from debuttressing to final adjustment, including spatiotemporal changes which could be used as an analogue for other developing paraglacial sediment slope failures.

Prior to debuttressing, sediment slopes are fairly stable, supported and formed by glacier advance and the presence of glacial ice. From observations at Sam Slip and Passchendale Slip in this thesis, minor slope instability can occur for several years prior to debuttressing. Timelapse monitoring of both sediment slope failures provided insight into how and when sediment slopes deform. Initially, failure is slow and occurs primarily as steady sliding with little to no debris flow activity, with movement rates up to 30 cm per day. Rock falls and topples can be seen in some cases, if the supporting slope is compromised and occurs from both rock and sediment slopes which have been undercut by glacier retreat or by failure of hillslopes downhill. Like Fey et al. (2017) who found peak movement rates were reached when the glacier terminus lay half-way along the landslide toe, similar results were seen here with maximum movement rates increasing at this point, sometimes exceeding 1 m per day, then plateauing following continued debuttressing to remain largely stable at less than 10 cm per day. Failure during this phase of sediment slope development is strongly controlled by glacier retreat, with seasonal fluctuations in landslide movement coinciding with seasonal fluctuations in glacier extent. Increased downwasting and glacier thinning in summer coincided with increased landsliding in summer, with downwasting allowing for controlled sliding of the sediment slope failures. Although glacier retreat is considered to be the primary trigger of slope failure, movement is heavily modulated by rainfall, particularly up until the glacier terminus reaches midway along the landslide toe i.e., when peak movement rates are achieved. Following this, as the landslide beings to slow down, rainfall leads to increased debris flow occurrence which can be seen as abrupt changes in displacement in Chapter 5.

As the slope is finally debuttressed, debris flows and rainfall induced landslide become the dominant process impacting upon slope stability. Minor gullying was induced in the two years

following debuttressing at Sam Slip, indicating this process begins rapidly and could give an indication for other sites as to when debuttressing occurred. From several studies by Curry and Ballantyne (1999), Ballantyne (2002b), Ballantyne (2002a), Curry et al. (2006) and Kuschel et al. (2020) this process takes approximately 50 -150 years from gully initiation to gully infilling and a reduction in gully relief. The final stage of adjustment, as defined by Eichel et al., (2018) involved the revegetation of the slope or alternatively, reworking of sediment during the next period of glacier advance. Overall, adjustment takes place over several centuries with the most rapid changes occurring in the first five to ten years of paraglacial adjustment, during debuttressing through to debris flow dominated slope failures and gully formation.

6.3 Paraglacial landslide impacts

Although a focus within this thesis and within recent literature has been on understanding underlying controls on paraglacial landslide development to determine how and why they fail, early studies and indeed this thesis have also focused on the broader environmental impacts of paraglacial landsliding. This is important for a number of reasons. As landslides fail (whether this occurs through rapid or gradual failure) they produce and transport sediment and can be a major influencing factor controlling the fluvial entrainment of sediment, sediment budgets and sediment connectivity. The impacts of landsliding are also not restricted to the immediate area; as seen in Chapters 3,4 and 5 landslide development can lead to headscarp retrogression, superficial marginal failures and alterations to valley and glacier morphology. Both changes in sedimentation as a result of failure and changes in hills lope morphology outside the original scope of the landslide area increase the hazard potential of landslides. Increased sediment supply to valleys and rivers could lead to debris flows, flooding, river channel avulsion and aggradation (Evans et al., 2001, Korup et al., 2004, Korup, 2005b, Knapp et al., 2020). A notable feature of paraglacial landslides compared to landslides conditioned by other means is that although the often fail gradually over thousands of years, they deliver high rates of sediment over long periods of time. In fact sedimentation rates during paraglacial adjustment in proglacial systems can be ten times higher than during periods of quiescence (Church and Ryder, 1972, Curry and Ballantyne, 1999, Ballantyne, 2002a). This is particularly true for sediment slopes, highlighted in this thesis by movement rates exceeding 1 m per day during debuttressing. To begin assessing the short, medium and long-term impacts of paraglacial hillslope adjustment, observations are summarised in the following paragaphs on the alteration of hillslope and valley morphology, modes of sediment delivery and potential implications from continued development of the hillslopes identified and discussed in this thesis.

The most immediate impacts of landsliding on the surrounding environment occur in the area closest to the landslide. Headscarp retrogression and tension crack formation are common processes occurring in susceptible hillslopes with the necessary preconditions, where destabilisation and undermining of a hillslope from landslide movement leads to instability further up the hillslope (Wang et al., 2016). In the case of the Mueller Rockslide, several main scarps can be seen within the

headscarp zone and are represented in the field as large toppling blocks which are structurally controlled. Above the rockslide, in the vicinity of Mueller Hut and extending almost to the eastern ridge line, a number of minor scarps and tension cracks are seen, dipping westwards and aligning with discontinuities within the rockslide. Structural or tectonically controlled discontinuities are a common control over headscarp retrogression in rock slopes (Travelletti et al., 2013, Gschwind et al., 2019) however, they themselves do not cause headscarp retrogression but merely constrain it. Complex interconnected landslide systems and retrogressive zones have been documented in several paraglacial landslides including the Spriana Landslide (Riva et al., 2018) and the Marzell Rockslide (Fey et al., 2017). Of particular note is time-dependancy modelling completed by Riva et al. (2018) which showed clear growth of the Spriana Landslide over several thousand years, including the formation of several "headscarps" and continued retrogression upslope with the growth of a basal sliding plane. Should the necessary preconditions be present i.e. favourable bedding or fracture orientations, retrogression forming multiple stepped scarps or headscarps may be common in paraglacial rockslopes as the glacier provides sufficient support for these scarps to form without leading to catastrophic failure. In the case of the Mueller Rockslide, the maximum extent of the rockslide may have initially stopped at the lower margin of the headscarp, before growing gradually over the >8000 year history of the rockslide. This has now resulted in a complex and often discontinuous headscarp zone marked by multiple scarps and which is now beginning to extend onto the ridgeline as a result of recent glacier retreat and destabilise and weaken the surrounding hillslope. Through allowing the gradual deformation of the rockslope, the Mueller Glacier may have increased the size of the Mueller Rockslide by supporting the slope sufficiently to allow for a through-going basal sliding plane to develop and impact the ridgeline.

Widespread impacts of paraglacial hillslope failures are not only restricted to the upper slopes through retrogression; the area most immediately impacted by landsliding is the area below the landslide including in this instance the buttressing glacier and the glacial valley in which the landslide occurs. Both the Mueller Rockslide and the sediment slope failures at Fox Glacier have been impacting the immediate proglacial area in different ways. At Fox Glacier, widespread sediment deposition at the base of the affected hillslopes has led to rapid alluvial fan grown and displacement of the valley floor caused by the landslide body pushing into the proglacial zone. At Mueller Glacier, the Mueller Rockslide toe has now grown and expanded into the valley by several hundred meters and continued movement of the rockslide will likely block the valley. Unusual interactions are also seen between each landslide and their buttressing glaciers; the Mueller Rockslide appears to deform and thin the Mueller Glacier (Chapter 4) causing the glacier terminus to become elongate and crevassed, where it lies against the rockslide toe. At Fox Glacier, timelapse imagery shows sediment delivery directly underneath the glacier as opposed to onto the glacier. Neither effect has been noted or discussed in the literature before although McColl and Davies (2013) have shown the Mueller Glacier to deform from landslide movement in the past. When investigating landslide-glacier interactions, emphasis is

usually placed on the impact glaciers play in enhancing or reducing slope instability (McColl and Davies, 2013, Storni et al., 2020) or have found landslide material to commonly be deposited supra-glacially (Deline, 2009, Hewitt, 2009, Vacco et al., 2010, Reznichenko et al., 2011, Deline et al., 2015b, Dunning et al., 2015). While the impacts of landsliding on glaciers have been noted in this thesis, it is beyond the scope of this research to provide detailed analysis of these processes and is recommended for future work. In particular, gaining an understanding of how sediment is entrained by glacier ice when it is deposited sub glacially would be beneficial to determine how this impacts glaciers, connectivity and sediment transportation to the proglacial zone.

Implications of continued paraglacial landslide development can be wide-ranging and difficult to determine prior to their occurrence. However by observing how the Mueller Rockslide and the Fox Glacier sediment slope failures are currently developing, inferences can be made about the next stages of their development. At Mueller Rockslide, continued movement is likely to partially or fully block the Mueller Glacier valley creating a landslide darn. As discussed in Chapter 4, this may occur due to gradual movement like the slope is currently experiencing, or it is likely to occur if the landslide fails rapidly. Through the formation of a landslide darn, a proglacial lake may form as the Mueller Glacier continues to retreat, although due to the narrowness of the Mueller Glacier valley, the size of the landslide (~200 Mrn3) and the large blocky material which makes up the Mueller Rockslide, the darn may be relatively stable. Should the darn itself fail, or if the darn is overtopped by the proglacial lake through a Glacial Lake Outburst Flood (GLOF) flooding down valley would be likely and would extend to the surrounding campground, Mount Cook Village and access roads.

At Fox Glacier, predicting the long term impacts of landslide development are easier, as the sediment slopes become dominated by debris flows and gullying, in a similar pattern to previously discussed examples (Curry and Ballantyne, 1999, Ballantyne, 2002b, Curry et al., 2006, Mercier et al., 2009). Complete adjustment of the sediment slopes at Fox Glacier is expected to take about 150 years based on the rate of adjustment seen in the aforementioned references. Adjustment within the proglacial zone will likely take longer; high volumes of sediment may remain in the catchment for centuries, fed from additional slope failures up valley. The hillslopes at Fox Glacier may be further destabilised by seismic activity as they lie within 5 km of the Alpine Fault, with a large earthquake on the fault likely to occur within the century (Berryman et al., 2012). It is this rapid rate of adjustment, combined with high sediment turnover (~ 10,000,000 m' volumetric change in 4 years) which makes the sediment adjustment at Fox Glacier particularly hazard. With the exception of the Mueller Rockslide failing, the more immediate impacts of paraglacial hillslope adjustment with be seen at Fox Glacier in the corning decades. Access to the glacier is already blocked with the road washed out repeatedly from debris flow activity down valley. Closer to the glacier terminus, rockfall and debris flow activity is ongoing and pose a risk to glacier tourism within the area. Due to high connectivity at the site, sediment delivery to the proglacial zone is beginning to result in

aggradation and avulsion within the immediate area and down valley in the Fox Glacier sandur. Remobilisation of paraglacial sediment within proglacial zones is a common occurrence (Baewert and Morche, 2014) and with the high rainfall totals within the Fox Glacier area, there will be an abundant source of sediment available for transport during flood events.

As a final contribution, the short, medium and long-term impacts are summarised below for both sediment and rock slope failures, based on observations at Fox Glacier and Mueller Glacier. Short-term impacts are classified as impacts seen within the next decades, medium-term impacts are those seen within the next century and long-term impacts are those seen after the next century. Short-term, a reduction in movement rates is expected at Mueller Rockslide as the hillslope continues to be debuttressed by the glacier. Continued growth of the landslide toe is expected although the rockslide is not expected to block the valley within the next few years. Increased fracturing of the surrounding rock mass is expected and may increase at the top of the slope and within the lower landslide area. Continued deformation of the Mueller Glacier is also expected, with the glacier pushed to the west resulting in a long, extended glacier lobe. Future ice cauldroning may also be seen as the glacier continues to retreat and thin. At Fox Glacier, failure of Passchendale Slip will continue and accelerate over the next few years before movement rates reduce by the end of the decade. At this time, further sediment slope failures are likely to activate up valley and further rock fall may be seen on the northern margin of the valley. Gullying of Sam Slip will be well underway and alluvial fan development at the base of Sam Slip will continue and expand. Increased sediment connectivity and sedimentation rates at the site will make it particularly susceptible to flooding, with reworking of the proglacial sandur commonly occurring during this time. Medium-term, both sites are likely to be impacted by an earthquake on the Alpine Fault which could result in rapid and catastrophic failure at both locations. Should this occur, as a worst-case scenario, damming of the valleys may occur followed by flooding, debris flow activity and dam failure if the right conditions were met. If the sites are not subjected to a large earthquake (although this is unlikely given New Zealand's position on a plate boundary) both landslides will continue to deform with a reduction in movement rates. Sediment failure rates at Fox Glacier will decrease steadily as the Passchendale Slip is also fully debuttressed and debris flow activity becomes the dominant erosive process. Sedimentation rates during this time will still be a magnitude higher than during interglacial periods as gullying continually removes sediment from the hillslopes and transports it the proglacial zone. As with the short-term effects, flooding and sediment reworking would be common during this time. At the Mueller Rockslide, failure may or may not occur although as the landslide toe continues to grow into the glacier valley and the landslide interacts with the valley floor this would become less likely. Long-term, Sam Slip and Passchendale Slip will adjust completely, with gullying exhausting sediment availability on the hillslope although high sediment volumes will remain in the proglacial zone. Investigating the impacts of high sediment accumulations in the pro glacial zone is beyond the scope of this thesis however overseas examples show total paraglacial adjustment of the proglacial

zone through reworking can occur indefinitely, should sediment continue to be added to the system (Ballantyne, 2002a). At Mueller Glacier, should movement continue, the valley will likely be dammed by the glacier and the formation of a proglacial lake may have begun. Outside of repeated glacial cycles, the greatest hazard to impact upon the Mueller Rockslide will be earthquakes and the site will be exposed to strong earthquakes in the future. These will continue to progressively weaken the hillslope and may or may not act as a trigger for failure. Given the sites location in a high seismic zone, its proximity to the Mueller Glacier and its growth into the valley, the rockslide will likely fail in the future, caused by earthquakes or future glacier advance which would destabilise and erode the toe of the rockslide. Overall, the risks of catastrophic failure for the sediment slopes at Fox Glacier will decrease in the future as sediment supply is exhausted and increase in the future for the Mueller Rockslide as it is progressively weakened by external triggers.

6.4 Conclusions

This thesis has presented an investigation into the formation and associated impacts of paraglacial landsliding through movement monitoring, subsurface investigations and laboratory techniques. Methodologies including but not limited to geophysics, geotechnical mapping, crack meter monitoring and timelapse photo analysis have been successfully combined to provide insight in to the development of paraglacial rock and sediment slope failures. Both rock and sediment slopes exhibit some similarity in movement patterns during debuttressing; landslide movement increases as the glacier terminus approaches midway along the landslide toe with movement rates decreasing when the glacier terminus reaches half way along the landslide toe. But the timescales over which they deform are vastly different, as are their movement drivers and the impacts they have on the surrounding area. Conditioning of paraglacial rockslope failures occurs thousands of years prior to debuttressing, as does failure with scarp development seen at least 8000 years prior to debuttressing. Structural controls like bedding orientation may predispose certain rockslopes to accelerated movement and potential failure with toppling dominated rockslides exhibiting faster movement rates. In sediment slopes, debuttressing plays a fundamental role in inducing failure with movement monitoring showing a near instantaneous response of sediment slopes to seasonal changes in glacier retreat. In fact, debris flow activity was minor at the study site (Fox Glacier) and was not documented until the end of the study period when debuttressing was complete.

This thesis has highlighted the diversity and transient nature of paraglacial sediment slope development compared to overseas studies. Valley morphology appears to enhance or reduce connectivity, and sediment storage on valley slopes may not be assumed for paraglacial environments with sediment directly transported to the proglacial zone ready for remobilisation.

This thesis also investigated the impacts paraglacial hillslope response has on the surrounding environment, and the hazards posed by these events. These effects can be wide ranging spatially, and variable in their likelihood of occurrence and importance. Rock slope deformation can

produce headscarp retrogression and movement of several centimetres per year. In the valley floor, growth of the landslide toe shows the potential to develop into a landslide dam. In sediment slopes, sedimentation rates were ten times higher than previous reported in other paraglacial sediment slope studies. Combined with high connectivity between the hillslope and valley floor, large volumes of sediment are being delivered into the proglacial zone.

Both rock and sediment slopes also showed unusual interactions with their corresponding glaciers. Rock slope deformation lead to the pinching out and narrowing of the Mueller Glacier plus additional crevassing of the glacier and formation of ice cauldrons, previously unseen outside of geothermal areas. Sediment slope deformation led to the direct delivery of sediment underneath the Fox Glacier potentially altering how sediment is entrained through the glacier terminus. These impacts are not only limited to the environment; they have the potential to place human life at risk with increased sediment ready for mobilisation during flood events as glacier retreat continues.

This research has advanced the understanding of paraglacial hillslope development but to mitigate future risk direct focus should be placed on their continued development through this current phase of contemporary debuttressing. Identifying common factors which could predefine certain paraglacial hillslopes for accelerated or rapid failure would be a useful prediction tool i.e. does toppling oriented discontinuities truly increase the risk of paraglacial rockslopes failing rapidly. Additional focus should be placed on quantifying the response of sediment slopes as the implications of these slope failures are being seen almost immediately and will continue over the short term, acting as a hazard for decades into the future.

7. Bibliography

AGLIARDI, F., CROSTA, G. & ZANCHI, A. 2001. Structural constraints on deep-seated slope deformation kinematics. *Engineering Geology,* 59**,** 83-102.
AGLIARDI, F., CROSTA, G. B., ZANCHI, A. & RAVAZZI, C. 2009a. Onset and timing of deep-seated gravitational slope deformations in the eastern Alps, Italy. *Geomorphology,* 103**,** 113-129.
AGLIARDI, F., ZANCHI, A. & CROSTA, G. 2009b. Tectonic vs. gravitational morphostructures in the central Eastern Alps (Italy): constraints on the recent evolution of the mountain range. *Tectonophysics* 474**,** 250-270.
ALLEN, S., GRUBER, S., OWENS, I. 2009. Exploring steep bedrock permafrost and its relationship with recent slope failures in the Southern Alps of New Zealand. *Journal of Permafrost and Periglacial Processes* 20**,** 345-356.
AMBROSI, C. & CROSTA, G. 2011. Valley shape influence on deformation mechanisms of rock slopes. *Geological Society, London, Special Publications,* 351**,** 215-233.
AMITRANO, D. 2006. Rupture by damage accumulation in rocks. *International Journal of Fracture,* 139**,** 369-381.
ARCHIBALD, G. C., CAREY J.M., RIES. W.F., MCCOLL. S.T. 2016. *Geological inspection and baseline monitoring of Mueller Hut, Aoraki/ Mt Cook National Park*. GNS Science Consultancy Report 2016/80 June 2016.
ARINGOLI, D., FARABOLLINI, P., GIACOPETTI, M., MATERAZZI, M., PAGGI, S., PAMBIANCHI, G., PIERANTONI, P. P., PISTOLESI, E., PITTS, A. & TONDI, E. 2016. The August 24th 2016 Accumoli earthquake: Surface faulting and deep-seated gravitational slope deformation (DSGSD) in the Monte Vettore area. *Annals of Geophysics* 59.
ATKINSON, B. 1984. Subcritical crack growth in geological materials. *Journal of Geophysical Research: Solid Earth,* 89**,** 4077-4114.
AUGUSTINUS, P. Rock mass strength and the stability of some glacial valley slopes. International Journal of Rock Mechanics and Mining Sciences and Geomechanics Abstracts, 1996. 28A-29A.
AUGUSTINUS, P. 1995. Glacial valley cross-profile development: the influence of in situ rock stress and rock mass strength, with examples from the Southern Alps, New Zealand. *Geomorphology,* 14**,** 87-97.
BADGER, T. C. 2002. Fracturing within anticlines and its kinematic control on slope stability. *Environmental Engineering Geoscience,* 8**,** 19-33.
BAEWERT, H. & MORCHE, D. 2014. Coarse sediment dynamics in a proglacial fluvial system (Fagge River, Tyrol). *Geomorphology,* 218**,** 88-97.
BALDIS, C. T. & LIAUDAT, D. 2019. Rockslides and rock avalanches in the Central Andes of Argentina and their possible association with permafrost degradation. *Permafrost and Periglacial Processes,* 30**,** 330-347.
BALLANTYNE, C. K. 2000a. Paraglacial adjustment of rock slopes: causes and consequences. *Indian Journal of Geography and Environment,* 5**,** 1-22.
BALLANTYNE, C. K. 2002a. A general model of paraglacial landscape response. *The Holocene,* 12**,** 371-376.
BALLANTYNE, C. K. 2002b. Paraglacial geomorphology. *Quaternary Science Reviews,* 21**,** 1935-2017.
BALLANTYNE, C. K. & BENN, D. I. 1994. Paraglacial Slope Adjustment and Resedlmenfation following Recent Glacier Retreat, Fåbergstølsdalen, Norway. *Arctic and Alpine Research,* 26**,** 255-269.
BALLANTYNE, C. K. & STONE, J. J. T. H. 2004. The Beinn Alligin rock avalanche, NW Scotland: cosmogenic 10Be dating, interpretation and significance. *The Holocene,* 14**,** 448-453.
BALLANTYNE, C. K. & STONE, J. 2013. Timing and periodicity of paraglacial rock-slope failures in the Scottish Highlands. *Geomorphology,* 186**,** 150-161.
BALLANTYNE, C. K., WILSON, P., SCHNABEL, C. 2013. Lateglacial rock slope failures in north-west Ireland: age, causes and implications. *Journal of Quaternary Science,* 28**,** 789-802.
BALLANTYNE, C. K. J. 2000b. Paraglacial adjustment of rock slopes: causes and consequences. *Indian Journal of Geography Environmental,* 5**,** 1-22.

BALLANTYNE, C. K. 2002c. A general model of paraglacial landscape response. *The Holocene,* 12**,** 371-376.
BARBANO, M. S., PAPPALARDO, G., PIRROTTA, C. & MINEO, S. 2014. Landslide triggers along volcanic rock slopes in eastern Sicily (Italy). *Natural Hazards,* 73**,** 1587-1607.
BARBARANO, M., AGLIARDI, F., CROSTA, G. B. & ZANCHI, A. 2015. Inherited and active tectonic controls on the Piz Dora DSGSD (Val Müstair, Switzerland). *Engineering geology for society and territory-volume 2.* Springer.
BAUMANN, S., ANDERSON, B., CHINN, T., MACKINTOSH, A., COLLIER, C., LORREY, A. M., RACK, W., PURDIE, H. & EAVES, S. 2020. Updated inventory of glacier ice in New Zealand based on 2016 satellite imagery. *Journal of Glaciology***,** 1-14.
BECK, A. C. 1968. Gravity faulting as a mechanism of topographic adjustment. *New Zealand Journal of Geology and Geophysics,* 11**,** 191-199.
BERRYMAN, K. R., COCHRAN, U. A., CLARK, K. J., BIASI, G. P., LANGRIDGE, R. M. & VILLAMOR, P. 2012. Major earthquakes occur regularly on an isolated plate boundary fault. *Science,* 336**,** 1690-1693.
BESSETTE-KIRTON, E. K. & COE, J. 2020. A 36-year record of rock avalanches in the Saint Elias Mountains of Alaska, with implications for future hazards. *Frontiers in Earth Science* 8**,** 293.
BLAIR JR, R. 1994. Moraine and valley wall collapse due to rapid deglaciation in Mount Cook National Park, New Zealand. *Mountain Research and Development***,** 347-358.
BLIKRA, L. H. & CHRISTIANSEN, H. 2014. A field-based model of permafrost-controlled rockslide deformation in northern Norway. *Geomorphology,* 208**,** 34-49.
BOVIS, M. J. & JAKOB, M. 1999. The role of debris supply conditions in predicting debris flow activity. *Earth surface processes and landforms,* 24**,** 1039-1054.
BOVIS, M. 1990. Rock-slope deformation at affliction creek, southern Coast Mountains, British Columbia. *Canadian Journal of Earth Sciences,* 27**,** 243-254.
BOVIS, M. 1982. Uphill-facing (antislope) scarps in the Coast Mountains, southwest British Columbia. *Geological Society of America Bulletin,* 93**,** 804-812.
BRACKEN, L. J., TURNBULL, L., WAINWRIGHT, J., BOGAART, P. 2015. Sediment connectivity: a framework for understanding sediment transfer at multiple scales. *Earth Surface Processes and Landforms,* 40**,** 177-188.
BRIDEAU, M.-A., MCDOUGALL, S., STEAD, D., EVANS, S. G., COUTURE, R., TURNER, K. 2012. Three-dimensional distinct element modelling and dynamic runout analysis of a landslide in gneissic rock, British Columbia, Canada. *Bulletin of Engineering Geology and the Environment,* 71**,** 467-486.
BRIDEAU, M.-A., YAN, M. & STEAD, D. 2009. The role of tectonic damage and brittle rock fracture in the development of large rock slope failures. *Geomorphology,* 103**,** 30-49.
BROMHEAD, E. & IBSEN, M. 2004. Bedding-controlled coastal landslides in Southeast Britain between Axmouth and the Thames Estuary. *Landslides* 1**,** 131-141.
BRÖNNIMANN, C. S. 2011. *Effect of groundwater on landslide triggering*. EPFL.
CAMONES, L. A. M., DO AMARAL VARGAS JR, E., DE FIGUEIREDO, R. P. & VELLOSO, R. Q. 2013. Application of the discrete element method for modeling of rock crack propagation and coalescence in the step-path failure mechanism. *Engineering Geology,* 153**,** 80-94.
CARDINALI, M., ARDIZZONE, F., GALLI, M., GUZZETTI, F. & REICHENBACH, P. Landslides triggered by rapid snow melting: the December 1996–January 1997 event in Central Italy. Proceedings 1st Plinius Conference on Mediterranean Storms, 2000. Citeseer, 439-448.
CARRIVICK, J. L., JAMES, W. H., GRIMES, M., SUTHERLAND, J. L. & LORREY, A. M. 2020. Ice thickness and volume changes across the Southern Alps, New Zealand, from the little ice age to present. *Scientific reports,* 10**,** 1-10.
CARRIVICK, J. L., RUSHMER, E. 2009. Inter-and intra-catchment variations in proglacial geomorphology: an example from Franz Josef Glacier and Fox Glacier, New Zealand. *Arctic, Antarctic, and Alpine Research,* 41**,** 18-36.
CAVALLI, M., TREVISANI, S., COMITI, F. & MARCHI, L. 2013. Geomorphometric assessment of spatial sediment connectivity in small Alpine catchments. *Geomorphology,* 188**,** 31-41.

CHIGIRA, M., HARIYAMA, T. & YAMASAKI, S. 2013. Development of deep-seated gravitational slope deformation on a shale dip-slope: observations from high-quality drill cores. *Tectonophysics,* 605**,** 104-113.

CHIGIRA, M. & KIHO, K. 1994. Deep-seated rockslide-avalanches preceded by mass rock creep of sedimentary rocks in the Akaishi Mountains, central Japan. *Engineering Geology,* 38**,** 221-230.

CHIGIRA, M., MOHAMAD, Z., SIAN, L. C. & KOMOO, I. 2011. Landslides in weathered granitic rocks in Japan and Malaysia. *Bulletin of the Geological Society of Malaysia*.

CHIGIRA, M., WANG, W.-N., FURUYA, T. & KAMAI, T. 2003. Geological causes and geomorphological precursors of the Tsaoling landslide triggered by the 1999 Chi-Chi earthquake, Taiwan. *Engineering Geology,* 68**,** 259-273.

CHINN, T. 1996. New Zealand glacier responses to climate change of the past century. *New Zealand Journal of Geology and Geophysics,* 39**,** 415-428.

CHURCH, M. & RYDER, J. M. 1972. Paraglacial sedimentation: a consideration of fluvial processes conditioned by glaciation. *Geological Society of America Bulletin,* 83**,** 3059-3072.

CHURCH, M. & SLAYMAKER, O. 1989. Holocene disequilibrium of sediment yield in British Columbia. *Nature,* 327**,** 452-454.

CLARKE, B. A. & BURBANK, D. W. 2011. Quantifying bedrock-fracture patterns within the shallow subsurface: Implications for rock mass strength, bedrock landslides, and erodibility. *Journal of Geophysical Research: Earth Surface,* 116**,** n/a-n/a. Available: 10.1029/2011jf001987

COE, J. A., BESSETTE-KIRTON, E. K. & GEERTSEMA, M. 2017. Increasing rock-avalanche size and mobility in Glacier Bay National Park and Preserve, Alaska detected from 1984 to 2016 Landsat imagery. *Landslides***,** 1-15.

COE, J. A. J. L. 2020. Bellwether sites for evaluating changes in landslide frequency and magnitude in cryospheric mountainous terrain: a call for systematic, long-term observations to decipher the impact of climate change. *Landslides***,** 1-19.

COOK, S. J., PORTER, P. R. & BENDALL, C. 2013. Geomorphological consequences of a glacier advance across a paraglacial rock avalanche deposit. *Geomorphology,* 189**,** 109-120.

COQUIN, J., MERCIER, D., BOURGEOIS, O., COSSART, E. & DECAULNE, A. 2015. Gravitational spreading of mountain ridges coeval with Late Weichselian deglaciation: impact on glacial landscapes in Tröllaskagi, northern Iceland. *Quarternary Science Reviews* 107**,** 197-213.

COROMINAS, J., MAVROULI, O. & RUIZ-CARULLA, R. 2018. Magnitude and frequency relations: are there geological constraints to the rockfall size? *Landslides,* 15**,** 829-845.

COROMINAS, J. & MOYA, J. 1999. Reconstructing recent landslide activity in relation to rainfall in the Llobregat River basin, Eastern Pyrenees, Spain. *Geomorphology,* 30**,** 79-93.

COSSART, E. Do deglaciated mountainslopes contribute significantly to paraglacial sediment fluxes? EGU General Assembly Conference Abstracts, 2013.

COSSART, E., BRAUCHER, R., FORT, M., BOURLÈS, D. & CARCAILLET, J. 2008. Slope instability in relation to glacial debuttressing in alpine areas (Upper Durance catchment, southeastern France): evidence from field data and 10Be cosmic ray exposure ages. *Geomorphology,* 95**,** 3-26.

COSSART, E., MERCIER, D., DECAULNE, A. & FEUILLET, T 2013. An overview of the consequences of paraglacial landsliding on deglaciated mountain slopes: typology, timing and contribution to cascading fluxes. *Quaternaire. Revue de l'Association française pour l'étude du Quaternaire,* 24**,** 13-24.

COSSART, É. J. 2008. Landform connectivity and waves of negative feedbacksduring the paraglacial period, a case study: the Tabuc subcatchment since the end of the Little Ice Age (massif des Écrins, France). *Géomorphologie: relief, processus, environnement,* 14**,** 249-260.

COSTA, J. E. & SCHUSTER, R. L. 1988. The formation and failure of natural dams. *Geological Society of America Bulletin,* 100**,** 1054-1068.

COUTURE, R. & EVANS, S. A rock topple-rock avalanche, near Goat Mountain, Cariboo Mountains, British Columbia, Canada. Proceedings, 9th Congress, International Association of Engineering Geology and the Environment, Durban, South Africa, Conference CD, 2002.

COX, S. C., BARRELL, D.J.A. 2007. *Geology of the Aoraki area.* . GNS Science.
CRANDELL, D., MILLER, C. D., GLICKEN, H., CHRISTIANSEN, R. & NEWHALL, C. J. G. 1984. Catastrophic debris avalanche from ancestral Mount Shasta volcano, California. *Geology,* 12**,** 143-146.
CROSTA, G. & AGLIARDI, F. 2003. Failure forecast for large rock slides by surface displacement measurements. *Canadian Geotechnical Journal,* 40**,** 176-191.
CROSTA, G., DI PRISCO, C., FRATTINI, P., FRIGERIO, G., CASTELLANZA, R. & AGLIARDI, F. J. L. 2014. Chasing a complete understanding of the triggering mechanisms of a large rapidly evolving rockslide. *Landslides,* 11**,** 747-764.
CROZIER, M. & GLADE, T. 2005a. Landslide hazard and risk: issues, concepts and approach. *Landslide hazard and risk***,** 1-40.
CROZIER, M. J. 1986. *Landslides: causes, consequences & environment*, Taylor & Francis.
CROZIER, M. J. & GLADE, T. 2005b. Landslide hazard and risk: issues, concepts and approach. *Landslide hazard and risk***,** 1-40.
CROZIER, M. 2010. Deciphering the effect of climate change on landslide activity: A review. *Geomorphology,* 124**,** 260-267.
CRUDEN, D. M. 1991. A simple definition of a landslide. *Bulletin of Engineering Geology and the Environment,* 43**,** 27-29.
CURRY, A., CLEASBY, V. & ZUKOWSKYJ, P. 2006. Paraglacial response of steep, sediment-mantled slopes to post-'Little Ice Age'glacier recession in the central Swiss Alps. *Journal of Quaternary Science: Published for the Quaternary Research Association,* 21**,** 211-225.
CURRY, A. M. 1999. Paraglacial modification of slope form. *Earth Surface Processes and Landforms: The Journal of the British Geomorphological Research Group,* 24**,** 1213-1228.
CURRY, A. M. 2020. Paraglacial rock-slope failure following deglaciation in western Norway. *Landscapes and Landforms of Norway.* Springer.
CURRY, A. M. & BALLANTYNE, C. K. 1999. Paraglacial modification of glacigenic sediment. *Geografiska Annaler: Series A, Physical Geography,* 81**,** 409-419.
CURRY, A. M., SANDS, T. B. & PORTER, P. R. 2009a. Geotechnical controls on a steep lateral moraine undergoing paraglacial slope adjustment. *Geological Society, London, Special Publications,* 320**,** 181-197.
CURRY, A. M., SANDS, T. B. & PORTER, P. 2009b. Geotechnical controls on a steep lateral moraine undergoing paraglacial slope adjustment. *Geological Society, London, Special Publications,* 320**,** 181-197.
DAI, C., HIGMAN, B., LYNETT, P. J., JACQUEMART, M., HOWAT, I. M., LILJEDAHL, A. K., DUFRESNE, A., FREYMUELLER, J. T., GEERTSEMA, M. & WARD JONES, M. 2020. Detection and assessment of a large and potentially-tsunamigenic periglacial landslide in Barry Arm, Alaska. *Geophysical Research Letters***,** e2020GL089800.
DAVIES, T. R., KORUP, O. 2010. Sediment cascades in active landscapes. *Sediment Cascades: An Integrated Approach***,** 89-115.
DAVIS, J. L. & ANNAN, A. 1989. Ground-penetrating radar for high-resolution mapping of soil and rock stratigraphy 1. *Geophysical Prospecting,* 37**,** 531-551.
DE GIORGI, L. & LEUCCI, G. 2014. Detection of hazardous cavities below a road using combined geophysical methods. *Surveys in geophysics,* 35**,** 1003-1021.
DELINE, P., GRUBER, S., DELALOYE, R., FISCHER, L., GEERTSEMA, M., GIARDINO, M., HASLER, A., KIRKBRIDE, M., KRAUTBLATTER, M. & MAGNIN, F. 2015a. Ice loss and slope stability in high-mountain regions. *Snow and Ice-related Hazards, Risks and Disasters.* Elsevier.
DELINE, P., HEWITT, K., REZNICHENKO, N. & SHUGAR, D. 2015b. Rock avalanches onto glaciers. *Landslide hazards, risks and disasters.* Elsevier.
DELINE, P. 2009. Interactions between rock avalanches and glaciers in the Mont Blanc massif during the late Holocene. *Quarternary Science Reviews,* 28**,** 1070-1083.
DRAEBING, D. & EICHEL, J. 2018. Divergence, convergence, and path dependency of paraglacial adjustment of alpine lateral moraine slopes. *Land degradation & development,* 29**,** 1979-1990.

DRAEBING, D., KRAUTBLATTER, M. & DIKAU, R. 2014. Interaction of thermal and mechanical processes in steep permafrost rock walls: a conceptual approach. *Geomorphology,* 226**,** 226-235.

DRAEBING, D. & KRAUTBLATTER, M. 2012. P-wave velocity changes in freezing hard low-porosity rocks: a laboratory-based time-average model. *The Cryosphere,* 6**,** 1163-1174.

DRAMIS, F. & SORRISO-VALVO, M. 1994. Deep-seated gravitational slope deformations, related landslides and tectonics. *Engineering Geology,* 38**,** 231-243.

DUNNING, S. A., ROSSER, N. J., MCCOLL, S. T. & REZNICHENKO, N. V. 2015. Rapid sequestration of rock avalanche deposits within glaciers. *Nature communications,* 6**,** 7964.

DURGIN, P. 1977. Landslides and the weathering of granitic rocks. *Reviews in Engineering Geology,* 3**,** 127-131.

EBERHARDT, E., STEAD, D., COGGAN, J. & SCIENCES, M. 2004. Numerical analysis of initiation and progressive failure in natural rock slopes—the 1991 Randa rockslide. *International Journal of Rock Mechanics,* 41**,** 69-87.

EBERHARDT, E., STEAD, D. & LOEW, S. Progressive Failure, Rock Mass Fatigue and Early Warning Applied to Deep-Seated Rock Slope Failures. ISRM Progressive Rock Failure Conference, 2017. International Society for Rock Mechanics and Rock Engineering.

EICHEL, J., DRAEBING, D. & MEYER, N. 2018. From active to stable: Paraglacial transition of Alpine lateral moraine slopes. *Land degradation & development,* 29**,** 4158-4172.

EL BEDOUI, S., BOIS, T., JOMARD, H., SANCHEZ, G., LEBOURG, T., TRICS, E., GUGLIELMI, Y., BOUISSOU, S., CHEMENDA, A. & ROLLAND, Y. J. G. S., LONDON, SPECIAL PUBLICATIONS 2011. Paraglacial gravitational deformations in the SW Alps: a review of field investigations, 10Be cosmogenic dating and physical modelling. *Geological Society, London, Special Publications,* 351**,** 11-25.

EMMER, A., KLIMEŠ, J., HÖLBLING, D., ABAD, L., DRAEBING, D., SKALÁK, P., ŠTĚPÁNEK, P. & ZAHRADNÍČEK, P. 2020. Distinct types of landslides in moraines associated with the post-LIA glacier thinning: Observations from the Kinzl Glacier, Huascarán, Peru. *Science of the Total Environment***,** 139997.

EVANS, S. G., HUNGR, O. & CLAGUE, J. 2001. Dynamics of the 1984 rock avalanche and associated distal debris flow on Mount Cayley, British Columbia, Canada; implications for landslide hazard assessment on dissected volcanoes. *Engineering Geology,* 61**,** 29-51.

FAN, X., DUFRESNE, A., SUBRAMANIAN, S. S., STROM, A., HERMANNS, R., STEFANELLI, C. T., HEWITT, K., YUNUS, A. P., DUNNING, S. & CAPRA, L. J. 2020. The formation and impact of landslide dams–State of the art. *Earth-Science Reviews,* 203**,** 103116.

FERNANDES, M., OLIVA, M. & VIEIRA, G. 2020. Paraglacial slope failures in the Aran valley (Central Pyrenees). *Quaternary International,* 566**,** 24-38.

FEY, C., WICHMANN, V. & ZANGERL, C. J. G. 2017. Reconstructing the evolution of a deep seated rockslide (Marzell) and its response to glacial retreat based on historic and remote sensing data. *Geomorphology,* 298**,** 72-85.

FITZHARRIS, B. & GARR, C. 1995. Simulation of past variability in seasonal snow in the Southern Alps, New Zealand. *Annals of Glaciology,* 21**,** 377-382.

FROUDE, M. J., PETLEY, D. 2018. Global fatal landslide occurrence from 2004 to 2016. *Natural Hazards Earth System Sciences,* 18**,** 2161-2181.

GANERØD, G. V., GRØNENG, G., RØNNING, J. S., DALSEGG, E., ELVEBAKK, H., TØNNESEN, J. F., KVELDSVIK, V., EIKEN, T., BLIKRA, L. H. & BRAATHEN, A. 2008. Geological model of the Åknes rockslide, western Norway. *Engineering Geology,* 102**,** 1-18. Available: http://dx.doi.org/10.1016/j.enggeo.2008.01.018

GARDNER, J. S. & HEWITT, K. 1990. A surge of Bualtar Glacier, Karakoram Range, Pakistan: a possible landslide trigger. *Journal of Glaciology,* 36**,** 159-162.

GATTINONI, P., SCESI, L., ARIENI, L. & CANAVESI, M. J. L. 2012. The February 2010 large landslide at Maierato, Vibo Valentia, Southern Italy. *Landslides,* 9**,** 255-261.

GEERTSEMA, M., CLAGUE, J. J., SCHWAB, J. W. & EVANS, S. G. 2006. An overview of recent large catastrophic landslides in northern British Columbia, Canada. *Engineering Geology,* 83**,** 120-143.
GELLATLY, A. F. J. G. J. 1985. Historical records of glacier fluctuations in Mt Cook National Park, New Zealand: a century of change. *Geographical Journal***,** 86-99.
GERRARD, J. 1994. The landslide hazard in the Himalayas: geological control and human action. *Geomorphology and Natural Hazards.* Elsevier.
GHIROTTI, M., MARTIN, S. & GENEVOIS, R. J. G. S., LONDON, SPECIAL PUBLICATIONS 2011. The Celentino deep-seated gravitational slope deformation (DSGSD): structural and geomechanical analyses (Peio Valley, NE Italy). *Geological Society, London, Special Publications,* 351**,** 235-251.
GISCHIG, V., PREISIG, G., EBERHARDT, E. 2016. Numerical investigation of seismically induced rock mass fatigue as a mechanism contributing to the progressive failure of deep-seated landslides. *Rock Mechanics Rock Engineering,* 49**,** 2457-2478.
GLASTONBURY, J. & FELL, R. 2008a. A decision analysis framework for the assessment of likely post-failure velocity of translational and compound natural rock slope landslides. *Canadian Geotechnical Journal,* 45**,** 329-350.
GLASTONBURY, J. & FELL, R. 2008b. Geotechnical characteristics of large slow, very slow, and extremely slow landslides. *Canadian Geotechnical Journal,* 45**,** 984-1005.
GLASTONBURY, J. & FELL, R. 2010. Geotechnical characteristics of large rapid rock slides. *Canadian Geotechnical Journal,* 47**,** 116-132.
GLUEER, F., LOEW, S. & MANCONI, A. 2019. Paraglacial history and structure of the Moosfluh Landslide (1850–2016), Switzerland. *Geomorphology*.
GOSSE, J. C. & PHILLIPS, F. 2001. Terrestrial in situ cosmogenic nuclides: theory and application. *Quarternary Science Reviews,* 20**,** 1475-1560.
GRÄMIGER, L. M., MOORE, J. R., GISCHIG, V. S., IVY-OCHS, S. & LOEW, S. 2017. Beyond debuttressing: Mechanics of paraglacial rock slope damage during repeat glacial cycles. *Journal of Geophysical Research: Earth Surface,* 122**,** 1004-1036.
GRÄMIGER, L. M., MOORE, J. R., GISCHIG, V. S., LOEW, S., FUNK, M. & LIMPACH, P. 2020. Hydromechanical rock slope damage during Late Pleistocene and Holocene glacial cycles in an Alpine valley. *Journal of Geophysical Research: Earth Surface,* 125**,** e2019JF005494.
GRUBER, S., HOELZLE, M. & HAEBERLI, W. 2004. Permafrost thaw and destabilization of Alpine rock walls in the hot summer of 2003. *Geophysical Research Letters,* 31.
GSCHWIND, S., LOEW, S. & WOLTER, A. 2019. Multi-stage structural and kinematic analysis of a retrogressive rock slope instability complex (Preonzo, Switzerland). *Engineering Geology,* 252**,** 27-42.
GUDE, M. & BARSCH, D. 2005. Assessment of geomorphic hazards in connection with permafrost occurrence in the Zugspitze area (Bavarian Alps, Germany). *Geomorphology,* 66**,** 85-93.
GUDMUNDSSON, M. T. 2021. Ice Cauldron. *Encyclopedia of Planetary Landforms.* New York, NY: Springer New York. Available: 10.1007/978-1-4614-9213-9_192-1
GUPTA, V. 2005. The relationship between tectonic stresses, joint patterns and landslides. *Journal of Nepal Geological Society,* 31**,** 51-58.
GUZZETTI, F., CARDINALI, M. & REICHENBACH, P. 1996. The influence of structural setting and lithology on landslide type and pattern. *Environmental & Engineering Geoscience,* 2**,** 531-555.
HAAS, F., HECKMANN, T., WICHMANN, V., BECHT, M. 2012. Runout analysis of a large rockfall in the Dolomites/Italian Alps using LIDAR derived particle sizes and shapes. *Earth Surface Processes and Landforms,* 37**,** 1444-1455.
HAEBERLI, W., SCHAUB, Y. & HUGGEL, C. 2017. Increasing risks related to landslides from degrading permafrost into new lakes in de-glaciating mountain ranges. *Geomorphology,* 293**,** 405-417.
HALLET, B., HUNTER, L. & BOGEN, J. 1996. Rates of erosion and sediment evacuation by glaciers: A review of field data and their implications. *Global and Planetary Change,* 12**,** 213-235.

HANCOX, G. T. 1998. *Pilot study for Baseline Geological Inspection of DOC Backcountry Huts: Inspections of alpine hut sites in the Mt Cook and Westland National Parks, March 1998.* . Institute of Geological and Nuclear Sciences Client Report 43713B.

HARRISON, S. & WINCHESTER, V. 1997. Age and nature of paraglacial debris cones along the margins of the San Rafael Glacier, Chilean Patagonia. *The Holocene,* 7**,** 481-487.

HAUCK, C., MÜHLL, D. V. 2003. Inversion and interpretation of two-dimensional geoelectrical measurements for detecting permafrost in mountainous regions. *Permafrost and Periglacial Processes,* 14**,** 305-318.

HAVENITH, H.-B., JONGMANS, D., ABDRAKHMATOV, K., TREFOIS, P., DELVAUX, D. & TORGOEV, I. A. 2000. Geophysical Investigations Of Seismically Induced Surface Effects: Case Study Of A Landslide In The Suusamyr Valley, Kyrgyzstan. *Surveys in Geophysics,* 21**,** 351-370. Available: 10.1023/a:1006788808145

HAVENITH, H.-B., JONGMANS, D., FACCIOLI, E., ABDRAKHMATOV, K. & BARD, P.-Y. 2002. Site Effect Analysis around the Seismically Induced Ananevo Rockslide, Kyrgyzstan. *Bulletin of the Seismological Society of America,* 92**,** 3190-3209. Available: 10.1785/0120010206

HECKMANN, T., CAVALLI, M., CERDAN, O., FOERSTER, S., JAVAUX, M., LODE, E., SMETANOVÁ, A., VERICAT, D. & BRARDINONI, F. 2018. Indices of sediment connectivity: opportunities, challenges and limitations. *Earth Science Reviews,* 187**,** 77-108.

HECKMANN, T. & SCHWANGHART, W. 2013. Geomorphic coupling and sediment connectivity in an alpine catchment—Exploring sediment cascades using graph theory. *Geomorphology,* 182**,** 89-103.

HEINCKE, B., GÜNTHER, T., DALSEGG, E., RØNNING, J. S., GANERØD, G. V. & ELVEBAKK, H. 2010. Combined three-dimensional electric and seismic tomography study on the Åknes rockslide in western Norway. *Journal of Applied Geophysics,* 70**,** 292-306. Available: 10.1016/j.jappgeo.2009.12.004

HEINCKE, B., MAURER, H., GREEN, A. G., WILLENBERG, H., SPILLMANN, T. & BURLINI, L. 2006. Characterizing an unstable mountain slope using shallow 2D and 3D seismic tomography. *Geophysics,* 71**,** B241-B256. Available: 10.1190/1.2338823

HELMSTETTER, A. & GARAMBOIS, S. J. 2010. Seismic monitoring of Séchilienne rockslide (French Alps): Analysis of seismic signals and their correlation with rainfalls. *Journal of Geophysical Research: Earth Surface,* 115.

HERMAN, F., ANDERSON, B. & LEPRINCE, S. J. 2011. Mountain glacier velocity variation during a retreat/advance cycle quantified using sub-pixel analysis of ASTER images. *Journal of Glaciology,* 57**,** 197-207.

HEWITT, K. 2009. Rock avalanches that travel onto glaciers and related developments, Karakoram Himalaya, Inner Asia. *Geomorphology,* 103**,** 66-79.

HIGMAN, B., SHUGAR, D. H., STARK, C. P., EKSTRÖM, G., KOPPES, M. N., LYNETT, P., DUFRESNE, A., HAEUSSLER, P. J., GEERTSEMA, M. & GULICK, S. 2018. The 2015 landslide and tsunami in Taan Fiord, Alaska. *Scientific reports,* 8**,** 1-12.

HILGER, P., HERMANNS, R. L., CZEKIRDA, J., MYHRA, K. S., GOSSE, J. C. & ETZELMÜLLER, B. 2020. Permafrost as a first order control on long-term rock-slope deformation in (Sub-) Arctic Norway. *Quarternary Science Reviews,* 251**,** 106718.

HOLM, K., BOVIS, M. & JAKOB, M. 2004. The landslide response of alpine basins to post-Little Ice Age glacial thinning and retreat in southwestern British Columbia. *Geomorphology,* 57**,** 201-216.

HOU, Y., CHIGIRA, M. & TSOU, C.-Y. 2014. Numerical study on deep-seated gravitational slope deformation in a shale-dominated dip slope due to river incision. *Engineering Geology,* 179**,** 59-75.

HOVIUS, N. 1995. *A geological hazard assessment for the lower Fox Valley, anno 1994.* . Department of Conservation, Wellington.

HUANG, D., CEN, D., MA, G. & HUANG, R. 2015. Step-path failure of rock slopes with intermittent joints. *Landslides,* 12**,** 911-926.

HUGENHOLTZ, C. H., MOORMAN, B. J., BARLOW, J. & WAINSTEIN, P. A. 2008a. Large-scale moraine deformation at the Athabasca Glacier, Jasper National Park, Alberta, Canada. *Landslides,* 5**,** 251-260.

HUGENHOLTZ, C. H., MOORMAN, B. J., BARLOW, J. & WAINSTEIN, P. A. 2008b. Large-scale moraine deformation at the Athabasca Glacier, Jasper National Park, Alberta, Canada. 5**,** 251-260.

HUGGEL, C., CLAGUE, J. J., KORUP, O. 2012. Is climate change responsible for changing landslide activity in high mountains? *Earth Surface Processes and Landforms,* 37**,** 77-91.

HUGGEL, C., ZGRAGGEN-OSWALD, S., HAEBERLI, W., KÄÄB, A., POLKVOJ, A., GALUSHKIN, I. & EVANS, S. 2005. The 2002 rock/ice avalanche at Kolka/Karmadon, Russian Caucasus: assessment of extraordinary avalanche formation and mobility, and application of QuickBird satellite imagery. *Natural Hazards and Earth System Sciences*.

HUMAIR, F., PEDRAZZINI, A., EPARD, J.-L., FROESE, C. R. & JABOYEDOFF, M. J. T. 2013. Structural characterization of Turtle Mountain anticline (Alberta, Canada) and impact on rock slope failure. *Tectonophysics,* 605**,** 133-148.

HUNGR, O. 2007. Dynamics of rapid landslides. *Progress in landslide science.* Springer.

HUNGR, O., LEROUEIL, S. & PICARELLI, L. 2014. The Varnes classification of landslide types, an update. *Landslides,* 11**,** 167-194.

IVERSON, R. M. 2000. Landslide triggering by rain infiltration. *Water resources research,* 36**,** 1897-1910.

JABOYEDOFF, M., PENNA, I., PEDRAZZINI, A., BAROŇ, I. & CROSTA, G. B. 2013. An introductory review on gravitational-deformation induced structures, fabrics and modeling. *Tectonophysics,* 605**,** 1-12.

JACKSON JR, L. E., MACDONALD, G. M. & WILSON, M. C. 1982. Paraglacial origin for terraced river sediments in Bow Valley, Alberta. *Canadian Journal of Earth Sciences,* 19**,** 2219-2231.

JAKOB, M. 2005a. Debris-flow hazard analysis. *Debris-flow hazards and related phenomena.* Springer.

JAKOB, M. 2005b. A size classification for debris flows. *Engineering geology,* 79**,** 151-161.

JAKOB, M., HUNGR, O. & JAKOB, D. M. 2005. *Debris-flow hazards and related phenomena*, Springer.

JAMES, M. R., HOW, P. & WYNN, P. M. 2016. Pointcatcher software: analysis of glacial time-lapse photography and integration with multitemporal digital elevation models. *Journal of Glaciology,* 62**,** 159-169.

JAMES, M. R. & ROBSON, S. 2014. Mitigating systematic error in topographic models derived from UAV and ground-based image networks. *Earth Surface Processes and Landforms,* 39**,** 1413-1420.

JIJUN, L., DERBYSHIRE, E. & SHUYING, X. Glacial and paraglacial sediments of the Hunza Valley north west Karakoram, Pakistan: a preliminary analysis. The international Karakoram project. International conference, 1984. 496-535.

JOHNSON, P. 1984. Paraglacial conditions of instability and mass movement. A discussion. *Zeitschrift für Geomorphologie Stuttgar,* 28**,** 235-250.

KÄÄB, A., STROZZI, T., DELALOYE, R., AMBROSI, C. & DEBELLA GILO, M. J. E. 2009. Paraglacial rock mass movements in response to glacier retreat. Examples from Aletsch Glacier, Swiss Alps. *EGUGA***,** 11838.

KAGEYAMA, M., PEYRON, O., PINOT, S., TARASOV, P., GUIOT, J., JOUSSAUME, S. & RAMSTEIN, G. 2001. The Last Glacial Maximum climate over Europe and western Siberia: a PMIP comparison between models and data. *Climate Dynamics,* 17**,** 23-43.

KEEFER, D. K. 2002. Investigating landslides caused by earthquakes–a historical review. *Surveys in geophysics,* 23**,** 473-510.

KELLERER-PIRKLBAUER, A., PROSKE, H. & STRASSER, V. 2010. Paraglacial slope adjustment since the end of the Last Glacial Maximum and its long-lasting effects on secondary mass wasting processes: Hauser Kaibling, Austria. *Geomorphology,* 120**,** 65-76.

KENNER, R., PHILLIPS, M., DANIOTH, C., DENIER, C., THEE, P. & ZGRAGGEN, A. 2011. Investigation of rock and ice loss in a recently deglaciated mountain rock wall using terrestrial laser scanning: Gemsstock, Swiss Alps. *Cold Regions Science and Technology,* 67**,** 157-164.

KERR, T., HENDERSON, R. & SOOD, A. 2018. The precipitation distribution across Westland Tai Poutini national park. *Journal of Hydrology (New Zealand),* 57**,** 1.
KEUSCHNIG, M., HARTMEYER, I., HÖFER-ÖLLINGER, G., SCHOBER, A., KRAUTBLATTER, M. & SCHROTT, L. 2015. Permafrost-related mass movements: Implications from a rock slide at the Kitzsteinhorn, Austria. *Engineering Geology for Society and Territory-Volume 1.* Springer.
KILBURN, C. R. & PETLEY, D. N. 2003. Forecasting giant, catastrophic slope collapse: lessons from Vajont, Northern Italy. *Geomorphology,* 54**,** 21-32.
KIRKBRIDE, M. P., DELINE, P. 2018. Spatial heterogeneity in the paraglacial response to post-Little Ice Age deglaciation of four headwater cirques in the Western Alps. *Land degradation & development,* 29**,** 3127-3140.
KIRKBRIDE, M. P., WARREN, C. R. 1999. Tasman Glacier, New Zealand: 20th-century thinning and predicted calving retreat. *Global and Planetary Change,* 22**,** 11-28.
KLICHE, C. A. 1999. *Rock slope stability*.
KNAPP, S., ANSELMETTI, F. S., LEMPE, B., KRAUTBLATTER, M. 2020. Impact of an 0.2 km3 Rock Avalanche on Lake Eibsee (Bavarian Alps, Germany)–Part II: Catchment Response to Consecutive Debris Avalanche and Debris Flow. *Earth Surface Processes and Landforms*.
KORUP, O. 2005a. Geomorphic imprint of landslides on alpine river systems, southwest New Zealand. *Earth Surface Processes and Landforms,* 30**,** 783-800.
KORUP, O. 2005b. Large landslides and their effect on sediment flux in South Westland, New Zealand. *Earth Surface Processes and Landforms,* 30**,** 305-323.
KORUP, O., MCSAVENEY, M. J. & DAVIES, T. R. 2004. Sediment generation and delivery from large historic landslides in the Southern Alps, New Zealand. *Geomorphology,* 61**,** 189-207.
KORUP, O. 2005c. Geomorphic hazard assessment of landslide dams in South Westland, New Zealand: fundamental problems and approaches. *Geomorphology,* 66**,** 167-188.
KOS, A., AMANN, F., STROZZI, T., DELALOYE, R., VON RUETTE, J. & SPRINGMAN, S. 2016. Contemporary glacier retreat triggers a rapid landslide response, Great Aletsch Glacier, Switzerland. *Geophysical Research Letters,* 43**,** 12,466-12,474.
KRAUTBLATTER, M. & DRAEBING, D. 2014. Pseudo 3D - P-wave refraction seismic monitoring of permafrost in steep unstable bedrock. *Journal of Geophysical Research: Earth Surface,* 119**,** 287-299. Available: 10.1002/2012jf002638
KRAUTBLATTER, M., FUNK, D. & GÜNZEL, F. K. 2013. Why permafrost rocks become unstable: a rock–ice-mechanical model in time and space. *Earth Surface Processes and Landforms,* 38**,** 876-887.
KRAUTBLATTER, M., VERLEYSDONK, S., FLORES-OROZCO, A. & KEMNA, A. J. 2010. Temperature-calibrated imaging of seasonal changes in permafrost rock walls by quantitative electrical resistivity tomography (Zugspitze, German/Austrian Alps). *Journal of Geophysical Research: Earth Surface,* 115.
KUSCHEL, E., ZANGERL, C., PROKOP, A., BERNARD, E., TOLLE, F. & FRIEDT, J.-M. Paraglacial adjustment of sediment-mantled slopes through landslide processes in the vicinity of the Austre Lovénbreen glacier (Ny-Ålesund, Svalbard). EGU General Assembly Conference Abstracts, 2020. 9509.
LACROIX, P., BIÈVRE, G., PATHIER, E., KNIESS, U. & JONGMANS, D. 2018. Use of Sentinel-2 images for the detection of precursory motions before landslide failures. *Remote Sensing of Environment* 215**,** 507-516.
LANE, S. N., BAKKER, M., GABBUD, C., MICHELETTI, N. & SAUGY, J.-N. 2017. Sediment export, transient landscape response and catchment-scale connectivity following rapid climate warming and Alpine glacier recession. *Geomorphology,* 277**,** 210-227.
LEBOURG, T., RISS, J. & PIRARD, E. 2004. Influence of morphological characteristics of heterogeneous moraine formations on their mechanical behaviour using image and statistical analysis. *Engineering Geology,* 73**,** 37-50.
LEITH, K., MOORE, J. R., AMANN, F. & LOEW, S. J. 2014a. Subglacial extensional fracture development and implications for Alpine Valley evolution. *Journal of Geophysical Research: Earth Surface,* 119**,** 62-81.

LEITH, K., MOORE, J. R., AMANN, F. & LOEW, S. J. 2014b. In situ stress control on microcrack generation and macroscopic extensional fracture in exhuming bedrock. *Journal of Geophysical Research: Earth Surface,* 119**,** 594-615.
LIFTON, N., SATO, T. & DUNAI, T. J. 2014. Scaling in situ cosmogenic nuclide production rates using analytical approximations to atmospheric cosmic-ray fluxes. *Earth and Planetary Science Letters,* 386**,** 149-160.
LILLIE, A., GUNN, B. 1964. Steeply plunging folds in the sealy range, southern Alps. *New Zealand Journal of Geology and Geophysics,* 7**,** 403-423.
LOEW, S., GSCHWIND, S., GISCHIG, V., KELLER-SIGNER, A. & VALENTI, G. J. L. 2017. Monitoring and early warning of the 2012 Preonzo catastrophic rockslope failure. *Landslides,* 14**,** 141-154.
LONG, D. G. 1974. Glacial and paraglacial genesis of conglomeratic rocks of the Chibougamau Formation (Aphebian), Chibougamau, Quebec. *Canadian Journal of Earth Sciences,* 11**,** 1236-1252.
MACFARLANE, D. 2009. Observations and predictions of the behaviour of large, slow-moving landslides in schist, Clyde Dam reservoir, New Zealand. *Engineering Geology,* 109**,** 5-15.
MAHR, T. 1977. Deep—Reaching gravitational deformations of high mountain slopes. *Bulletin of the International Association of Engineering Geology,* 16**,** 121-127.
MALAMUD, B. D., TURCOTTE, D. L., GUZZETTI, F. & REICHENBACH, P. 2004. Landslides, earthquakes, and erosion. *Earth and Planetary Science Letters,* 229**,** 45-59.
MALET, J.-P., LAIGLE, D., REMAÎTRE, A. & MAQUAIRE, O. 2005. Triggering conditions and mobility of debris flows associated to complex earthflows. *Geomorphology,* 66**,** 215-235.
MANCINI, D. & LANE, S. 2020. Changes in sediment connectivity following glacial debuttressing in an Alpine valley system. *Geomorphology,* 352**,** 106987.
MANCONI, A., GLUER, F. & LOEW, S. 2017. Rapid evolution of the paraglacial Moosfluh rock slope instability (Swiss Alps) captured by Sentinel-1. *EGUGA***,** 4594.
MARCOTT, S. A., SHAKUN, J. D., CLARK, P. U. & MIX, A. C. 2013. A reconstruction of regional and global temperature for the past 11,300 years. *Science,* 339**,** 1198-1201.
MARGIELEWSKI, W. 2006. Structural control and types of movements of rock mass in anisotropic rocks: case studies in the Polish Flysch Carpathians. *Geomorphology,* 77**,** 47-68.
MARINOS, P. & HOEK, E. GSI: a geologically friendly tool for rock mass strength estimation. ISRM international symposium, 2000. International Society for Rock Mechanics and Rock Engineering.
MARTINOTTI, G., GIORDAN, D., GIARDINO, M. & RATTO, S. 2011. Controlling factors for deep-seated gravitational slope deformation (DSGSD) in the Aosta Valley (NW Alps, Italy). *Geological Society, London, Special Publications,* 351**,** 113-131.
MARZEION, B., COGLEY, J. G., RICHTER, K. & PARKES, D. 2014. Attribution of global glacier mass loss to anthropogenic and natural causes. *Science,* 345**,** 919-921.
MATSUI, T., SAN, K. 1992. Finite element slope stability analysis by shear strength reduction technique. *Soils Foundations,* 32**,** 59-70.
MCCOLL, S. T. 2012a. Paraglacial rock-slope stability. *Geomorphology,* 153**,** 1-16.
MCCOLL, S. T. 2012b. *Paraglacial Rockslope Stability.* PhD, University of Canterbury.
MCCOLL, S. T. & DAVIES, T. R. 2013. Large ice-contact slope movements: glacial buttressing, deformation and erosion. *Earth Surface Processes and Landforms,* 38**,** 1102-1115.
MCCOLL, S. T., DAVIES, T. R., MCSAVENEY, M. J. 2012. The effect of glaciation on the intensity of seismic ground motion. *Earth Surface Processes and Landforms,* 37**,** 1290-1301.
MCCOLL, S. T. & DRAEBING, D. 2019. Rock slope instability in the proglacial zone: State of the Art. *Geomorphology of Proglacial Systems.* Springer.
MCSAVENEY, M. J., DAVIES, T. R. & ASHBY, G. L. 2003. *The fatal Ramsay Glacier rockfall of 9 November 2002.* Institute of Geological & Nuclear Sciences science report
MEIGS, A., KRUGH, W. C., DAVIS, K. & BANK, G. 2006. Ultra-rapid landscape response and sediment yield following glacier retreat, Icy Bay, southern Alaska. *Geomorphology,* 78**,** 207-221.
MERCIER, D., COQUIN, J., FEUILLET, T., DECAULNE, A., COSSART, E., JÓNSSON, H. P. & SÆMUNDSSON, Þ. 2017. Are Icelandic rock-slope failures paraglacial? Age evaluation of

seventeen rock-slope failures in the Skagafjörður area, based on geomorphological stacking, radiocarbon dating and tephrochronology. *Geomorphology,* 296**,** 45-58.
MERCIER, D., COSSART, E., DECAULNE, A., FEUILLET, T., JÓNSSON, H. P. & SÆMUNDSSON, Þ. 2013. The Höfðahólar rock avalanche (sturzström): Chronological constraint of paraglacial landsliding on an Icelandic hillslope. *The holocene,* 23**,** 432-446.
MERCIER, D., DECAULNE, A., COSSART, E., FEUILLET, T., SÆMUNDSSON, Þ. & JÓNSSON, H. P. 2011. Dating of a rock avalanche in Skagafjörður, Northern Iceland: pieces of evidence of a paraglacial origin. *Geophysical Research Abstracts-Proceedings of EGU General Assembly,* 13.
MERCIER, D., ÉTIENNE, S., SELLIER, D. & ANDRÉ, M. F. 2009. Paraglacial gullying of sediment-mantled slopes: a case study of Colletthøgda, Kongsfjorden area, West Spitsbergen (Svalbard). *Earth Surface Processes and Landforms: The Journal of the British Geomorphological Research Group,* 34**,** 1772-1789.
MERIC, O., GARAMBOIS, S., JONGMANS, D., WATHELET, M., CHATELAIN, J. L. & VENGEON, J. M. 2005. Application of geophysical methods for the investigation of the large gravitational mass movement of Séchilienne, France. *Canadian Geotechnical Journal,* 42**,** 1105-1115. Available: 10.1139/t05-034
MOLNAR, P. 2004. Interactions among topographically induced elastic stress, static fatigue, and valley incision. *Journal of Geophysical Research: Earth Surface,* 109.
MOORE, D. & MATHEWS, W. 1978. The Rubble Creek landslide, southwestern British Columbia. *Canadian Journal of Earth Sciences,* 15**,** 1039-1052.
MÜLLER, B. U. 1999. Paraglacial sedimentation and denudation processes in an Alpine valley of Switzerland. An approach to the quantification of sediment budgets. *Geodinamica Acta,* 12**,** 291-301.
NARANJO, J. A. & FRANCIS, P. 1987. High velocity debris avalanche at Lastarria volcano in the north Chilean Andes. *Bulletin of Volcanology,* 49**,** 509-514.
NAUDET, V., LAZZARI, M., PERRONE, A., LOPERTE, A., PISCITELLI, S. & LAPENNA, V. 2008. Integrated geophysical and geomorphological approach to investigate the snowmelt-triggered landslide of Bosco Piccolo village (Basilicata, southern Italy). *Engineering Geology,* 98**,** 156-167.
NISHII, R., MATSUOKA, N., DAIMARU, H. & YASUDA, M. 2013. Precursors and triggers of an alpine rockslide in Japan: the 2004 partial collapse during a snow-melting period. *Landslides,* 10**,** 75-82.
NOETZLI, J., HOELZLE, M. & HAEBERLI, W. Mountain permafrost and recent Alpine rock-fall events: a GIS-based approach to determine critical factors. Proceedings of the 8th International Conference on Permafrost, 2003. Swets & Zeitlinger Lisse, Zürich, 827-832.
OERLEMANS, J., ANDERSON, B., HUBBARD, A., HUYBRECHTS, P., JOHANNESSON, T., KNAP, W., SCHMEITS, M., STROEVEN, A., VAN DE WAL, R. & WALLINGA, J. 1998. Modelling the response of glaciers to climate warming. *Climate Dynamics,* 14**,** 267-274.
OPPIKOFER, T., JABOYEDOFF, M., PEDRAZZINI, A., DERRON, M. H. & BLIKRA, L. H. 2011. Detailed DEM analysis of a rockslide scar to characterize the basal sliding surface of active rockslides. *Journal of Geophysical Research: Earth Surface,* 116.
OSWALD, P., STRASSER, M., HAMMERL, C. & MOERNAUT, J. 2021. Seismic control of large prehistoric rockslides in the Eastern Alps. *Nature communications,* 12**,** 1-8.
OWEN, G., HIEMSTRA, J. F., MATTHEWS, J. A. & MCEWEN, L. J. 2010. Landslide-glacier interaction in a neoparaglacial setting at tverrbytnede, jotunheimen, southern norway. *Geografiska Annaler: Series A, Physical Geography,* 92**,** 421-436.
PÁNEK, T., HRADECKÝ, J., MINÁR, J., HUNGR, O. & DUŠEK, R. 2009. Late Holocene catastrophic slope collapse affected by deep-seated gravitational deformation in flysch: Ropice Mountain, Czech Republic. *Geomorphology,* 103**,** 414-429.
PÁNEK, T. & KLIMEŠ, J. 2016. Temporal behavior of deep-seated gravitational slope deformations: A review. *Earth Science Reviews,* 156**,** 14-38.
PÁNEK, T., TÁBOŘÍK, P., KLIMEŠ, J., KOMÁRKOVÁ, V., HRADECKÝ, J. & ŠŤASTNÝ, M. 2011. Deep-seated gravitational slope deformations in the highest parts of the Czech Flysch Carpathians:

Evolutionary model based on kinematic analysis, electrical imaging and trenching. *Geomorphology,* 129**,** 92-112.
PATTON, A. I., RATHBURN, S. L. & CAPPS, D. M. J. G. 2019. Landslide response to climate change in permafrost regions. *Geomorphology,* 340**,** 116-128.
PERRAS, M. A., DIEDERICHS, M. S. 2014. A review of the tensile strength of rock: concepts and testing. *Geotechnical geological engineering* 32**,** 525-546.
PETLEY, D. 2012. Global patterns of loss of life from landslides. *Geology,* 40**,** 927-930.
PHILLIPS, M., HABERKORN, A., DRAEBING, D., KRAUTBLATTER, M., RHYNER, H. & KENNER, R. 2016. Seasonally intermittent water flow through deep fractures in an Alpine rock ridge: Gemsstock, central Swiss Alps. *Cold Regions Science and Technology,* 125**,** 117-127. Available: 10.1016/j.coldregions.2016.02.010
PREMCHITT, J., BRAND, E. & PHILLIPSON, H. 1986. Landslides caused by rapid groundwater changes. *Geological Society, London, Engineering Geology Special Publications,* 3**,** 87-94.
PRICE, N. J. & COSGROVE, J. W. 1990. *Analysis of geological structures*, Cambridge University Press.
PURDIE, H., ANDERSON, B., CHINN, T., OWENS, I., MACKINTOSH, A. & LAWSON, W. 2014. Franz Josef and Fox Glaciers, New Zealand: historic length records. *Global and Planetary Change,* 121**,** 41-52.
PURDIE, H., BROOK, M. & FULLER, I. 2008. Seasonal variation in ablation and surface velocity on a temperate maritime glacier: Fox Glacier, New Zealand. *Arctic, Antarctic, and Alpine Research,* 40**,** 140-147.
PURDIE, H., GOMEZ, C. & ESPINER, S. 2015. Glacier recession and the changing rockfall hazard: Implications for glacier tourism. *New Zealand Geographer,* 71**,** 189-202.
PUTNAM, A. E., DENTON, G. H., SCHAEFER, J. M., BARRELL, D. J., ANDERSEN, B. G., FINKEL, R. C., SCHWARTZ, R., DOUGHTY, A. M., KAPLAN, M. R. & SCHLÜCHTER, C. J. N. G. 2010. Glacier advance in southern middle-latitudes during the Antarctic Cold Reversal. *Nature Geoscience,* 3**,** 700-704.
RADBRUCH-HALL, D. H. 1978. Gravitational creep of rock masses on slopes. *Developments in Geotechnical Engineering.* Elsevier.
RAVANEL, L., MAGNIN, F. & DELINE, P. 2017. Impacts of the 2003 and 2015 summer heatwaves on permafrost-affected rock-walls in the Mont Blanc massif. *Science of the Total Environment,* 609**,** 132-143.
REZNICHENKO, N. V., DAVIES, T. R. & ALEXANDER, D. J. 2011. Effects of rock avalanches on glacier behaviour and moraine formation. *Geomorphology,* 132**,** 327-338.
REZNICHENKO, N. V., DAVIES, T. R., WINKLER, S. 2016. Revised palaeoclimatic significance of Mueller Glacier moraines, Southern Alps, New Zealand. *Earth Surface Processes and Landforms,* 41**,** 196-207.
RICHARDS, L. & READ, S. New Zealand greywacke characteristics and influences on rock mass behaviour. 11th ISRM Congress, 2007. International Society for Rock Mechanics and Rock Engineering.
RIVA, F., AGLIARDI, F., AMITRANO, D. & CROSTA, G. B. 2018. Damage-based time-dependent modeling of paraglacial to postglacial progressive failure of large rock slopes. *Journal of Geophysical Research: Earth Surface,* 123**,** 124-141.
ROE, G. H., BAKER, M. B. & HERLA, F. 2017. Centennial glacier retreat as categorical evidence of regional climate change. *Nature geoscience,* 10**,** 95-99.
ROY, S., PURDIE, H., GOMEZ, C., WASSMER, P. & SCHUSTER, M. 2015. *Rockfall at Fox Glacier: a Hazard Analysis using Structure from Motion and Spatial Modelling.*
RYDER, J. 1971. The stratigraphy and morphology of para-glacial alluvial fans in south-central British Columbia. *Canadian Journal of Earth Sciences,* 8**,** 279-298.
SANDMEIER, K. J. 2012. *REFLEXW Version 7.0 Manual*, Karlsruhe.
SARA, W. A. 1968. Franz Josef and Fox Glaciers, 1951–1967. *New Zealand Journal of Geology and Geophysics,* 11**,** 768-780.

SATTLER, K., ANDERSON, B., MACKINTOSH, A., NORTON, K. & DE RÓISTE, M. 2016. Estimating permafrost distribution in the maritime Southern Alps, New Zealand, based on climatic conditions at rock glacier sites. *Frontiers in Earth Science,* 4**,** 4.

SCHAEFER, J. M., DENTON, G. H., KAPLAN, M., PUTNAM, A., FINKEL, R. C., BARRELL, D. J., ANDERSEN, B. G., SCHWARTZ, R., MACKINTOSH, A. & CHINN, T. J. S. 2009. High-frequency Holocene glacier fluctuations in New Zealand differ from the northern signature. *Science,* 324**,** 622-625.

SCHERLER, D., BOOKHAGEN, B. & STRECKER, M. R. 2011. Spatially variable response of Himalayan glaciers to climate change affected by debris cover. *Nature geoscience,* 4**,** 156.

SCHOPPER, N., MERGILI, M., FRIGERIO, S., CAVALLI, M. & POEPPL, R. 2019. Analysis of lateral sediment connectivity and its connection to debris flow intensity patterns at different return periods in the Fella River system in northeastern Italy. *Science of the Total Environment,* 658**,** 1586-1600.

SCHULZ, W. H., GALLOWAY, S. L. & HIGGINS, J. D. 2012. Evidence for earthquake triggering of large landslides in coastal Oregon, USA. *Geomorphology,* 141**,** 88-98.

SCHUSTER, R. L. 1996. *LANDSLIDES: INVESTIGATION AND MITIGATION. CHAPTER 2-SOCIOECONOMIC SIGNIFICANCE OF LANDSLIDES*.

SCHUSTER, R. L. & COSTA, J. E. PERSPECTIVE ON LANDSLIDE DAMS. Landslide Dams: Processes, Risk, and Mitigation. Proceedings of a Session in Conjunction with the ASCE Convention., 1986. 1-20.

SEPÚLVEDA, S. A., ALFARO, A., LARA, M., CARRASCO, J., OLEA-ENCINA, P., REBOLLEDO, S. & GARCÉS, M. 2021. An active large rock slide in the Andean paraglacial environment: The Yerba Loca landslide, central Chile. *Landslides,* 18**,** 697-705.

SHAKESBY, R. A. & MATTHEWS, J. A. 1996. Glacial activity and paraglacial landsliding in the Devensian Lateglacial: evidence from Craig Cerrig-gleisiad and Fan Dringarth, Fforest Fawr (Brecon Beacons), South Wales. *Geological Journal,* 31**,** 143-157.

SHULMEISTER, J., DAVIES, T. R., EVANS, D. J., HYATT, O. M. & TOVAR, D. S. 2009. Catastrophic landslides, glacier behaviour and moraine formation–A view from an active plate margin. *Quarternary Science Reviews,* 28**,** 1085-1096.

SLAYMAKER, O. 2009. Proglacial, periglacial or paraglacial? *Geological Society, London, Special Publications,* 320**,** 71-84.

SLAYMAKER, O.2011. Criteria to distinguish between periglacial, proglacial and paraglacial environments. *Quaestiones Geographicae,* 30**,** 85-94.

SOSIO, R., CROSTA, G. B. & HUNGR, O. 2008. Complete dynamic modeling calibration for the Thurwieser rock avalanche (Italian Central Alps). *Engineering Geology,* 100**,** 11-26.

SPRINGMAN, S., JOMMI, C. & TEYSSEIRE, P. 2003. Instabilities on moraine slopes induced by loss of suction: a case history. *Geotechnique,* 53**,** 3-10.

STEAD, D. & WOLTER, A. 2015. A critical review of rock slope failure mechanisms: the importance of structural geology. *Journal of Structural Geology,* 74**,** 1-23.

STEFANELLI, C. T., SEGONI, S., CASAGLI, N. & CATANI, F. 2016. Geomorphic indexing of landslide dams evolution. *Engineering Geology,* 208**,** 1-10.

STOCK, G. M., UHRHAMMER, R. A. 2010. Catastrophic rock avalanche 3600 years BP from El Capitan, Yosemite Valley, California. *Earth Surface Processes and Landforms,* 35**,** 941-951.

STORNI, E., HUGENTOBLER, M., MANCONI, A. & LOEW, S. 2020. Monitoring and analysis of active rockslide-glacier interactions (Moosfluh, Switzerland). *Geomorphology,* 371**,** 107414.

STURMAN, A., WANNER, H. 2001. A comparative review of the weather and climate of the Southern Alps of New Zealand and the European Alps. *Mountain Research and Development***,** 359-369.

STURZENEGGER, M., STEAD, D., GOSSE, J., WARD, B. & FROESE, C. 2015. Reconstruction of the history of the Palliser rockslide based on 36 Cl terrestrial cosmogenic nuclide dating and debris volume estimations. *Landslides,* 12**,** 1097-1106.

STURZENEGGER, M. & STEAD, D. 2012. The Palliser Rockslide, Canadian Rocky Mountains: characterization and modeling of a stepped failure surface. *Geomorphology,* 138**,** 145-161.

SWANSON, F. J., OYAGI, N. & TOMINAGA, M. Landslide dams in Japan. Landslide dams: processes, risk, and mitigation, 1986. ASCE, 131-145.
TANNANT, D., GIORDAN, D. & MORGENROTH, J. 2017. Characterization and analysis of a translational rockslide on a stepped-planar slip surface. *Engineering Geology,* 220**,** 144-151.
TRAVELLETTI, J., MALET, J.-P., SAMYN, K., GRANDJEAN, G. & JABOYEDOFF, M. 2013. Control of landslide retrogression by discontinuities: evidence by the integration of airborne-and ground-based geophysical information. *Landslides,* 10**,** 37-54.
VACCO, D. A., ALLEY, R. B., POLLARD, D. 2010. Glacial advance and stagnation caused by rock avalanches. *Earth Planetary Science Letters,* 294**,** 123-130.
VANDERGOES, M. J., DIEFFENBACHER-KRALL, A. C., NEWNHAM, R. M., DENTON, G. H. & BLAAUW, M. 2008. Cooling and changing seasonality in the southern Alps, New Zealand during the Antarctic cold reversal. *Quarternary Science Reviews,* 27**,** 589-601.
VEHLING, L., BAEWERT, H., GLIRA, P., MOSER, M., ROHN, J. & MORCHE, D. 2017. Quantification of sediment transport by rockfall and rockslide processes on a proglacial rock slope (Kaunertal, Austria). *Geomorphology,* 287**,** 46-57.
WALTER, F., AMANN, F., KOS, A., KENNER, R., PHILLIPS, M., DE PREUX, A., HUSS, M., TOGNACCA, C., CLINTON, J. & DIEHL, T. 2020. Direct observations of a three million cubic meter rock-slope collapse with almost immediate initiation of ensuing debris flows. *Geomorphology,* 351**,** 106933.
WANG, B., VARDON, P., HICKS, M. 2016. Investigation of retrogressive and progressive slope failure mechanisms using the material point method. *Computers Geotechnics,* 78**,** 88-98.
WANG, J.-J., ZHAO, D., LIANG, Y. & WEN, H. 2013. Angle of repose of landslide debris deposits induced by 2008 Sichuan Earthquake. *Engineering Geology,* 156**,** 103-110.
WEGMANN, M., GUDMUNDSSON, G. H., HAEBERLI, W. 1998. Permafrost changes in rock walls and the retreat of Alpine glaciers: a thermal modelling approach. *Permafrost and Periglacial Processes,* 9**,** 23-33.
WESTOBY, M. J., BRASINGTON, J., GLASSER, N. F., HAMBREY, M. J. & REYNOLDS, J. M. 2012. 'Structure-from-Motion'photogrammetry: A low-cost, effective tool for geoscience applications. *Geomorphology,* 179**,** 300-314.
WILLIAMS, H. B. & KOPPES, M. N. 2019. A comparison of glacial and paraglacial denudation responses to rapid glacial retreat. *Annals of Glaciology***,** 1-14.
WINKLER, S. 2000. The 'Little Ice Age'maximum in the Southern Alps, New Zealand: preliminary results at Mueller Glacier. *The Holocene,* 10**,** 643-647.
WOHL, E., BRIERLEY, G., CADOL, D., COULTHARD, T. J., COVINO, T., FRYIRS, K. A., GRANT, G., HILTON, R. G., LANE, S. N., MAGILLIGAN, F. J. 2019. Connectivity as an emergent property of geomorphic systems. *Earth Surface Processes and Landforms,* 44**,** 4-26.
WYRWOLL, K. 1977. Causes of rock-slope failure in a cold area: Labrador-Ungava. *Geological Society of America Reviews in Engineering Geology,* 3**,** 59-67.
YIN, Y., WANG, F. & SUN, P. 2009. Landslide hazards triggered by the 2008 Wenchuan earthquake, Sichuan, China. *Landslides,* 6**,** 139-152.
YIN, Y., XING, A. T. 2012. Aerodynamic modeling of the Yigong gigantic rock slide-debris avalanche, Tibet, China. *Bulletin of Engineering Geology and the Environment,* 71**,** 149-160.
ZÊZERE, J., FERREIRA, A., RODRIGUES, M. 1999. Landslides in the North of Lisbon Region (Portugal): conditioning and triggering factors. *Physics Chemistry of the Earth, Part A: Solid Earth Geodesy,* 24**,** 925-934.

8. Appendix

8.1 DRC 16 ONLINE STATEMENT OF CONTRIBUTION FORMS

MASSEY UNIVERSITY
TE KUNENGA KI PŪREHUROA
UNIVERSITY OF NEW ZEALAND

GRADUATE RESEARCH SCHOOL

STATEMENT OF CONTRIBUTION
DOCTORATE WITH PUBLICATIONS/MANUSCRIPTS

We, the candidate and the candidate's Primary Supervisor, certify that all co-authors have consented to their work being included in the thesis and they have accepted the candidate's contribution as indicated below in the *Statement of Originality*.

Name of candidate:	Emma Cody
Name/title of Primary Supervisor:	Dr Samuel McColl
In which chapter is the manuscript /published work:	Chapter 3

Please select one of the following three options:

(●) The manuscript/published work is published or in press

- Please provide the full reference of the Research Output:

Cody, E., Draebing, D., McColl, S., Cook, S., & Brideau, M.-A. (2020). Geomorphology and geological controls of an active paraglacial rockslide in the New Zealand Southern Alps. Landslides, 17, 755-776.

( ) The manuscript is currently under review for publication – please indicate:

- The name of the journal:

- The percentage of the manuscript/published work that was contributed by the candidate: 80.00

- Describe the contribution that the candidate has made to the manuscript/published work:

Emma Cody wrote the journal article and created figures for the article. They were responsible for the review process during publishing and completed field work, data acquisition and processing for all methodologies.
Sam McColl assisted with writing, revisions and Figures 1 and 2. They also participated in field work and data acquisition.
Daniel Draebing assisted with manuscript writing field work and seismic data acquisition and

( ) It is intended that the manuscript will be published, but it has not yet been submitted to a journal

Candidate's Signature:	Emma Cody Digitally signed by Emma Cody Date: 2020.10.06 09:46:55 +13'00'
Date:	06-Oct-2020
Primary Supervisor's Signature:	
Date:	6 May 2022

This form should appear at the end of each thesis chapter/section/appendix submitted as a manuscript/ publication or collected as an appendix at the end of the thesis.

MASSEY UNIVERSITY
TE KUNENGA KI PŪREHUROA
UNIVERSITY OF NEW ZEALAND

GRADUATE RESEARCH SCHOOL

STATEMENT OF CONTRIBUTION
DOCTORATE WITH PUBLICATIONS/MANUSCRIPTS

We, the candidate and the candidate's Primary Supervisor, certify that all co-authors have consented to their work being included in the thesis and they have accepted the candidate's contribution as indicated below in the *Statement of Originality*.

Name of candidate:	Emma Cody
Name/title of Primary Supervisor:	Dr Samuel McColl
In which chapter is the manuscript /published work:	Chapter 4

Please select one of the following three options:

○ The manuscript/published work is published or in press

- Please provide the full reference of the Research Output:

○ The manuscript is currently under review for publication – please indicate:

- The name of the journal:

- The percentage of the manuscript/published work that was contributed by the candidate: 80.00

- Describe the contribution that the candidate has made to the manuscript/published work:

Emma Cody wrote the draft manuscript and created all figures. They completed or assisted with field work, data collection and analysis for all methodologies.
Sam McColl completed field work and assisted with processes of the annual survey data.
Daniel Draebing assisted with field work and crack meter installation and processing
Processing of cosmogenic samples was completed at GNS and Victoria University of Wellington.

◉ It is intended that the manuscript will be published, but it has not yet been submitted to a journal

Candidate's Signature:	Emma Cody Digitally signed by Emma Cody Date: 2020.10.06 09:46:55 +13'00'
Date:	06-Oct-2020
Primary Supervisor's Signature:	
Date:	6 May 2022

This form should appear at the end of each thesis chapter/section/appendix submitted as a manuscript/ publication or collected as an appendix at the end of the thesis.

MASSEY UNIVERSITY
TE KUNENGA KI PŪREHUROA
UNIVERSITY OF NEW ZEALAND

GRADUATE RESEARCH SCHOOL

STATEMENT OF CONTRIBUTION
DOCTORATE WITH PUBLICATIONS/MANUSCRIPTS

We, the candidate and the candidate's Primary Supervisor, certify that all co-authors have consented to their work being included in the thesis and they have accepted the candidate's contribution as indicated below in the *Statement of Originality*.

Name of candidate:	Emma Cody
Name/title of Primary Supervisor:	Dr Samuel McColl
In which chapter is the manuscript /published work:	5

Please select one of the following three options:

(●) The manuscript/published work is published or in press

- Please provide the full reference of the Research Output:

Cody, E., Anderson, B.M., McColl, S.T., Fuller, I.C., & Purdie, H.L. (2020). Paraglacial adjustment of sediment slopes during and immediately after glacial debuttressing. Geomorphology, 371, 107411.

( ) The manuscript is currently under review for publication – please indicate:

- The name of the journal:

- The percentage of the manuscript/published work that was contributed by the candidate: 80.00

- Describe the contribution that the candidate has made to the manuscript/published work:

Emma Cody wrote the research article and created all figures. They were responsible for the review process and analysed data for the manuscript.
Brian Anderson installed the monitoring equipment and assisted with the processing of data, including the creation of the DEM.
Sam McColl and Ian Fuller assisted with reviewing the manuscript and data collection.
Heather Purdie created a DEM used in the study

( ) It is intended that the manuscript will be published, but it has not yet been submitted to a journal

Candidate's Signature:	Emma Cody Digitally signed by Emma Cody Date: 2020.10.06 09:59:28 +13'00'
Date:	06-Oct-2020
Primary Supervisor's Signature:	
Date:	6 May 2022

This form should appear at the end of each thesis chapter/section/appendix submitted as a manuscript/ publication or collected as an appendix at the end of the thesis.